

# Robust Fixed-Structure Controller Synthesis

by

**Joseph R. Corrado**

Graduate Student

School of Aerospace Engineering

Georgia Institute of Technology

**Wassim M. Haddad**

Graduate Advisor

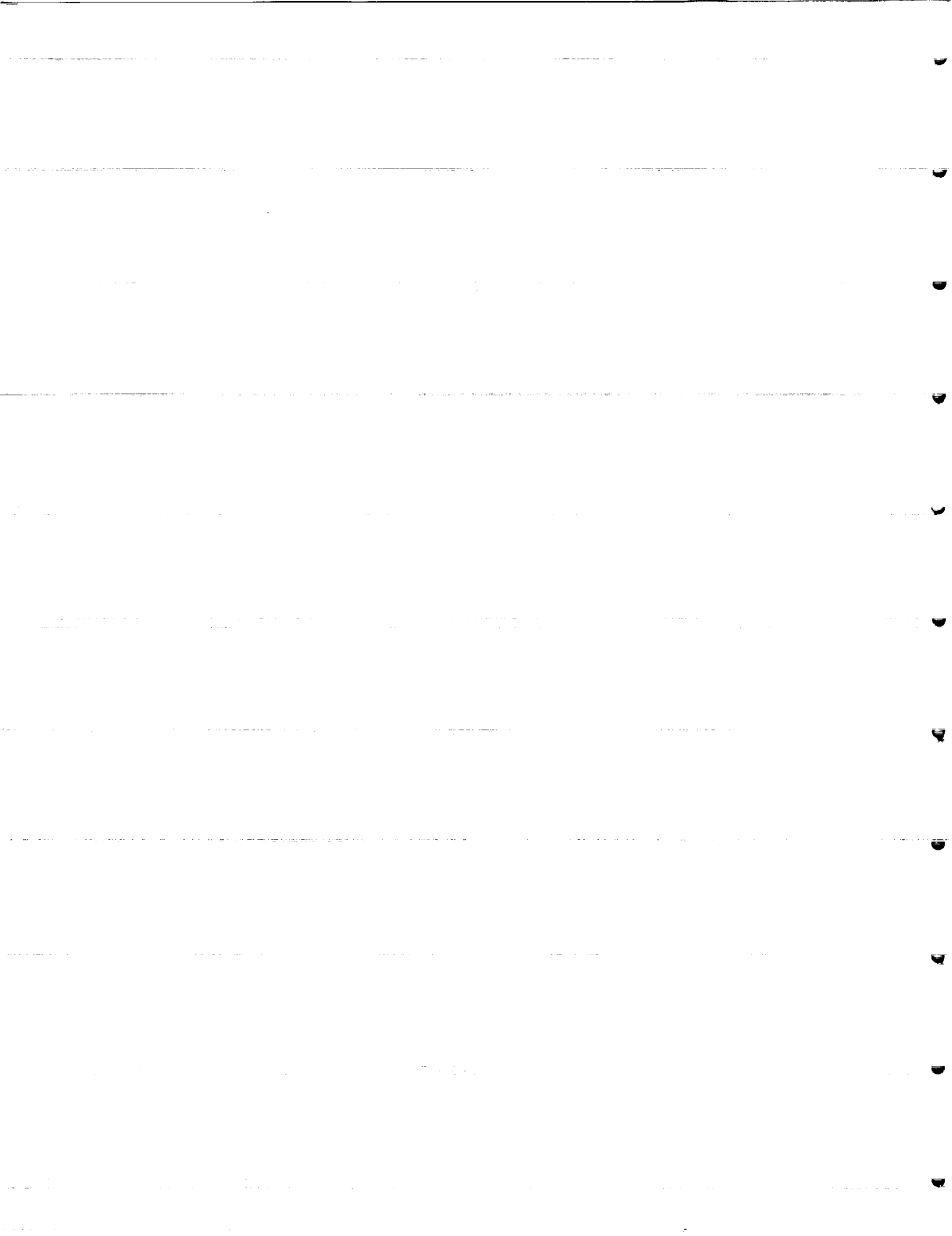
School of Aerospace Engineering

Georgia Institute of Technology

June, 2000



School of Aerospace Engineering  
Atlanta, GA 30332-0150 U.S.A.  
Phone/Fax: (404) 894-3474



# Acknowledgements

This research was conducted at the School of Aerospace Engineering at the Georgia Institute of Technology with the support provided by the National Aeronautics and Space Administration under Grant NGT 4-52405 with Dr. K. Gupta serving as technical monitor.



# Contents

Acknowledgements	iii
List of Tables	xi
List of Figures	xiii
Notation	xvii
Summary	xix
<b>1 Introduction</b>	<b>1</b>
1.1. Robust Fixed-Structure Control Design: Motivation and Overview . .	1
1.2. Brief Outline of the Dissertation . . . . .	7
<b>2 Fixed-Structure Control Framework</b>	<b>11</b>
2.1. Introduction . . . . .	11
2.2. Performance Constraints . . . . .	15
2.3. Quasi-Newton Gradient Optimization . . . . .	18
2.4. Structural Dynamics Modeling of the ACTEX Flight Experiment . .	19
2.5. Fixed-Structure Synthesis for the ACTEX Flight Experiment . . . .	21
2.6. Simulation Results . . . . .	24
2.7. Conclusion . . . . .	30

<b>3</b>	<b>Stable <math>\mathcal{H}_2</math>-Optimal Controller Synthesis</b>	<b>31</b>
3.1.	Introduction . . . . .	31
3.2.	Stable $\mathcal{H}_2$ -Optimal Control . . . . .	33
3.3.	Design Equations . . . . .	34
3.4.	Optimization Algorithm . . . . .	36
3.5.	Spring-Mass-Damper Example . . . . .	37
3.6.	Two-Mass Example . . . . .	45
3.7.	Conclusion . . . . .	48
<b>4</b>	<b><math>\mathcal{H}_2</math>-Optimal Synthesis of Controllers with Relative Degree Two</b>	<b>49</b>
4.1.	Introduction . . . . .	49
4.2.	$\mathcal{H}_2$ -Optimal Relative Degree Two Control . . . . .	50
4.3.	Relative Degree Two Controller Synthesis . . . . .	52
4.4.	Control Design Process . . . . .	53
4.5.	Two-Mass Example . . . . .	54
4.6.	Three Mass Example . . . . .	56
4.7.	Coupled Rotating Disk Example . . . . .	58
4.8.	Conclusion . . . . .	61
<b>5</b>	<b>Robust Fixed-Structure Controller Synthesis using the Implicit Small Gain Bound</b>	<b>63</b>
5.1.	Introduction . . . . .	63
5.2.	Robust Stability and Performance Problem . . . . .	64
5.3.	Sufficient Conditions for Robust Stability and Performance . . . . .	65
5.4.	Uncertainty Structure and the Implicit Small Gain Guaranteed Cost Bound . . . . .	66

5.5. Robust Controller Synthesis via the Implicit Small Gain Guaranteed Cost Bound . . . . .	70
5.6. Two-Mass Example . . . . .	75
5.7. Three-Mass Example . . . . .	81
5.8. Conclusion . . . . .	83
<b>6 Robust Resilient Dynamic Controllers for Systems with Parametric Uncertainty and Controller Gain Variations</b>	<b>85</b>
6.1. Introduction . . . . .	85
6.2. Robust Stability and Performance . . . . .	87
6.3. Sufficient Conditions for Robust Stability and Performance . . . . .	89
6.4. Multiplicative Controller Uncertainty Structure and Guaranteed Cost Bound . . . . .	92
6.5. Decentralized Static Output Feedback Formulation . . . . .	94
6.6. Sufficient Conditions for Fixed-Order Resilient Compensation with Multiplicative Uncertainty . . . . .	97
6.7. Additive Controller Uncertainty and Guaranteed Cost Bound . . . . .	99
6.8. Decentralized Static Output Feedback Formulation . . . . .	102
6.9. Sufficient Conditions for Fixed-Order Resilient Compensation with Additive Uncertainty . . . . .	104
6.10. Quasi-Newton Optimization Algorithm . . . . .	105
6.11. Second-Order Unstable System . . . . .	105
6.12. Two-Mass Benchmark Problem . . . . .	107
6.13. Conclusion . . . . .	109
<b>7 Fixed-Structure Controller Design for Axial Flow Compression Systems</b>	<b>117</b>

7.1. Introduction . . . . .	117
7.2. Output Feedback Disturbance Rejection Control for Axial Flow Compression Systems . . . . .	120
7.3. Sufficient Conditions for Closed-Loop Stability and Disturbance Rejection . . . . .	125
7.4. Reduced-Order Dynamic Control for Axial Flow Compressors . . . . .	131
7.5. Active Dynamic Control of an Axial Flow Compressor . . . . .	134
7.6. Conclusion . . . . .	140
<b>8 Fixed-Structure Controller Synthesis for Real and Complex Multiple Block-Structured Uncertainty</b>	<b>141</b>
8.1. Introduction . . . . .	141
8.2. Absolute Stability Criterion with Generalized Positive Real Stability Multipliers . . . . .	142
8.3. Stability Multiplier Structure . . . . .	145
8.4. Decentralized Static Output Feedback Formulation . . . . .	149
8.5. Specialization to Centralized Strictly Proper Dynamic Compensation	153
8.6. Robust Stability and Performance . . . . .	156
8.7. Sufficient Conditions for Fixed-Order Robust Compensation with Dy- namic Multipliers . . . . .	157
8.8. Quasi-Newton Optimization Algorithm . . . . .	160
8.9. Conclusion . . . . .	161
<b>9 Concluding Remarks and Recommendations for Future Research</b>	<b>163</b>
9.1. Conclusions . . . . .	163
9.2. Recommendations for Future Research . . . . .	165

Appendix

169

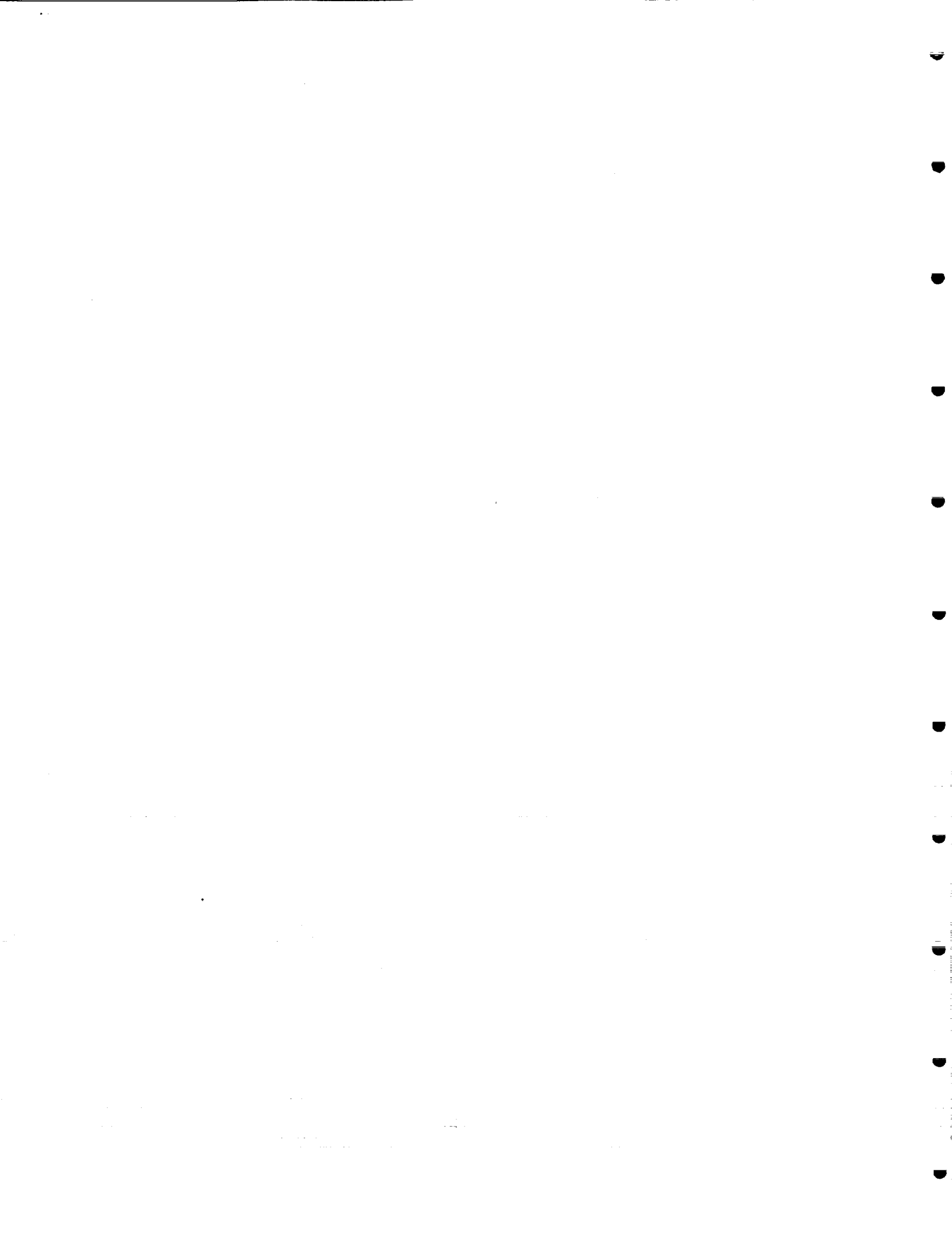
References

175



# List of Tables

2.1	$\mathcal{H}_2$ costs for various controller configurations and weightings . . . . .	25
2.2	Optimal controller parameters for controller configuration 1 . . . . .	25
3.1	$\mathcal{H}_2$ costs for various stable stabilization techniques . . . . .	43
3.2	$\mathcal{H}_2$ costs for various stable stabilization techniques . . . . .	47

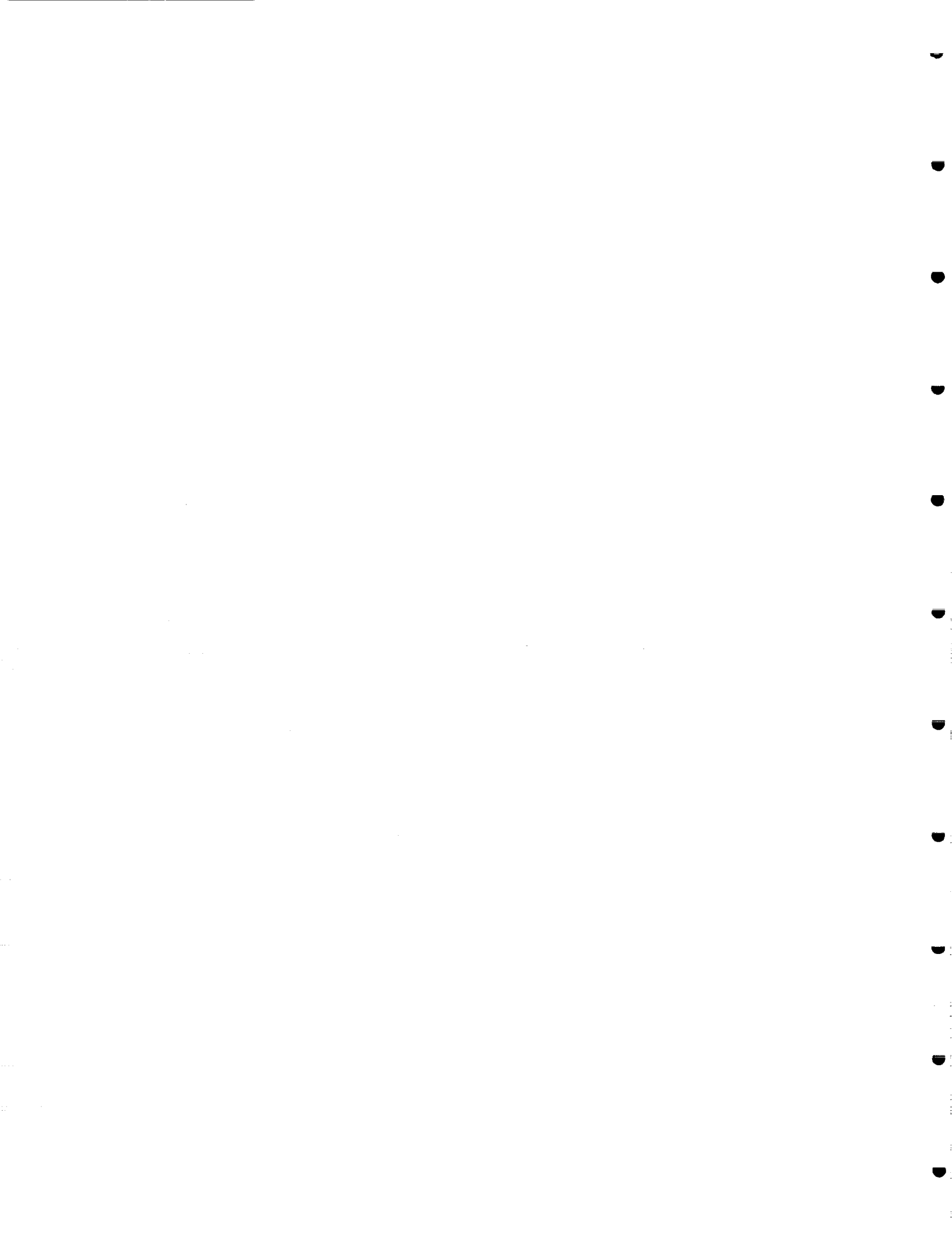


# List of Figures

2.1	Decentralized Static Output Feedback Framework . . . . .	12
2.2	ACTEX flight experiment . . . . .	20
2.3	Open-loop impulse response . . . . .	25
2.4	Closed-loop impulse response, $R_2 = 1$ . . . . .	26
2.5	Closed-loop impulse response, $R_2 = 0.01$ . . . . .	27
2.6	Closed-loop impulse response, $R_2 = 0.0001$ . . . . .	27
2.7	Closed-loop control effort, $R_2 = 1$ . . . . .	28
2.8	Closed-loop control effort, $R_2 = 0.01$ . . . . .	28
2.9	Closed-loop control effort, $R_2 = 0.0001$ . . . . .	29
2.10	Bode plots for open-loop and closed-loop systems . . . . .	29
3.1	Bode plots of LQG and stable $\mathcal{H}_2$ controllers ( $\rho = 0.0288$ ) . . . . .	38
3.2	Nyquist plots of the loop gain for LQG (left) and stable $\mathcal{H}_2$ (right) controllers ( $\eta = 1, \rho = 0.0288$ ) . . . . .	39
3.3	Impulse response of closed-loop system with LQG and stable $\mathcal{H}_2$ controllers ( $\eta = 1, \rho = 2.88 \times 10^{-8}$ ) . . . . .	40
3.4	Location of controller eigenvalues and $\mathcal{H}_2$ cost versus $\rho$ . . . . .	41
3.5	$\mathcal{H}_2$ cost versus control weighting for various-order stable $\mathcal{H}_2$ controllers ( $\rho = 0.0288$ ) . . . . .	42
3.6	Stable $\mathcal{H}_2$ controller cost versus $\rho$ . . . . .	43

3.7	Bode plots of stable $\mathcal{H}_2$ controllers versus $\rho$ . . . . .	44
3.8	Two-mass system . . . . .	45
3.9	$\mathcal{H}_2$ cost versus control weighting ( $\rho = 0.04752$ ) . . . . .	47
4.1	Relative degree two controller set-up . . . . .	52
4.2	Bode plots of LQG and relative degree two controllers . . . . .	55
4.3	Bode plots of LQG and relative degree two controllers . . . . .	57
4.4	Bode plots of LQG and relative degree two controllers . . . . .	58
4.5	Bode plots of LQG and relative degree two controllers . . . . .	59
4.6	Bode plots of LQG and relative degree two controllers . . . . .	60
5.1	Two-mass system . . . . .	76
5.2	Dependence of the $\mathcal{H}_2$ cost on the damped natural frequency of the second mode: Colocated case . . . . .	78
5.3	Frequency responses of implicit small gain controllers: Colocated case	79
5.4	Dependence of the $\mathcal{H}_2$ cost on the damped natural frequency of the second mode: Noncolocated case . . . . .	80
5.5	Frequency responses of implicit small gain controllers: Noncolocated case . . . . .	80
5.6	Three-mass system . . . . .	81
5.7	Dependence of the $\mathcal{H}_2$ cost on $k_2$ . . . . .	82
5.8	Frequency response of the implicit small gain controller . . . . .	82
6.1	Decentralized static output feedback: Multiplicative controller uncer- tainty . . . . .	95
6.2	Decentralized static output feedback: Additive controller uncertainty	103
6.3	Two mass oscillator . . . . .	107

6.4	Dependence of the $\mathcal{H}_2$ cost on the controller error parameter . . . . .	109
6.5	Asymptotic stability regions . . . . .	110
6.6	Loop gain Nyquist plots . . . . .	110
6.7	Dependence of the $\mathcal{H}_2$ cost on the controller error parameter . . . . .	111
6.8	Asymptotic stability regions . . . . .	111
6.9	Loop gain Nyquist plots . . . . .	112
6.10	Loop gain Nyquist plots . . . . .	112
6.11	Dependence of the $\mathcal{H}_2$ cost on the controller error parameter . . . . .	113
6.12	Loop gain Nyquist plots . . . . .	113
6.13	Dependence of the $\mathcal{H}_2$ cost on the controller error parameter . . . . .	114
6.14	Asymptotic stability regions . . . . .	114
6.15	Loop gain Nyquist plots . . . . .	115
6.16	Loop gain Nyquist plots . . . . .	115
7.1	Compressor system geometry . . . . .	121
7.2	Regions, $\mathcal{D}_c$ , satisfying the sector bound (7.47) . . . . .	130
7.3	Phase portrait of pressure versus flow . . . . .	135
7.4	Phase portrait of pressure versus flow . . . . .	135
7.5	Phase portrait of pressure versus flow with exogenous disturbances . . . . .	136
7.6	Stall cell amplitude versus time . . . . .	137
7.7	Compressor flow versus time . . . . .	137
7.8	Pressure rise in compressor versus time . . . . .	138
7.9	Throttle opening versus time . . . . .	138
7.10	Integral squared performance versus time . . . . .	139
8.1	Standard feedback uncertainty representation . . . . .	143
8.2	Decentralized static output feedback framework . . . . .	150



# Notation

In this dissertation, we use the following notation:

$\mathbb{R}, \mathbb{C}$	real numbers, complex numbers
$\mathbb{R}^n, \mathbb{C}^n$	$n \times 1$ real column vectors, $n \times 1$ complex column vectors
$\mathbb{R}^{n \times m}, \mathbb{C}^{n \times m}$	$n \times m$ real matrices, $n \times m$ complex matrices
$\mathbb{N}^n, \mathbb{P}^n$	$n \times n$ nonnegative definite matrices, $n \times n$ positive definite matrices
$\mathbb{S}^n, \mathbb{E}$	$n \times n$ symmetric matrices, expectation
$I_n, \otimes$	$n \times n$ identity, Kronecker product
$A^T, A^*, A^{-1}$	transpose of $A$ , complex conjugate transpose of $A$ , inverse of $A$
$\text{tr } A, \mathcal{R}(A)$	trace of $A$ , range space of $A$
$\text{He } G$	Hermitian part of arbitrary complex matrix $G$
	$\text{He } G \triangleq \frac{1}{2}(G + G^*)$
$\text{Sh } G$	Skew-Hermitian part of arbitrary complex matrix $G$
	$\text{Sh } G \triangleq \frac{1}{2}(G - G^*)$

For convenience, we define the following terms:

$$\Sigma \triangleq BR_2^{-1}B^T, \quad \bar{\Sigma} \triangleq C^T V_2^{-1}C.$$

We also define the dimensions of the various signals below:

$x(t) \in \mathbb{R}^n$	is the plant state vector
$x_c(t) \in \mathbb{R}^{n_c}$	is the controller state vector
$u(t) \in \mathbb{R}^m$	is the control input signal
$w(t) \in \mathbb{R}^d$	is a unit-intensity, zero-mean, Gaussian white noise signal
$d(t) \in \mathbb{R}^s$	is the uncertainty input signal
$y(t) \in \mathbb{R}^l$	is the measurement output signal
$z(t) \in \mathbb{R}^p$	is the performance output signal
$e(t) \in \mathbb{R}^r$	is the uncertainty output signal

Furthermore, we define the order of the closed-loop system to be  $\tilde{n} \triangleq n + n_c$ , where

$n$  is the order of the plant and  $n_c$  is the order of the compensator. We also define the following closed-loop matrices:

$$\tilde{x}(t) \triangleq \begin{bmatrix} x(t) \\ x_c(t) \end{bmatrix}, \quad \tilde{A} \triangleq \begin{bmatrix} A & BC_c \\ B_c C & A_c + B_c DC_c \end{bmatrix}, \quad \tilde{B}_0 \triangleq \begin{bmatrix} B_0 \\ B_c F_1 \end{bmatrix}, \quad \tilde{D} \triangleq \begin{bmatrix} D_1 \\ B_c D_2 \end{bmatrix},$$

$$\tilde{C}_0 \triangleq [ C_0 \quad F_2 C_c ], \quad \tilde{E} \triangleq [ E_1 \quad E_2 C_c ].$$

Finally, we define

$$\tilde{R} \triangleq \tilde{E}^T \tilde{E} = \begin{bmatrix} R_1 & 0 \\ 0 & C_c^T R_2 C_c \end{bmatrix},$$

where  $R_1 \triangleq E_1^T E_1$ ,  $R_2 \triangleq E_2^T E_2$ , and  $R_{12} \triangleq E_1^T E_2 = 0$ , and

$$\tilde{V} \triangleq \tilde{E}^T \tilde{E} = \begin{bmatrix} V_1 & 0 \\ 0 & B_c V_2 B_c^T \end{bmatrix},$$

where  $V_1 \triangleq D_1 D_1^T$ ,  $V_2 \triangleq D_2 D_2^T$ , and  $V_{12} \triangleq D_1 D_2^T = 0$ .

# Summary

The ability to develop an integrated control system design methodology for robust high performance controllers satisfying multiple design criteria and real world hardware constraints constitutes a challenging task. The increasingly stringent performance specifications required for controlling such systems necessitates a trade-off between controller complexity and robustness. The principle challenge of the minimal complexity robust control design is to arrive at a tractable control design formulation in spite of the extreme complexity of such systems. Hence, design of minimal complexity robust controllers for systems in the face of modeling errors has been a major preoccupation of system and control theorists and practitioners for the past several decades.

Although the theory for designing linear output feedback controllers is quite mature, the actual solution of the design equations can be a daunting task. This becomes even more difficult if an optimal reduced-order controller is sought. In this dissertation, we develop a general fixed-structure control design framework that addresses the following paradigm: Reduce control law complexity subject to the achievement of a specified accuracy in the face of a specified level of uncertainty.

The control law complexity is reduced by developing a decentralized static output feedback formulation for fixed-structure controller synthesis. The decentralized static output feedback formulation captures a large class of controller architectures within a common framework and allows a common numerical algorithm to be used

for computational purposes.

We first discuss this decentralized static output feedback framework and demonstrate its applicability on the space-based ACTEX control testbed. Since the strict architecture constraints of the ACTEX flight experiment preclude standard LQG and  $\mathcal{H}_\infty$  techniques, we show that the decentralized static output feedback formulation for fixed-structure controller synthesis can directly account for the controller architecture constraints and improve closed-loop performance by designing fixed-structure  $\mathcal{H}_2$ -optimal controllers.

The next problem we consider is fixed-structure stable  $\mathcal{H}_2$ -optimal controller synthesis using a multiobjective optimization technique. The problem is presented in the decentralized static output feedback framework developed for fixed-structure dynamic controller synthesis. A quasi-Newton/continuation algorithm is used to compute solutions to the necessary conditions. To demonstrate the approach, two numerical examples are considered. The first example is a second-order spring-mass-damper system and the second example is a fourth-order two-mass system, both of which are considered in the stable stabilization literature. The results are then compared with other methods of stable compensator synthesis.

Next we use a similar approach to consider fixed-structure  $\mathcal{H}_2$ -optimal relative degree two controller synthesis. By considering dynamic controllers structured to appear as the augmentation of two strictly proper dynamic controllers in series, the relative degree condition is guaranteed. Three examples are presented to demonstrate the effectiveness of this design technique.

We then explore the applicability of the implicit small gain guaranteed cost bound for controller synthesis. For flexibility in controller synthesis, we adopt the approach of fixed-structure controller design which allows consideration of arbitrary controller structures, including order, internal structure, and decentralization. Two numerical

examples that have been addressed by means of alternative guaranteed cost bounds are presented to demonstrate the fixed-structure/implicit small gain approach to robust controller synthesis.

One of the fundamental problems in feedback control design is the ability of the control system to maintain stability and performance in the face of system uncertainties. To this end, elegant multivariable robust control design frameworks such as  $\mathcal{H}_\infty$  control,  $\mathcal{L}_1$  control, and  $\mu$ -synthesis have been developed to address the robust stability and performance control problem. An implicit assumption inherent in these design frameworks is that the controller will be implemented exactly. In a recent paper by Keel and Bhattacharyya, it was shown that even though such frameworks are robust with respect to system uncertainty, they are extremely sensitive, or *fragile*, with respect to errors in the controller coefficients. Here we extend the robust fixed-structure controller synthesis approach to develop controllers which are robust to system uncertainties and non-fragile, or *resilient*, to controller gain variations.

Next, we develop linear, fixed-order pressure rise feedback dynamic compensators for axial flow compressors. Unlike the nonlinear static controllers proposed in the literature possessing gain at all frequencies, the proposed dynamic compensators explicitly account for compressor performance versus sensor accuracy, compressor performance versus processor throughput, and compressor performance versus disturbance rejection. Furthermore, the proposed controller is predicated on *only* pressure rise measurements, providing a considerable simplification in the sensing architecture over the bifurcation-based and backstepping controllers proposed in the literature.

Finally, we use a unifying absolute stability result for mixed uncertainty to obtain fixed-structure controllers and fixed-order stability multipliers which provide robust stability and performance. The robust controller synthesis technique proposed here permits the treatment of fully populated real uncertain blocks which may, in addition,

possess internal structure. The ability to address real uncertain blocks is based on the use of an appropriate class of multipliers whose structure is compatible with the real block uncertainty. Hence, tailoring the multipliers to the structure of the uncertainty not only leads to the ability to address more general uncertainty characterizations but can also lead to less conservative controllers than obtained from standard mixed- $\mu$  synthesis.





# CHAPTER 1

## Introduction

### 1.1. Robust Fixed-Structure Control Design: Motivation and Overview

The growing complexity of dynamic systems results in unavoidable discrepancies between real physical systems and the mathematical models used to describe them. These *uncertainties*, in turn, result in severe degradation of control system *performance*. Thus, one of the main objectives of feedback control system theory is to design controllers that are *robust* with respect to system uncertainties as well as guarantee specific performance objectives. The problem of robust control design constitutes a significant challenge in mathematical system theory which, at the same time, addresses a fundamental issue in the *practical* implementation of feedback control systems, namely, modeling uncertainty. Modeling uncertainty must be characterized and quantified so that it can be accounted for within the control design process. For example, the dynamics of large flexible space structures are highly nonlinear (due to geometric and material nonlinearities) but are commonly approximated by linear models. Furthermore, since flexible structures are inherently infinite dimensional systems, any finite dimensional approximation model will exhibit significant error, particularly as the modal frequency increases.

These uncertainties arising due to inexact modeling are referred to as *plant uncertainties* and are broadly classified into *parametric* and *nonparametric* uncertainties. Parametric uncertainty here describes errors that can be translated into uncertainty in the physical elements of some time-invariant state-space representation of the design model (i.e., perturbations or uncertainties in specific parameters of the physical system). On the other hand, nonparametric uncertainty is best viewed in the frequency domain and describes errors that have bounded gain but arbitrary phase (e.g., uncertainties due to unmodeled system dynamics or system linearization). The distinction of parametric versus nonparametric uncertainty in the plant model is of paramount importance in robust control design. For example, in the problem of vibration control of flexible space structures, if the stiffness matrix uncertainty is modeled as nonparametric uncertainty, then perturbations to the damping matrix will inadvertently be allowed. Consequently, stability and performance predictions for a given compensator will be extremely conservative, which limits achievable performance.

Hence, robust control theory mainly deals with two issues; namely, the qualitative issue of *robust stability* and the quantitative issue of *robust performance*. Robust stability addresses the stability of a given system in the face of uncertainties while robust performance addresses performance degradation due to system uncertainties over the region of robust stability. Often *worst case* performance of the system in the face of all possible uncertainties is addressed as a measure of robust performance.

Modern multivariable feedback control theory and application has been one of the most rapidly growing areas in the scientific and engineering communities for the past several decades. Some of the most fundamental advances in this field can be traced back to World War II. During the post-World War II era, the emergent superpowers turned their research focus to aerospace technology in order to compete in the race to space. One of the central achievements of this research effort was the development of

state-space based methods introduced in the West by R. E. Kalman in the 1960's [71, 72] which led to the Kalman filter [68, 73]. Another pivotal achievement of the early 1960's was the development of the Linear Quadratic Regulator (LQR) [4, 67, 80, 101] which, when combined with the Kalman filter, led to the formulation of the Linear Quadratic Gaussian (LQG) controller design methodology [4, 6, 67, 80, 107]. These revolutionary breakthroughs in optimal navigation and control led to the successful launch of the Apollo mission which resulted in the first manned moon landing on July 20, 1969.

One of the most attractive features of the LQG controller design methodology is the characterization of the optimal compensator gains via a system of two decoupled Riccati equations. A number of commercially available computational tools offer efficient solutions to standard Riccati equations. Unfortunately, however, the dimension of an LQG controller is always equal to the dimension of the design plant. Since on-board processors have limited throughput and uncertainty is always present in the system, this necessitates robust minimal complexity controllers which further renders LQG controllers impractical for many applications. This has motivated the study of optimal fixed-order controllers. Balanced truncation techniques [124] were used to reduce the order of the plant or the designed full-order controller, however these reduced-order controllers could not even guarantee closed-loop stability, let alone performance. Another approach, developed to *directly* synthesize fixed-order controllers, is the fixed-structure control framework developed in [62, 63]. In this approach, the compensator structure is fixed *a priori* and the optimization is performed over the compensator parameters. The application of fixed-structure control theory to the fixed-order controller design problem yields a characterization of the optimal fixed-order controllers via a set of coupled Riccati and Lyapunov equations, each containing a projection matrix which motivated the name "optimal projection

equations" in [62, 63].

At the same time as the development of the LQG controller, the work on absolute stability theory which forms the basis of modern robust control theory was being pioneered by the Romanian mathematician V. M. Popov [102]. Absolute stability theory addresses the stability of feedback systems whose forward path contains a dynamic linear time-invariant system and whose feedback path contains a memoryless (possibly time-varying) nonlinearity (uncertainty). These stability criteria are generally stated in terms of the linear system and apply to every element of a specified class of nonlinearities. Research efforts in this direction were vigorously pursued in the former Soviet Union by V. A. Yakubovich [116–120] and Y. Z. Tsypkin [109]. In the United States, progress along the same direction was made by R. E. Kalman [69], E. I. Jury [65, 66], R. W. Brockett [19, 20], J. L. Willems [20], and K. S. Narendra [91–94]. The significant progress made towards resolving the absolute stability problem is now well documented in research monographs, such as Aizerman and Gantmacher [1], Lefschetz [82], and Popov [103]. A more modern treatment of the subject is given by Safonov [104] while excellent book treatments are presented in Narendra and Taylor [94] and Vidyasagar [111].

Since all real-world systems exhibit nonlinear behavior and possess numerous uncertainties (due to such phenomena as exogenous disturbances, noise, mathematical modeling errors, unmodeled nonlinear dynamics, unmodeled high frequency dynamics, and unmodeled actuator and sensor dynamics), a viable controller synthesis methodology must be able to account for system nonlinearities and uncertainties. The problem of accurately controlling system performance variables whose dynamics contain significant nonlinearities and uncertainties poses a challenging problem in control system design. The critical issues of system uncertainty can be traced back to H. S. Black's 1927 patent where large loop gains were proposed for addressing

the problem of uncertainty [17, 28]. In classical single-input, single-output control design techniques based on the Nyquist criterion and Bode gain and phase plots, the question of robustness to system uncertainty was addressed by requiring that the overall closed-loop system possess prespecified *relative* stability margins, i.e., gain and phase margins. The issue of parametric plant uncertainty, however, was largely neglected. Even though, as demonstrated by Kalman [70], optimal linear quadratic state-feedback regulators possess guaranteed robustness properties, i.e.,  $\infty$  dB upward and 6 dB downward gain margins and  $\pm 60^\circ$  phase margin, these robustness properties are misleading since the guaranteed gain and phase margins are valid only for uncertainty at the system input. Furthermore, it was shown in [55] that the robustness properties of LQR designs could diminish with increasing parametric system uncertainty. Finally, these robustness guarantees are nonexistent in observer-based LQG controllers [4, 29].

In the late 1970's and early 1980's, a renewed research interest emerged in addressing plant uncertainty which led to an accelerated progress in the field of robust control (see [28] for a representative collection of papers on this topic). A main motivation for this growing research effort appears to be the ever increasing complexity of the modern systems within the engineering field (such as large flexible structures, advanced tactical fighter aircraft, and variable-cycle gas turbine engines, to name a few), as well as complex economic and biological systems. Thus the predominant considerations in control law design for modern engineering systems have become control law complexity and control law robustness, respectively. Indeed, with increasing system complexity comes increasing (and usually overriding concern with) system cost, reliability, and maintainability, whereas with increasing accuracy requirements come increasingly complex control systems. Since, generally speaking, the more complex the control system, the more it costs, the less reliable it is, and the harder it is

to maintain, it follows that high accuracy requirements conflict with control system complexity requirements in highly complex systems. In fact, they are also in conflict with each other through the specification of control law robustness. In an attempt to capture robustness guarantees within observer based designs, Doyle and Stein [32,33] proposed a two-stage analysis/synthesis recovery framework that led to the LQG/LTR methodology [108] yielding dynamic compensators with recovered LQR-type margins. However, the LQG/LTR methodology is limited to the recovery of LQR margins and employs high-gain feedback. In addition, this design framework is not applicable to plants with non-minimum phase zeros and involves inversion of the plant which leads to controllers which are extremely sensitive to parametric uncertainty.

One approach to controller synthesis in the presence of unstructured uncertainty is the well known  $\mathcal{H}_\infty$  methodology. Several authors have shown that the  $\mathcal{H}_\infty$  problem can be solved via a pair of modified Riccati equations [11, 31, 45, 99]. However, as is also well known, this methodology is highly conservative for parametric uncertainty. Using a Lyapunov bounding framework, the authors in [12, 13, 88] addressed the problem of robust analysis and synthesis in the face of parametric uncertainty. Several bounding functions were considered in [12], while [10] extended the quadratic bounding technique of [100] to robust fixed-order controller synthesis. Alternative approaches to robust stability and performance in the presence of parametric uncertainty are discussed in [28, 77, 100]. However, a major drawback of the conventional Lyapunov bounding techniques [48] is their inability to restrict time-variation of the parametric perturbations. In a recent series of papers [46, 48–50, 52], a refined Lyapunov function technique was developed to overcome some of the current limitations of Lyapunov function theory for the problem of robust stability and performance in the presence of constant real parameter uncertainty. The authors in [46, 48–50, 52] extend the rich theory of absolute stability to develop parameter-dependent Lyapunov

functions that guarantee robust stability and performance in the presence of constant real parametric uncertainty. Finally, using frequency domain stability criteria, the authors in [57, 61] demonstrate that the seemingly remote modern robust stability and performance tools based on the structured singular value [30, 123] can be directly connected to absolute stability theory via selection of stability multipliers for various classes of nonlinearities. Hence, [46, 48–50, 52, 57] provide an alternative approach to mixed- $\mu$  synthesis [122], while avoiding the standard  $D$ ,  $N$ - $K$  iteration and curve fitting procedure.

Prior experience with the state-space techniques and the LQG controllers prompted many researchers to seek state-space-based robust controller synthesis methods that essentially try to mimic the solution features of the LQG controller, i.e., controller gains based on solutions to modified Riccati equations. Recent advances along these lines are given in [10, 11, 13, 31, 45, 46, 52, 57, 76, 88, 99, 100]. Furthermore, the optimal projection equation approach of Hyland and Bernstein [62, 63] has been extended to the problem of robust controller synthesis in the presence of unstructured system uncertainty [11, 45, 88], arbitrary time-varying parameter uncertainty [10, 12, 13, 88], and constant real parameter uncertainty [46, 48–50, 52, 57] via the quadratic Lyapunov bounding framework developed in [44].

## 1.2. Brief Outline of the Report

In this research, we will build on the results of [14, 95] in several directions. In Chapter 2, we formulate the decentralized static output feedback problem for fixed-structure controller synthesis. This formulation captures a large class of controller architectures within a common framework and allows a common numerical algorithm to be used for computational purposes. This framework will provide the basis for

much of the subsequent controller synthesis, such as the stable  $\mathcal{H}_2$ -optimal controller synthesis discussed in Chapter 3. In this chapter, a multiobjective optimization technique is used to optimize the  $\mathcal{H}_2$  cost of the closed-loop system while maintaining controller stability. The decentralized static output feedback framework is also exploited in Chapter 4 when we consider  $\mathcal{H}_2$ -optimal relative degree two controller synthesis.

Next, in Chapter 5, we consider the applicability of the implicit small gain guaranteed cost bound for controller synthesis. In Chapter 6, the decentralized static output feedback framework is used to develop controllers with the ability to maintain control system stability and performance in the face of system uncertainties, which could even include variations in the controller gains. Then, in Chapter 7, we use the fixed-architecture control methodology to develop linear, fixed-order pressure rise feedback dynamic compensators for axial flow compressors. Unlike the nonlinear static controllers proposed in the literature possessing gain at all frequencies, the proposed dynamic compensators explicitly account for compressor performance and is predicated on *only* pressure rise measurements, providing a considerable simplification in the sensing architecture over the bifurcation-based and backstepping controllers proposed in the literature.

Finally, in Chapter 8, we use a unifying absolute stability result for mixed uncertainty to obtain fixed-structure controllers and fixed-order stability multipliers which provide robust stability and performance. The robust controller synthesis technique proposed here permits the treatment of fully populated real uncertain blocks which may, in addition, possess internal structure. The ability to address real uncertain blocks is based on the use of an appropriate class of multipliers whose structure is compatible with the real block uncertainty. Hence, tailoring the multipliers to the structure of the uncertainty not only leads to the ability to address more general

uncertainty characterizations but can also lead to less conservative controllers than obtained from the standard mixed- $\mu$  synthesis techniques.

Finally, in Chapter 9, conclusions and recommendations for future research are discussed.



# CHAPTER 2

## Fixed-Structure Control Framework

### 2.1. Introduction

This chapter reviews the decentralized static output feedback problem formulation for fixed-structure controller synthesis. As shown in [14, 95], the decentralized static output feedback format captures a large class of controller architectures within a common framework and allows a common numerical algorithm to be used for computational purposes.

Consider the  $(m + q + 1)$ -vector-input,  $(m + q + 1)$ -vector-output decentralized system shown in Figure 2.1, where  $w$  is the exogenous disturbance input,  $z$  is the performance variable, the signals  $y_i$  and  $u_i$ ,  $i = 1, \dots, m$ , are measurement and control signals, respectively, and  $e_i$  and  $d_i$ ,  $i = 1, \dots, q$ , are used to account for model uncertainty. The decentralized static output feedback multi vector-input, multi vector-output system shown in Figure 2.1 is characterized by the dynamics

$$\dot{\tilde{x}}(t) = \mathcal{A}\tilde{x}(t) + \sum_{j=1}^m \mathcal{B}_{u_j} u_j(t) + \sum_{k=1}^q \mathcal{B}_{d_k} d_k(t) + \mathcal{B}_w w(t), \quad t \in [0, \infty), \quad (2.1)$$

$$y_i(t) = \mathcal{C}_{y_i} \tilde{x}(t) + \sum_{j=1}^m \mathcal{D}_{y u_{ij}} u_j(t) + \sum_{k=1}^q \mathcal{D}_{y d_{ik}} d_k(t) + \mathcal{D}_{y w_i} w(t), \quad i = 1, 2, \dots, m, \quad (2.2)$$

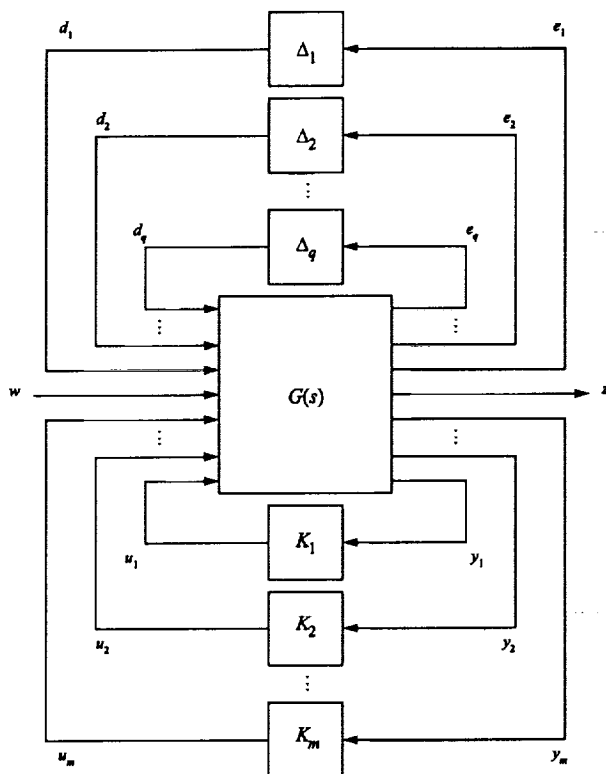


**Figure 2.1:** Decentralized Static Output Feedback Framework

$$e_i(t) = C_{e_i} \tilde{x}(t) + \sum_{j=1}^m \mathcal{D}_{eu_{ij}} u_j(t) + \sum_{k=1}^q \mathcal{D}_{ed_{ik}} d_k(t) + \mathcal{D}_{ew_i} w(t), \quad i = 1, 2, \dots, q, \quad (2.3)$$

$$z(t) = C_z \tilde{x}(t) + \sum_{j=1}^m \mathcal{D}_{zu_j} u_j(t) + \sum_{k=1}^q \mathcal{D}_{zd_k} d_k(t) + \mathcal{D}_{zw} w(t). \quad (2.4)$$

In the above formulation, model uncertainty is represented by the decentralized static output feedback map

$$d_i(t) = \Delta_i e_i(t), \quad i = 1, \dots, q, \quad (2.5)$$

where the uncertain matrices  $\Delta_i$  are not necessarily distinct. To represent decentralized static output feedback control with possibly repeated gains, we consider

$$u_i(t) = \mathcal{K}_i y_i(t), \quad i = 1, \dots, m, \quad (2.6)$$

where the matrices  $\mathcal{K}_i$  are not necessarily distinct. Reordering the variables in (2.5)

and (2.6) if necessary and defining

$$\hat{u}(t) = \begin{bmatrix} u_1(t) \\ \vdots \\ u_m(t) \end{bmatrix}, \quad \hat{y}(t) = \begin{bmatrix} y_1(t) \\ \vdots \\ y_m(t) \end{bmatrix}, \quad \hat{d}(t) = \begin{bmatrix} d_1(t) \\ \vdots \\ d_q(t) \end{bmatrix}, \quad \hat{e}(t) = \begin{bmatrix} e_1(t) \\ \vdots \\ e_q(t) \end{bmatrix}, \quad (2.7)$$

$$\mathcal{B}_u \triangleq [\mathcal{B}_{u_1} \ \cdots \ \mathcal{B}_{u_m}], \quad \mathcal{B}_d \triangleq [\mathcal{B}_{d_1} \ \cdots \ \mathcal{B}_{d_q}], \quad \mathcal{D}_{zu} \triangleq [\mathcal{D}_{zu_1} \ \cdots \ \mathcal{D}_{zu_m}], \quad (2.8)$$

$$\mathcal{C}_y \triangleq \begin{bmatrix} \mathcal{C}_{y_1} \\ \vdots \\ \mathcal{C}_{y_m} \end{bmatrix}, \quad \mathcal{D}_{yu} \triangleq \begin{bmatrix} \mathcal{D}_{yu_{11}} & \cdots & \mathcal{D}_{yu_{1m}} \\ \vdots & \ddots & \vdots \\ \mathcal{D}_{yu_{m1}} & \cdots & \mathcal{D}_{yu_{mm}} \end{bmatrix}, \quad \mathcal{D}_{yd} \triangleq \begin{bmatrix} \mathcal{D}_{yd_{11}} & \cdots & \mathcal{D}_{yd_{1q}} \\ \vdots & \ddots & \vdots \\ \mathcal{D}_{yd_{m1}} & \cdots & \mathcal{D}_{yd_{mq}} \end{bmatrix}, \quad (2.9)$$

$$\mathcal{C}_e \triangleq \begin{bmatrix} \mathcal{C}_{e_1} \\ \vdots \\ \mathcal{C}_{e_q} \end{bmatrix}, \quad \mathcal{D}_{eu} \triangleq \begin{bmatrix} \mathcal{D}_{eu_{11}} & \cdots & \mathcal{D}_{eu_{1m}} \\ \vdots & \ddots & \vdots \\ \mathcal{D}_{eu_{q1}} & \cdots & \mathcal{D}_{eu_{qm}} \end{bmatrix}, \quad \mathcal{D}_{ed} \triangleq \begin{bmatrix} \mathcal{D}_{ed_{11}} & \cdots & \mathcal{D}_{ed_{1q}} \\ \vdots & \ddots & \vdots \\ \mathcal{D}_{ed_{q1}} & \cdots & \mathcal{D}_{ed_{qq}} \end{bmatrix}, \quad (2.10)$$

$$\mathcal{D}_{zd} \triangleq [\mathcal{D}_{zd_1} \ \cdots \ \mathcal{D}_{zd_q}], \quad \mathcal{D}_{yw} \triangleq \begin{bmatrix} \mathcal{D}_{yw_1} \\ \vdots \\ \mathcal{D}_{yw_m} \end{bmatrix}, \quad \mathcal{D}_{ew} \triangleq \begin{bmatrix} \mathcal{D}_{ew_1} \\ \vdots \\ \mathcal{D}_{ew_q} \end{bmatrix}, \quad (2.11)$$

(2.5) and (2.6) can be rewritten

$$\hat{d}(t) = \Delta \hat{e}(t), \quad (2.12)$$

$$\hat{u}(t) = \mathcal{K} \hat{y}(t), \quad (2.13)$$

where  $\Delta$  and  $\mathcal{K}$  have the form

$$\Delta \triangleq \text{block-diag} [I_{\psi_1} \otimes \Delta_1, \dots, I_{\psi_v} \otimes \Delta_v], \quad (2.14)$$

$$\mathcal{K} \triangleq \text{block-diag} [I_{\phi_1} \otimes \mathcal{K}_1, \dots, I_{\phi_g} \otimes \mathcal{K}_g], \quad (2.15)$$

where  $v$  is the number of *distinct* uncertainties  $\Delta_i \in \mathbb{C}^{p_i \times f_i}$  or  $\mathbb{R}^{p_i \times f_i}$ ,  $\psi_i$  is the number of repetitions of uncertainty  $\Delta_i$ ,  $g$  is the number of *distinct* gains  $\mathcal{K}_i \in \mathbb{R}^{r_i \times c_i}$  and  $\phi_i$  is the number of repetitions of gain  $\mathcal{K}_i$ . Note that  $\mathcal{K}_1, \dots, \mathcal{K}_g$  are not necessarily square matrices, and  $\sum_{i=1}^v \psi_i = q$  and  $\sum_{i=1}^g \phi_i = m$ . Furthermore, define the matrices

$Q_{Lij}$  and  $Q_{Rij}$  to be

$$Q_{Lij} \triangleq \begin{bmatrix} 0_{r_1 \phi_1 \times r_i} \\ 0_{r_2 \phi_2 \times r_i} \\ \vdots \\ 0_{r_{i-1} \phi_{i-1} \times r_i} \\ 0_{r_i(j-1) \times r_i} \\ I_{r_i} \\ 0_{r_i(\phi_i-j) \times r_i} \\ 0_{r_{i+1} \phi_{i+1} \times r_i} \\ \vdots \\ 0_{r_v \phi_v \times r_i} \end{bmatrix}, \quad Q_{Rij} \triangleq \begin{bmatrix} 0_{c_1 \phi_1 \times c_i} \\ 0_{c_2 \phi_2 \times c_i} \\ \vdots \\ 0_{c_{i-1} \phi_{i-1} \times c_i} \\ 0_{c_i(j-1) \times c_i} \\ I_{c_i} \\ 0_{c_i(\phi_i-j) \times c_i} \\ 0_{c_{i+1} \phi_{i+1} \times c_i} \\ \vdots \\ 0_{c_v \phi_v \times c_i} \end{bmatrix}^T, \quad (2.16)$$

where  $i = 1, \dots, v$ , and  $j = 1, \dots, \phi_i$ .

With the definitions in (2.7)–(2.11), the transfer function  $G(s)$  from  $[\hat{u}^T, \hat{d}^T, w^T]^T$  to  $[\hat{y}^T, \hat{e}^T, z^T]^T$  of the decentralized system has the realization

$$G(s) \sim \left[ \begin{array}{c|ccc} \mathcal{A} & \mathcal{B}_u & \mathcal{B}_d & \mathcal{B}_w \\ \hline \mathcal{C}_y & \mathcal{D}_{yu} & \mathcal{D}_{yd} & \mathcal{D}_{yw} \\ \mathcal{C}_e & \mathcal{D}_{eu} & \mathcal{D}_{ed} & \mathcal{D}_{ew} \\ \mathcal{C}_z & \mathcal{D}_{zu} & \mathcal{D}_{zd} & \mathcal{D}_{zw} \end{array} \right], \quad (2.17)$$

which represents the linear, time-invariant dynamic system

$$\dot{\tilde{x}}(t) = \mathcal{A}\tilde{x}(t) + \mathcal{B}_u\hat{u}(t) + \mathcal{B}_d\hat{d}(t) + \mathcal{B}_w w(t), \quad t \in [0, \infty), \quad (2.18)$$

$$\hat{y}(t) = \mathcal{C}_y\tilde{x}(t) + \mathcal{D}_{yu}\hat{u}(t) + \mathcal{D}_{yd}\hat{d}(t) + \mathcal{D}_{yw}w(t), \quad (2.19)$$

$$\hat{e}(t) = \mathcal{C}_e\tilde{x}(t) + \mathcal{D}_{eu}\hat{u}(t) + \mathcal{D}_{ed}\hat{d}(t) + \mathcal{D}_{ew}w(t), \quad (2.20)$$

$$z(t) = \mathcal{C}_z\tilde{x}(t) + \mathcal{D}_{zu}\hat{u}(t) + \mathcal{D}_{zd}\hat{d}(t) + \mathcal{D}_{zw}w(t), \quad (2.21)$$

which is equivalent to (2.1)–(2.4). Furthermore, by rewriting the decentralized control signals (2.6) in the compact form given by (2.13), the closed-loop system realization from  $[\hat{d}^T, w^T]^T$  to  $[\hat{e}^T, z^T]^T$  is given by

$$\tilde{G}(s) \sim \left[ \begin{array}{c|cc} \tilde{A} & \tilde{B}_0 & \tilde{D} \\ \hline \tilde{C}_0 & \tilde{D}_0 & \tilde{D}_1 \\ \tilde{E} & \tilde{E}_1 & \tilde{E}_0 \end{array} \right], \quad (2.22)$$

where

$$\begin{aligned}\tilde{A} &\triangleq \mathcal{A} + \mathcal{B}_u \mathcal{K} L_{\mathcal{K}}^{-1} \mathcal{C}_y, & \tilde{B}_0 &\triangleq \mathcal{B}_d + \mathcal{B}_u \mathcal{K} L_{\mathcal{K}}^{-1} \mathcal{D}_{yd}, & \tilde{D} &\triangleq \mathcal{B}_w + \mathcal{B}_u \mathcal{K} L_{\mathcal{K}}^{-1} \mathcal{D}_{yw}, \\ \tilde{C}_0 &\triangleq \mathcal{C}_e + \mathcal{D}_{eu} \mathcal{K} L_{\mathcal{K}}^{-1} \mathcal{C}_y, & \tilde{D}_0 &\triangleq \mathcal{D}_{ed} + \mathcal{D}_{eu} \mathcal{K} L_{\mathcal{K}}^{-1} \mathcal{D}_{yd}, & \tilde{D}_1 &\triangleq \mathcal{D}_{ew} + \mathcal{D}_{eu} \mathcal{K} L_{\mathcal{K}}^{-1} \mathcal{D}_{yw}, \\ \tilde{E} &\triangleq \mathcal{C}_z + \mathcal{D}_{zu} \mathcal{K} L_{\mathcal{K}}^{-1} \mathcal{C}_y, & \tilde{E}_1 &\triangleq \mathcal{D}_{zd} + \mathcal{D}_{zu} \mathcal{K} L_{\mathcal{K}}^{-1} \mathcal{D}_{yd}, & \tilde{E}_0 &\triangleq \mathcal{D}_{zw} + \mathcal{D}_{zu} \mathcal{K} L_{\mathcal{K}}^{-1} \mathcal{D}_{yw},\end{aligned}$$

and where  $L_{\mathcal{K}} \triangleq I - \mathcal{D}_{yu} \mathcal{K}$ . Note that we assume  $\det(L_{\mathcal{K}}) \neq 0$  for all  $\mathcal{K}$  given by (2.15) to ensure the well-posedness of the feedback interconnection.

## 2.2. Performance Constraints

The decentralized static output feedback framework can be used to help synthesize controllers that are optimal with respect to user-chosen performance criteria. A performance criterion consists of a cost function and one or more constraints. The cost function represents some characteristic of the controlled system which a desirable controller will minimize, while the constraints represent properties that an acceptable controller must have. An example of a cost function is an induced norm of the closed-loop transfer function, while examples of constraints include asymptotic stability of the nominal closed-loop system or robust stability with respect to uncertainties of a certain size and/or structure.

As an example, consider the  $\mathcal{H}_2$ -optimal centralized strictly proper dynamic control (Linear Quadratic Gaussian) problem. Here we will consider the  $n^{\text{th}}$ -order stabilizable and detectable plant with noisy measurements, uncertainty signals, and performance variables given by

$$\dot{x}(t) = Ax(t) + Bu(t) + B_0d(t) + D_1w(t), \quad t \in [0, \infty), \quad (2.23)$$

$$y(t) = Cx(t) + Du(t) + F_1d(t) + D_2w(t), \quad (2.24)$$

$$e(t) = C_0x(t) + F_2u(t), \quad (2.25)$$

$$z(t) = E_1 x(t) + E_2 u(t). \quad (2.26)$$

To recast this system into the decentralized static output feedback format, we first define the decentralized control signals to be

$$u_1(t) = A_c y_1(t), \quad u_2(t) = B_c y_2(t), \quad u_3(t) = C_c y_3(t). \quad (2.27)$$

Note that we can also write the control signals (2.27) in the compact form given by (2.13), where, for the centralized strictly proper dynamic control problem,  $\mathcal{K}$  takes the form

$$\mathcal{K} \triangleq \begin{bmatrix} A_c & 0 & 0 \\ 0 & B_c & 0 \\ 0 & 0 & C_c \end{bmatrix}. \quad (2.28)$$

Further note that  $Q_{Lij}$  and  $Q_{Rij}$  are given by

$$Q_{L11} = \begin{bmatrix} I_{n_c} \\ 0_{n_c \times n_c} \\ 0_{m \times n_c} \end{bmatrix}, \quad Q_{L21} = \begin{bmatrix} 0_{n_c \times n_c} \\ I_{n_c} \\ 0_{m \times n_c} \end{bmatrix}, \quad Q_{L31} = \begin{bmatrix} 0_{n_c \times m} \\ 0_{n_c \times m} \\ I_m \end{bmatrix},$$

$$Q_{R11} = [I_{n_c} \quad 0_{n_c \times l} \quad 0_{n_c \times n_c}], \quad Q_{R21} = [0_{l \times n_c} \quad I_l \quad 0_{l \times n_c}], \quad Q_{R31} = [0_{n_c} \quad 0_{n_c \times l} \quad I_{n_c}].$$

With these definitions, the closed-loop system is given by

$$\begin{aligned} \dot{\tilde{x}}(t) &= \mathcal{A} \tilde{x}(t) + \sum_{i=1}^3 \mathcal{B}_{u_i} u_i(t) + \mathcal{B}_w w(t), \quad t \in [0, \infty), \\ y_i(t) &= \mathcal{C}_{y_i} \tilde{x}(t) + \sum_{j=1}^3 \mathcal{D}_{y_{u_{ij}}} u_j(t) + \mathcal{D}_{y_w} w(t), \quad i = 1, 2, 3, \\ z(t) &= \mathcal{C}_z \tilde{x}(t) + \sum_{i=1}^3 \mathcal{D}_{z u_i} u_i(t), \end{aligned}$$

where

$$\mathcal{A} = \begin{bmatrix} A & 0 \\ 0 & 0 \end{bmatrix}, \quad \mathcal{B}_{u_1} = \begin{bmatrix} 0 \\ I \end{bmatrix}, \quad \mathcal{B}_{u_2} = \begin{bmatrix} 0 \\ I \end{bmatrix}, \quad \mathcal{B}_{u_3} = \begin{bmatrix} B \\ 0 \end{bmatrix}, \quad \mathcal{B}_w = \begin{bmatrix} D_1 \\ 0 \end{bmatrix},$$

$$\mathcal{C}_{y_1} = [0 \quad I], \quad \mathcal{C}_{y_2} = [C \quad 0], \quad \mathcal{C}_{y_3} = [0 \quad I],$$

$$\mathcal{D}_{y_{u_{11}}} = 0, \quad \mathcal{D}_{y_{u_{12}}} = 0, \quad \mathcal{D}_{y_{u_{13}}} = 0, \quad \mathcal{D}_{y_{u_{21}}} = 0, \quad \mathcal{D}_{y_{u_{22}}} = 0, \quad \mathcal{D}_{y_{u_{23}}} = D,$$

$$\mathcal{D}_{yu_{31}} = 0, \quad \mathcal{D}_{yu_{32}} = 0, \quad \mathcal{D}_{yu_{33}} = 0, \quad \mathcal{D}_{yw_1} = 0, \quad \mathcal{D}_{yw_2} = D_2, \quad \mathcal{D}_{yw_3} = 0,$$

$$C_z = [ E_1 \ 0 ], \quad \mathcal{D}_{zu_1} = 0, \quad \mathcal{D}_{zu_2} = 0, \quad \mathcal{D}_{zu_3} = E_2.$$

The LQG problem can now be defined as

$$\min_{\mathcal{K} \in \mathcal{K}_s} \|\tilde{G}_{zw}(s)\|_2^2, \quad (2.29)$$

where  $\mathcal{K}_s$  is the set of all  $\mathcal{K}$  of the form (2.28) such that  $\tilde{A}$  is stable.

If  $\mathcal{K} \in \mathcal{K}_s$ , then

$$\|\tilde{G}_{zw}(s)\|_2^2 = \text{tr } \tilde{Q}\tilde{R}, \quad (2.30)$$

where  $\tilde{Q}$  is the unique, nonnegative definite solution to the Lyapunov equation

$$0 = \tilde{A}\tilde{Q} + \tilde{Q}\tilde{A}^T + \tilde{V}. \quad (2.31)$$

Necessary conditions for optimality involve a Lagrangian function that accounts for the constraint (2.31). The Lagrangian for the  $\mathcal{H}_2$ -optimal control problem is given by

$$\mathcal{L}(\tilde{P}, \tilde{Q}, A_c, B_c, C_c) = \text{tr } \tilde{Q}\tilde{R} + \text{tr } \tilde{P} [\tilde{A}\tilde{Q} + \tilde{Q}\tilde{A}^T + \tilde{V}], \quad (2.32)$$

where  $\tilde{P} \in \mathbb{N}^{\tilde{n}}$  is a Lagrange multiplier, and the partial derivatives of  $\mathcal{L}(\tilde{P}, \tilde{Q}, A_c, B_c, C_c)$  are given by

$$\frac{\partial \mathcal{L}}{\partial \tilde{P}} = \tilde{A}\tilde{Q} + \tilde{Q}\tilde{A}^T + \tilde{V}, \quad (2.33)$$

$$\frac{\partial \mathcal{L}}{\partial \tilde{Q}} = \tilde{A}^T \tilde{P} + \tilde{P} \tilde{A} + \tilde{R}, \quad (2.34)$$

$$\frac{\partial \mathcal{L}}{\partial \mathcal{K}_i} = 2Q_{L_{ij}}^T \tau \left[ B_u^T \tilde{P} \tilde{Q} C_y^T + B_u^T \tilde{P} \tilde{D} \mathcal{D}_{yw}^T + \mathcal{D}_{zu}^T \tilde{E} \tilde{Q} C_y^T \right] L_{\mathcal{K}}^{-T} Q_{R_{ij}}^T, \quad (2.35)$$

$$i = 1, 2, 3, \quad j = 1,$$

where  $\tau = I + \mathcal{D}_{yu}^T L_{\mathcal{K}}^{-T} \mathcal{K}^T$ .

Finally, although the LQG problem does not account for model uncertainty, for completeness we note that, for centralized strictly proper dynamic control problems

where the model uncertainty for the nominal system matrices  $(A, B, C, D)$  is modeled as

$$\Delta A = B_0 \Delta C_0, \quad \Delta B = B_0 \Delta F_2, \quad \Delta C = F_1 \Delta C_0, \quad \Delta D = F_1 \Delta F_2,$$

the matrices  $\mathcal{B}_d$ ,  $\mathcal{C}_e$ ,  $\mathcal{D}_{eu}$ , and  $\mathcal{D}_{yd}$  have the form

$$\mathcal{B}_d = \begin{bmatrix} B_0 \\ 0 \end{bmatrix}, \quad \mathcal{C}_e = [ C_0 \ 0 ], \quad \mathcal{D}_{eu} = [ 0 \ 0 \ F_2 ], \quad \mathcal{D}_{yd} = \begin{bmatrix} 0 \\ F_1 \\ 0 \end{bmatrix}.$$

### 2.3. Quasi-Newton Gradient Optimization

Once the problem has been posed in terms of the gradients of an associated Lagrangian, a general-purpose BFGS quasi-Newton algorithm is used to solve the non-linear optimization problem. The line-search portions of the algorithm were modified to include a constraint-checking subroutine which decreases the length of the search direction vector until it lies entirely within the allowable set of parameters that yield a stable closed-loop system. This modification ensures that the cost function remains defined at every point in the line-search process. Numerical experience indicates that this subroutine is usually invoked only during the first few iterations of a synthesis problem. For details of the algorithm, see [35].

One requirement of gradient-based optimization algorithms is an initial stabilizing design. Here, this was usually accomplished by using either the LQG controller for full-order designs or a balanced truncation of the LQG controller to obtain a reduced-order design.

## 2.4. Structural Dynamics Modeling of the ACTEX Flight Experiment

To demonstrate the applicability of the decentralized static output feedback format for controller design, we present the ACTEX flight experiment. This testbed provides a unique opportunity for users to implement and test controllers on a space-based platform. However, the hardware environment has several features that must be accounted for when specifying control algorithms. First, the feedback control algorithms that can be implemented on ACTEX are fixed gain, and thus adaptive controllers cannot be used. Furthermore, these fixed-gain controllers are analog, which avoids sampling effects. Finally, the implementable analog controllers have a prespecified structure in which only the filter gains and natural frequencies can be modified. Since this constraint does not permit implementation of dynamic compensators of arbitrary structure, standard LQG and  $\mathcal{H}_\infty$  methods cannot be applied.

We thus show that the decentralized static output feedback formulation of fixed-structure controller synthesis can directly account for the control-structure constraints of the ACTEX flight experiment. Specifically, we show that the ACTEX controller structure can be written as a decentralized static output feedback problem. Having done this, we then proceed to apply our techniques to obtain  $\mathcal{H}_2$ -optimal feedback controllers for suppressing broadband disturbances.

The ACTEX flight experiment consists of a plate connected to a satellite by three struts, as shown in Figure 2.2. Each strut is equipped with its own control piezo-actuator as well as a colocated and nearly colocated sensor. A disturbance can be introduced to the experimental package through each of the three control actuators, or through a disturbance actuator on the plate. In addition, each of the three control actuators has an independent decentralized analog controller.

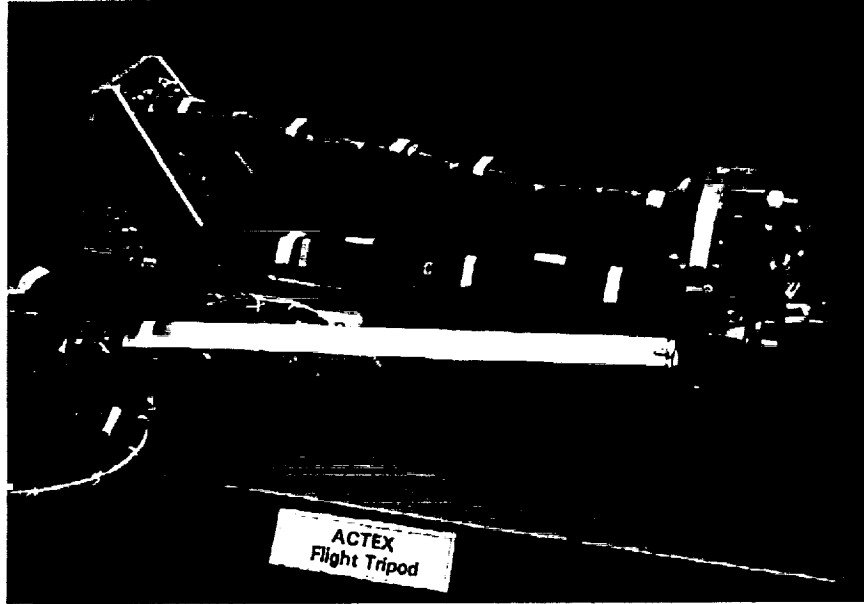


Figure 2.2: ACTEX flight experiment

Several experiments have been run on the ACTEX package, with telemetry returned for identification purposes. Measurements were taken from onboard accelerometers, sensor inputs, and actuator outputs, sampled at 4 kHz. Using this data, identification was performed on the plant from the strut 1 actuator to the strut 1 nearly-colocated sensor. For frequencies below 200 Hz, these dynamics can be represented by (2.23)–(2.24) where

$$A = \begin{bmatrix} -1.56 & 77.98 & 0 & 0 \\ -77.98 & -1.56 & 0 & 0 \\ 0 & 0 & -0.25 & 24.99 \\ 0 & 0 & -24.99 & -0.25 \end{bmatrix}, \quad B = \begin{bmatrix} -1.10 \\ -0.21 \\ -0.11 \\ 0.03 \end{bmatrix}, \quad D_1 = \begin{bmatrix} -1.10 & 0 \\ -0.21 & 0 \\ -0.11 & 0 \\ 0.03 & 0 \end{bmatrix},$$

$$C = [ -0.15 \quad 0.70 \quad 1.83 \quad 6.88 ], \quad D = 1, \quad D_2 = [ 0 \quad 0.1 ].$$

Finally, we define the performance signals (2.26) based on the output measurements so that the closed-loop system reduces the vibrations seen by the sensors. Specifically, we have

$$E_1 = \begin{bmatrix} -0.15 & 0.70 & 1.83 & 6.88 \\ 0 & 0 & 0 & 0 \end{bmatrix}, \quad E_2 = \alpha \begin{bmatrix} 0 \\ 1 \end{bmatrix}.$$

## 2.5. Fixed-Structure Synthesis for the ACTEX Flight Experiment

Since continuous-time controllers are implemented on ACTEX, hardware constraints place a limit on the form that the controllers may take. Each of the three struts on ACTEX has a decentralized controller, available in three fourth-order configurations and a sixth-order configuration, as shown below

$$G_{c1}(s) = \frac{k_3\omega_1^2}{s^2 + 0.3\omega_1s + \omega_1^2} + \frac{k_4\omega_2^2}{s^2 + 0.3\omega_2s + \omega_2^2}, \quad (2.36)$$

$$G_{c2}(s) = \frac{k_3\omega_2^2}{s^2 + 0.3\omega_2s + \omega_2^2} \cdot \frac{\omega_1s}{s^2 + 0.3\omega_1s + \omega_1^2}, \quad (2.37)$$

$$G_{c3}(s) = \frac{k_3\omega_2^2}{s^2 + 0.3\omega_2s + \omega_2^2} \cdot \frac{\omega_1^2}{s^2 + 0.3\omega_1s + \omega_1^2}, \quad (2.38)$$

$$G_{c4}(s) = \frac{k_3\omega_3^2}{s^2 + 0.3\omega_3s + \omega_3^2} \cdot \frac{\omega_2}{s^2 + 0.3\omega_2s + \omega_2^2} \cdot \frac{\omega_1s}{s^2 + 0.3\omega_1s + \omega_1^2}, \quad (2.39)$$

where  $\omega_1, \omega_2, \omega_3, k_3,$  and  $k_4$  are subject to the constraints

$$\begin{aligned} 0 &\leq \omega_1, \omega_2, \omega_3 \leq 1024, \\ -16 &\leq k_3 \leq 16, \\ -8 &\leq k_4 \leq 8. \end{aligned} \quad (2.40)$$

Now, we consider the controller associated with strut 1, and express the controller in the decentralized static output feedback framework. Controller configuration 1, given by (2.36), can be expressed in dynamic compensator form as

$$\begin{aligned} A_c &= \begin{bmatrix} 0 & 1 & 0 & 0 \\ -\omega_1^2 & -0.3\omega_1 & 0 & 0 \\ 0 & 0 & 0 & 1 \\ 0 & 0 & -\omega_2^2 & -0.3\omega_2 \end{bmatrix}, & B_c &= \begin{bmatrix} 0 \\ 1 \\ 0 \\ 1 \end{bmatrix}, \\ C_c &= [k_3\omega_1^2 \quad 0 \quad k_4\omega_2^2 \quad 0]. \end{aligned}$$

Controller configurations 2 through 4, given by (2.37)–(2.39), can be expressed similarly and are given in the Appendix.

Having specified the form of the controller, we consider the  $\mathcal{H}_2$  synthesis problem. The  $\mathcal{H}_2$  norm of the closed-loop transfer function  $\tilde{G}_{zw}(s)$  is given by (2.30). In order to design  $\mathcal{H}_2$ -optimal controllers for the ACTEX experiment, we pose the following optimization problem: Determine  $\mathcal{K}$  that minimizes

$$J(\mathcal{K}) = \text{tr } \tilde{Q}\tilde{R}, \quad (2.41)$$

where  $\tilde{Q} \in \mathbb{N}^{\tilde{n}}$  satisfies (2.31). The necessary conditions for optimality can be derived by forming the Lagrangian (2.32). The partial derivatives with respect to  $\tilde{Q}$  and  $\tilde{P}$  in (2.32) are given by (2.33) and (2.34). To obtain the partial derivative of the Lagrangian with respect to the free parameters in the controller gains, we first specify the controller configuration. As an example, we consider controller configuration 1, given by (2.36). The settings for each of the other controller configurations are given in the Appendix.

For controller configuration 1, the block-diagonal matrix  $\mathcal{K}$  has the form (2.28). Note that this controller has four free optimization parameters; namely,  $\omega_1$ ,  $\omega_2$ ,  $k_3$ , and  $k_4$ . Thus, we construct the matrix

$$K = \begin{bmatrix} \omega_1 & 0 & 0 & 0 \\ 0 & \omega_2 & 0 & 0 \\ 0 & 0 & k_3 & 0 \\ 0 & 0 & 0 & k_4 \end{bmatrix},$$

and note that

$$\mathcal{K} = K_0 + L_1KR_1 + L_2KKR_2 + L_3KKM_3KR_3,$$

where

$$K_0 = \begin{bmatrix} 0 & 1 & 0 & 0 & 0 & 0 & 0 & 0 & 0 \\ 0 & 0 & 0 & 0 & 0 & 0 & 0 & 0 & 0 \\ 0 & 0 & 0 & 1 & 0 & 0 & 0 & 0 & 0 \\ 0 & 0 & 0 & 0 & 0 & 0 & 0 & 0 & 0 \\ 0 & 0 & 0 & 0 & 0 & 0 & 0 & 0 & 0 \\ 0 & 0 & 0 & 0 & 1 & 0 & 0 & 0 & 0 \\ 0 & 0 & 0 & 0 & 0 & 0 & 0 & 0 & 0 \\ 0 & 0 & 0 & 0 & 1 & 0 & 0 & 0 & 0 \\ 0 & 0 & 0 & 0 & 0 & 0 & 0 & 0 & 0 \end{bmatrix},$$

$$L_1 = \begin{bmatrix} 0 & 0 & 0 & 0 \\ -0.3 & 0 & 0 & 0 \\ 0 & 0 & 0 & 0 \\ 0 & -0.3 & 0 & 0 \\ 0 & 0 & 0 & 0 \\ 0 & 0 & 0 & 0 \\ 0 & 0 & 0 & 0 \\ 0 & 0 & 0 & 0 \\ 0 & 0 & 0 & 0 \end{bmatrix}, \quad L_2 = \begin{bmatrix} 0 & 0 & 0 & 0 \\ -1 & 0 & 0 & 0 \\ 0 & 0 & 0 & 0 \\ 0 & -1 & 0 & 0 \\ 0 & 0 & 0 & 0 \\ 0 & 0 & 0 & 0 \\ 0 & 0 & 0 & 0 \\ 0 & 0 & 0 & 0 \\ 0 & 0 & 0 & 0 \end{bmatrix}, \quad L_3 = \begin{bmatrix} 0 & 0 & 0 & 0 \\ 0 & 0 & 0 & 0 \\ 0 & 0 & 0 & 0 \\ 0 & 0 & 0 & 0 \\ 0 & 0 & 0 & 0 \\ 0 & 0 & 0 & 0 \\ 0 & 0 & 0 & 0 \\ 0 & 0 & 0 & 0 \\ 1 & 1 & 0 & 0 \end{bmatrix},$$

$$R_1 = \begin{bmatrix} 0 & 0 & 0 & 0 \\ 1 & 0 & 0 & 0 \\ 0 & 0 & 0 & 0 \\ 0 & 1 & 0 & 0 \\ 0 & 0 & 0 & 0 \\ 0 & 0 & 0 & 0 \\ 0 & 0 & 0 & 0 \\ 0 & 0 & 0 & 0 \\ 0 & 0 & 0 & 0 \end{bmatrix}^T, \quad R_2 = \begin{bmatrix} 1 & 0 & 0 & 0 \\ 0 & 0 & 0 & 0 \\ 0 & 1 & 0 & 0 \\ 0 & 0 & 0 & 0 \\ 0 & 0 & 0 & 0 \\ 0 & 0 & 0 & 0 \\ 0 & 0 & 0 & 0 \\ 0 & 0 & 0 & 0 \\ 0 & 0 & 0 & 0 \end{bmatrix}^T, \quad R_3 = \begin{bmatrix} 0 & 0 & 0 & 0 \\ 0 & 0 & 0 & 0 \\ 0 & 0 & 0 & 0 \\ 0 & 0 & 0 & 0 \\ 0 & 0 & 0 & 0 \\ 0 & 0 & 1 & 0 \\ 0 & 0 & 0 & 0 \\ 0 & 0 & 0 & 1 \\ 0 & 0 & 0 & 0 \end{bmatrix}^T, \quad M_3 = \begin{bmatrix} 0 & 0 & 1 & 0 \\ 0 & 0 & 0 & 1 \\ 0 & 0 & 0 & 0 \\ 0 & 0 & 0 & 0 \end{bmatrix},$$

Now with  $\mathcal{K}$  in terms of  $K$ , we can take the derivative of the Lagrangian with respect to  $K$ . Define the following notation

$$\begin{aligned} \tau &\triangleq I + \mathcal{D}_{yu}^T L_{\mathcal{K}}^{-T} \mathcal{K}^T, & \hat{A} &\triangleq \tau \mathcal{B}_u^T \tilde{P} \tilde{Q} \mathcal{C}_y^T L_{\mathcal{K}}^{-T}, \\ \hat{D} &\triangleq \tau \mathcal{B}_u^T \tilde{P} \tilde{D} \mathcal{D}_{yw}^T L_{\mathcal{K}}^{-T}, & \hat{E} &\triangleq \tau \mathcal{D}_{zu}^T \tilde{E} \tilde{Q} \mathcal{C}_y^T L_{\mathcal{K}}^{-T}. \end{aligned}$$

The derivative of the Lagrangian with respect to  $K$  is given by

$$\begin{aligned} \frac{1}{2} \frac{\partial \mathcal{L}}{\partial K} &= \text{diag}\{L_1^T \hat{A} R_1^T + L_2^T \hat{A} R_2^T K + K L_2^T \hat{A} R_2^T + L_3^T \hat{A} R_3^T K M_3^T K + K L_3^T \hat{A} R_3^T K M_3^T \\ &\quad + M_3^T K K L_3^T \hat{A} R_3^T + L_1^T \hat{D} R_1^T + L_2^T \hat{D} R_2^T K + K L_2^T \hat{D} R_2^T + L_3^T \hat{D} R_3^T K M_3^T K \end{aligned}$$

$$\begin{aligned}
& +KL_3^T \hat{D}R_3^T KM_3^T + M_3^T KKL_3^T \hat{D}R_3^T + L_1^T \hat{E}R_1^T + L_2^T \hat{E}R_2^T K + KL_2^T \hat{E}R_2^T \\
& +L_3^T \hat{E}R_3^T KM_3^T K + KL_3^T \hat{E}R_3^T KM_3^T + M_3^T KKL_3^T \hat{E}R_3^T \}.
\end{aligned}$$

## 2.6. Simulation Results

As mentioned in Section 2.3, one requirement of gradient-based optimization algorithms is an initial stabilizing design. Initial designs showed that for large values of  $\omega_i$ ,  $i = 1, 2, 3$ , the cost function depended very weakly upon these values. Therefore,  $\omega_i$ ,  $i = 1, 2, 3$ , were initially chosen to be 48, 72, and 96, respectively. Furthermore, since the open-loop system was stable, an initial stabilizing design could be obtained by setting  $k_3 = k_4 = 0$ . With these values set, the BFGS quasi-Newton algorithm was applied to find the  $\mathcal{H}_2$ -optimal solution for a given fixed-structure controller configuration.

The ACTEX experiment is a lightly damped flexible structure, as can be seen by the impulse response shown in Figure 2.3, where  $x(0) = [0 \ 0 \ 0 \ 1]^T$ . For each of the four different controller configurations, three different controllers were designed by setting the control weighting matrix  $R_2$  to 1, 0.01, and 0.0001. The  $\mathcal{H}_2$  cost of these controllers can be seen in Table 2.1. It is seen that the  $\mathcal{H}_2$  performance is best for the first controller configuration. In fact, the fourth controller configuration ran into parameter limits (2.40), as explained in Section 2.3. Therefore, the optimization routine terminated due to a boundary constraint rather than a small gradient condition. It can also be seen from Table 2.1 that the  $\mathcal{H}_2$  cost of the closed-loop system decreases with increasing controller authority.

The optimal controller parameters for the first controller configuration are given in Table 2.2. We can see from the output signals of the impulse response in Figure 2.4 that with  $R_2 = 1$  the controller does not attenuate the vibrations significantly. How-

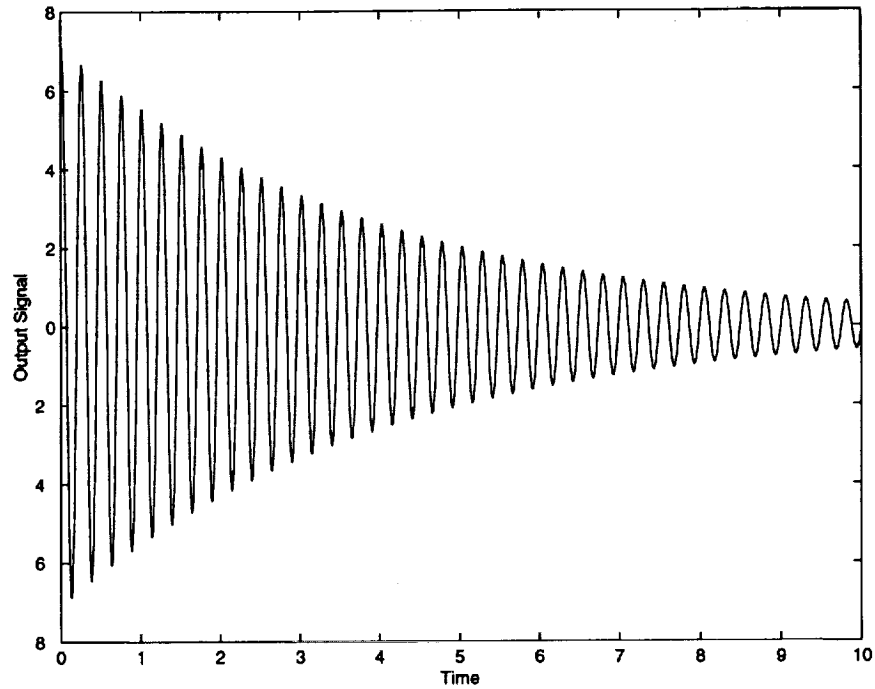


Figure 2.3: Open-loop impulse response

	Config. 1	Config. 2	Config. 3	Config. 4
$R_2 = 1$	0.5825	0.6774	0.6774	0.6782
$R_2 = 0.01$	0.2444	0.5601	0.5601	0.5613
$R_2 = 0.0001$	0.1910	0.5495	0.5495	0.5507

Table 2.1:  $\mathcal{H}_2$  costs for various controller configurations and weightings

	$\omega_1$	$\omega_2$	$k_3$	$k_4$
$R_2 = 1$	26.6460	80.0602	0.1352	0.0074
$R_2 = 0.01$	36.4434	99.1179	0.3195	0.4025
$R_2 = 0.0001$	37.3664	123.8404	0.2081	0.6314

Table 2.2: Optimal controller parameters for controller configuration 1

ever, as the controller authority is increased, the attenuation becomes greater, as seen in Figure 2.5 and Figure 2.6, though this does increase the control effort expended, as shown in Figures 2.7–2.9, which could lead to actuator saturation. Finally, Figure 2.10 shows the Bode plots of the open-loop and closed-loop systems. It is seen that the size of the first peak in the closed-loop response is decreased as the controller authority is increased. Another important feature of the closed-loop frequency response is the high-frequency roll-off. Since the ACTEX system model has a relative degree of zero, designing a controller without high-frequency roll-off would result in a closed-loop system which possesses gain at all frequencies, thus unmodeled high-frequency dynamics could destabilize the closed-loop system, whereas these dynamics would be attenuated with a strictly proper dynamic controller.

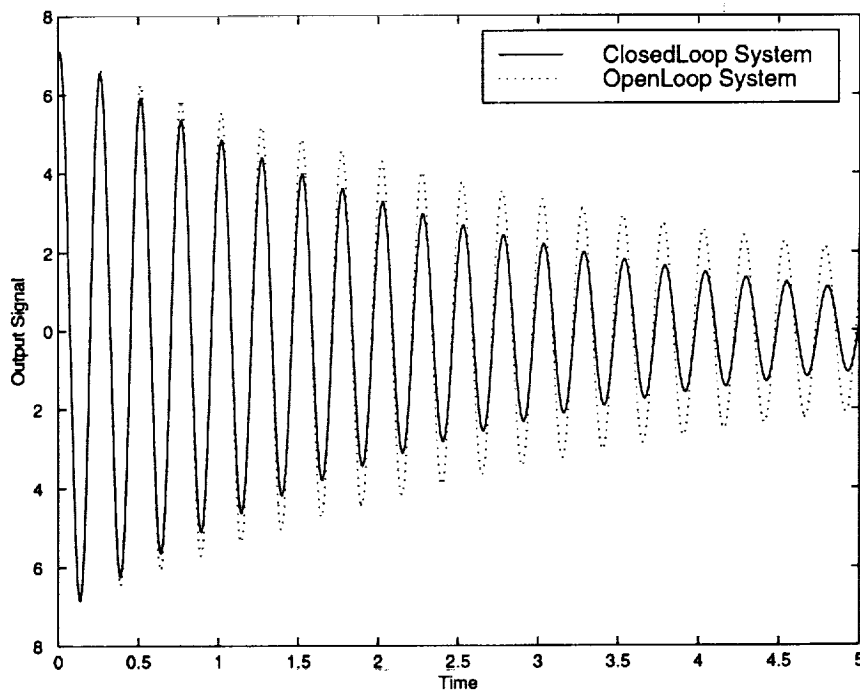


Figure 2.4: Closed-loop impulse response,  $R_2 = 1$

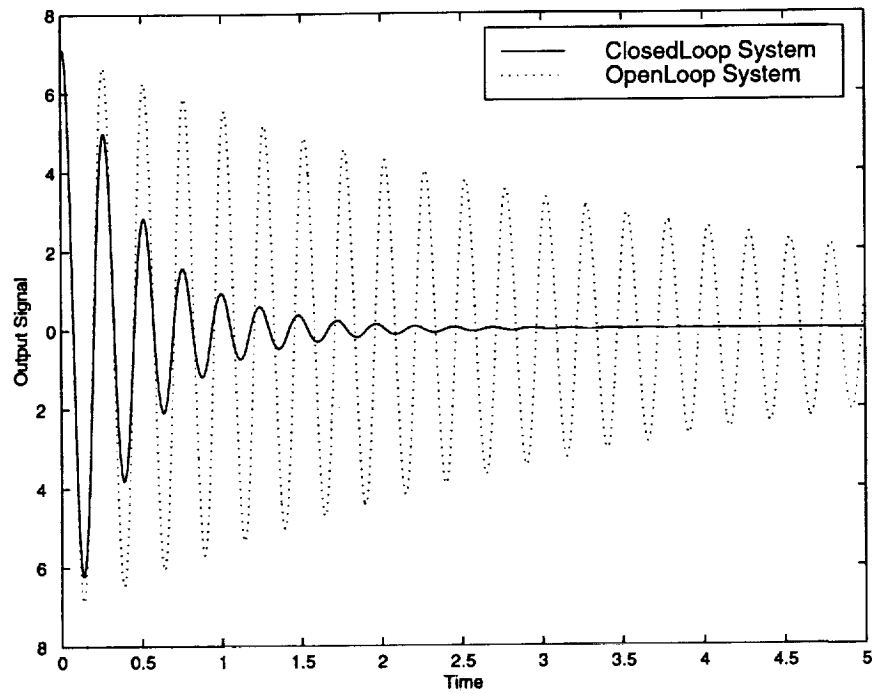


Figure 2.5: Closed-loop impulse response,  $R_2 = 0.01$

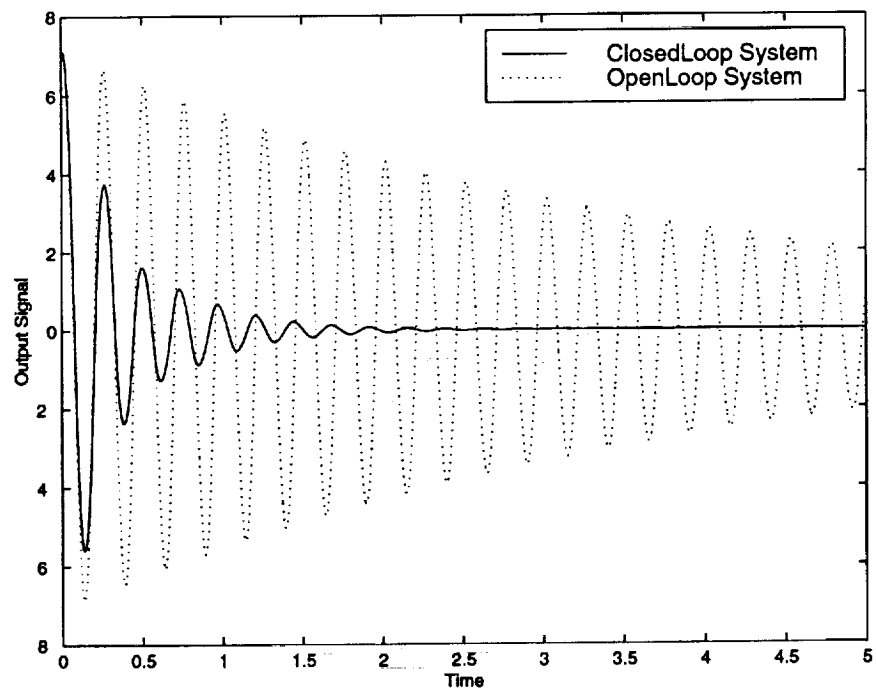


Figure 2.6: Closed-loop impulse response,  $R_2 = 0.0001$

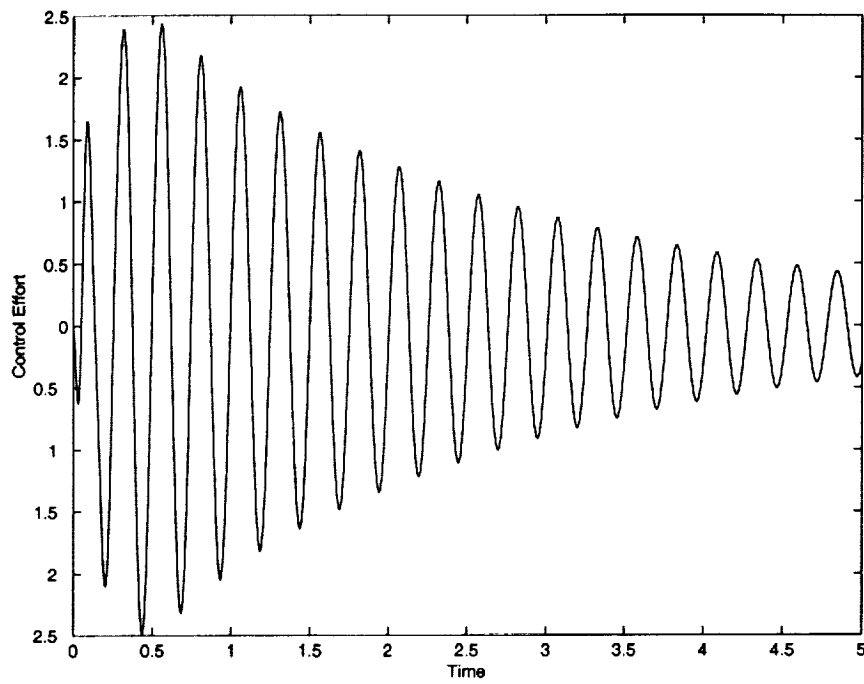


Figure 2.7: Closed-loop control effort,  $R_2 = 1$

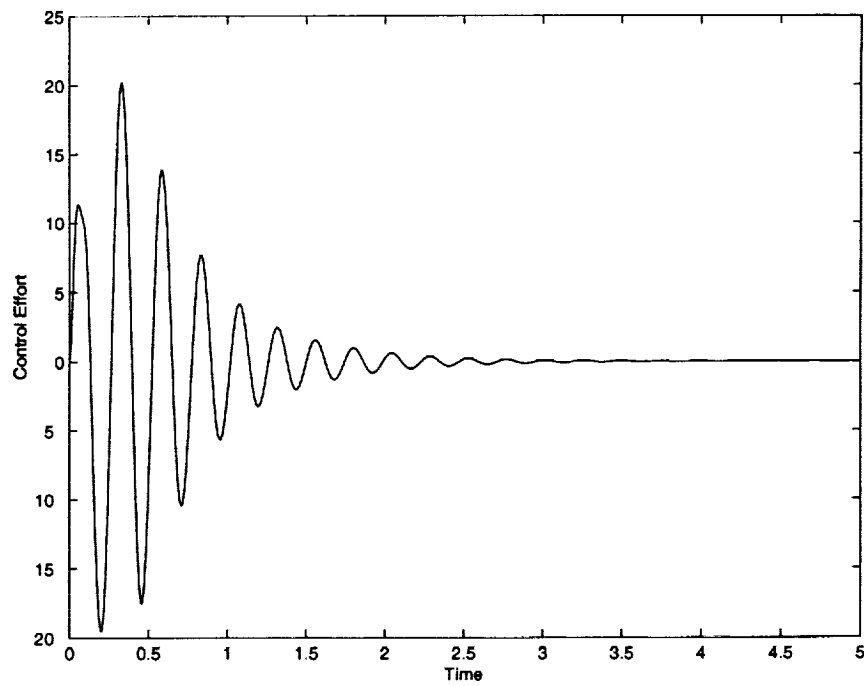


Figure 2.8: Closed-loop control effort,  $R_2 = 0.01$

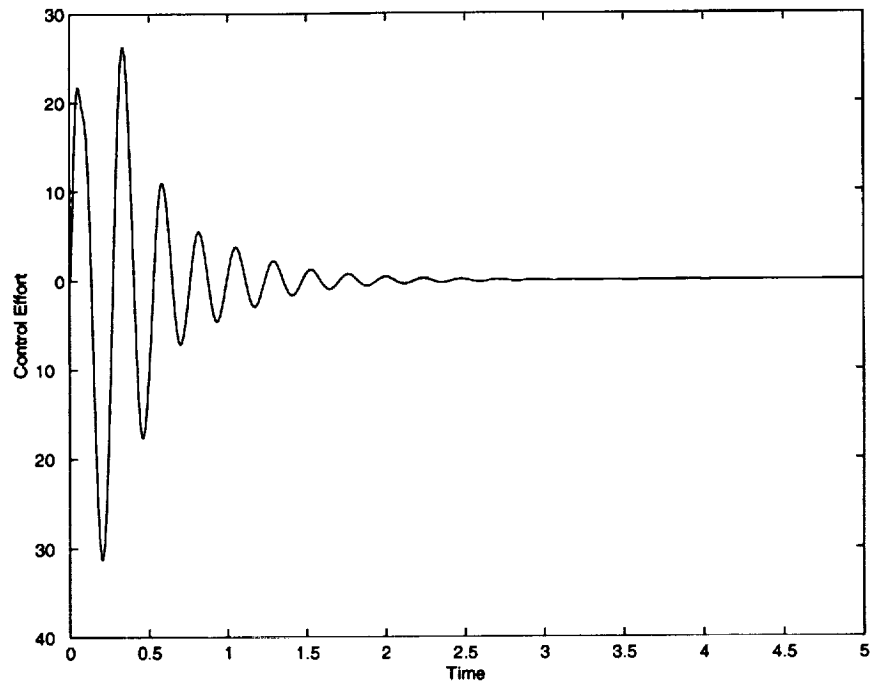


Figure 2.9: Closed-loop control effort,  $R_2 = 0.0001$

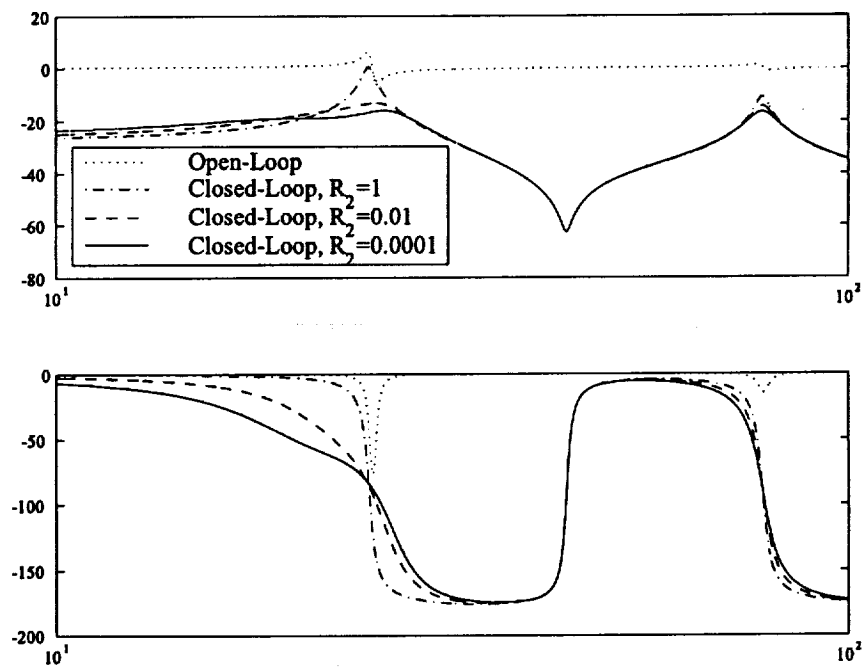


Figure 2.10: Bode plots for open-loop and closed-loop systems

## 2.7. Conclusion

In this chapter we introduced the decentralized static output feedback format. Specifically, we showed how dynamic output feedback control problems can be transformed into a decentralized static output feedback form. By using this format, a numerical optimization scheme can be used to optimize the controller gains with respect to a given cost function and constraint equation. Furthermore, we demonstrated the effectiveness of this framework on the ACTEX flight experiment.

## CHAPTER 3

# Stable $\mathcal{H}_2$ -Optimal Controller Synthesis

### 3.1. Introduction

It is well known that even though LQG synthesis will stabilize the nominal closed-loop system, it can produce controllers with unstable dynamics, especially at high authority levels. Of course, for certain plants, specifically those that do not satisfy the parity interlacing property [121], only unstable controllers are stabilizing. However, even for stable plants, LQG synthesis often produces unstable controllers, thus requiring Nyquist encirclements of the critical point. These encirclements and the resulting multiple gain margins, which must be maintained by the input actuators, can be jeopardized by actuator saturation and startup dynamics [87]. Therefore, whenever possible, it is desirable to implement only stable controllers.

Several modifications of LQG theory have been proposed to obtain stable compensators. Several of these techniques involve either modified Riccati equations [64, 112, 113] or constrained weights [59, 60]. Thus the resulting controllers may sacrifice performance for controller stability. In [43, 86, 87], an augmented cost technique was proposed to obtain stable controllers without unnecessarily sacrificing performance. However, even though the authors in [87] give an excellent discussion on the

implementation issues surrounding stable versus unstable controllers, they focus on multiple-model control, and therefore the cost function to be optimized is a weighted average of a number of system costs and does not give any insight into the trade-off between system performance and controller stability margin.

The purpose of this paper is to provide a control-system design framework for  $\mathcal{H}_2$ -optimal strong stabilization. To achieve this goal we formulate the  $\mathcal{H}_2$ -optimal stable control problem within the context of decentralized static output feedback control which provides a general framework for fixed-structure dynamic controller synthesis [14, 34]. In particular, in order to guarantee stable stabilization, a multiobjective problem, reminiscent of scalarization techniques for Pareto optimization, is treated by forming a convex combination of the  $\mathcal{H}_2$  norm of the closed-loop system and a weighted  $\mathcal{H}_2$  norm of the controller. It is shown that as the trade-off parameter is varied to obtain better  $\mathcal{H}_2$  system performance, the controller eigenvalues approach the imaginary axis. Thus the control engineer can decide if additional performance improvements warrant the resulting reduction in the stability margin of the controller.

Two examples from the stable stabilization literature are considered here. The first example is a second-order spring-mass-damper system and the second example is a fourth-order two-mass system involving two flexible modes. The  $\mathcal{H}_2$  cost of the stable controllers developed for the first example, though larger than that of the LQG controller, was comparable to the lowest cost possible by a stable controller. For the second example, the difference between the  $\mathcal{H}_2$  cost of the stable controller and the unstable LQG controller is negligible.

## 3.2. Stable $\mathcal{H}_2$ -Optimal Control

In this section we state the  $\mathcal{H}_2$ -optimal stable stabilization problem. Specifically, given the  $n^{\text{th}}$ -order plant

$$\dot{x}(t) = Ax(t) + Bu(t) + D_1w(t), \quad t \in [0, \infty), \quad (3.1)$$

with noisy measurements

$$y(t) = Cx(t) + D_2w(t), \quad (3.2)$$

and performance variables

$$z(t) = E_1x(t) + E_2u(t), \quad (3.3)$$

determine an  $n_c^{\text{th}}$ -order strictly proper dynamic compensator

$$\dot{x}_c(t) = A_c x_c(t) + B_c y(t), \quad (3.4)$$

$$u(t) = C_c x_c(t), \quad (3.5)$$

such that the  $\mathcal{H}_2$  performance criterion

$$J(A_c, B_c, C_c) \triangleq \lim_{t \rightarrow \infty} \frac{1}{t} \mathbb{E} \int_0^t z^T(s) z(s) ds, \quad (3.6)$$

is minimized and the compensator dynamics matrix  $A_c$  is asymptotically stable.

The closed-loop system (3.1)–(3.5) is given by

$$\dot{\tilde{x}}(t) = \tilde{A}\tilde{x}(t) + \tilde{D}w(t), \quad t \in [0, \infty), \quad (3.7)$$

$$z(t) = \tilde{E}\tilde{x}(t). \quad (3.8)$$

The closed-loop transfer function from disturbances  $w$  to performance variables  $z$  is given by

$$G_{zw}(s) \triangleq \tilde{E}(sI_{\tilde{n}} - \tilde{A})^{-1}\tilde{D}.$$

Next, we define a weighted controller transfer function from plant output  $y$  to plant input  $u$  by

$$G_c(s) \triangleq E_2 C_c (sI_{n_c} - A_c)^{-1} B_c D_2.$$

Hence, the fixed-structure  $\mathcal{H}_2$ -optimal stable control problem is defined as:

$$\min_{(A_c, B_c, C_c)} \|G_{zw}(s)\|_2^2$$

subject to

$$\|G_c(s)\|_2^2 < \infty.$$

### 3.3. Design Equations

The  $\mathcal{H}_2$  norm of  $G_{zw}(s)$  is given by

$$\|G_{zw}(s)\|_2^2 = \text{tr } \tilde{Q} \tilde{R}, \quad (3.9)$$

where  $\tilde{Q} \in \mathbb{N}^{\tilde{n}}$  is the unique nonnegative definite solution to the algebraic Lyapunov equation

$$0 = \tilde{A} \tilde{Q} + \tilde{Q} \tilde{A}^T + \tilde{V}. \quad (3.10)$$

Furthermore, if  $A_c$  is stable, then the  $\mathcal{H}_2$  norm of the weighted transfer function of the controller  $G_c(s) = E_2 C_c (sI_{n_c} - A_c)^{-1} B_c D_2$  is given by

$$\|G_c(s)\|_2^2 = \text{tr } Q_c C_c^T R_2 C_c, \quad (3.11)$$

where  $Q_c \in \mathbb{N}^{n_c}$  is the unique nonnegative definite solution to the algebraic Lyapunov equation

$$0 = A_c Q_c + Q_c A_c^T + B_c V_2 B_c^T. \quad (3.12)$$

To obtain (3.11) and (3.12) in terms of  $\mathcal{K}$ , given by

$$\mathcal{K} \triangleq \begin{bmatrix} A_c & 0 & 0 \\ 0 & B_c & 0 \\ 0 & 0 & C_c \end{bmatrix}, \quad (3.13)$$

we define the matrices  $Q_{L_{ij}}$  and  $Q_{R_{ij}}$ ,  $i = 1, 2, 3$ ,  $j = 1$ , as given by (2.16), so that

$$\begin{aligned} A_c &= Q_{L_{11}}^T \mathcal{K} Q_{R_{11}}^T, \\ B_c &= Q_{L_{21}}^T \mathcal{K} Q_{R_{21}}^T, \\ C_c &= Q_{L_{31}}^T \mathcal{K} Q_{R_{31}}^T. \end{aligned}$$

Thus, (3.11) and (3.12) become

$$\|G_c(s)\|_2^2 = \text{tr } Q_c Q_{R_{31}} \mathcal{K}^T Q_{L_{31}} R_2 Q_{L_{31}}^T \mathcal{K} Q_{R_{31}}^T, \quad (3.14)$$

and

$$0 = Q_{L_{11}}^T \mathcal{K} Q_{R_{11}}^T Q_c + Q_c Q_{R_{11}} \mathcal{K}^T Q_{L_{11}} + Q_{L_{21}}^T \mathcal{K} Q_{R_{21}}^T V_2 Q_{R_{21}} \mathcal{K}^T Q_{L_{21}}, \quad (3.15)$$

respectively.

In order to design  $\mathcal{H}_2$ -optimal stable controllers we pose the following multiobjective optimization problem: For  $\rho \in [0, 1]$ , determine  $\mathcal{K}$  that minimizes

$$\mathcal{J}(\mathcal{K}) = (1 - \rho) \text{tr } \bar{Q} \bar{R} + \rho \text{tr } Q_c Q_{R_{31}} \mathcal{K}^T Q_{L_{31}} R_2 Q_{L_{31}}^T \mathcal{K} Q_{R_{31}}^T, \quad (3.16)$$

where  $\bar{Q} \in \mathbb{N}^{\bar{n}}$ ,  $Q_c \in \mathbb{N}^{n_c}$  satisfy (3.10) and (3.15), respectively. Note that (3.16) involves a convex combination of the  $\mathcal{H}_2$  norm of the closed-loop system and the weighted  $\mathcal{H}_2$  norm of the controller. By including the  $\mathcal{H}_2$  cost of the controller in the objective function, we can guarantee that the controller is stable as long as the objective function is finite. By varying  $\rho \in [0, 1]$ , (3.16) can be viewed as the scalar representation of a multiobjective cost. To achieve the best closed-loop performance with a stable controller, we only want to use the  $\mathcal{H}_2$  cost of the controller as a constraint, and thus we set  $\rho > 0$  to be small so that the contribution to the multiobjective cost due to the  $\mathcal{H}_2$  cost of the controller is negligible compared to the contribution due to the  $\mathcal{H}_2$  cost of the closed-loop system. Thus, the optimization routine will

minimize the cost of the closed-loop system and not attempt to minimize the  $\mathcal{H}_2$  cost of the compensator. However, increasing the trade-off parameter  $\rho$  will increase the controller stability margin. Finally, note that by letting  $\rho \rightarrow 0$ , we recover the  $\mathcal{H}_2$ -optimal control problem.

The necessary conditions for optimality can be derived by forming the Lagrangian

$$\begin{aligned} \mathcal{L}(\tilde{P}, \tilde{Q}, P_c, Q_c, \mathcal{K}) = & (1 - \rho) \operatorname{tr} \tilde{Q} \tilde{R} + \rho \operatorname{tr} Q_c Q_{R_{31}} \mathcal{K}^T Q_{L_{31}} R_2 Q_{L_{31}}^T \mathcal{K} Q_{R_{31}}^T \\ & + \operatorname{tr} \tilde{P} [\tilde{A} \tilde{Q} + \tilde{Q} \tilde{A}^T + \tilde{V}] + \operatorname{tr} P_c [Q_{L_{11}}^T \mathcal{K} Q_{R_{11}}^T Q_c \\ & + Q_c Q_{R_{11}} \mathcal{K}^T Q_{L_{11}} + Q_{L_{21}}^T \mathcal{K} Q_{R_{21}}^T V_2 Q_{R_{21}} \mathcal{K}^T Q_{L_{21}}], \quad (3.17) \end{aligned}$$

where  $\tilde{P} \in \mathbb{N}^{\tilde{n}}$  and  $P_c \in \mathbb{N}^{n_c}$  are Lagrange multipliers. The partial derivatives with respect to the free parameters in (3.17) are given by

$$\begin{aligned} \frac{\partial \mathcal{L}}{\partial \tilde{Q}} &= \tilde{A}^T \tilde{P} + \tilde{P} \tilde{A} + (1 - \rho) \tilde{R}, \\ \frac{\partial \mathcal{L}}{\partial \tilde{P}} &= \tilde{A} \tilde{Q} + \tilde{Q} \tilde{A}^T + \tilde{V}, \\ \frac{\partial \mathcal{L}}{\partial Q_c} &= A_c^T P_c + P_c A_c + \rho C_c^T R_2 C_c, \\ \frac{\partial \mathcal{L}}{\partial P_c} &= A_c Q_c + Q_c A_c^T + B_c V_2 B_c^T, \end{aligned}$$

$$\frac{\partial \mathcal{L}}{\partial A_c} = Q_{L_{11}}^T \frac{\partial \mathcal{L}}{\partial \mathcal{K}} Q_{R_{11}}^T, \quad \frac{\partial \mathcal{L}}{\partial B_c} = Q_{L_{21}}^T \frac{\partial \mathcal{L}}{\partial \mathcal{K}} Q_{R_{21}}^T, \quad \frac{\partial \mathcal{L}}{\partial C_c} = Q_{L_{31}}^T \frac{\partial \mathcal{L}}{\partial \mathcal{K}} Q_{R_{31}}^T,$$

where

$$\begin{aligned} \frac{\partial \mathcal{L}}{\partial \mathcal{K}} = & B_u^T \tilde{P} \tilde{Q} C_y^T + B_u^T \tilde{P} \tilde{V} D_{yw}^T + (1 - \rho) D_{zu}^T \tilde{E} \tilde{Q} C_y^T \\ & + \rho Q_{L_{31}} R_2 Q_{L_{31}}^T \mathcal{K} Q_{R_{31}}^T Q_c Q_{R_{31}} + Q_{L_{11}} P_c Q_c Q_{R_{11}} + Q_{L_{21}} Q_{L_{21}}^T \mathcal{K} Q_{R_{21}}^T V_2 Q_{R_{21}}. \end{aligned}$$

### 3.4. Optimization Algorithm

As noted in Section 2.3, one requirement of gradient-based optimization algorithms is an initial stabilizing design. For plants satisfying the parity interlacing property,

initialization can be accomplished by using sufficiently low authority compensators [24]. This was accomplished here by multiplying the control weight  $E_2$  by a scalar  $\eta > 1$ . At sufficiently low authority, the LQG controllers tended to be stable. These low authority, stable, full-order controllers generally can then be truncated using an appropriate model reduction technique without destroying closed-loop stability. For decentralized control, this technique can be implemented in a sequential manner for each channel to obtain initializing gains with the given structure. These low authority LQG designs are used to initialize a low authority optimization algorithm. The optimized controller gains are then used to sequentially initialize higher authority problems until eventually the desired controller authority level is regained. At this point, the trade-off parameter  $\rho$  is varied until the best  $\mathcal{H}_2$  performance is attained in the face of a desired controller stability margin.

### 3.5. Spring-Mass-Damper Example

Consider the spring-mass-damper system given by the state space realization [42, 60]

$$\begin{aligned}\dot{x}(t) &= \begin{bmatrix} 0 & 1 \\ -3 & -4 \end{bmatrix} x(t) + \begin{bmatrix} 0 \\ 1 \end{bmatrix} u(t), \\ y(t) &= \begin{bmatrix} 2 & 1 \end{bmatrix} x(t).\end{aligned}$$

The matrices  $D_1$ ,  $D_2$ ,  $E_1$ , and  $E_2$  are chosen to be

$$D_1 = \begin{bmatrix} 35 & 0 \\ -61 & 0 \end{bmatrix}, \quad D_2 = \begin{bmatrix} 0 & 1 \end{bmatrix}, \quad E_1 = \begin{bmatrix} 52.9150 & 8.9443 \\ 0 & 0 \end{bmatrix}, \quad E_2 = \begin{bmatrix} 0 \\ 1 \end{bmatrix}.$$

For the given data, the LQG controller is unstable. To initialize the  $\mathcal{H}_2$ -optimal stable control problem, the control weighting was increased by multiplying  $E_2$  by  $\eta = 16$ , as described in Section 3.4. This stable LQG design was used as a starting point for the quasi-Newton algorithm which found optimal stable compensators as  $\eta$  was

decremented back to unity, returning the control authority to its original value.

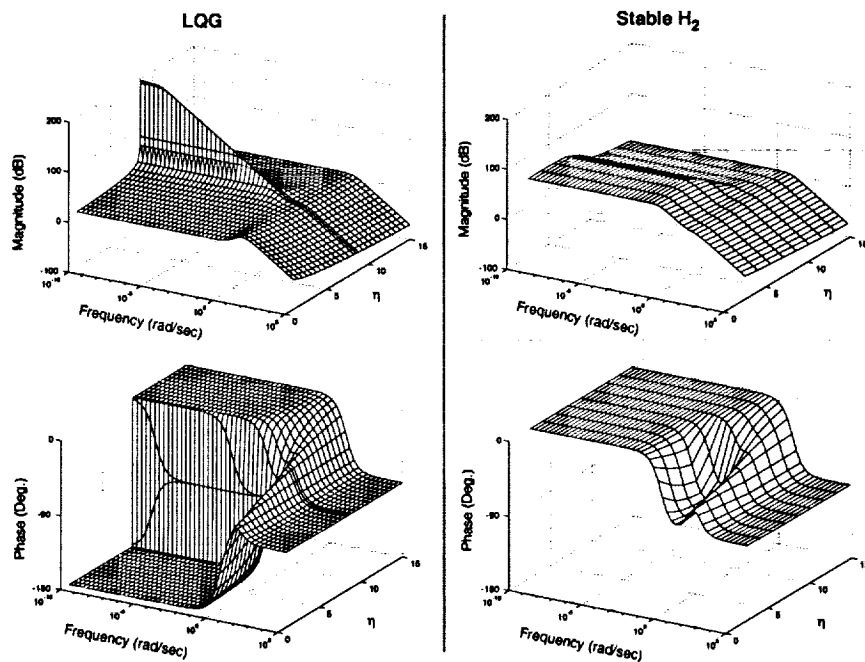
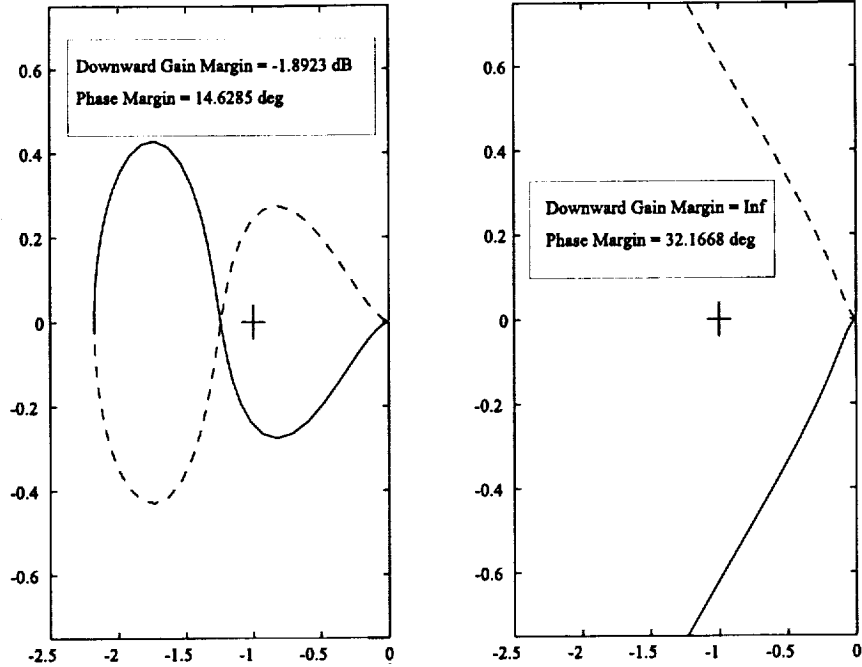


Figure 3.1: Bode plots of LQG and stable  $\mathcal{H}_2$  controllers ( $\rho = 0.0288$ )

As can be seen in Figure 3.1, increasing the authority toward a critical level ( $\eta = 8.58$ ) causes the gain of the LQG controller to approach infinity, at which point the low frequency phase jumps  $-180^\circ$  and the gain begins to decrease, though the controller must now be unstable to maintain closed-loop stability. At this point, it can be seen that the gain of the  $\mathcal{H}_2$ -optimal stable controllers increase as well, though not as drastically as the LQG design, and the  $\mathcal{H}_2$ -optimal stable controllers always have a phase of  $0^\circ$  at low frequencies. The Nyquist plots of the LQG controller and the stable controller at full control authority, as seen in Figure 3.2, show the poor gain margins of the unstable LQG controller.

Since the loop gain with the  $\mathcal{H}_2$ -optimal stable controller in feedback is much larger than that with the LQG controller at full authority, the impulse responses of the LQG controller and the stable controller were simulated to compare the actual



**Figure 3.2:** Nyquist plots of the loop gain for LQG (left) and stable  $\mathcal{H}_2$  (right) controllers ( $\eta = 1$ ,  $\rho = 0.0288$ )

control effort needed to bring the closed-loop system back to the equilibrium. These comparisons are shown in Figure 3.3. As expected, the performance of the system with the LQG controller is better than the performance of the system with the  $\mathcal{H}_2$ -optimal stable controller. However, note that even though the loop gain of the stable controller is much larger than that of the LQG controller, the control effort used by the stable controller is significantly less than that used by the LQG controller and hence is less likely to saturate the system actuators, which could cause closed-loop instabilities to occur when an unstable controller is used.

Once the control authority was increased to the desired level, the value of the parameter  $\rho$  was varied to study the trade-off between the  $\mathcal{H}_2$  cost of the system and the stability level of the compensator. Figure 3.4 shows the position of the controller ( $n_c = 2$ ) eigenvalues as a function of  $\rho$  as well as the  $\mathcal{H}_2$  cost of the closed-loop system

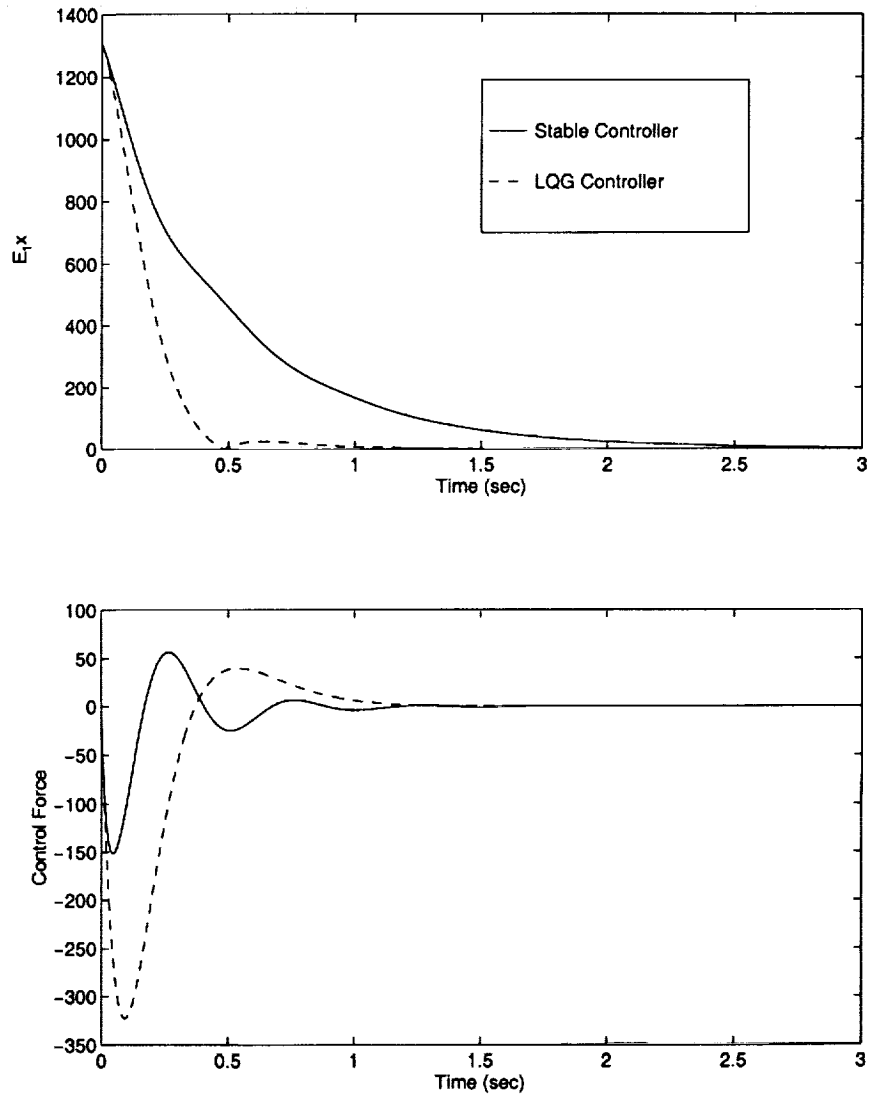


**Figure 3.3:** Impulse response of closed-loop system with LQG and stable  $\mathcal{H}_2$  controllers ( $\eta = 1$ ,  $\rho = 2.88 \times 10^{-8}$ )

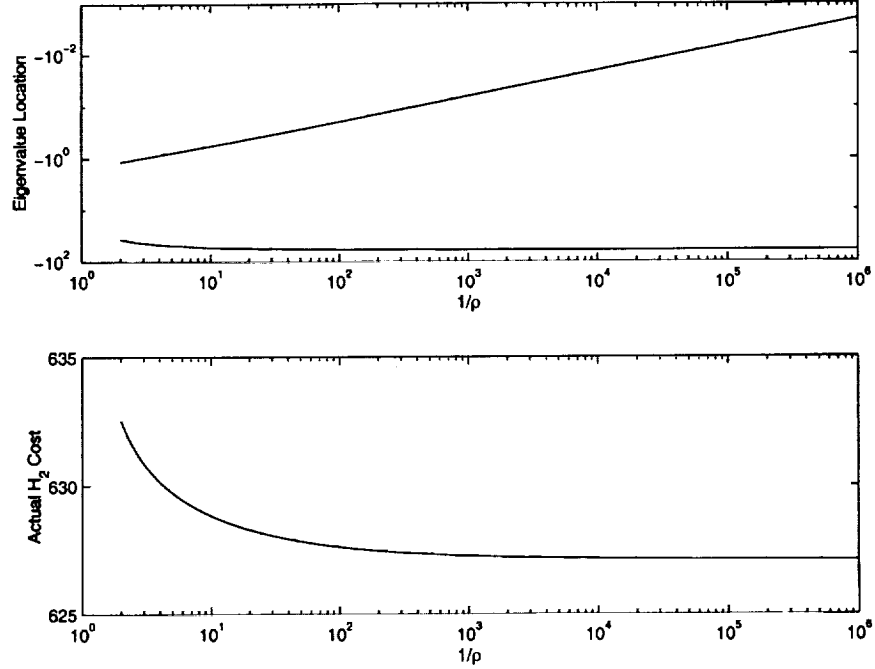


**Figure 3.4:** Location of controller eigenvalues and  $\mathcal{H}_2$  cost versus  $\rho$

as a function of  $\rho$ . By studying the resulting trade-off, the control engineer can decide if subsequent cost reductions justify bringing the controller eigenvalues closer to the stability boundary.

For  $\rho = 0.5$ , the controller transfer function is given by

$$G_c(s) = \frac{-274.21s - 4183.8}{s^2 + 38.324s + 43.539}, \quad (3.18)$$

which has eigenvalues at  $\lambda_1 = -37.152$  and  $\lambda_2 = -1.1719$ , while, for  $\rho = 5 \times 10^{-7}$ , the controller transfer function is given by

$$G_c(s) = \frac{-504.93s - 9744.5}{s^2 + 60.543s + 0.086523}, \quad (3.19)$$

which has eigenvalues at  $\lambda_1 = -60.541$  and  $\lambda_2 = -0.0014292$ .

Since, as stated in [42], the lowest possible cost via stable stabilization for this example is given by a 4<sup>th</sup>-order controller, we used the present framework to obtain stable 4<sup>th</sup>-, 6<sup>th</sup>-, and 8<sup>th</sup>-order controllers to quantify the benefits of expanded-order

control. Specifically, these expanded-order  $\mathcal{H}_2$ -optimal stable controllers were initialized by adding one, two, and three stable modes to a full-order stable LQG controller, at which point the optimization algorithm was applied. The corresponding closed-loop costs, computed at various levels of control authority, are shown in Figure 3.5. At lower levels of controller authority, the stable controllers have nearly identical costs to the LQG controllers. As the authority is increased, the closed-loop cost associated with the stable controllers becomes noticeably worse than the LQG controllers, however it is noticeably better than the best stable LQG design (i.e., the LQG design with  $\eta = 8.58$ ). At the specified control authority ( $\eta = 1$ ), the dependence of the augmented cost function on the controller cost was decreased by decreasing the variable  $\rho$ .

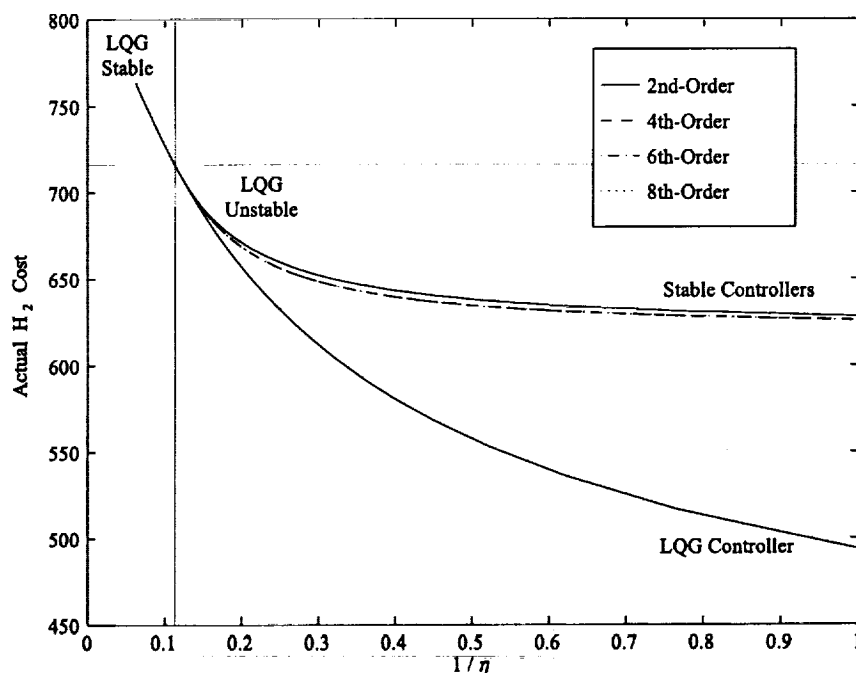


**Figure 3.5:**  $\mathcal{H}_2$  cost versus control weighting for various-order stable  $\mathcal{H}_2$  controllers ( $\rho = 0.0288$ )

As seen in Figure 3.6, the full-order controller has the highest  $\mathcal{H}_2$  cost, followed

by the controller with one extra mode. The other two controllers, however, have nearly identical closed-loop costs, suggesting that arbitrarily high-order controllers may not achieve significant performance improvements. Since decreasing  $\rho$  decreases the dependence of the cost function  $J$  on the weighted  $\mathcal{H}_2$  cost of the controller, the controller loop gain increases greatly as  $\rho$  becomes smaller, as shown in Figure 3.7.

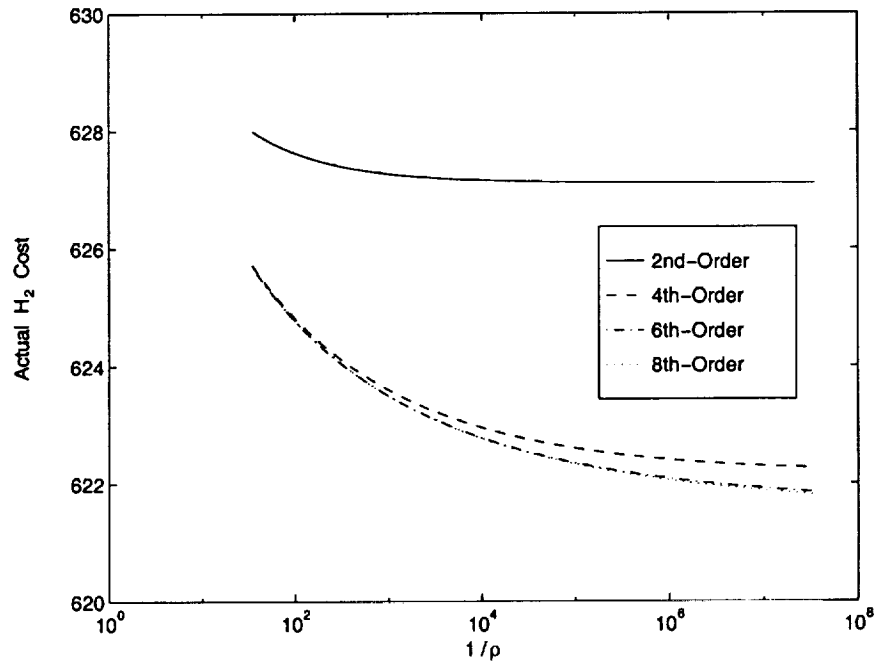


Figure 3.6: Stable  $\mathcal{H}_2$  controller cost versus  $\rho$

	2nd-Order	4th-Order	6th-Order	8th-Order
Fixed - Structure	627.11	622.20	621.73	621.67
Ganesh [42] (Optimal)	N/A	622.73	N/A	N/A
Ganesh (Sub-Optimal)	N/A	628.40	N/A	N/A
Halevi [60] (First Result)	678.97	N/A	N/A	N/A
Halevi (After Tuning)	637.18	N/A	N/A	N/A
Stable LQG ( $\eta = 8.58$ )	713.02	N/A	N/A	N/A

Table 3.1:  $\mathcal{H}_2$  costs for various stable stabilization techniques

As can be seen in Table 3.1, the  $\mathcal{H}_2$ -optimal stable controllers obtained here com-

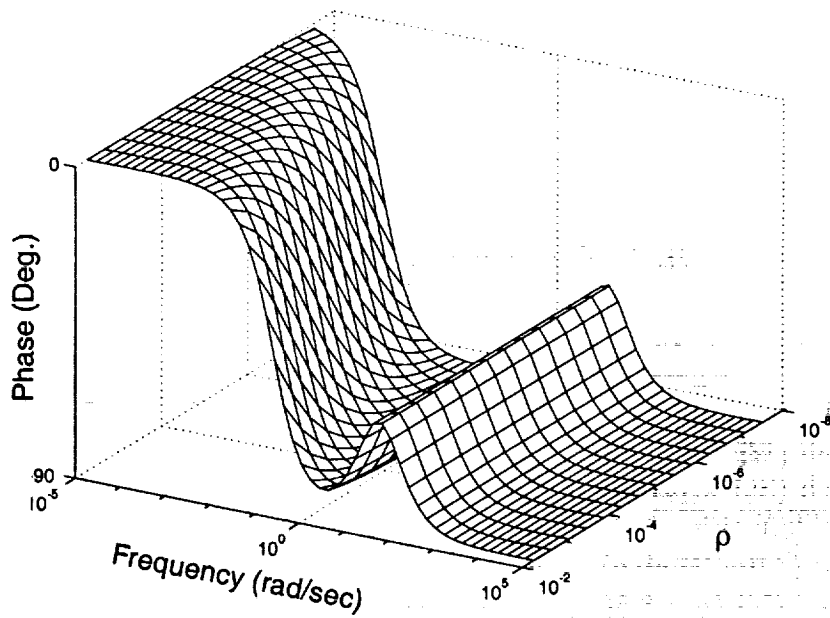
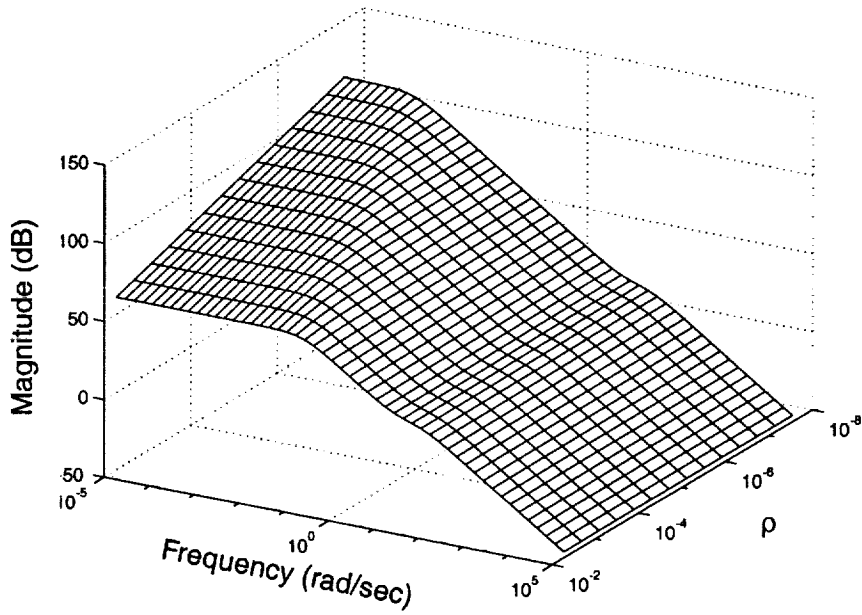


Figure 3.7: Bode plots of stable  $\mathcal{H}_2$  controllers versus  $\rho$

pare favorably to earlier results. In [60], the design weights were constrained in such a way as to yield stable controllers. Even with a tuning procedure, however, those costs are larger than what was obtained using the present framework. In [42], a nonlinear programming approach was used to obtain  $\mathcal{H}_2$ -optimal controllers, but only for SISO systems. However, as can be seen, the  $\mathcal{H}_2$  cost is slightly larger than the fourth-order controllers designed here. In fact, the optimal controllers obtained in [42] had two poles located at the origin, and thus the controller was merely conditionally stable. The stability boundary was then pushed back to  $s = -0.5$  to yield a stable controller. It should be noted that the cost obtained by the second-order controller synthesized using our method was 627.1, whereas in [60], it is stated that the minimum cost possible by a second-order stable compensator is 628, though this may be simply a numerical artifact. Also listed is the  $\mathcal{H}_2$  cost of an LQG design with  $\eta$  chosen as low as possible while still yielding a stable controller, which is significantly larger than all other methods considered.

### 3.6. Two-Mass Example

Consider the dynamic system [113] shown in Figure 3.8. The equations of motion

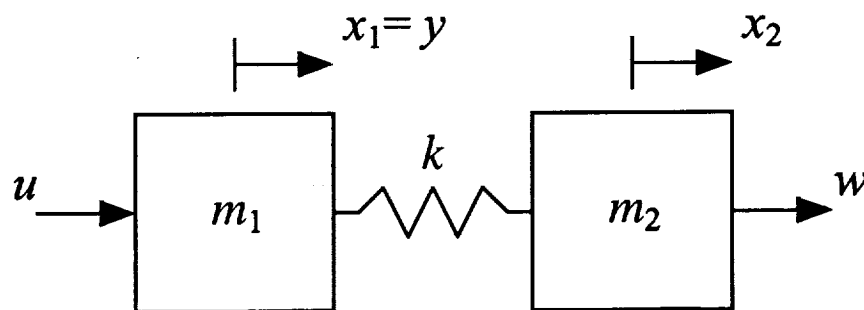


Figure 3.8: Two-mass system

for this system are given by

$$\begin{aligned} m_1 \ddot{x}_1(t) + k(x_1(t) - x_2(t)) &= u(t), \\ m_2 \ddot{x}_2(t) + k(x_2(t) - x_1(t)) &= 0. \end{aligned}$$

Here we consider the case of a colocated sensor and actuator pair, where the output is given by  $y = x_1$ . Letting  $m_1 = m_2 = k = 1$  yields the plant state space realization

$$\begin{aligned} \dot{x}(t) &= \begin{bmatrix} 0 & 0 & 1 & 0 \\ 0 & 0 & 0 & 1 \\ -1 & 1 & 0 & 0 \\ 1 & -1 & 0 & 0 \end{bmatrix} x(t) + \begin{bmatrix} 0 \\ 0 \\ 1 \\ 0 \end{bmatrix} u(t), \\ y(t) &= [1 \ 0 \ 0 \ 0] x(t). \end{aligned}$$

As in [113], the matrices  $D_1$ ,  $D_2$ ,  $E_1$ , and  $E_2$  are chosen to be

$$D_1 = \begin{bmatrix} 0 & 0 \\ 0 & 0 \\ 0 & 0 \\ 68 & 0 \end{bmatrix}, \quad D_2 = [0 \ 1], \quad E_1 = \begin{bmatrix} 1 & 0 & 1 & 0 \\ 0 & 0 & 0 & 0 \end{bmatrix}, \quad E_2 = \begin{bmatrix} 0 \\ 0.01 \end{bmatrix}.$$

For this example, a full-order and a reduced-order  $\mathcal{H}_2$ -optimal stable controller were designed. The control authority was chosen to be sufficiently low so that the LQG controller was stable. This controller was then used to initialize the optimization algorithm.

The same general trends can be observed here as in the first example, though in this case, even when full authority is achieved, the  $\mathcal{H}_2$  cost of the full-order stable controller rivals the performance of the unstable  $\mathcal{H}_2$ -optimal LQG controller, which would be apparent in Figure 3.9 if the curves were not directly on each other. In fact, the relative difference in the  $\mathcal{H}_2$  costs is merely  $9.7114 \times 10^{-4} \%$ . For this reason, expanded-order controllers could not give further cost improvements to justify their increased complexity, and thus were not designed for this example. Also, the initial value of  $\rho$  was sufficiently small that further reductions did not improve the  $\mathcal{H}_2$  cost of

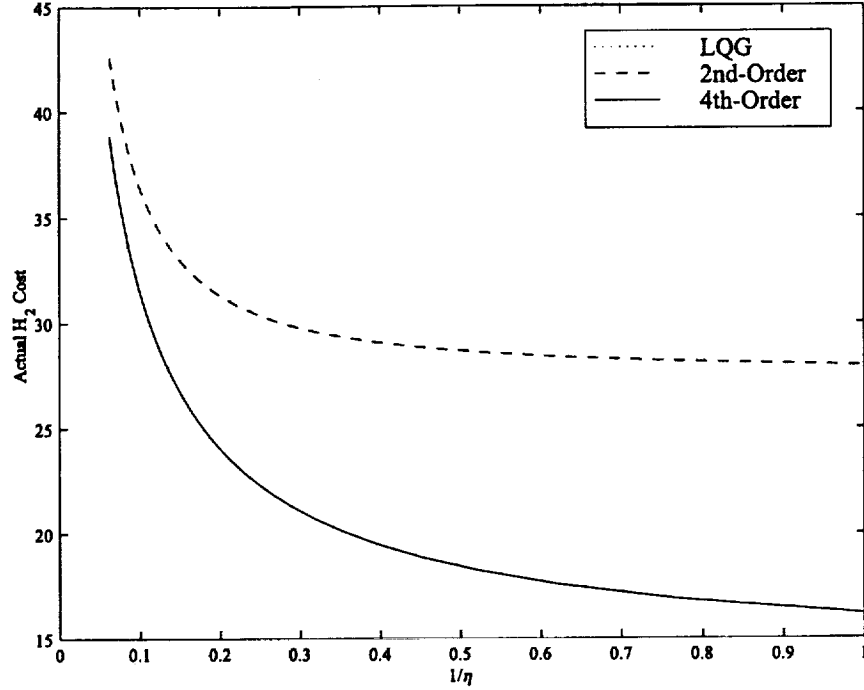


Figure 3.9:  $\mathcal{H}_2$  cost versus control weighting ( $\rho = 0.04752$ )

the closed-loop system. Table 3.2 compares the performance of the  $\mathcal{H}_2$ -optimal stable controller designs with the LQG controller, the best stable LQG controller (i.e., the LQG controller with  $\eta$  chosen as low as possible while still yielding a stable controller), and the full-order controller designed in [113], which used an over-bounding approach along with parameter tunings to obtain stable controllers.

	2nd-Order	4th-Order
LQG	N/A	16.175703
Fixed - Structure	27.9340	16.175782
Wang [113]	N/A	16.261138
Stable LQG ( $\eta = 12.21$ )	N/A	34.334324

Table 3.2:  $\mathcal{H}_2$  costs for various stable stabilization techniques

The ability of this stable controller to achieve an  $\mathcal{H}_2$  performance nearly identical to that of the LQG controller was then explored. After running numerous examples,

it appears that a minimum phase open-loop stable plant (such as the first example) will yield a significant performance degradation when the controller is constrained to be stable. However, a minimum phase, open-loop unstable plant does not seem to exhibit this lack of performance, as demonstrated by this example. Further investigation seems to show that  $\mathcal{H}_2$ -optimal stable controllers designed for non-minimum phase, open-loop unstable plants will also show performance degradation over an LQG controller, whereas no appreciable loss of performance occurred when a  $\mathcal{H}_2$ -optimal stable controller was designed for a non-minimum phase, open-loop stable plant.

### 3.7. Conclusion

In this chapter we investigated a scheme to synthesize  $\mathcal{H}_2$ -optimal controllers by including the  $\mathcal{H}_2$  cost of the controller in the Lagrangian and using a multiobjective optimization technique. The problem was formulated in a decentralized static output feedback framework, which facilitated the use of a quasi-Newton optimization algorithm. This technique was applied to two numerical examples. It was numerically shown that for some systems, namely minimum phase, open-loop unstable or non-minimum phase, open-loop stable plants, a stable controller can rival the performance of an unstable  $\mathcal{H}_2$ -optimal LQG controller and yet not be constrained by the loop margins of unstable controllers. For other systems, however, there could be a significant degradation in performance by requiring the controller to remain stable, although this technique provided controllers yielding the minimal  $\mathcal{H}_2$  closed-loop cost for all stable linear controllers.

## CHAPTER 4

# $\mathcal{H}_2$ -Optimal Synthesis of Controllers with Relative Degree Two

### 4.1. Introduction

It is well known that modern multivariable control design frameworks such as  $\mathcal{H}_2$  and  $\mathcal{H}_\infty$  control yield dynamic compensators with relative degree zero or one. Hence, the structure of the dynamic feedback controller is such that the measured system output appears explicitly in the control signal or in the control rate signal [85]. In the single-input/single-output system case, the resulting controller transfer function is non-strictly proper with relative degree zero or strictly proper with relative degree one. In this case, the Bode plot of the controller transfer function at best rolls off at 20 dB per decade. Alternatively, for relative degree  $r$  controllers, the Bode plot of the compensator has a high frequency roll-off of  $20r$  dB per decade.

High frequency roll-off is particularly useful when the system under consideration is a lightly damped flexible structure. Since flexible structure models are by necessity truncated to a finite number of modes, it is desirable for the frequency response to roll off as quickly as possible after the gain crossover frequency so that unmodeled high frequency system dynamics are not excited by the controller dynamics.

For single-input/single-output systems, where the  $\mathcal{H}_2$  norm corresponds to the area under the Bode plot and the  $\mathcal{H}_\infty$  norm corresponds to the maximum magnitude of the Bode plot, roll-off rates cannot be specified solely by minimization techniques on these norms. Loop shaping weighting functions can be used in the controller design process, but these specify the frequency where the roll-off starts, not the roll-off rate. Furthermore, these techniques also tend to result in high-order controllers when frequency weighting is included in the design process. In this section we extend the fixed-structure controller design framework of [14, 95] and [34] to design  $\mathcal{H}_2$ -optimal relative degree two controllers for multi-input/multi-output systems. Since we cast the relative degree two design problem within the fixed-structure control framework, fixed-order (i.e., full- and reduced-order) controllers can be designed with increased roll-off rates at the gain crossover frequency. Even though the proposed framework can be easily extended to include desired weighting functions for loop shaping, we do not do so here to facilitate the presentation.

The proposed  $\mathcal{H}_2$ -optimal relative degree two controller design technique is applied to several structural control problems, showing that the resulting relative degree two controller incurs minimal increase in  $\mathcal{H}_2$  performance over the optimal LQG controller while enforcing a 20 dB per decade increase in the roll-off rate at the gain crossover frequency.

## 4.2. $\mathcal{H}_2$ -Optimal Relative Degree Two Control

In this section we state the  $\mathcal{H}_2$ -optimal relative degree two control problem. Specifically, given the  $n^{\text{th}}$ -order stabilizable and detectable system

$$\dot{x}(t) = Ax(t) + Bu(t) + D_1w(t), \quad t \in [0, \infty), \quad (4.1)$$

$$y(t) = Cx(t) + D_2w(t), \quad (4.2)$$

$$z(t) = E_1 x(t) + E_2 u(t), \quad (4.3)$$

determine an  $n_c^{\text{th}}$ -order relative degree two dynamic compensator

$$\dot{x}_{c1}(t) = A_{c1} x_{c1}(t) + B_{c1} y(t), \quad (4.4)$$

$$\dot{x}_{c2}(t) = A_{c2} x_{c2}(t) + B_{c2} v(t), \quad (4.5)$$

$$v(t) = C_{c1} x_{c1}(t), \quad (4.6)$$

$$u(t) = C_{c2} x_{c2}(t), \quad (4.7)$$

where  $x_{c1}(t) \in \mathbb{R}^{n_{c1}}$ ,  $x_{c2}(t) \in \mathbb{R}^{n_{c2}}$ , and  $n_c \triangleq n_{c1} + n_{c2}$ , such that the  $\mathcal{H}_2$  performance criterion

$$J(A_{c1}, A_{c2}, B_{c1}, B_{c2}, C_{c1}, C_{c2}) \triangleq \lim_{t \rightarrow \infty} \frac{1}{t} \mathbb{E} \int_0^t [x^T(s) R_1 x(s) + u^T(s) R_2 u(s)] ds, \quad (4.8)$$

is minimized.

Note that the dynamic controller (4.4)–(4.7) corresponds to a cascade interconnection of the two controllers in the feedback loop (see Figure 4.1) so that the controller transfer function realization is given by

$$G_c(s) = G_{c2} G_{c1}(s) \sim \left[ \begin{array}{c|c} A_c & B_c \\ \hline C_c & 0 \end{array} \right], \quad (4.9)$$

where

$$A_c \triangleq \begin{bmatrix} A_{c1} & 0 \\ B_{c2} C_{c1} & A_{c2} \end{bmatrix}, \quad B_c \triangleq \begin{bmatrix} B_{c1} \\ 0 \end{bmatrix}, \quad C_c \triangleq [0 \quad C_{c2}]. \quad (4.10)$$

Note that since  $B_{c2}$  is always multiplied with  $C_{c1}$ ,  $B_{c2} C_{c1}$  can be considered a single free parameter, thus leaving only five controller gains over which to optimize, instead of six. Finally, we note that this framework can be easily extended to address the design of (vector) relative degree  $r$  controllers by considering a cascade interconnection of  $r$  dynamic controllers in the feedback loop.

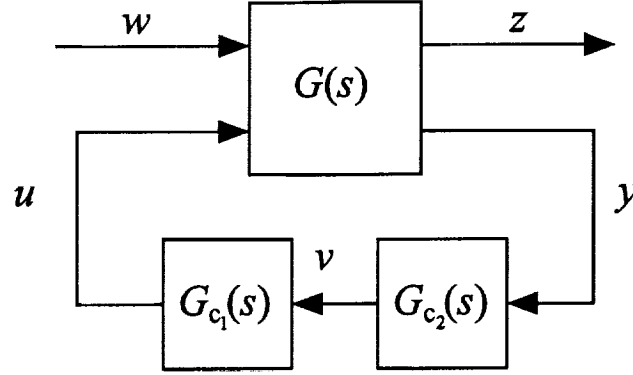


Figure 4.1: Relative degree two controller set-up

### 4.3. Relative Degree Two Controller Synthesis

In this section we use the decentralized static output feedback framework as described in Section 2.1 to design  $\mathcal{H}_2$ -optimal relative degree two dynamic compensators. Specifically, we define

$$\mathcal{K} \triangleq \text{block-diag}[A_{c_1}, A_{c_2}, B_{c_1}, B_{c_2}C_{c_1}, C_{c_2}].$$

Now, if  $\tilde{A}$  is asymptotically stable for a given feedback gain  $\mathcal{K} \in \mathbb{R}^{(2n_c+m) \times (2n_c+l)}$  it follows that the  $\mathcal{H}_2$  performance criterion (4.8) is given by

$$J(\mathcal{K}) = \|\tilde{G}_{zw}(s)\|_2^2 = \text{tr } \tilde{P}\tilde{V}, \quad (4.11)$$

where  $\tilde{P} \in \mathbb{N}^{\tilde{n}}$  is the unique nonnegative definite solution to the algebraic Lyapunov equation

$$0 = \tilde{A}^T \tilde{P} + \tilde{P} \tilde{A} + \tilde{R}. \quad (4.12)$$

Now, the necessary conditions for optimality can be derived by forming the Lagrangian

$$\mathcal{L}(\tilde{P}, \tilde{Q}, \mathcal{K}) = \text{tr} \left\{ \tilde{P}\tilde{V} + \tilde{Q} \left[ \tilde{A}^T \tilde{P} + \tilde{P} \tilde{A} + \tilde{R} \right] \right\}, \quad (4.13)$$

where  $\tilde{Q} \in \mathbb{N}^{\tilde{m}}$  is a Lagrange multiplier. The gradient expressions with respect to the free parameters in (4.13) are given by

$$\frac{\partial \mathcal{L}}{\partial \tilde{P}} = \tilde{A}\tilde{Q} + \tilde{Q}\tilde{A}^T + \tilde{V}, \quad (4.14)$$

$$\frac{\partial \mathcal{L}}{\partial \tilde{Q}} = \tilde{A}^T\tilde{P} + \tilde{P}\tilde{A} + \tilde{R}, \quad (4.15)$$

$$\frac{\partial \mathcal{L}}{\partial \mathcal{K}_i} = 2Q_{L_{ij}}^T \tau \left[ B_u^T \tilde{P} \tilde{Q} C_y^T + B_u^T \tilde{P} \tilde{D} D_{yw}^T + D_{zu}^T \tilde{E} \tilde{Q} C_y^T \right] L_{\mathcal{K}}^{-T} Q_{R_{ij}}^T, \quad (4.16)$$

$$i = 1, 2, 3, 4, 5, \quad j = 1,$$

where  $\tau = I + D_{yu}^T L_{\mathcal{K}}^{-T} \mathcal{K}^T$  and

$$\mathcal{K}_1 = A_{c_1}, \quad \mathcal{K}_2 = A_{c_2}, \quad \mathcal{K}_3 = B_{c_1}, \quad \mathcal{K}_4 = B_{c_2} C_{c_1}, \quad \mathcal{K}_5 = C_{c_2}.$$

## 4.4. Control Design Process

The initial stabilizing design for the relative degree two controller was obtained by computing the balanced truncation of the full-order LQG controller to obtain a reduced-order LQG controller corresponding to the controller in the feedback loop with the lower order. Note that since two controllers are being synthesized, it is not necessary for this first truncated controller to stabilize the system. This first designed controller was augmented to the plant. If  $G_{c_1}$  is designed first, the augmented plant realization is

$$\hat{G}(s) \sim \left[ \begin{array}{cc|cc} A & 0 & B & D_1 \\ B_{c_1}C & A_{c_1} & B_{c_1}D & B_{c_1}D_2 \\ \hline 0 & C & 0 & 0 \\ \hline E_1 & 0 & E_2 & E_0 \end{array} \right], \quad (4.17)$$

whereas if  $G_{c_2}$  is designed first, the augmented plant realization is

$$\hat{G}(s) \sim \left[ \begin{array}{cc|cc} A & BC_{c_2} & 0 & D_1 \\ 0 & A_{c_2} & B_{c_2} & 0 \\ \hline C & DC_{c_2} & 0 & D_2 \\ \hline E_1 & E_2C_{c_2} & 0 & E_0 \end{array} \right]. \quad (4.18)$$

Note that in the first case, the  $\hat{D}_2$  term is identically zero, whereas in the second case, the  $\hat{E}_2$  term is zero. Thus these augmented matrices result in a singular control problem. This was overcome by replacing these terms with nonzero matrices structured such that  $\hat{D}_1\hat{D}_2^T = 0$  or  $\hat{E}_1^T\hat{E}_2 = 0$ , as appropriate. Once an LQG controller was designed on this “artificial” system, the dynamics of the original system were tested, and if the closed-loop was asymptotically stable, these designed controllers were used as the initial controllers for the gradient search algorithm. For details of the algorithm, see [35].

## 4.5. Two-Mass Example

Consider a two-mass-spring-damper system with a colocated sensor/actuator pair and state space realization in real normal coordinates given by

$$\begin{aligned} \dot{x}(t) &= \begin{bmatrix} -0.0002 & 0.2208 & 0 & 0 \\ -0.2208 & -0.0002 & 0 & 0 \\ 0 & 0 & -0.0103 & 1.4320 \\ 0 & 0 & -1.4320 & -0.0103 \end{bmatrix} x(t) + \begin{bmatrix} -0.1439 \\ 0.2168 \\ -0.0426 \\ 1.1890 \end{bmatrix} u(t), \\ y(t) &= \begin{bmatrix} -0.0545 & 0.0819 & -0.0352 & 0.8181 \end{bmatrix} x(t). \end{aligned}$$

The weighting matrices  $D_1$ ,  $D_2$ ,  $E_1$ , and  $E_2$  were chosen so that LQG synthesis would place a notch at the second mode. This is accomplished when [40]

$$D_1 = \begin{bmatrix} 0 & 0 \\ 1 & 0 \\ 0 & 0 \\ 0 & 0 \end{bmatrix}, \quad D_2 = \begin{bmatrix} 0 & 1 \end{bmatrix}, \quad E_1 = \begin{bmatrix} 1 & 0 & 0 & 0 \\ 0 & 0 & 0 & 0 \end{bmatrix}, \quad E_2 = \begin{bmatrix} 0 \\ 1 \end{bmatrix}.$$

For this system, the two controllers in the feedback loop ( $G_{c_1}$  and  $G_{c_2}$ ) were chosen to be of order two. Initializing reduced-order LQG controllers were designed, and the gradient search algorithm was initiated. The Bode plots of the loop gain of the full-order LQG controller and of the relative degree two controller, along with dotted lines representing the respective high frequency asymptotes, are shown in Figure 4.2. The

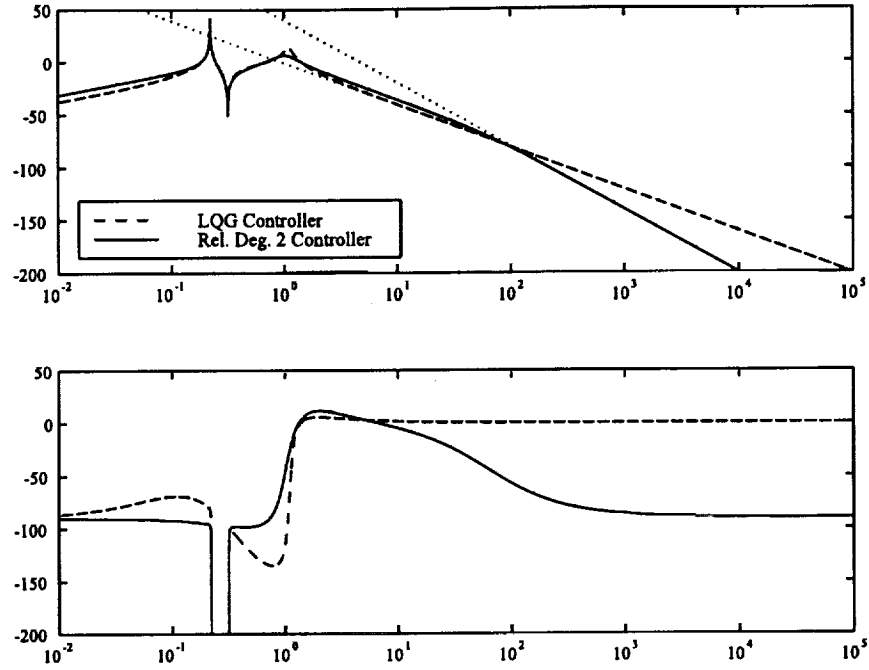


Figure 4.2: Bode plots of LQG and relative degree two controllers

$\mathcal{H}_2$ -optimal LQG cost is 3.9734 and the  $\mathcal{H}_2$ -optimal relative degree two controller is 4.0743 which corresponds to only a 2.5% increase over the  $\mathcal{H}_2$ -optimal LQG controller cost. This marginal increase in the  $\mathcal{H}_2$  cost is not surprising since  $\mathcal{H}_2$ -optimal relative degree two controllers are sought.

The transfer function for the LQG controller is

$$G_{c(\text{LQG})}(s) = \frac{-0.9090s^3 - 0.1073s^2 - 1.8660s - 0.1817}{s^4 + 0.3629s^3 + 1.2425s^2 + 0.6170s + 0.1443},$$

which has natural frequencies at 0.345 rad/sec and 1.10 rad/sec. The relative degree two controller transfer function is given by

$$G_{c(\text{Rel. Deg. 2})}(s) = \frac{-99.9827s^2 - 2.0960s - 205.2481}{s^4 + 64.6193s^3 + 46.1170s^2 + 34.9138s + 77.6907}.$$

This transfer function has a natural frequency at 1.02 rad/sec and break frequencies at 0.862 rad/sec and 0.015 rad/sec. Thus it is seen in this case that constraining the

controller to be of relative degree two does not push the controller poles out to such high frequencies that the extra 20 dB/decade roll-off is not useful.

## 4.6. Three Mass Example

Consider the three-mass system given by the state-space realization ([52])

$$\begin{aligned} \dot{x}(t) &= \begin{bmatrix} 0 & 0 & 0 & 1 & 0 & 0 \\ 0 & 0 & 0 & 0 & 1 & 0 \\ 0 & 0 & 0 & 0 & 0 & 1 \\ -1 & 1 & 0 & 0 & 0 & 0 \\ 1 & -2 & 1 & 0 & 0 & 0 \\ 0 & 1 & -1 & 0 & 0 & 0 \end{bmatrix} x(t) + \begin{bmatrix} 0 \\ 0 \\ 0 \\ 0 \\ 0 \\ 1 \end{bmatrix} u(t), \\ y(t) &= [1 \ 1 \ 0 \ 0 \ 0 \ 0] x(t). \end{aligned}$$

The weighting matrices  $D_1$ ,  $D_2$ ,  $E_1$ , and  $E_2$  are chosen to be

$$D_1 = \begin{bmatrix} 0 & 0 \\ 0 & 0 \\ 0 & 0 \\ 1 & 0 \\ 0 & 0 \\ 0 & 0 \end{bmatrix}, \quad D_2 = [0 \ 1], \quad E_1 = \begin{bmatrix} 1 & 1 & 0 & 0 & 0 & 0 \\ 0 & 0 & 0 & 0 & 0 & 0 \end{bmatrix}, \quad E_2 = \begin{bmatrix} 0 \\ 1 \end{bmatrix}.$$

For this system, two different relative degree two controllers were designed. The first was designed with the first controller in the feedback loop of order two and the second of order four. The Bode plots of the loop gain of the full-order LQG controller and of this relative degree two controller are shown in Figure 4.3. Again, the increase in the  $\mathcal{H}_2$  cost is only 9% above the optimal value.

The transfer function for the LQG controller is

$$G_{c(\text{LQG})}(s) = \frac{-2.4070s^5 - 0.1479s^4 - 10.1266s^3 - 1.3616s^2 - 8.3374s - 2.000}{s^6 + 3.1221s^5 + 8.8738s^4 + 15.8141s^3 + 21.5012s^2 + 17.8508s + 13.3444},$$

which has natural frequencies at 1.30 rad/sec, 1.55 rad/sec, and 1.82 rad/sec. The relative degree two controller transfer function is given by

$$G_{c(\text{RD } 2)}(s) = \frac{-332.2810s^4 - 11569s^3 - 679770s^2 - 1186900s - 293090}{s^6 + 182.4514s^5 + 12699s^4 + 392630s^3 + 4634100s^2 + 3606700s + 2212100}.$$

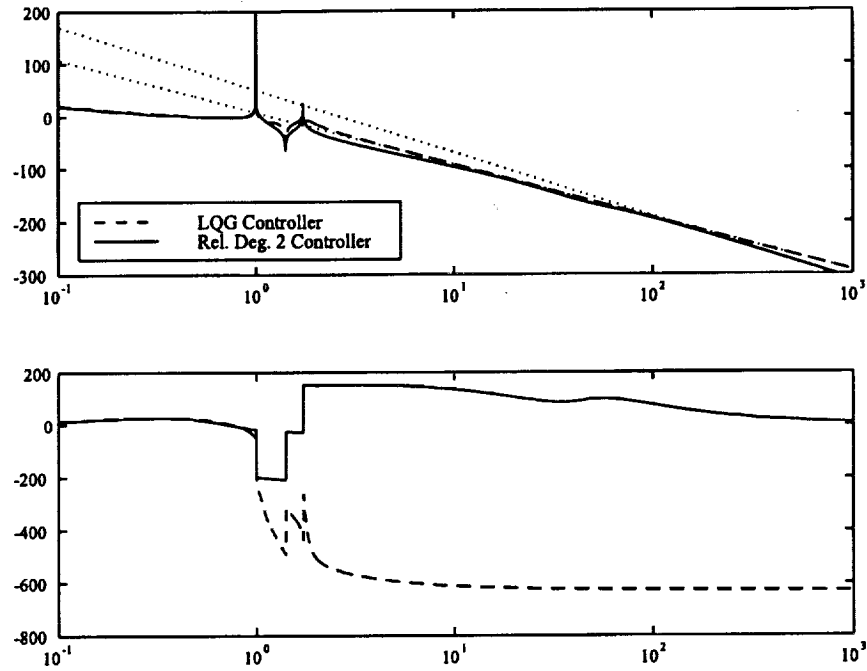


**Figure 4.3:** Bode plots of LQG and relative degree two controllers

This transfer function has natural frequencies at 0.715 rad/sec, 34.6 rad/sec, and 60.1 rad/sec. In this case, the relative degree two controller does have much higher frequency poles, so that the extra 20 dB/decade roll-off does not occur until higher frequencies are encountered, as seen in the figure.

The second relative degree two controller was designed with the first controller in the feedback loop of order four and the second of order two. The Bode plots of the loop gain of the full-order LQG controller and of this relative degree two controller are shown in Figure 4.4. For this configuration, however, the  $\mathcal{H}_2$  cost of the relative degree two controller is less than that of the first relative degree two controller designed. In particular, the increase in the  $\mathcal{H}_2$  cost for this controller is only 2.9% above the optimal value.

The transfer function of this relative degree two controller is

$$G_{c(RD2)}(s) = \frac{-130.3438s^4 - 582.6117s^3 - 258.0451s^2 - 679.4487s - 176.8302}{s^6 + 56.0271s^5 + 811.7752s^4 + 1118.0s^3 + 2196.9s^2 + 1630.2s + 1186.4}$$

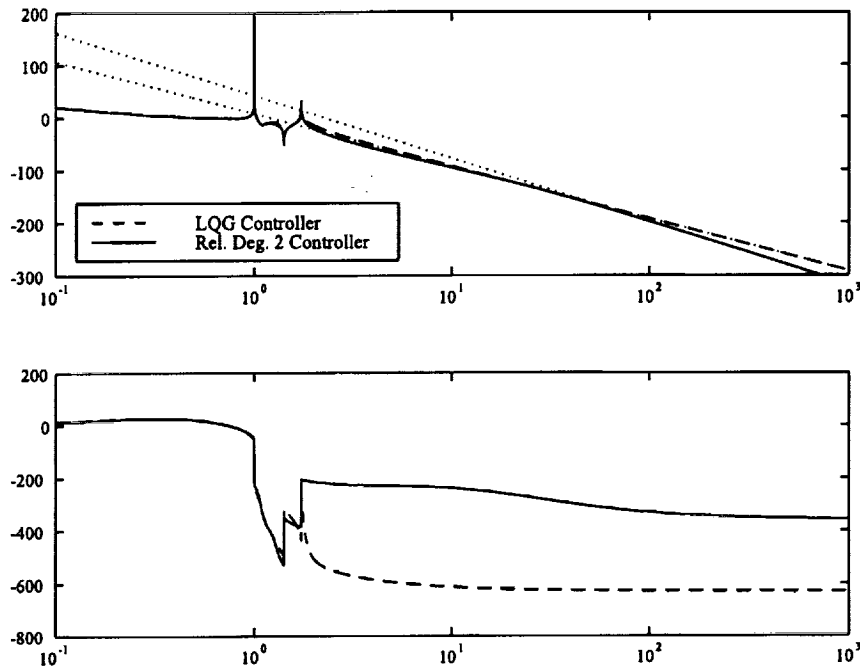


Figure 4.4: Bode plots of LQG and relative degree two controllers

which has natural frequencies at 0.975 rad/sec and 1.30 rad/sec, and break frequencies at 0.0417 rad/sec and 0.0326 rad/sec. In this case, the relative degree two controller does not have higher frequency poles, so that the roll-off is more pronounced than in the first configuration.

## 4.7. Coupled Rotating Disk Example

Consider the coupled rotating disk problem given in [22] with state space realization in real normal coordinates given by

$$\dot{x}(t) = \begin{bmatrix} -0.1610 & 1 & 0 & 0 & 0 & 0 & 0 & 0 \\ -6.0040 & 0 & 1 & 0 & 0 & 0 & 0 & 0 \\ -0.5822 & 0 & 0 & 1 & 0 & 0 & 0 & 0 \\ -9.9835 & 0 & 0 & 0 & 1 & 0 & 0 & 0 \\ -0.4073 & 0 & 0 & 0 & 0 & 1 & 0 & 0 \\ -3.9820 & 0 & 0 & 0 & 0 & 0 & 1 & 0 \\ 0 & 0 & 0 & 0 & 0 & 0 & 0 & 1 \\ 0 & 0 & 0 & 0 & 0 & 0 & 0 & 0 \end{bmatrix} x(t) + \begin{bmatrix} 0 \\ 0 \\ 0.00640 \\ 0.00235 \\ 0.07130 \\ 1.00020 \\ 0.10450 \\ 0.99550 \end{bmatrix} u(t),$$

$$y(t) = [1 \ 0 \ 0 \ 0 \ 0 \ 0 \ 0 \ 0] x(t).$$

The weighting matrices  $D_1$ ,  $D_2$ ,  $E_1$ , and  $E_2$  are chosen to be

$$D_1 = \begin{bmatrix} 0 & 0 \\ 0 & 0 \\ 0.00640 & 0 \\ 0.00235 & 0 \\ 0.07130 & 0 \\ 1.00020 & 0 \\ 0.10450 & 0 \\ 0.99550 & 0 \end{bmatrix}, \quad D_2 = [0 \ 1], \quad E_1 = \begin{bmatrix} 0 & 0 \\ 0 & 0 \\ 0 & 0 \\ 0.00055 & 0 \\ 0.01100 & 0 \\ 0.00132 & 0 \\ 0.01800 & 0 \end{bmatrix}^T, \quad E_2 = \begin{bmatrix} 0 \\ 1 \end{bmatrix}.$$

For this system, two different relative degree two controllers were designed. The first was designed with the first controller in the feedback loop of order two and the second of order six. The Bode plots of the loop gain of the full-order LQG controller and of this relative degree two controller are shown in Figure 4.5. Here, the increase in the

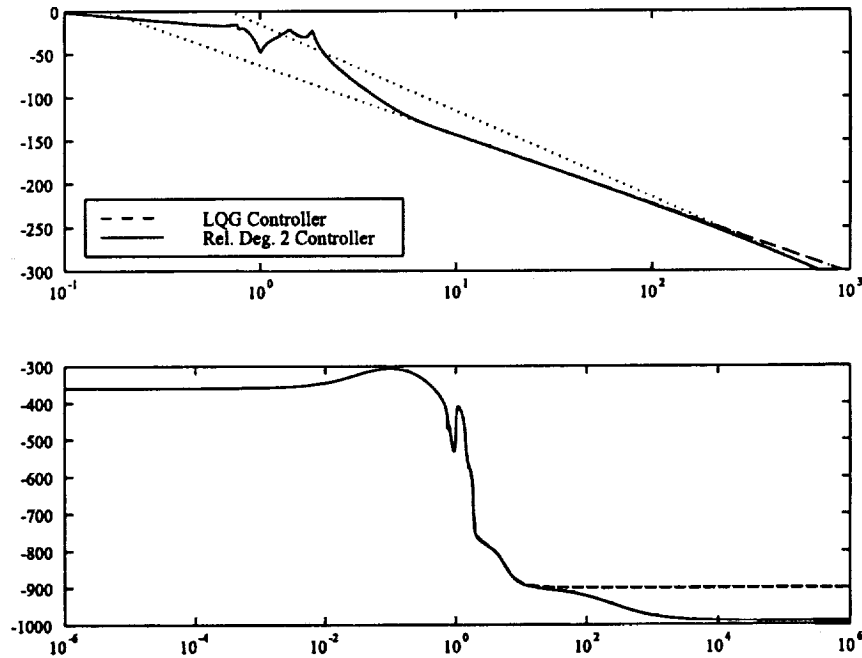


**Figure 4.5:** Bode plots of LQG and relative degree two controllers

$\mathcal{H}_2$  cost is a scant 0.0238% above the optimal value.

The transfer function for the LQG controller is

$$G_{c(\text{LQG})}(s) = \frac{-0.1102s^7 - 0.0210s^6 - 0.6637s^5 - 0.0843s^4 - 1.1105s^3 - 0.0793s^2 - 0.4500s - 0.0152}{s^8 + 1.3183s^7 + 6.8596s^6 + 7.3937s^5 + 14.1279s^4 + 11.4920s^3 + 9.2199s^2 + 4.5193s + 1.3859}$$

which has natural frequencies at 0.548 rad/sec, 0.820 rad/sec, 1.41 rad/sec, and 1.86 rad/sec. The relative degree two controller transfer function is given by

$$G_{c(\text{RD } 2)}(s) = \frac{-28.0400s^6 - 8051.5s^5 - 1122.6s^4 - 20797s^3 - 1486.7s^2 - 9550.1s - 321.8893}{s^8 + 569.3318s^7 + 75307s^6 + 93453s^5 + 244920s^4 + 215410s^3 + 186610s^2 + 95718s + 29437}$$

This transfer function has natural frequencies at 0.549 rad/sec, 0.819 rad/sec, and 1.40 rad/sec, and break frequencies at 0.00485 rad/sec and 0.00276 rad/sec.

The second relative degree two controller was designed with the first controller in the feedback loop of order six and the second of order two. The Bode plots of the loop gain of the full-order LQG controller and of this relative degree two controller are shown in Figure 4.6. For this configuration, however, the  $\mathcal{H}_2$  cost of the relative degree

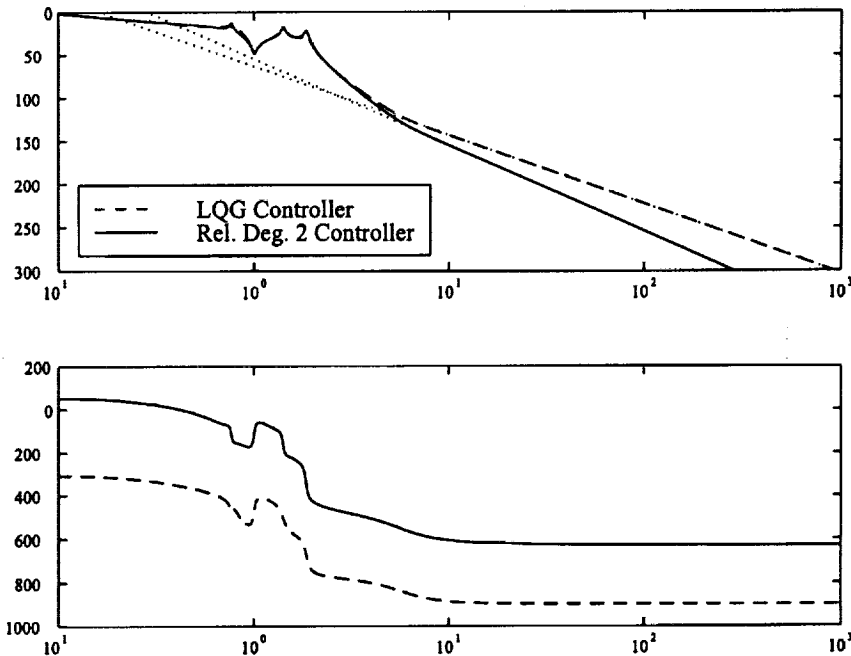


Figure 4.6: Bode plots of LQG and relative degree two controllers

two controller is slightly more than that of the first relative degree two controller

designed, but the increase in the  $\mathcal{H}_2$  cost for this controller is only 0.864% above the optimal value.

The transfer function of this relative degree two controller is

$$G_{c(\text{RD } 2)}(s) = \frac{-0.2916s^6 - 0.1042s^5 - 0.7773s^4 - 0.1187s^3 - 0.3535s^2 - 0.0118s - 2.9883 \times 10^{-11}}{s^8 + 3.1635s^7 + 7.3610s^6 + 10.8948s^5 + 11.4236s^4 + 8.2630s^3 + 3.9038s^2 + 1.0973s + 2.0906 \times 10^{-9}},$$

which has natural frequencies at 0.548 rad/sec, 0.820 rad/sec, 1.41 rad/sec, and 1.86 rad/sec.

## 4.8. Conclusion

In this chapter we proposed a scheme to synthesize  $\mathcal{H}_2$ -optimal relative degree two controllers by cascading two controllers in the feedback loop and optimizing over the five free controller parameters. The problem was formulated in a decentralized static output feedback framework, which facilitated the use of a quasi-Newton optimization algorithm. This technique was applied to three numerical examples. It was shown that constraining the controller to have a relative degree of at least two only marginally increased the  $\mathcal{H}_2$  cost of the closed-loop system, though it was noted that the order of the separate controllers in the feedback loop does significantly affect the  $\mathcal{H}_2$  cost of the closed-loop system and the natural frequencies and break frequencies of the controller dynamics.



# CHAPTER 5

## Robust Fixed-Structure Controller Synthesis using the Implicit Small Gain Bound

### 5.1. Introduction

One of the principal objectives of robust control theory is to synthesize feedback controllers with *a priori* guarantees of robust stability and performance. In  $\mu$ -synthesis [37, 97] these guarantees are achieved by means of bounds involving frequency-dependent scales and multipliers which account for the structure of the uncertainty as well as its real or complex nature. An alternative robustness approach involves bounding the effect of real or complex uncertain parameters on the  $\mathcal{H}_2$  performance of the closed-loop system. These guaranteed cost bounds take the form of modifications to the usual Lyapunov equation to provide bounds for robust stability and  $\mathcal{H}_2$  performance.

A diverse collection of guaranteed cost bounds have been developed. An overview of many of the early guaranteed cost bounds can be found in [12], while positive-real-type guaranteed cost bounds are discussed in [47]. More recently, Popov-type guaranteed cost bounds have provided links with frequency-dependent scales and multipliers while providing reliable bounds for the peak real structured singular value

[15, 52, 106]. Finally, the introduction of shift terms has been shown to reduce the conservatism of guaranteed cost bounds [38, 54, 74] for structured real uncertainty without requiring frequency-dependent scales and multipliers.

The goal of this research is to explore the applicability of the implicit small gain guaranteed cost bound of [54] to controller synthesis. As shown in [54], unlike the quadratic stability bounded-real type bound of [76, 100], the implicit small gain bound can distinguish between real and complex uncertainty and is particularly effective in capturing internal uncertainty structure. For flexibility in controller synthesis, we adopt the approach of fixed-structure controller synthesis [62] which allows consideration of arbitrary controller structures, including order, internal structure, and decentralization [34].

To demonstrate the fixed-structure/implicit small gain approach to robust controller synthesis, we consider two examples that have been addressed by means of alternative guaranteed cost bounds. The first example, which involves two flexible modes, was used in [40] to illustrate the Maximum Entropy technique, while the second example, which involves three flexible modes, was considered in [52, 106] to illustrate fixed-structure Popov synthesis.

## 5.2. Robust Stability and Performance Problem

In this section we state the robust stability and performance problem. This problem involves a set  $\mathcal{U} \subset \mathbb{R}^{n \times n}$  of uncertain perturbations  $da$  of the nominal system matrix  $A$ . The objective of this problem is to determine a fixed-order, strictly proper dynamic compensator  $(A_c, B_c, C_c)$  that stabilizes the plant for all variations in  $\mathcal{U}$  and minimizes the worst-case  $\mathcal{H}_2$  norm of the closed-loop system. In this section and the following section no explicit structure is assumed for the elements of  $\mathcal{U}$ . In Section 5.4

the structure of  $\mathcal{U}$  will be specified.

**Robust Stability and Performance Problem.** Given the  $n^{\text{th}}$ -order stabilizable and detectable system

$$\dot{x}(t) = (A + \Delta A)x(t) + Bu(t) + D_1w(t), \quad t \in [0, \infty), \quad (5.1)$$

$$y(t) = Cx(t) + D_2w(t), \quad (5.2)$$

determine an  $n_c^{\text{th}}$ -order dynamic compensator

$$\dot{x}_c(t) = A_c x_c(t) + B_c y(t), \quad (5.3)$$

$$u(t) = C_c x_c(t), \quad (5.4)$$

such that the closed-loop system (5.1)–(5.4) is asymptotically stable for all  $\Delta A \in \mathcal{U}$  and the performance criterion

$$J(A_c, B_c, C_c) \triangleq \sup_{\Delta A \in \mathcal{U}} \limsup_{t \rightarrow \infty} \frac{1}{t} \mathbb{E} \int_0^t [x^T(s)R_1x(s) + u^T(s)R_2u(s)] ds, \quad (5.5)$$

is minimized.

For each uncertain variation  $\Delta A \in \mathcal{U}$ , the closed-loop system (5.1)–(5.4) can be written as

$$\dot{\tilde{x}}(t) = (\tilde{A} + \Delta \tilde{A})\tilde{x}(t) + \tilde{D}w(t), \quad t \in [0, \infty), \quad (5.6)$$

where  $\Delta \tilde{A} \triangleq \begin{bmatrix} \Delta A & 0 \\ 0 & 0 \end{bmatrix}$ .

### 5.3. Sufficient Conditions for Robust Stability and Performance

In practice, steady-state performance is only of interest when the undisturbed closed-loop system is robustly stable over  $\mathcal{U}$ . The following result is immediate.

**Lemma 5.1.** Let  $(A_c, B_c, C_c)$  be given and assume that  $\tilde{A} + \Delta \tilde{A}$  is asymptotically

stable for all  $\Delta A \in \mathcal{U}$ . Then

$$J(A_c, B_c, C_c) = \sup_{\Delta A \in \mathcal{U}} \text{tr } \tilde{P}_{\Delta \tilde{A}} \tilde{V}, \quad (5.7)$$

where  $\tilde{P}_{\Delta \tilde{A}} \in \mathbb{N}^{\tilde{n}}$  is the unique nonnegative definite solution to

$$0 = (\tilde{A} + \Delta \tilde{A})^T \tilde{P}_{\Delta \tilde{A}} + \tilde{P}_{\Delta \tilde{A}} (\tilde{A} + \Delta \tilde{A}) + \tilde{R}. \quad (5.8)$$

The key step in guaranteeing robust stability and performance is to replace the uncertain terms in the Lyapunov equation (5.8) by a bounding function  $\Omega$ .

**Theorem 5.1** [12]. Let  $(A_c, B_c, C_c)$  be given, let  $\Omega : \mathbb{N}^{\tilde{n}} \rightarrow \mathbb{S}^{\tilde{n}}$  be such that

$$\Delta \tilde{A}^T \tilde{P} + \tilde{P} \Delta \tilde{A} \leq \Omega(\tilde{P}), \quad \Delta A \in \mathcal{U}, \quad \tilde{P} \in \mathbb{N}^{\tilde{n}}, \quad (5.9)$$

and suppose there exists  $\tilde{P} \in \mathbb{N}^{\tilde{n}}$  satisfying

$$0 = \tilde{A}^T \tilde{P} + \tilde{P} \tilde{A} + \Omega(\tilde{P}) + \tilde{R}. \quad (5.10)$$

Then  $(\tilde{A} + \Delta \tilde{A}, \tilde{E})$  is detectable for all  $\Delta A \in \mathcal{U}$  if and only if  $\tilde{A} + \Delta \tilde{A}$  is asymptotically stable for all  $\Delta A \in \mathcal{U}$ . In this case,

$$\tilde{P}_{\Delta \tilde{A}} \leq \tilde{P}, \quad \Delta A \in \mathcal{U}, \quad (5.11)$$

where  $\tilde{P}_{\Delta \tilde{A}}$  is given by (5.8), and

$$J(A_c, B_c, C_c) \leq \text{tr } \tilde{P} \tilde{V}. \quad (5.12)$$

## 5.4. Uncertainty Structure and the Implicit Small Gain Guaranteed Cost Bound

We now assign explicit structure to the set  $\mathcal{U}$  and bounding function  $\Omega(\tilde{P})$ . Specifically, the uncertainty set  $\mathcal{U}$  is defined by

$$\mathcal{U} = \left\{ \Delta A \in \mathbb{R}^{n \times n} : \Delta A = \sum_{i=1}^r \delta_i A_i, |\delta_i| \leq \gamma^{-1}, i = 1, \dots, r \right\}, \quad (5.13)$$

where  $\gamma$  is a positive number and, for  $i = 1, \dots, r$ ,  $A_i \in \mathbb{R}^{n \times n}$  is a fixed matrix denoting the structure of the parametric uncertainty and  $\delta_i$  is an uncertain real parameter. Note that  $\mathcal{U}$  given by (5.13) includes repeated parameters without loss of generality. For example, if  $\delta_1 = \delta_2$  then replace  $A_1$  with  $A_1 + A_2$  and discard  $\delta_2$  and  $A_2$ . Furthermore,  $\mathcal{U}$  includes real full block uncertainty. For example, if  $\Delta A = \begin{bmatrix} \delta_1 & \delta_2 \\ \delta_3 & \delta_4 \end{bmatrix}$ , then  $\Delta A = \sum_{i=1}^4 \delta_i A_i$ , where  $A_1 = \begin{bmatrix} 1 & 0 \\ 0 & 0 \end{bmatrix}$  and likewise for  $A_2, A_3$ , and  $A_4$ . Finally, for  $i = 1, \dots, r$ , letting  $A_i = B_i C_i$ , where  $B_i \in \mathbb{R}^{n \times q_i}$ ,  $C_i \in \mathbb{R}^{q_i \times n}$ , and  $q_i \leq n$ , and defining  $B_0 \triangleq [B_1 \ \dots \ B_r]$  and  $C_0 \triangleq [C_1^T \ \dots \ C_r^T]^T$ ,  $\mathcal{U}$  can be written as the real parameter uncertainty set considered in [37]

$$\mathcal{U} \triangleq \{ \Delta A \in \mathbb{R}^{n \times n} : \Delta A = B_0 \Delta C_0, \Delta \in \Delta_\gamma \}, \quad (5.14)$$

where

$$\Delta_\gamma \triangleq \{ \Delta \in \mathbb{R}^{q \times q} : \Delta = \text{block-diag}[\delta_1 I_{q_1}, \dots, \delta_r I_{q_r}], |\delta_i| \leq \gamma^{-1}, i = 1, \dots, r \}, \quad (5.15)$$

and where  $q \triangleq \sum_{i=1}^r q_i$ . Since an uncertainty set of the form (5.14) can always be written in the form of (5.13) by partitioning  $B_0$  and  $C_0$  as above and defining  $A_i \triangleq B_i C_i$ ,  $i = 1, \dots, r$ , robust stability of  $\tilde{A} + \Delta \tilde{A}$  for all  $\Delta A \in \mathcal{U}$  is equivalent to the robust stability of the feedback interconnection of  $\tilde{G}(s) \triangleq \tilde{C}_0 (sI_{\tilde{n}} - \tilde{A})^{-1} \tilde{B}_0$  and  $\Delta$ , where  $\tilde{B}_0 \triangleq [B_0^T \ 0]^T$ ,  $\tilde{C}_0 \triangleq [C_0 \ 0]$ , and  $\Delta \in \Delta_\gamma$ .

With the uncertainty set  $\mathcal{U}$  given by (5.13), the closed-loop system (5.6) has structured uncertainty of the form

$$\Delta \tilde{A} = \sum_{i=1}^r \delta_i \tilde{A}_i, \quad (5.16)$$

where

$$\tilde{A}_i \triangleq \begin{bmatrix} A_i & 0 \\ 0 & 0 \end{bmatrix}, \quad i = 1, \dots, r.$$

We now introduce a specific choice of the bound  $\Omega(\tilde{P})$  satisfying (5.9) for the structure of  $\mathcal{U}$  as specified by (5.13). For  $i = 1, \dots, r$ , let  $\tilde{S}_i \in \mathbb{R}^{\tilde{n} \times \tilde{n}}$  and define

$$\tilde{Z}_i \triangleq [(\tilde{S}_i + \tilde{S}_i^T)^2]^{\frac{1}{2}}.$$

Note that  $-\tilde{Z}_i \leq \alpha(\tilde{S}_i + \tilde{S}_i^T) \leq \tilde{Z}_i$  for all  $\alpha \in [-1, 1]$ . If  $\tilde{S}_i$  is skew symmetric then  $\tilde{Z}_i = 0$ . Furthermore, for  $i = 1, \dots, r$ , define  $\tilde{I}_i \triangleq [\tilde{S}_i \quad \tilde{A}_i^T][\tilde{S}_i \quad \tilde{A}_i^T]^\dagger$ , where  $(\cdot)^\dagger$  denotes the Moore-Penrose generalized inverse. Note that  $\tilde{I}_i$  is symmetric and idempotent, that is,  $\tilde{I}_i = \tilde{I}_i^T = \tilde{I}_i^2$ . Furthermore, since  $\tilde{I}_i[\tilde{S}_i \quad \tilde{A}_i^T] = [\tilde{S}_i \quad \tilde{A}_i^T]$ , it follows that  $\tilde{I}_i\tilde{S}_i = \tilde{S}_i$  and  $\tilde{A}_i\tilde{I}_i = \tilde{A}_i$ . If  $\tilde{S}_i = \tilde{A}_i$  and  $\tilde{A}_i$  is an EP matrix [21], that is,  $\mathcal{R}(\tilde{A}_i) = \mathcal{R}(\tilde{A}_i^T)$ , then  $\tilde{I}_i = \tilde{A}_i^\dagger\tilde{A}_i$ . Recall that normal matrices (and thus symmetric and skew-symmetric matrices) are EP.

**Proposition 5.1** [54]. For  $i = 1, \dots, r$ , let  $\alpha_i \in \mathbb{R}$ ,  $\beta_i > 0$ , and let  $\tilde{S}_i \in \mathbb{R}^{\tilde{n} \times \tilde{n}}$ . Then (5.9) is satisfied with  $\Omega(\tilde{P})$  given by

$$\Omega(\tilde{P}) = \sum_{i=1}^r \left[ \gamma^{-2}(\alpha_i\tilde{S}_i + \beta_i\tilde{A}_i^T\tilde{P})^T(\alpha_i\tilde{S}_i + \beta_i\tilde{A}_i^T\tilde{P}) + \gamma^{-1}\beta_i^{-1}|\alpha_i|\tilde{Z}_i + \beta_i^{-2}\tilde{I}_i \right]. \quad (5.17)$$

**Remark 5.1.** As discussed in [54], if  $\delta_i$  is assumed to be complex for some  $i$ , then it can be shown that  $\Omega(\tilde{P})$  given by (5.17) does *not* satisfy (5.9). Hence, unlike the quadratic stability bound of [76, 100], the bound (5.17) can distinguish between real and complex uncertainty.

Combining Theorem 5.1 with Proposition 5.1 yields the following result. For convenience define the shifted dynamics matrix  $\tilde{A}_{s\gamma} \triangleq \tilde{A} + \gamma^{-2} \sum_{i=1}^r \alpha_i \beta_i \tilde{A}_i \tilde{S}_i$ .

**Theorem 5.2.** For  $i = 1, \dots, r$ , let  $\alpha_i \in \mathbb{R}$ ,  $\beta_i > 0$ , and let  $\tilde{S}_i \in \mathbb{R}^{\tilde{n} \times \tilde{n}}$ . Furthermore, suppose there exists a matrix  $\tilde{P} \in \mathbb{N}^{\tilde{n}}$  satisfying

$$0 = \tilde{A}_{s\gamma}^T \tilde{P} + \tilde{P} \tilde{A}_{s\gamma} + \sum_{i=1}^r \left[ \gamma^{-2}(\alpha_i^2 \tilde{S}_i^T \tilde{S}_i + \beta_i^2 \tilde{P} \tilde{A}_i \tilde{A}_i^T \tilde{P}) + \gamma^{-1} \beta_i^{-1} |\alpha_i| \tilde{Z}_i + \beta_i^{-2} \tilde{I}_i \right] + \tilde{R}. \quad (5.18)$$

Then  $(\tilde{A} + \Delta\tilde{A}, \tilde{E})$  is detectable for all  $\Delta A \in \mathcal{U}$  if and only if  $\tilde{A} + \Delta\tilde{A}$  is asymptotically stable for all  $\Delta A \in \mathcal{U}$ . In this case,

$$\tilde{P}_{\Delta\tilde{A}} \leq \tilde{P}, \quad \Delta A \in \mathcal{U}, \quad (5.19)$$

where  $\tilde{P}_{\Delta\tilde{A}}$  satisfies (5.8), and

$$J(A_c, B_c, C_c) \leq \text{tr } \tilde{P}\tilde{V}. \quad (5.20)$$

**Remark 5.2.** If  $\tilde{A}_{s\gamma}$  is asymptotically stable then the existence of a matrix  $\tilde{P} \in \mathbb{N}^n$  satisfying (5.18) is equivalent to the existence of a frequency-domain condition guaranteeing robust stability of  $\tilde{A} + \Delta\tilde{A}$ ,  $\Delta A \in \mathcal{U}$ , in terms of an *implicit* small gain condition involving the shifted dynamics matrix  $\tilde{A}_{s\gamma}$  which is a function of the uncertainty set bound  $\gamma$ . For details see [54].

To apply Theorem 5.2 to controller synthesis, we use the Riccati equation (5.18) to guarantee that the closed-loop system is robustly stable. This leads to the following optimization problem.

**Optimization Problem.** Determine  $(A_c, B_c, C_c)$  that minimizes  $\mathcal{J}(A_c, B_c, C_c) \triangleq \text{tr } \tilde{P}\tilde{V}$ , where  $\tilde{P} \in \mathbb{N}^n$  satisfies (5.18) and such that  $(A_c, B_c, C_c)$  is controllable and observable.

The relationship between the Optimization Problem and the Robust Stability and Performance Problem is straightforward, as shown by the following proposition.

**Proposition 5.2.** Let  $(A_c, B_c, C_c)$  be given. If  $\tilde{P} \in \mathbb{N}^n$  satisfies (5.18) and  $(\tilde{A} + \Delta\tilde{A}, \tilde{E})$  is detectable for all  $\Delta A \in \mathcal{U}$ , then  $\tilde{A} + \Delta\tilde{A}$  is asymptotically stable for all  $\Delta A \in \mathcal{U}$ , and  $J(A_c, B_c, C_c) \leq \mathcal{J}(A_c, B_c, C_c)$ .

**Proof.** Since (5.18) has a solution  $\tilde{P} \in \mathbb{N}^n$  and  $(\tilde{A} + \Delta\tilde{A}, \tilde{E})$  is detectable for all  $\Delta A \in \mathcal{U}$ , the hypotheses of Theorem 5.2 are satisfied so that robust stability and

robust performance are guaranteed. Now,  $J(A_c, B_c, C_c) \leq \mathcal{J}(A_c, B_c, C_c)$  is merely a restatement of (5.20).  $\square$

It follows from Proposition 5.2 that the satisfaction of (5.18) along with the generic detectability condition leads to robust stability along with an upper bound for the  $\mathcal{H}_2$  performance. Hence, by deriving necessary conditions for the Optimization Problem we obtain sufficient conditions for characterizing dynamic output feedback controllers guaranteeing robust stability and performance.

## 5.5. Robust Controller Synthesis via the Implicit Small Gain Guaranteed Cost Bound

In this section we state constructive sufficient conditions for characterizing fixed-order (i.e., full- and reduced-order) robust controllers. These results are obtained by minimizing the worst-case  $\mathcal{H}_2$  cost bound (5.20) subject to (5.18). The following result is required for the statement of the main theorem.

**Lemma 5.2** [62]. Let  $\hat{Q}, \hat{P} \in \mathbb{N}^n$  and suppose that  $\text{rank } \hat{Q}\hat{P} = n_c$ . Then there exist  $n_c \times n$  matrices  $G, \Gamma$  and an invertible matrix  $M \in \mathbb{R}^{n_c \times n_c}$ , unique except for a change of basis in  $\mathbb{R}^{n_c}$ , such that

$$\hat{Q}\hat{P} = G^T M \Gamma, \quad \Gamma G^T = I_{n_c}. \quad (5.21)$$

Furthermore, the  $n \times n$  matrices  $\tau \triangleq G^T \Gamma$  and  $\tau_\perp \triangleq I_n - \tau$  are idempotent and have rank  $n_c$  and  $n - n_c$ , respectively.

To apply Theorem 5.2 to robust controller synthesis, let  $\tilde{S}_i, i = 1, \dots, r$ , have the form

$$\tilde{S}_i = \begin{bmatrix} S_i & 0_{n \times n_c} \\ 0_{n_c \times n} & 0_{n_c \times n_c} \end{bmatrix}, \quad (5.22)$$

where  $S_i \in \mathbb{R}^{n \times n}$ . With  $\tilde{S}_i, i = 1, \dots, r$ , given by (5.22) it can be shown that

$$\tilde{I}_i = \begin{bmatrix} \hat{I}_i & 0_{n \times n_c} \\ 0_{n_c \times n} & 0_{n_c \times n_c} \end{bmatrix}, \quad \tilde{Z}_i = \begin{bmatrix} Z_i & 0_{n \times n_c} \\ 0_{n_c \times n} & 0_{n_c \times n_c} \end{bmatrix},$$

where  $\hat{I}_i = [S_i \ A_i^T][S_i \ A_i^T]^\dagger$  and  $Z_i = [(S_i + S_i^T)^2]^\frac{1}{2}$ . Furthermore, for convenience in stating the main theorem, define the notation

$$A_{s\gamma} = A + \gamma^{-2} \sum_{i=1}^r \alpha_i \beta_i A_i S_i.$$

**Theorem 5.3.** Let  $n_c \leq n$  and suppose there exist matrices  $P, Q, \hat{P}, \hat{Q} \in \mathbb{N}^n$  satisfying

$$0 = A_{s\gamma}^T P + P A_{s\gamma} + R_1 + \sum_{i=1}^r \left[ \gamma^{-2} (\alpha_i^2 S_i^T S_i + \beta_i^2 P A_i A_i^T P) + \gamma^{-1} \beta_i^{-1} |\alpha_i| Z_i + \beta_i^{-2} \hat{I}_i \right] - P \Sigma P + \tau_\perp^T P \Sigma P \tau_\perp, \quad (5.23)$$

$$0 = [A_{s\gamma} + \sum_{i=1}^r \gamma^{-2} \beta_i^2 A_i A_i^T (P + \hat{P})] Q + Q [A_{s\gamma} + \sum_{i=1}^r \gamma^{-2} \beta_i^2 A_i A_i^T (P + \hat{P})]^T + V_1 - Q \bar{\Sigma} Q + \tau_\perp Q \bar{\Sigma} Q \tau_\perp^T, \quad (5.24)$$

$$0 = (A_{s\gamma} - Q \bar{\Sigma} + \sum_{i=1}^r \gamma^{-2} \beta_i^2 A_i A_i^T P)^T \hat{P} + \hat{P} (A_{s\gamma} - Q \bar{\Sigma} + \sum_{i=1}^r \gamma^{-2} \beta_i^2 A_i A_i^T P) + \sum_{i=1}^r \gamma^{-2} \beta_i^2 \hat{P} A_i A_i^T \hat{P} + P \Sigma P - \tau_\perp^T P \Sigma P \tau_\perp, \quad (5.25)$$

$$0 = (A_{s\gamma} - \Sigma P + \sum_{i=1}^r \gamma^{-2} \beta_i^2 A_i A_i^T P) \hat{Q} + \hat{Q} (A_{s\gamma} - \Sigma P + \sum_{i=1}^r \gamma^{-2} \beta_i^2 A_i A_i^T P)^T + Q \bar{\Sigma} Q - \tau_\perp Q \bar{\Sigma} Q \tau_\perp^T, \quad (5.26)$$

$$\text{rank } \hat{Q} = \text{rank } \hat{P} = \text{rank } \hat{Q} \hat{P} = n_c, \quad (5.27)$$

and let  $A_c, B_c$ , and  $C_c$  be given by

$$A_c = \Gamma (A_{s\gamma} - Q \bar{\Sigma} - \Sigma P + \gamma^{-2} \sum_{i=1}^r \beta_i^2 A_i A_i^T P) G^T, \quad (5.28)$$

$$B_c = \Gamma Q C^T V_2^{-1}, \quad (5.29)$$

$$C_c = -R_2^{-1} B^T P G^T. \quad (5.30)$$

Then  $(\tilde{A} + \Delta\tilde{A}, \tilde{E})$  is detectable for all  $\Delta A \in \mathcal{U}$  if and only if  $\tilde{A} + \Delta\tilde{A}$  is asymptotically stable for all  $\Delta A \in \mathcal{U}$ . In this case, the worst-case  $\mathcal{H}_2$  performance criterion (5.7) satisfies the bound

$$J(A_c, B_c, C_c) \leq \text{tr} [PV_1 + Q(P\Sigma P - \tau_\perp^\text{T} P \Sigma P \tau_\perp - \gamma^{-2} \sum_{i=1}^r \hat{P} A_i A_i^\text{T} \hat{P})] \quad (5.31)$$

$$\begin{aligned} &= \text{tr} \left[ QR_1 + P(Q\bar{\Sigma}Q - \tau_\perp Q\bar{\Sigma}Q\tau_\perp^\text{T}) \right. \\ &\quad \left. - \hat{Q} \left( \sum_{i=1}^r \gamma^{-2} \alpha_i^2 S_i^\text{T} S_i + \gamma^{-1} \beta_i^{-1} |\alpha_i| Z_i + \beta_i^{-2} \hat{I}_i \right) \right]. \end{aligned} \quad (5.32)$$

**Proof.** The proof is constructive in nature. We first obtain necessary conditions for the Optimization Problem and show by construction that these conditions serve as sufficient conditions for closed-loop stability. Specifically, it can be shown (see [13] for a similar construction) that the existence of  $P, Q, \hat{P}, \hat{Q} \in \mathbb{N}^n$  satisfying (5.23)–(5.26) implies the existence of  $\tilde{P} \in \mathbb{N}^{\tilde{n}}$  satisfying (5.18) where  $\tilde{P}$  is given by

$$\tilde{P} = \begin{bmatrix} P + \hat{P} & -\hat{P}G^\text{T} \\ -G\hat{P} & G\hat{P}G^\text{T} \end{bmatrix}.$$

Now, the proof of robust stability and the upper bound on  $\mathcal{H}_2$  performance (5.5) for all uncertain perturbations  $\Delta A \in \mathcal{U}$  follows from Theorem 5.2.

Next, to optimize (5.20) subject to constraint (5.18) over the open set

$$\begin{aligned} \mathcal{S} \triangleq \{ & (\tilde{P}, A_c, B_c, C_c) : \tilde{P} \in \mathbb{P}^{\tilde{n}}, \tilde{A}_{s\gamma} + \gamma^{-2} \sum_{i=1}^r A_i \beta_i^\text{T} \beta_i A_i^\text{T} \tilde{P} \\ & \text{is asymptotically stable and } (A_c, B_c, C_c) \text{ is minimal} \} \end{aligned}$$

form the Lagrangian

$$\begin{aligned} \mathcal{L}(A_c, B_c, C_c, \tilde{Q}, \tilde{P}, \lambda) \triangleq & \text{tr} \left[ \lambda \tilde{P} \tilde{V} + \tilde{Q} \left\{ \tilde{A}_{s\gamma}^\text{T} \tilde{P} + \tilde{P} \tilde{A}_{s\gamma} + \tilde{R} \right. \right. \\ & \left. \left. + \sum_{i=1}^r \left[ \gamma^{-2} (\alpha_i^2 \tilde{S}_i^\text{T} \tilde{S}_i + \beta_i^2 \tilde{P} \tilde{A}_i \tilde{A}_i^\text{T} \tilde{P}) + \gamma^{-1} \beta_i^{-1} |\alpha_i| \tilde{Z}_i + \beta_i^{-2} \tilde{I}_i \right] \right\} \right], \end{aligned} \quad (5.33)$$

where the Lagrange multipliers  $\lambda \geq 0$  and  $\tilde{Q} \in \mathbb{R}^{\tilde{n} \times \tilde{n}}$  are not both zero. We thus obtain

$$\frac{\partial \mathcal{L}}{\partial \tilde{P}} = (\tilde{A}_{s\gamma} + \gamma^{-2} \sum_{i=1}^r \beta_i^2 A_i A_i^T \tilde{P}) \tilde{Q} + \tilde{Q} (\tilde{A}_{s\gamma} + \gamma^{-2} \sum_{i=1}^r \beta_i^2 A_i A_i^T \tilde{P})^T + \lambda \tilde{V}. \quad (5.34)$$

Setting  $\frac{\partial \mathcal{L}}{\partial \tilde{P}} = 0$  yields

$$0 = (\tilde{A}_{s\gamma} + \gamma^{-2} \sum_{i=1}^r \beta_i^2 A_i A_i^T \tilde{P}) \tilde{Q} + \tilde{Q} (\tilde{A}_{s\gamma} + \gamma^{-2} \sum_{i=1}^r \beta_i^2 A_i A_i^T \tilde{P})^T + \lambda \tilde{V}. \quad (5.35)$$

Since  $\tilde{A}_{s\gamma} + \gamma^{-2} \sum_{i=1}^r \beta_i^2 A_i A_i^T \tilde{P}$  is assumed to be asymptotically stable, setting  $\lambda = 0$  implies  $\tilde{Q} = 0$ . Hence, it can be assumed without loss of generality that  $\lambda = 1$ . Furthermore,  $\tilde{Q}$  is nonnegative definite. The remainder of the proof follows as in [13]. Briefly, the principal steps are as follows.

Step 1. Compute  $\frac{\partial \mathcal{L}}{\partial A_c}$ ,  $\frac{\partial \mathcal{L}}{\partial B_c}$ , and  $\frac{\partial \mathcal{L}}{\partial C_c}$ .

Step 2. Partition (5.18) and (5.35) into six equations (a)-(f) corresponding to the  $n \times n$ ,  $n \times n_c$ , and  $n_c \times n_c$  sub-blocks of  $\tilde{P}$  and  $\tilde{Q}$ , respectively. Next, since the compensator triple  $(A_c, B_c, C_c)$  is controllable and observable, using a minor extension of the result from [2] and Lemma 12.2 of [115], (c) implies that the lower-right  $n_c \times n_c$  block of  $\tilde{P}$  is positive definite. Using similar arguments we can show that the lower-right  $n_c \times n_c$  block of  $\tilde{Q}$  is positive definite. See [13] for details.

Step 3. Form (b) times the  $n \times n_c$  sub-block of  $\tilde{Q}$  plus the  $n_c \times n_c$  sub-block of  $\tilde{Q}$  times (c) to define the projection matrix  $\tau$  and the new variables  $P$ ,  $Q$ ,  $\hat{P}$ ,  $\hat{Q}$ ,  $G$ , and  $\Gamma$ .

Step 4. Use the result of Step 1 and Step 3 to solve for the compensator gains (5.28)–(5.30).

Step 5. Manipulate (a), (b), (d), and (e) to yield (5.23)–(5.26).

Step 6. Use the results of Step 3 to show that (5.20) is equivalent to (5.31).

For a detailed exposition of a similar proof, see [13].  $\square$

**Remark 5.3.** In the full-order case, set  $n_c = n$  so that  $G = \Gamma = \tau = I_n$  and  $\tau_\perp = 0$ . In this case the last term in each of (5.23)–(5.26) is zero and (5.26) is superfluous.

Theorem 5.3 provides constructive sufficient conditions that yield dynamic feedback gains  $A_c$ ,  $B_c$ , and  $C_c$  for robust stability and performance. When solving (5.23)–(5.26) numerically, the values of  $\gamma$ ,  $\alpha_i$ ,  $\beta_i$ , and  $S_i$ ,  $i = 1, \dots, r$ , can be adjusted to examine trade-offs between  $\mathcal{H}_2$  performance and robustness. As discussed in [54], to further reduce conservatism, one can view the scalars  $\alpha_i$  and  $\beta_i$  as free parameters and optimize the worst-case  $\mathcal{H}_2$  performance bound  $\mathcal{J} = \text{tr } \tilde{P}\tilde{V}$  with respect to  $\alpha_i$  and  $\beta_i$ . The simplest case to consider is the case where  $\tilde{S}_i$  is skew-symmetric or, equivalently,  $\tilde{Z}_i = 0$ . In this case

$$\frac{\partial \mathcal{J}}{\partial \alpha_i} = 2\beta_i \gamma^{-2} \text{tr } \tilde{P} \tilde{A}_i \tilde{S}_i \tilde{Q} + 2\alpha_i \gamma^{-2} \text{tr } \tilde{S}_i^T \tilde{S}_i \tilde{Q} = 0 \quad (5.36)$$

and

$$\frac{\partial \mathcal{J}}{\partial \beta_i} = 2\alpha_i \gamma^{-2} \text{tr } \tilde{P} \tilde{A}_i \tilde{S}_i \tilde{Q} + 2\beta_i \gamma^{-2} \text{tr } \tilde{P} \tilde{A}_i \tilde{A}_i^T \tilde{P} \tilde{Q} - 2\beta_i^{-3} \text{tr } \tilde{I}_i \tilde{Q} = 0, \quad (5.37)$$

where  $\tilde{Q}$  satisfies

$$0 = \left( \tilde{A}_{s\gamma} + \sum_{i=1}^r \gamma^{-2} \beta_i^2 \tilde{A}_i \tilde{A}_i^T \tilde{P} \right) \tilde{Q} + \tilde{Q} \left( \tilde{A}_{s\gamma} + \sum_{i=1}^r \gamma^{-2} \beta_i^2 \tilde{A}_i \tilde{A}_i^T \tilde{P} \right)^T + \tilde{V}. \quad (5.38)$$

Furthermore, in this case,

$$\frac{\partial^2 \mathcal{J}}{\partial \alpha_i^2} = 2\gamma^{-2} \text{tr} \tilde{S}_i \tilde{Q} \tilde{S}_i^T \geq 0, \quad (5.39)$$

$$\frac{\partial^2 \mathcal{J}}{\partial \beta_i^2} = 2\gamma^{-2} \text{tr} \tilde{A}_i^T \tilde{P} \tilde{Q} \tilde{P} \tilde{A}_i + 6\beta_i^{-4} \text{tr} \tilde{I}_i \tilde{Q} \geq 0, \quad (5.40)$$

and

$$\frac{\partial^2 \mathcal{J}}{\partial \alpha_i^2} \frac{\partial^2 \mathcal{J}}{\partial \beta_i^2} - \left( \frac{\partial^2 \mathcal{J}}{\partial \alpha_i \partial \beta_i} \right)^2 = 16\gamma^{-2} \beta_i^{-4} \text{tr} \tilde{I}_i \tilde{Q} \text{tr} \tilde{S}_i \tilde{Q} \tilde{S}_i^T \geq 0, \quad (5.41)$$

which imply that (5.36) and (5.37) provide necessary conditions for a local minimum.

In the case  $\tilde{Z}_i \neq 0$  we need to consider the cases  $\alpha_i = 0$  and  $\alpha_i \neq 0$  since  $\mathcal{J}$  is not differentiable at  $\alpha_i = 0$ . First, let  $\alpha_i = 0$ . In this case

$$\frac{\partial \mathcal{J}}{\partial \beta_i} = 2\beta_i \gamma^{-2} \text{tr} \tilde{P} \tilde{A}_i \tilde{A}_i^T \tilde{P} \tilde{Q} - 2\beta_i^{-3} \text{tr} \tilde{I}_i \tilde{Q} = 0, \quad (5.42)$$

where  $\tilde{Q}$  satisfies (5.38) with  $\alpha_i = 0$ . Next, consider the case where  $\alpha_i \neq 0$ . In this case

$$\frac{\partial \mathcal{J}}{\partial \alpha_i} = 2\beta_i \gamma^{-2} \text{tr} \tilde{P} \tilde{A}_i \tilde{S}_i \tilde{Q} + 2\alpha_i \gamma^{-2} \text{tr} \tilde{S}_i^T \tilde{S}_i \tilde{Q} + \gamma^{-1} \beta_i^{-1} \text{sgn} \alpha_i \text{tr} \tilde{Z}_i \tilde{Q} = 0 \quad (5.43)$$

and

$$\frac{\partial \mathcal{J}}{\partial \beta_i} = 2\alpha_i \gamma^{-2} \text{tr} \tilde{P} \tilde{A}_i \tilde{S}_i \tilde{Q} + 2\beta_i \gamma^{-2} \text{tr} \tilde{P} \tilde{A}_i \tilde{A}_i^T \tilde{P} \tilde{Q} - \gamma^{-1} \beta_i^{-2} |\alpha_i| \text{tr} \tilde{Z}_i \tilde{Q} - 2\beta_i^{-3} \text{tr} \tilde{I}_i \tilde{Q} = 0 \quad (5.44)$$

where  $\tilde{Q}$  satisfies (5.38) and  $\text{sgn} \alpha_i \triangleq \frac{|\alpha_i|}{\alpha_i}$ . By using (5.36) and (5.37) (or (5.43) and (5.44) for non-skew-symmetric  $\tilde{S}_i$ ) within a numerical optimization algorithm, the optimal robust reduced-order controllers and scaling parameters  $\alpha_i, \beta_i, i = 1, \dots, r$ , can be determined simultaneously.

## 5.6. Two-Mass Example

Consider the dynamic system shown in Figure 5.1, which represents a flexible structure with uncertain high-frequency dynamics [40]. The equations of motion for

this system are

$$m_1 \ddot{x}_1 + c_1 \dot{x}_1 - c_2(\dot{x}_2 - \dot{x}_1) + k_1 x_1 - k_2(x_2 - x_1) = u,$$

$$m_2 \ddot{x}_2 + c_2(\dot{x}_2 - \dot{x}_1) + k_2(x_2 - x_1) = 0.$$

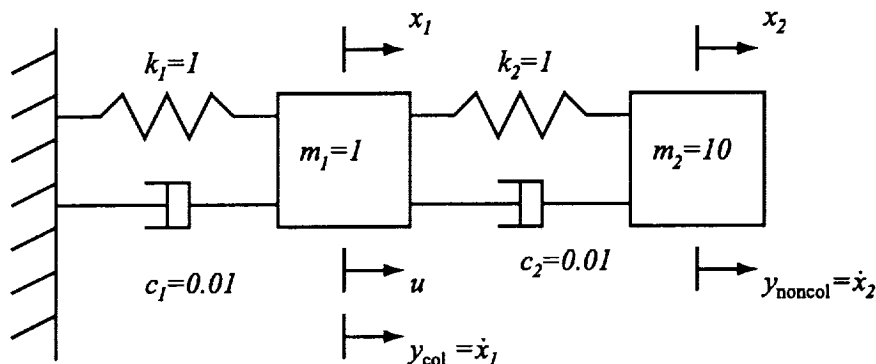


Figure 5.1: Two-mass system

We first consider the case of a colocated sensor and actuator pair, where the output is given by  $y_{\text{col}} = \dot{x}_1$ . Letting  $m_1 = 1$ ,  $m_2 = 10$ ,  $k_1 = k_2 = 1$ , and  $c_1 = c_2 = 0.01$  and transforming to real normal coordinates yields the plant state space realization

$$\dot{x} = \begin{bmatrix} -0.0002 & 0.2208 & 0 & 0 \\ -0.2208 & -0.0002 & 0 & 0 \\ 0 & 0 & -0.0103 & 1.4320 \\ 0 & 0 & -1.4320 & -0.0103 \end{bmatrix} x + \begin{bmatrix} -0.1439 \\ 0.2168 \\ -0.0426 \\ 1.1890 \end{bmatrix} u,$$

$$y_{\text{col}} = \begin{bmatrix} -0.0545 & 0.0819 & -0.0352 & 0.8181 \end{bmatrix} x.$$

As in [40], the matrices  $D_1$ ,  $D_2$ ,  $E_1$ , and  $E_2$  are chosen to be

$$D_1 = \begin{bmatrix} 0 & 0 \\ 1 & 0 \\ 0 & 0 \\ 0 & 0 \end{bmatrix}, \quad D_2 = \begin{bmatrix} 0 & 1 \end{bmatrix}, \quad E_1 = \begin{bmatrix} 1 & 0 & 0 & 0 \\ 0 & 0 & 0 & 0 \end{bmatrix}, \quad D_1 = \begin{bmatrix} 0 \\ 1 \end{bmatrix},$$

so that the LQG compensator places a notch at the second modal frequency. Uncertainty in the damped natural frequency of the second mode  $\omega_{d2} = 1.432$  is modeled

by choosing

$$A_1 = \begin{bmatrix} 0 & 0 & 0 & 0 \\ 0 & 0 & 0 & 0 \\ 0 & 0 & 0 & 1 \\ 0 & 0 & -1 & 0 \end{bmatrix}.$$

The quasi-Newton optimization algorithm discussed in Section 2.3 was used to compute full-order controllers ( $n_c = n$ ) that minimize the cost bound  $\mathcal{J}$  for several values of  $\gamma$ . The actual  $\mathcal{H}_2$  cost was computed for a range of values of the damped natural frequency of the second mode for the LQG controller and for the implicit small gain (with  $S_1 = A_1$  and  $\alpha_1$  and  $\beta_1$  obtained by (5.36) and (5.37)) and scaled Popov controllers [106] corresponding to  $\gamma = 15, 7$ , and  $2$ . The cost dependence is shown in Figure 5.2. As  $\gamma$  decreases, the  $\mathcal{H}_2$  cost of the nominal closed-loop system increases while the  $\mathcal{H}_2$  cost of the perturbed closed-loop system remains near the nominal value for a larger range of perturbations. The LQG controller stabilizes the closed-loop system for only small perturbations in the damped natural frequency of the second mode, while the implicit small gain controllers stabilize the closed-loop system and provide performance close to the optimal level even for large perturbations. Hence, robust performance over a large range of the uncertain parameter is achieved for only a small increase in the  $\mathcal{H}_2$  cost above the optimal. Also note that the robustness/performance tradeoffs of the implicit small gain controllers are comparable to those of the scaled Popov controllers which are obtained using frequency-dependent multipliers [106].

The frequency responses of the LQG controller and the implicit small gain controllers with  $\gamma = 15, 7$ , and  $2$  are shown in Figure 5.3. The LQG controller is unstable and achieves closed-loop stability and nominal performance by placing a notch at the nominal damped natural frequency  $\omega_{d2}$  of the uncertain second mode. Hence, closed-loop performance degrades considerably with the damped natural frequency of the second mode is perturbed. The implicit small gain controller with  $\gamma = 7$  has only

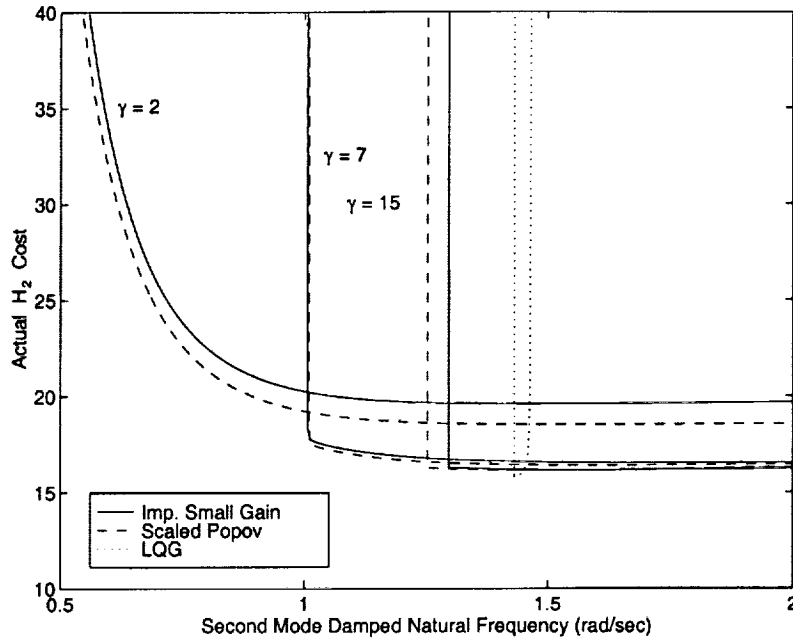


**Figure 5.2:** Dependence of the  $\mathcal{H}_2$  cost on the damped natural frequency of the second mode: Colocated case

a shallow notch near the damped natural frequency of the second mode, while the controller with  $\gamma = 2$  has no notch near that frequency. Hence, these controllers sacrifice nominal performance for improved robust performance over a larger range of the uncertain damped natural frequency. As  $\gamma$  decreases, the controllers guarantee robust performance over a larger range of  $\delta$ . Note that the controller obtained with  $\gamma = 2$  is positive real. Since the plant is a model of a flexible structure with a colocated sensor and actuator pair, it is also positive real, and thus the closed-loop system is asymptotically stable for all values of the uncertain damped natural frequency.

Next we consider the two-mass system of Figure 5.1 with a noncolocated sensor and actuator pair by choosing

$$y_{\text{noncol}} = \begin{bmatrix} -0.1063 & 0.1597 & 0.0018 & -0.0419 \end{bmatrix} x.$$

As in [40], we increase the matrix  $E_1$  by a factor of ten to enhance the notching characteristics of the LQG controller.

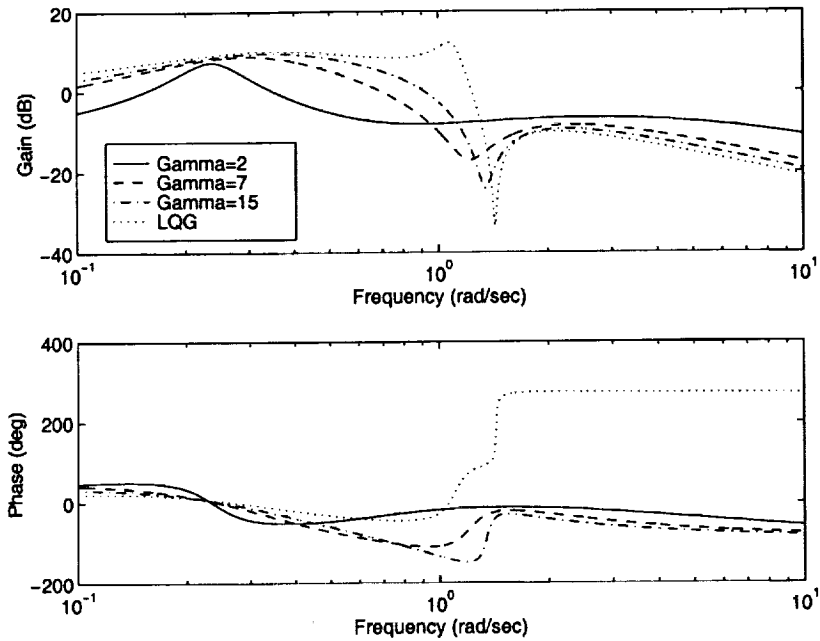


**Figure 5.3:** Frequency responses of implicit small gain controllers: Colocated case

The implicit small gain synthesis technique was used as before to compute full-order controllers ( $n_c = n$ ) that minimize  $\mathcal{J}$  for a range of  $\gamma$ . The actual  $\mathcal{H}_2$  cost was computed for a range of the damped natural frequency for the LQG controller and for the implicit small gain and scaled Popov controllers [106] corresponding to  $\gamma = 15$  and 4. The cost dependence is shown in Figure 5.4. In the noncolocated case, the LQG controller stabilizes the closed-loop system for a smaller range of the uncertain parameter than the unstable LQG controller for the colocated plant.

The frequency responses of the LQG controller and the implicit small gain controllers with  $\gamma = 15$  and  $\gamma = 4$  were computed and are shown in Figure 5.5. Since the plant is not positive real, robust performance cannot be achieved simply by obtaining positive real controllers, as in the colocated case. Instead, as seen in Figure 5.5, the controllers widen the notch at the nominal frequency of the uncertain mode, and the controller with  $\gamma = 15$  deepens the notch as well.

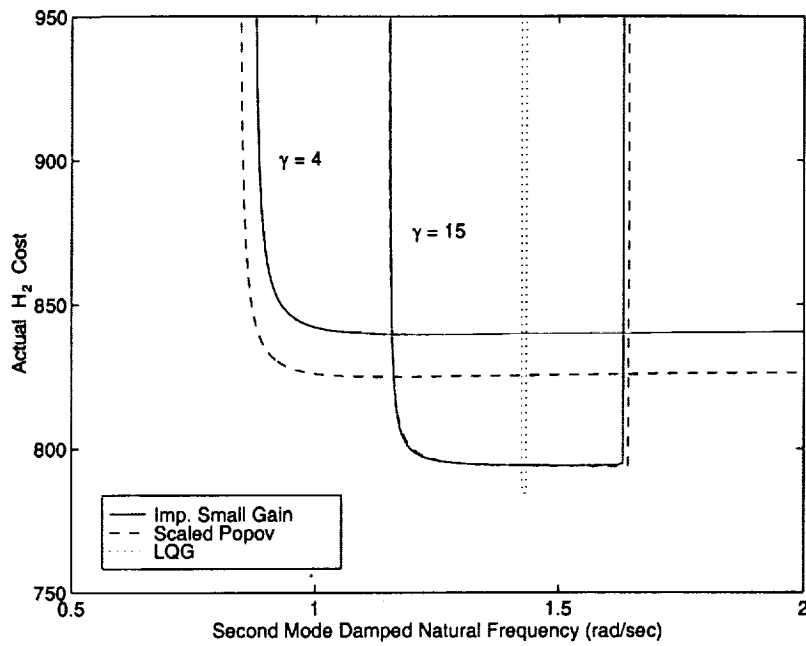


Figure 5.4: Dependence of the  $\mathcal{H}_2$  cost on the damped natural frequency of the second mode: Noncolocated case

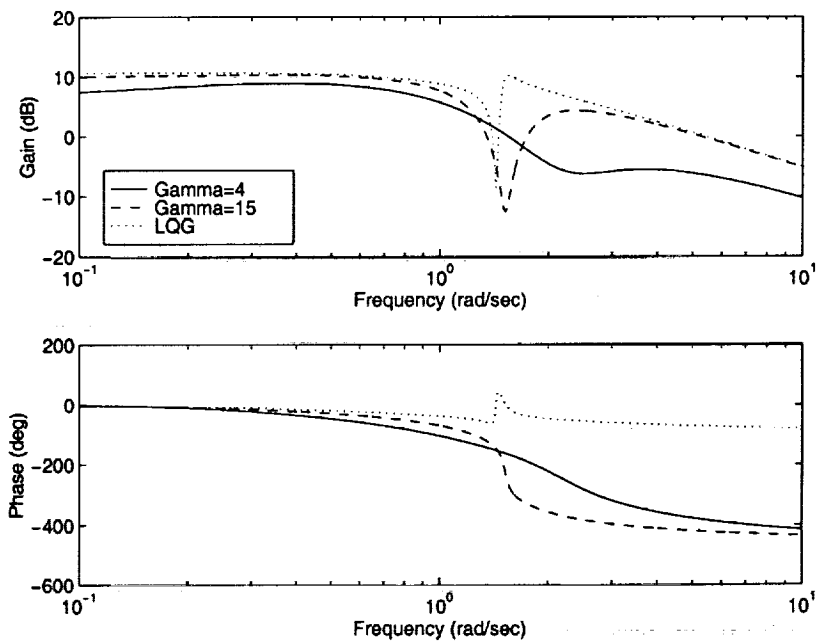


Figure 5.5: Frequency responses of implicit small gain controllers: Noncolocated case

## 5.7. Three-Mass Example

Consider the three-mass, two-spring system shown in Figure 5.6 with  $m_1 = m_2 = m_3 = 1$  and an uncertain spring stiffness  $k_2$  [52, 106]. A control force acts on mass 3 while the position and velocity of mass 1 are measured resulting in a noncolocated control problem. The nominal dynamics, with state variables defined in Figure 5.6, are given by

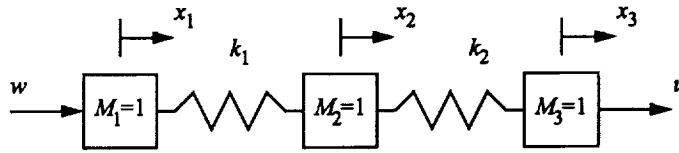


Figure 5.6: Three-mass system

$$A = \begin{bmatrix} 0 & 0 & 0 & 1 & 0 & 0 \\ 0 & 0 & 0 & 0 & 1 & 0 \\ 0 & 0 & 0 & 0 & 0 & 1 \\ -k_1 & k_1 & 0 & 0 & 0 & 0 \\ k_1 & -(k_1 + k_{2nom}) & k_{2nom} & 0 & 0 & 0 \\ 0 & k_{2nom} & -k_{2nom} & 0 & 0 & 0 \end{bmatrix}, \quad B = \begin{bmatrix} 0 \\ 0 \\ 0 \\ 0 \\ 0 \\ 1 \end{bmatrix}, \quad D_1 = \begin{bmatrix} 0 & 0 \\ 0 & 0 \\ 0 & 0 \\ 1 & 0 \\ 0 & 0 \\ 0 & 0 \end{bmatrix},$$

$$C = [1 \ 1 \ 0 \ 0 \ 0 \ 0], \quad D_2 = [0 \ 1],$$

and  $k_1 = k_{2nom} = 1$ . The actual spring stiffness of the second spring can be written as  $k_2 = k_{2nom} + \delta$  so that the actual dynamics are given by  $\Delta A = A + \delta A_1$ , where

$$A_1 = \begin{bmatrix} 0 & 0 & 0 & 0 & 0 & 0 \\ 0 & 0 & 0 & 0 & 0 & 0 \\ 0 & 0 & 0 & 0 & 0 & 0 \\ 0 & 0 & 0 & 0 & 0 & 0 \\ 0 & -1 & 1 & 0 & 0 & 0 \\ 0 & 1 & -1 & 0 & 0 & 0 \end{bmatrix}.$$

Furthermore, let

$$E_1 = \begin{bmatrix} 1 & 1 & 0 & 0 & 0 & 0 \\ 0 & 0 & 0 & 0 & 0 & 0 \end{bmatrix}, \quad E_2 = \begin{bmatrix} 0 \\ 1 \end{bmatrix}.$$

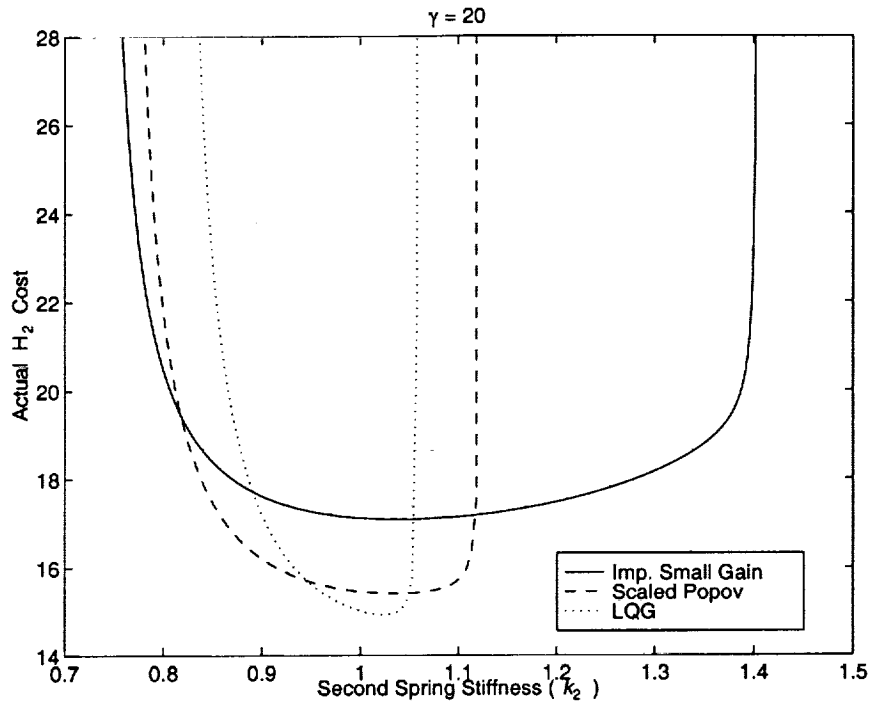


Figure 5.7: Dependence of the  $\mathcal{H}_2$  cost on  $k_2$

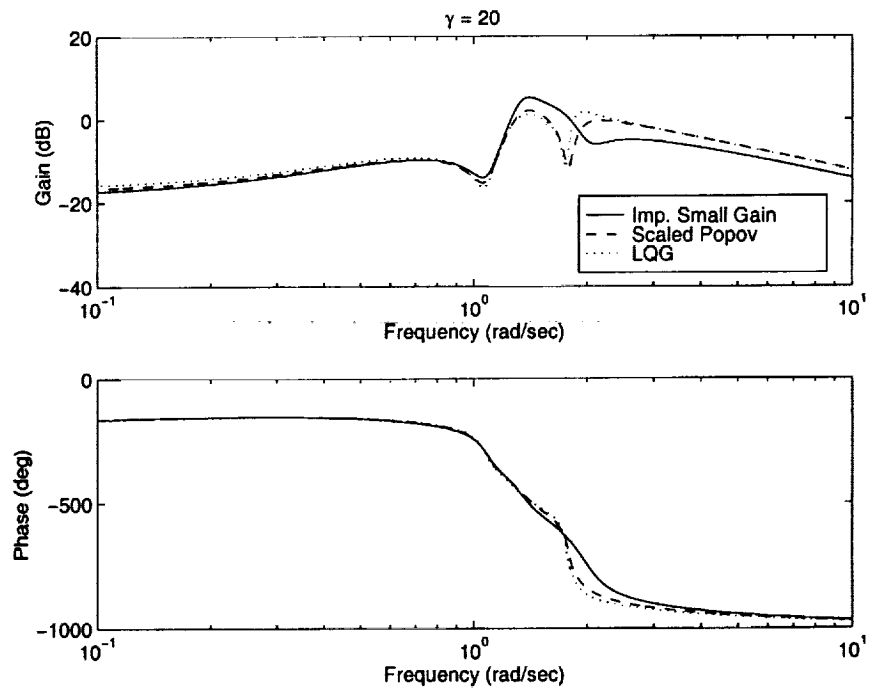
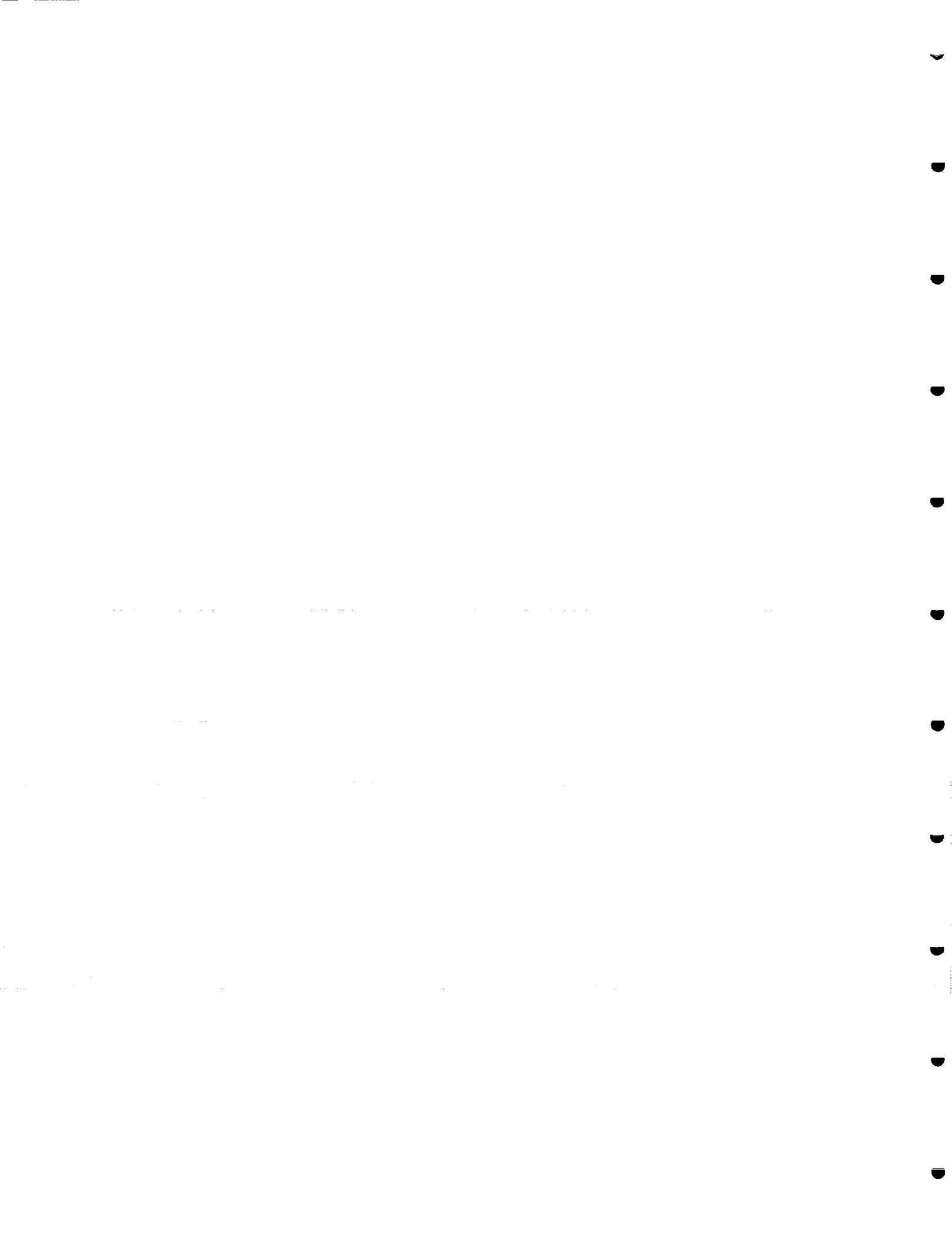


Figure 5.8: Frequency response of the implicit small gain controller

A full-order ( $n_c = n$ ) implicit small gain (with  $S_1 = A_1$  and  $\alpha_1$  and  $\beta_1$  obtained by (5.43) and (5.44)) compensator was designed with a value of  $\gamma = 20$ . The actual  $\mathcal{H}_2$  cost was computed for the LQG controller and for the implicit small gain and scaled Popov controllers corresponding to  $\gamma = 20$  for a range of the uncertain parameter  $\delta$ . The cost dependence is shown in Figure 5.7. Though a value of  $\gamma = 20$  corresponds to a parameter uncertainty of  $\delta = 0.05$ , it is seen that the implicit small gain controller is robust over a much larger range. Finally, the frequency responses of the LQG controller and the implicit small gain controller are shown in Figure 5.8.

## 5.8. Conclusion

This research extended the implicit small gain guaranteed cost bound [54] to controller synthesis. Specifically, the implicit small gain guaranteed cost bound was used to address the problem of robust stability and  $\mathcal{H}_2$  performance via fixed-order dynamic compensation. A quasi-Newton optimization algorithm was used to obtain robust controllers for several illustrative examples. The design examples considered demonstrated the effectiveness of the implicit small gain guaranteed cost bound. Finally, we note that the conservatism of the proposed implicit small gain guaranteed cost bound is difficult to predict and will depend upon the actual value of  $\tilde{P}$  determined by solving (5.18).



# CHAPTER 6

## Robust Resilient Dynamic Controllers for Systems with Parametric Uncertainty and Controller Gain Variations

### 6.1. Introduction

It is well known that unavoidable discrepancies between mathematical models and real-world systems can result in the degradation of control-system performance including instability. Thus it is not surprising that a considerable amount of research over the past two decades has concentrated on analysis and synthesis of feedback controllers that guarantee robustness with respect to system uncertainties in the design model (see [27] and the numerous references therein). These robust controller synthesis frameworks include the Youla parameterization of all stabilizing controllers [110],  $\mathcal{H}_2$  and  $\mathcal{H}_\infty$  (including desired weighting functions for loop shaping) synthesis [5, 39, 126],  $\mathcal{L}_1$  control design [25],  $\mu$ -synthesis for structured real and complex uncertainty [126], and robust fixed-structure controller synthesis [16]. Almost all of these techniques yield very high order controllers in relation to the original system order. A notable exception is the fixed-structure controller design methodology [16]

which directly accounts for controller complexity constraints, including controller order, within the control-system design process. However, an implicit assumption inherent in *all* of the above mentioned design frameworks is that the resulting robust controller will be implemented *exactly*. But in most applications (and, in particular, aerospace applications), reduction in size and cost of digital control hardware results in limitations in available computer memory and wordlength capabilities of the digital processor and the A/D and D/A converters. This further results in roundoff errors in numerical computations leading to controller implementation imprecision. Hence, any controller that is part of a feedback system must be insensitive to *some* amount of error with respect to its gains.

Within the context of robust controller synthesis, the above issues were first pointed out in the enlightening and very interesting paper entitled, "Robust, Fragile, or Optimal?" [75]. Specifically, the authors in [75] very elegantly point out that the powerful (weighted)  $\mathcal{H}_2$ , (weighted)  $\mathcal{H}_\infty$ ,  $\mathcal{L}_1$ , and  $\mu$  controller design approaches, even though quite robust with respect to system uncertainty, are surprisingly very sensitive with respect to errors in the controller coefficients resulting in vanishingly small stability margins. Of course, since the control system is part of the overall closed-loop system, the authors of [75] show through a series of examples that most of the elegant multivariable robust control frameworks discussed above destabilize the closed-loop system for extremely small perturbations in the controller coefficients. Hence, even though these controllers are robust (with respect to plant uncertainty) and in some cases optimal, they are extremely *fragile*! This further implies that the resulting controllers preclude the control-system designer from tuning the controller gains around a designed nominal controller which has been the creed of practicing control engineers to capture performance requirements which are not directly addressed within the original design problem. Finally, it is interesting to note that numerical experi-

ments seem to indicate that the fragility or brittleness of the controller is exacerbated with increasing controller order.

In this chapter, the robust fixed-structure guaranteed cost controller synthesis framework of [10, 13, 52] for systems with structured parametric uncertainty is extended to address the design of non-fragile or robust *resilient* fixed-order (i.e., full- and reduced-order) dynamic compensation. For flexibility in controller synthesis, we adopt the approach of fixed-structure controller design which allows consideration of arbitrary controller structure, including order, internal structure, and decentralization. Specifically, using quadratic Lyapunov bounds, a rigorous development of sufficient conditions for robust stability and worst-case  $\mathcal{H}_2$  performance via fixed-order dynamic compensation is presented for uncertain feedback systems wherein the controller can tolerate multiplicative or additive gain variations with respect to its nominal coefficients. These sufficient conditions are in the form of a coupled system of algebraic Riccati equations that characterize robust resilient reduced-order controllers. Hence, the proposed robust resilient controllers guarantee robust stability and robust performance in the face of both system uncertainty *and* controller errors. The proposed approach is applied on several numerical examples which clearly demonstrate the need for robust resilient control.

## 6.2. Robust Stability and Performance

In this section we state the robust stability and performance problem. This problem involves a set  $\mathcal{U} \subset \mathbb{R}^{n \times n}$  of uncertain plant perturbations  $\Delta A$  of the nominal dynamics  $A$  and a set  $\mathcal{U}_c \subset \mathbb{R}^{n_c \times n_c} \times \mathbb{R}^{n_c \times l} \times \mathbb{R}^{m \times n_c}$  of uncertain controller perturbations  $(\Delta A_c, \Delta B_c, \Delta C_c)$  of the nominal controller gain matrices  $(A_c, B_c, C_c)$ . The objective of this problem is to determine a fixed-order, strictly proper dynamic compensator  $(A_c, B_c, C_c)$  that stabilizes the plant for all variations in  $\mathcal{U} \times \mathcal{U}_c$  and minimizes the

worst-case  $\mathcal{H}_2$  norm of the closed-loop system. In this section and the following section no explicit structure is assumed for the elements of  $\mathcal{U} \times \mathcal{U}_c$ . In Section 6.4 and Section 6.7, two specific structures of the variations in  $\mathcal{U} \times \mathcal{U}_c$  will be introduced.

**Robust Stability and Performance Problem.** Given the  $n^{\text{th}}$ -order stabilizable and detectable uncertain system

$$\dot{x}(t) = (A + \Delta A)x(t) + Bu(t) + D_1w(t), \quad t \in [0, \infty), \quad (6.1)$$

$$y(t) = Cx(t) + D_2w(t), \quad (6.2)$$

determine an  $n_c^{\text{th}}$ -order robust resilient dynamic compensator  $(A_c, B_c, C_c)$  such that the closed-loop system consisting of (6.1), (6.2), and controller dynamics

$$\dot{x}_c(t) = (A_c + \Delta A_c)x_c(t) + (B_c + \Delta B_c)y(t), \quad (6.3)$$

$$u(t) = (C_c + \Delta C_c)x_c(t), \quad (6.4)$$

is asymptotically stable for all allowable plant uncertainties and controller gain variations  $(\Delta A, \Delta A_c, \Delta B_c, \Delta C_c) \in \mathcal{U} \times \mathcal{U}_c$  and the performance criterion

$$J(A_c, B_c, C_c) \triangleq \sup_{(\Delta A, \Delta A_c, \Delta B_c, \Delta C_c) \in \mathcal{U} \times \mathcal{U}_c} \limsup_{t \rightarrow \infty} \frac{1}{t} \mathbb{E} \int_0^t [x^T(s)R_1x(s) + u^T(s)R_2u(s)] ds, \quad (6.5)$$

is minimized.

For each uncertain plant and controller variation  $(\Delta A, \Delta A_c, \Delta B_c, \Delta C_c) \in \mathcal{U} \times \mathcal{U}_c$ , the closed-loop system (6.1)–(6.4) can be written as

$$\dot{\tilde{x}}(t) = (\tilde{A} + \Delta \tilde{A})\tilde{x}(t) + (\tilde{D} + \Delta \tilde{D})w(t), \quad t \in [0, \infty), \quad (6.6)$$

where

$$\Delta \tilde{A} \triangleq \begin{bmatrix} \Delta A & B\Delta C_c \\ \Delta B_c C & \Delta A_c \end{bmatrix}, \quad \Delta \tilde{D} \triangleq \begin{bmatrix} 0 \\ \Delta B_c D_2 \end{bmatrix},$$

and where the closed-loop disturbance  $(\tilde{D} + \Delta\tilde{D})w(t)$  has nonnegative definite intensity

$$\tilde{V}_\Delta \triangleq (\tilde{D} + \Delta\tilde{D})(\tilde{D} + \Delta\tilde{D})^T = \begin{bmatrix} V_1 & 0 \\ 0 & B_c V_2 B_c^T + \Delta B_c V_2 B_c^T + B_c V_2 \Delta B_c^T + \Delta B_c V_2 \Delta B_c^T \end{bmatrix}.$$

### 6.3. Sufficient Conditions for Robust Stability and Performance

In practice, steady-state performance is only of interest when the undisturbed closed-loop system is robustly stable over  $\mathcal{U} \times \mathcal{U}_c$ . The following result is immediate. For convenience, define

$$\tilde{R}_\Delta \triangleq (\tilde{E} + \Delta\tilde{E})^T (\tilde{E} + \Delta\tilde{E}) = \begin{bmatrix} R_1 & 0 \\ 0 & C_c^T R_2 C_c + \Delta C_c^T R_2 C_c + C_c^T R_2 \Delta C_c + \Delta C_c^T R_2 \Delta C_c \end{bmatrix},$$

where

$$\Delta\tilde{E} \triangleq [0 \quad E_2 \Delta C_c].$$

**Lemma 6.1.** Let  $(A_c, B_c, C_c)$  be given and assume that  $\tilde{A} + \Delta\tilde{A}$  is asymptotically stable for all plant and controller gain variations  $(\Delta A, \Delta A_c, \Delta B_c, \Delta C_c) \in \mathcal{U} \times \mathcal{U}_c$ . Then

$$J(A_c, B_c, C_c) = \sup_{(\Delta A, \Delta A_c, \Delta B_c, \Delta C_c) \in \mathcal{U} \times \mathcal{U}_c} \text{tr } \tilde{Q}_\Delta \tilde{R}_\Delta, \quad (6.7)$$

where  $\tilde{Q}_\Delta \in \mathbb{N}^n$ , is the unique nonnegative definite solution to

$$0 = (\tilde{A} + \Delta\tilde{A})\tilde{Q}_\Delta + \tilde{Q}_\Delta(\tilde{A} + \Delta\tilde{A})^T + \tilde{V}_\Delta. \quad (6.8)$$

The key step in guaranteeing robust stability and performance is to bound the uncertain terms  $\tilde{R}_\Delta$  in the cost function (6.7) and  $\Delta\tilde{A}\tilde{Q}_\Delta + \tilde{Q}_\Delta\Delta\tilde{A}^T$  and  $\tilde{V}_\Delta$  in the Lyapunov equation (6.8) by smooth bounding functions  $\Omega_i(\cdot)$ ,  $i = 1, 2, 3$ . For the statement of the next result, define the notation

$$\Delta\tilde{R} \triangleq \tilde{R}_\Delta - \tilde{R} = \begin{bmatrix} 0 & 0 \\ 0 & \Delta C_c^T R_2 C_c + C_c^T R_2 \Delta C_c + \Delta C_c^T R_2 \Delta C_c \end{bmatrix},$$

$$\Delta\tilde{V} \triangleq \tilde{V}_\Delta - \tilde{V} = \begin{bmatrix} 0 & 0 \\ 0 & \Delta B_c V_2 B_c^T + B_c V_2 \Delta B_c^T + \Delta B_c V_2 \Delta B_c^T \end{bmatrix}.$$

**Theorem 6.1.** Let  $A_c \in \mathbb{R}^{n_c \times n_c}$ ,  $B_c \in \mathbb{R}^{n_c \times l}$ , and  $C_c \in \mathbb{R}^{m \times n_c}$  be given and let  $\Omega_1 : \mathbb{N}^{\tilde{n}} \times \mathbb{R}^{n_c \times n_c} \times \mathbb{R}^{n_c \times l} \times \mathbb{R}^{m \times n_c} \rightarrow \mathbb{S}^{\tilde{n}}$ ,  $\Omega_2 : \mathbb{R}^{n_c \times l} \rightarrow \mathbb{S}^{\tilde{n}}$ , and  $\Omega_3 : \mathbb{R}^{m \times n_c} \rightarrow \mathbb{S}^{\tilde{n}}$ , be such that, for  $(\Delta A, \Delta A_c, \Delta B_c, \Delta C_c) \in \mathcal{U} \times \mathcal{U}_c$ , and  $\tilde{Q} \in \mathbb{N}^{\tilde{n}}$ ,

$$\Delta\tilde{A}\tilde{Q} + \tilde{Q}\Delta\tilde{A}^T \leq \Omega_1(\tilde{Q}, A_c, B_c, C_c), \quad (6.9)$$

$$\Delta\tilde{V} \leq \Omega_2(B_c), \quad (6.10)$$

$$\Delta\tilde{R} \leq \Omega_3(C_c), \quad (6.11)$$

and suppose there exists  $\tilde{Q} \in \mathbb{N}^{\tilde{n}}$  satisfying

$$0 = \tilde{A}\tilde{Q} + \tilde{Q}\tilde{A}^T + \Omega_1(\tilde{Q}, A_c, B_c, C_c) + \tilde{V} + \Omega_2(B_c). \quad (6.12)$$

Then

$$(\tilde{A} + \Delta\tilde{A}, \tilde{D} + \Delta\tilde{D}) \text{ is stabilizable for all } (\Delta A, \Delta A_c, \Delta B_c, \Delta C_c) \in \mathcal{U} \times \mathcal{U}_c, \quad (6.13)$$

if and only if  $\tilde{A} + \Delta\tilde{A}$  is asymptotically stable for all  $(\Delta A, \Delta A_c, \Delta B_c, \Delta C_c) \in \mathcal{U} \times \mathcal{U}_c$ .

In this case,

$$\tilde{Q}_\Delta \leq \tilde{Q}, \quad (\Delta A, \Delta A_c, \Delta B_c, \Delta C_c) \in \mathcal{U} \times \mathcal{U}_c, \quad (6.14)$$

where  $\tilde{Q}_\Delta$  is given by (6.8), and

$$J(A_c, B_c, C_c) \leq \mathcal{J}(A_c, B_c, C_c) \triangleq \text{tr } \tilde{Q} \left[ \tilde{R} + \Omega_3(C_c) \right]. \quad (6.15)$$

**Proof.** We stress that in (6.9),  $\tilde{Q}$  denotes an arbitrary element of  $\mathbb{N}^{\tilde{n}}$ , whereas in (6.12),  $\tilde{Q}$  denotes a specific solution of the modified Lyapunov equation (6.12). This minor abuse of notation considerably simplifies the presentation. Now, for  $(\Delta A, \Delta A_c, \Delta B_c, \Delta C_c) \in \mathcal{U} \times \mathcal{U}_c$ , (6.12) is equivalent to

$$\begin{aligned} 0 &= (\tilde{A} + \Delta\tilde{A})\tilde{Q} + \tilde{Q}(\tilde{A} + \Delta\tilde{A})^T \\ &\quad + \Omega_1(\tilde{Q}, A_c, B_c, C_c) - (\Delta\tilde{A}\tilde{Q} + \tilde{Q}\Delta\tilde{A}^T) + \tilde{V}_\Delta + \Omega_2(B_c) - \Delta\tilde{V}. \end{aligned} \quad (6.16)$$

Hence, by assumption, (6.16) has a solution  $\tilde{Q} \in \mathbb{N}^n$  for all  $(\Delta A, \Delta A_c, \Delta B_c, \Delta C_c) \in \mathcal{U} \times \mathcal{U}_c$  and, by (6.9) and (6.10),  $\Omega_1(\tilde{Q}, A_c, B_c, C_c) - (\Delta \tilde{A} \tilde{Q} + \tilde{Q} \Delta \tilde{A}^T)$  and  $\Omega_2(B_c) - \Delta \tilde{V}$  are nonnegative definite. Now, if the stabilizability condition (6.13) holds for all plant uncertainties and controller gain variations  $(\Delta A, \Delta A_c, \Delta B_c, \Delta C_c) \in \mathcal{U} \times \mathcal{U}_c$ , it follows from Theorem 3.6 of [115] that

$$\left( \tilde{A} + \Delta \tilde{A}, [\tilde{V}_\Delta + \Omega_1(\tilde{Q}, A_c, B_c, C_c) - (\Delta \tilde{A} \tilde{Q} + \tilde{Q} \Delta \tilde{A}^T) + \Omega_2(B_c) - \Delta \tilde{V}]^{\frac{1}{2}} \right)$$

is stabilizable for all  $(\Delta A, \Delta A_c, \Delta B_c, \Delta C_c) \in \mathcal{U} \times \mathcal{U}_c$ . It now follows from (6.16) and Lemma 12.2 of [115] that  $\tilde{A} + \Delta \tilde{A}$  is asymptotically stable for all plant uncertainties and controller gain variations  $(\Delta A, \Delta A_c, \Delta B_c, \Delta C_c) \in \mathcal{U} \times \mathcal{U}_c$ . Conversely, if  $\tilde{A} + \Delta \tilde{A}$  is asymptotically stable for all  $(\Delta A, \Delta A_c, \Delta B_c, \Delta C_c) \in \mathcal{U} \times \mathcal{U}_c$ , then (6.13) holds. Next, subtracting (6.8) from (6.16) yields

$$\begin{aligned} 0 &= (\tilde{A} + \Delta \tilde{A})(\tilde{Q} - \tilde{Q}_\Delta) + (\tilde{Q} - \tilde{Q}_\Delta)(\tilde{A} + \Delta \tilde{A})^T \\ &\quad + \Omega_1(\tilde{Q}, A_c, B_c, C_c) - (\Delta \tilde{A} \tilde{Q} + \tilde{Q} \Delta \tilde{A}^T) + \Omega_2(B_c) - \Delta \tilde{V}, \end{aligned}$$

or, equivalently, since  $\tilde{A} + \Delta \tilde{A}$  is asymptotically stable for all  $(\Delta A, \Delta A_c, \Delta B_c, \Delta C_c) \in \mathcal{U} \times \mathcal{U}_c$ ,

$$\begin{aligned} \tilde{Q} - \tilde{Q}_\Delta &= \int_0^\infty e^{(\tilde{A} + \Delta \tilde{A})t} \left[ \Omega_1(\tilde{Q}, A_c, B_c, C_c) - (\Delta \tilde{A} \tilde{Q} + \tilde{Q} \Delta \tilde{A}^T) + \Omega_2(B_c) - \Delta \tilde{V} \right] e^{(\tilde{A} + \Delta \tilde{A})^T t} dt \\ &\geq 0, \end{aligned}$$

which implies (6.14). The performance bound (6.15) is now an immediate consequence of (6.14) and (6.11) by noting that

$$J(A_c, B_c, C_c) = \sup_{\Delta \tilde{A} \in \mathcal{U} \times \mathcal{U}_c} \text{tr} \tilde{Q}_\Delta \tilde{R}_\Delta \leq \sup_{\Delta \tilde{A} \in \mathcal{U} \times \mathcal{U}_c} \text{tr} \tilde{Q} \tilde{R}_\Delta = \sup_{\Delta \tilde{A} \in \mathcal{U} \times \mathcal{U}_c} \text{tr} \tilde{Q} (\tilde{R} + \Delta \tilde{R}) \leq \text{tr} \tilde{Q} (\tilde{R} + \Omega_3(C_c)).$$

□

**Remark 6.1.** In applying Theorem 6.1 it may be convenient to replace Condition (6.13) with the stronger condition

$$\left( \tilde{A} + \Delta \tilde{A}, \left[ \tilde{V}_\Delta + \Omega_1(\tilde{Q}, A_c, B_c, C_c) - (\Delta \tilde{A} \tilde{Q} + \tilde{Q} \Delta \tilde{A}^T) + \Omega_2(B_c) - \Delta \tilde{V} \right]^{1/2} \right)$$

is stabilizable for all  $(\Delta A, \Delta A_c, \Delta B_c, \Delta C_c) \in \mathcal{U} \times \mathcal{U}_c$ , (6.17)

which is easier to verify in practice. Clearly, (6.17) is satisfied if  $\left[ \tilde{V}_\Delta + \Omega_1(\tilde{Q}, A_c, B_c, C_c) - (\Delta \tilde{A} \tilde{Q} + \tilde{Q} \Delta \tilde{A}^T) + \Omega_2(B_c) - \Delta \tilde{V} \right]$  is positive definite for all plant uncertainties and controller gain variations  $(\Delta A, \Delta A_c, \Delta B_c, \Delta C_c) \in \mathcal{U} \times \mathcal{U}_c$ . This will be the case, for example, if either  $\tilde{V}$  is positive definite or strict inequalities hold in (6.9) or (6.10).

## 6.4. Multiplicative Controller Uncertainty Structure and Guaranteed Cost Bound

Having established the theoretical basis for our approach, we now assign an explicit structure to the sets  $\mathcal{U}$  and  $\mathcal{U}_c$  and the bounding functions  $\Omega_1(\tilde{Q}, A_c, B_c, C_c)$ ,  $\Omega_2(B_c)$ , and  $\Omega_3(C_c)$ . Specifically, the uncertainty set  $\mathcal{U}$  capturing parametric plant uncertainty and the uncertainty set  $\mathcal{U}_c$  capturing multiplicative (relative) controller gain variations are defined by

$$\mathcal{U} \triangleq \{ \Delta A : \Delta A = B_0 F C_0, F^T F \leq \gamma^{-2} I_r \}, \quad (6.18)$$

$$\mathcal{U}_c \triangleq \{ (\Delta A_c, \Delta B_c, \Delta C_c) : \Delta A_c = \delta A_c, \Delta B_c = \delta B_c, \Delta C_c = \delta C_c, |\delta| \leq \gamma_c^{-1} \}, \quad (6.19)$$

where  $B_0 \in \mathbb{R}^{n \times s}$ ,  $C_0 \in \mathbb{R}^{r \times n}$  are fixed matrices denoting the structure of the plant uncertainty,  $F \in \mathbb{R}^{s \times r}$  is an uncertain matrix,  $\delta$  is an uncertain real parameter, and  $\gamma, \gamma_c$  are given positive numbers. With this uncertainty characterization, the closed-loop system (6.6) has structured uncertainty of the form

$$\Delta \tilde{A} = \tilde{B}_1 F \tilde{C}_1 + \delta \tilde{B}_2 \tilde{C}_2, \quad (6.20)$$

where

$$\tilde{B}_1 \triangleq \begin{bmatrix} B_0 \\ 0 \end{bmatrix}, \tilde{C}_1 \triangleq [C_0 \ 0], \tilde{B}_2 \triangleq \begin{bmatrix} 0 & 0 & B \\ I_{n_c} & I_{n_c} & 0 \end{bmatrix}, \tilde{C}_2 \triangleq \begin{bmatrix} 0 & A_c \\ B_c C & 0 \\ 0 & C_c \end{bmatrix}. \quad (6.21)$$

For the structure of  $\mathcal{U}$  and  $\mathcal{U}_c$  as specified by (6.18) and (6.19), the bounding functions  $\Omega_1(\tilde{Q}, A_c, B_c, C_c)$ ,  $\Omega_2(B_c)$ , and  $\Omega_3(C_c)$  can now be given a concrete form. For the statement of the next result, define  $\tilde{R}_{c_1} \triangleq \tilde{E}_{c_1}^T \tilde{E}_{c_1}$  and  $\tilde{V}_{c_1} \triangleq \tilde{D}_{c_1} \tilde{D}_{c_1}^T$ , where

$$\tilde{E}_{c_1} \triangleq [0 \ E_2 C_c], \quad \tilde{D}_{c_1} \triangleq \begin{bmatrix} 0 \\ B_c D_2 \end{bmatrix}.$$

**Proposition 6.1.** Let  $\alpha, \alpha_c > 0$ . Furthermore, let  $\mathcal{U}$  and  $\mathcal{U}_c$  be defined by (6.18) and (6.19), respectively, and define  $\Omega_1(\cdot)$ ,  $\Omega_2(\cdot)$ , and  $\Omega_3(\cdot)$  by

$$\Omega_1(\tilde{Q}, A_c, B_c, C_c) = \alpha \tilde{B}_1 \tilde{B}_1^T + \alpha_c \tilde{B}_2 \tilde{B}_2^T + \tilde{Q}(\alpha^{-1} \gamma^{-2} \tilde{C}_1^T \tilde{C}_1 + \alpha_c^{-1} \gamma_c^{-2} \tilde{C}_2^T \tilde{C}_2) \tilde{Q}, \quad (6.22)$$

$$\Omega_2(B_c) = (\gamma_c^{-2} + 2\gamma_c^{-1}) \tilde{V}_{c_1}, \quad (6.23)$$

$$\Omega_3(C_c) = (\gamma_c^{-2} + 2\gamma_c^{-1}) \tilde{R}_{c_1}. \quad (6.24)$$

Then (6.9)–(6.11) are satisfied.

**Proof.** Note that

$$\begin{aligned} 0 &\leq \begin{bmatrix} \alpha^{\frac{1}{2}} \tilde{B}_1 - \alpha^{-\frac{1}{2}} \tilde{Q} \tilde{C}_1^T F^T \\ \alpha_c^{\frac{1}{2}} \tilde{B}_2 - \alpha_c^{-\frac{1}{2}} \delta \tilde{Q} \tilde{C}_2^T \end{bmatrix} \begin{bmatrix} \alpha^{\frac{1}{2}} \tilde{B}_1 - \alpha^{-\frac{1}{2}} \tilde{Q} \tilde{C}_1^T F^T \\ \alpha_c^{\frac{1}{2}} \tilde{B}_2 - \alpha_c^{-\frac{1}{2}} \delta \tilde{Q} \tilde{C}_2^T \end{bmatrix}^T \\ &\leq \alpha \tilde{B}_1 \tilde{B}_1^T + \alpha_c \tilde{B}_2 \tilde{B}_2^T + \tilde{Q}(\alpha^{-1} \gamma^{-2} \tilde{C}_1^T \tilde{C}_1 + \alpha_c^{-1} \gamma_c^{-2} \tilde{C}_2^T \tilde{C}_2) \tilde{Q} - (\Delta \tilde{A} \tilde{Q} + \tilde{Q} \Delta \tilde{A}^T), \end{aligned}$$

which proves (6.9) with  $\mathcal{U}$  and  $\mathcal{U}_c$  given by (6.18) and (6.19), respectively. Next, note that

$$\Delta \tilde{V} = \begin{bmatrix} 0 & 0 \\ 0 & (\delta^2 + 2\delta) B_c V_2 B_c^T \end{bmatrix} \leq \begin{bmatrix} 0 & 0 \\ 0 & (\gamma_c^{-2} + 2\gamma_c^{-1}) B_c V_2 B_c^T \end{bmatrix} = \Omega_2(B_c),$$

which proves (6.10) with  $\mathcal{U}_c$  given by (6.19). Finally, a similar construction proves (6.11).  $\square$

Next, using Theorem 6.1 and Proposition 6.1 we have the following immediate result.

**Theorem 6.2.** Let  $\alpha, \alpha_c > 0$ , and suppose there exists a matrix  $\tilde{Q} \in \mathbb{N}^{\bar{n}}$  satisfying

$$\begin{aligned} 0 = & \tilde{A}\tilde{Q} + \tilde{Q}\tilde{A}^T + \tilde{Q}(\alpha^{-1}\gamma^{-2}\tilde{C}_1^T\tilde{C}_1 + \alpha_c^{-1}\gamma_c^{-2}\tilde{C}_2^T\tilde{C}_2)\tilde{Q} + \tilde{V} \\ & + \alpha\tilde{B}_1\tilde{B}_1^T + \alpha_c\tilde{B}_2\tilde{B}_2^T + (\gamma_c^{-2} + 2\gamma_c^{-1})\tilde{V}_{c_1}. \end{aligned} \quad (6.25)$$

Then  $(\tilde{A} + \Delta\tilde{A}, \tilde{D} + \Delta\tilde{D})$  is stabilizable for all  $(\Delta A, \Delta A_c, \Delta B_c, \Delta C_c) \in \mathcal{U} \times \mathcal{U}_c$  if and only if  $\tilde{A} + \Delta\tilde{A}$  is asymptotically stable for all  $(\Delta A, \Delta A_c, \Delta B_c, \Delta C_c) \in \mathcal{U} \times \mathcal{U}_c$ . In this case,

$$\tilde{Q}_\Delta \leq \tilde{Q}, \quad (\Delta A, \Delta A_c, \Delta B_c, \Delta C_c) \in \mathcal{U} \times \mathcal{U}_c, \quad (6.26)$$

where  $\tilde{Q}_\Delta$  satisfies (6.8), and

$$J(A_c, B_c, C_c) \leq \text{tr } \tilde{Q} \left[ \tilde{R} + (\gamma_c^{-2} + 2\gamma_c^{-1})\tilde{R}_{c_1} \right]. \quad (6.27)$$

## 6.5. Decentralized Static Output Feedback Formulation

In this section we use the fixed-structure control framework discussed in Chapter 2 to transform the Robust Stability and Performance Problem to a decentralized static output feedback setting. Specifically, note that for every dynamic controller (6.3), (6.4) with gain variations  $(\Delta A_c, \Delta B_c, \Delta C_c) \in \mathcal{U}_c$  given by (6.19), the uncertain closed-loop system (6.1)-(6.4) can be written as

$$\begin{bmatrix} \dot{x}(t) \\ \dot{x}_c(t) \end{bmatrix} = \begin{bmatrix} A + \Delta A & (1 + \delta)BC_c \\ (1 + \delta)B_c C & (1 + \delta)A_c \end{bmatrix} \begin{bmatrix} x(t) \\ x_c(t) \end{bmatrix} + \begin{bmatrix} D_1 \\ (1 + \delta)B_c D_2 \end{bmatrix} w(t). \quad (6.28)$$

Furthermore, by treating  $A_c$ ,  $B_c$ , and  $C_c$  as decentralized static output feedback gains with multiplicative (relative) uncertainty as shown in Figure 6.1, we can pull the uncertainty into the plant model obtaining

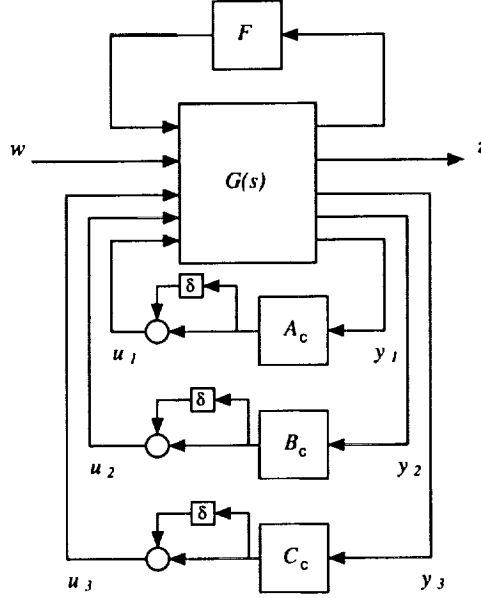


**Figure 6.1:** Decentralized static output feedback: Multiplicative controller uncertainty

$$\dot{\tilde{x}}(t) = (\mathcal{A} + \tilde{B}_1 F \tilde{C}_1) \tilde{x}(t) + (1 + \delta) \sum_{i=1}^3 \mathcal{B}_{u_i} u_i(t) + \mathcal{B}_w w(t), \quad t \in [0, \infty), \quad (6.29)$$

$$y_i(t) = \mathcal{C}_{y_i} \tilde{x}(t) + \mathcal{D}_{y w_i} w(t), \quad i = 1, 2, 3, \quad (6.30)$$

$$z(t) = \mathcal{C}_z \tilde{x}(t) + (1 + \delta) \sum_{i=1}^3 \mathcal{D}_{z u_i} u_i(t), \quad (6.31)$$

where  $u_i(t)$ ,  $i = 1, 2, 3$ , are given by

$$u_1(t) = A_c y_1(t), \quad u_2(t) = B_c y_2(t), \quad u_3(t) = C_c y_3(t). \quad (6.32)$$

Finally, by rewriting the decentralized control signals in the compact form

$$\hat{u}(t) = \mathcal{K} \hat{y}(t), \quad (6.33)$$

where

$$\hat{u}(t) \triangleq \begin{bmatrix} u_1(t) \\ \vdots \\ u_3(t) \end{bmatrix}, \quad \hat{y}(t) \triangleq \begin{bmatrix} y_1(t) \\ \vdots \\ y_3(t) \end{bmatrix}, \quad (6.34)$$

and  $\mathcal{K}$  is given by

$$\mathcal{K} \triangleq \begin{bmatrix} A_c & 0 & 0 \\ 0 & B_c & 0 \\ 0 & 0 & C_c \end{bmatrix}, \quad (6.35)$$

the uncertain closed-loop system is given by

$$\dot{\tilde{x}}(t) = (\tilde{A} + \Delta\tilde{A}) \tilde{x}(t) + (\tilde{D} + \Delta\tilde{D}) w(t), \quad (6.36)$$

$$z(t) = (\tilde{D} + \Delta\tilde{E}) \tilde{x}(t), \quad (6.37)$$

where

$$\Delta\tilde{A} \triangleq \tilde{B}_1 F \tilde{C}_1 + \delta\mathcal{B}_u \mathcal{K} \mathcal{C}_y, \quad \Delta\tilde{D} \triangleq \delta\mathcal{B}_u \mathcal{K} \mathcal{D}_{yw}, \quad \Delta\tilde{E} \triangleq \delta\mathcal{D}_{zu} \mathcal{K} \mathcal{C}_y.$$

Note that  $\tilde{B}_2 = \mathcal{B}_u$  and  $\tilde{C}_2 = \mathcal{K} \mathcal{C}_y$ .

We can now recast the Robust Stability and Performance Problem as the following Auxiliary Optimization Problem.

**Auxiliary Optimization Problem.** For given  $\alpha$ ,  $\alpha_c > 0$ , determine the block-diagonal controller matrix  $\mathcal{K} \in \mathbb{R}^{(2n_c+m) \times (2n_c+l)}$  that minimizes

$$\mathcal{J}(\mathcal{K}) = \text{tr } \tilde{Q} \left[ \tilde{R} + (\gamma_c^{-2} + 2\gamma_c^{-1}) \tilde{R}_{c_1} \right], \quad (6.38)$$

where  $\tilde{Q} \in \mathbb{N}^{\tilde{m}}$  satisfies (6.25).

It follows from Theorem 6.2 that the satisfaction of (6.25) for  $\tilde{Q} \in \mathbb{N}^{\tilde{m}}$  along with the generic stabilizability condition  $(\tilde{A} + \Delta\tilde{A}, \tilde{D} + \Delta\tilde{D})$  leads to closed-loop robust stability along with robust  $\mathcal{H}_2$  performance.

## 6.6. Sufficient Conditions for Fixed-Order Resilient Compensation with Multiplicative Uncertainty

In this section we state sufficient conditions for characterizing dynamic output feedback controllers guaranteeing robust stability and robust  $\mathcal{H}_2$  performance with respect to system plant uncertainty and multiplicative controller gain variations.

**Theorem 6.3.** Let  $\alpha, \alpha_c > 0$ . Suppose there exist matrices  $\tilde{Q}, \tilde{P} \in \mathbb{N}^{\tilde{n}}$  satisfying

$$0 = \tilde{A}\tilde{Q} + \tilde{Q}\tilde{A}^T + \tilde{Q} \left( \alpha^{-1}\gamma^{-2}\tilde{C}_1^T\tilde{C}_1 + \alpha_c^{-1}\gamma_c^{-2}\tilde{C}_2^T\tilde{C}_2 \right) \tilde{Q} + \tilde{V} \\ + \alpha\tilde{B}_1\tilde{B}_1^T + \alpha_c\tilde{B}_2\tilde{B}_2^T + (\gamma_c^{-2} + 2\gamma_c^{-1})\tilde{V}_{c_1}, \quad (6.39)$$

$$0 = \left[ \tilde{A} + \tilde{Q} \left( \alpha^{-1}\gamma^{-2}\tilde{C}_1^T\tilde{C}_1 + \alpha_c^{-1}\gamma_c^{-2}\tilde{C}_2^T\tilde{C}_2 \right) \right]^T \tilde{P} \\ + \tilde{P} \left[ \tilde{A} + \tilde{Q} \left( \alpha^{-1}\gamma^{-2}\tilde{C}_1^T\tilde{C}_1 + \alpha_c^{-1}\gamma_c^{-2}\tilde{C}_2^T\tilde{C}_2 \right) \right] + \tilde{R} + (\gamma_c^{-2} + 2\gamma_c^{-1})\tilde{R}_{c_1}, \quad (6.40)$$

and let  $(A_c, B_c, C_c)$  satisfy

$$0 = B_{u_1}^T \tilde{P} \tilde{Q} C_{y_1}^T + \alpha_c^{-1} \gamma_c^{-2} A_c C_y \tilde{Q} \tilde{P} \tilde{Q} C_{y_1}^T, \quad (6.41)$$

$$0 = B_{u_2}^T \tilde{P} \tilde{D} D_{y_{w2}}^T + B_{u_2}^T \tilde{P} \tilde{Q} C_{y_2}^T + \alpha_c^{-1} \gamma_c^{-2} B_c C_y \tilde{Q} \tilde{P} \tilde{Q} C_{y_2}^T \\ + (\gamma_c^{-2} + 2\gamma_c^{-1}) B_{u_2}^T \tilde{P} B_u \mathcal{K} D_{yw} D_{y_{w2}}^T, \quad (6.42)$$

$$0 = B_{u_3}^T \tilde{P} \tilde{Q} C_{y_3}^T + D_{z_{u3}}^T \tilde{E} \tilde{Q} C_{y_3}^T + \alpha_c^{-1} \gamma_c^{-2} C_c C_y \tilde{Q} \tilde{P} \tilde{Q} C_{y_3}^T \\ + (\gamma_c^{-2} + 2\gamma_c^{-1}) D_{z_{u3}}^T D_{zu} \mathcal{K} C_y \tilde{Q} C_{y_3}^T. \quad (6.43)$$

Then  $(\tilde{A} + \Delta\tilde{A}, \tilde{D} + \Delta\tilde{D})$  is stabilizable for all  $(\Delta A, \Delta A_c, \Delta B_c, \Delta C_c) \in \mathcal{U} \times \mathcal{U}_c$  if and only if  $\tilde{A} + \Delta\tilde{A}$  is asymptotically stable for all  $(\Delta A, \Delta A_c, \Delta B_c, \Delta C_c) \in \mathcal{U} \times \mathcal{U}_c$ . In this case, the worst-case  $\mathcal{H}_2$  performance of the closed-loop system (6.7) satisfies the bound

$$J(A_c, B_c, C_c) \leq \text{tr} \tilde{Q} \left[ \tilde{R} + (\gamma_c^{-2} + 2\gamma_c^{-1}) \tilde{R}_{c_1} \right]. \quad (6.44)$$

**Proof.** First we obtain necessary conditions for the Auxiliary Optimization Problem and then show, by construction, that these conditions serve as sufficient conditions for closed-loop stability and robust  $\mathcal{H}_2$  performance. Thus, to optimize (6.38) subject to (6.25), form the Lagrangian

$$\begin{aligned} \mathcal{L}(\mathcal{K}, \tilde{P}, \lambda) \triangleq & \text{tr} \left\{ \lambda \left[ \tilde{Q}\tilde{R} + (\gamma_c^{-2} + 2\gamma_c^{-1}) \tilde{Q}\tilde{R}_{c_1} \right] \right. \\ & + \tilde{P} \left[ \tilde{A}\tilde{Q} + \tilde{Q}\tilde{A}^T + \tilde{Q} \left( \alpha^{-1}\gamma^{-2}\tilde{C}_1^T\tilde{C}_1 + \alpha_c^{-1}\gamma_c^{-2}\tilde{C}_2^T\tilde{C}_2 \right) \tilde{Q} \right. \\ & \left. \left. + \tilde{V} + \alpha\tilde{B}_1\tilde{B}_1^T + \alpha_c\tilde{B}_2\tilde{B}_2^T + (\gamma_c^{-2} + 2\gamma_c^{-1}) \tilde{V}_{c_1} \right] \right\}, \end{aligned}$$

where the Lagrange multipliers  $\lambda \geq 0$  and  $\tilde{P} \in \mathbb{R}^{\tilde{n} \times \tilde{n}}$  are not both zero. By viewing  $\mathcal{K}$  and  $\tilde{Q}$  as independent variables, we obtain

$$\begin{aligned} \frac{\partial \mathcal{L}}{\partial \tilde{Q}} = & \left[ \tilde{A} + \tilde{Q} \left( \alpha^{-1}\gamma^{-2}\tilde{C}_1^T\tilde{C}_1 + \alpha_c^{-1}\gamma_c^{-2}\tilde{C}_2^T\tilde{C}_2 \right) \right]^T \tilde{P} \\ & + \tilde{P} \left[ \tilde{A} + \tilde{Q} \left( \alpha^{-1}\gamma^{-2}\tilde{C}_1^T\tilde{C}_1 + \alpha_c^{-1}\gamma_c^{-2}\tilde{C}_2^T\tilde{C}_2 \right) \right] + \lambda \left[ \tilde{R} + (\gamma_c^{-2} + 2\gamma_c^{-1}) \tilde{R}_{c_1} \right]. \end{aligned} \quad (6.45)$$

If  $\tilde{A} + \tilde{Q} \left( \alpha^{-1}\gamma^{-2}\tilde{C}_1^T\tilde{C}_1 + \alpha_c^{-1}\gamma_c^{-2}\tilde{C}_2^T\tilde{C}_2 \right)$  is Hurwitz, then  $\lambda = 0$  implies  $\tilde{P} = 0$ . Hence, it can be assumed without loss of generality that  $\lambda = 1$ . Furthermore, note that  $\tilde{P}$  is nonnegative definite. Thus the stationary conditions with  $\lambda = 1$  are given by

$$\begin{aligned} \frac{\partial \mathcal{L}}{\partial \tilde{Q}} = & \left[ \tilde{A} + \tilde{Q} \left( \alpha^{-1}\gamma^{-2}\tilde{C}_1^T\tilde{C}_1 + \alpha_c^{-1}\gamma_c^{-2}\tilde{C}_2^T\tilde{C}_2 \right) \right]^T \tilde{P} \\ & + \tilde{P} \left[ \tilde{A} + \tilde{Q} \left( \alpha^{-1}\gamma^{-2}\tilde{C}_1^T\tilde{C}_1 + \alpha_c^{-1}\gamma_c^{-2}\tilde{C}_2^T\tilde{C}_2 \right) \right] + \tilde{R} + (\gamma_c^{-2} + 2\gamma_c^{-1}) \tilde{R}_{c_1} = 0, \\ \frac{\partial \mathcal{L}}{\partial A_c} = & B_{u_1}^T \tilde{P} \tilde{Q} C_{y_1}^T + \alpha_c^{-1} \gamma_c^{-2} A_c C_y \tilde{Q} \tilde{P} \tilde{Q} C_{y_1}^T = 0, \\ \frac{\partial \mathcal{L}}{\partial B_c} = & B_{u_2}^T \tilde{P} \tilde{D} D_{y_{w2}}^T + B_{u_2}^T \tilde{P} \tilde{Q} C_{y_2}^T + \alpha_c^{-1} \gamma_c^{-2} B_c C_y \tilde{Q} \tilde{P} \tilde{Q} C_{y_2}^T \\ & + (\gamma_c^{-2} + 2\gamma_c^{-1}) B_{u_2}^T \tilde{P} B_u \mathcal{K} D_{y_w} D_{y_{w2}}^T = 0, \\ \frac{\partial \mathcal{L}}{\partial C_c} = & B_{u_3}^T \tilde{P} \tilde{Q} C_{y_3}^T + D_{z_{u3}}^T \tilde{E} \tilde{Q} C_{y_3}^T + \alpha_c^{-1} \gamma_c^{-2} C_c C_y \tilde{Q} \tilde{P} \tilde{Q} C_{y_3}^T \\ & + (\gamma_c^{-2} + 2\gamma_c^{-1}) D_{z_{u3}}^T D_{z_u} \mathcal{K} C_y \tilde{Q} C_{y_3}^T = 0, \end{aligned}$$

which are equivalent to (6.40)–(6.43). Equation (6.39) is a restatement of (6.25). It now follows from Theorem 6.2 that the stabilizability condition  $(\tilde{A} + \Delta\tilde{A}, \tilde{D} + \Delta\tilde{D})$

for all  $(\Delta A, \Delta A_c, \Delta B_c, \Delta C_c) \in \mathcal{U} \times \mathcal{U}_c$  is equivalent to the asymptotic stability of  $\tilde{A} + \Delta \tilde{A}$  for all  $(\Delta A, \Delta A_c, \Delta B_c, \Delta C_c) \in \mathcal{U} \times \mathcal{U}_c$ . Finally, the  $\mathcal{H}_2$  performance bound (6.44) is a restatement of (6.38).  $\square$

Equations (6.39)–(6.43) provide constructive sufficient conditions that yield dynamic controllers for robust resilient fixed-order (i.e., full- and reduced-order) output feedback compensation. In the design equations (6.40)–(6.42), one can view  $\alpha$  and  $\alpha_c$  as free parameters and optimize the performance criterion (6.38) with respect to  $\alpha$  and  $\alpha_c$ . In particular, setting  $\frac{\partial \mathcal{J}}{\partial \alpha} = 0$  and  $\frac{\partial \mathcal{J}}{\partial \alpha_c} = 0$  yields

$$\alpha = \frac{1}{\gamma} \left[ \frac{\text{tr } \tilde{P} \tilde{Q} \tilde{C}_1^T \tilde{C}_1 \tilde{Q}}{\text{tr } \tilde{P} \tilde{B}_1 \tilde{B}_1^T} \right]^{\frac{1}{2}}, \quad \alpha_c = \frac{1}{\gamma_c} \left[ \frac{\text{tr } \tilde{P} \tilde{Q} \tilde{C}_2^T \tilde{C}_2 \tilde{Q}}{\text{tr } \tilde{P} \tilde{B}_2 \tilde{B}_2^T} \right]^{\frac{1}{2}}. \quad (6.46)$$

It is important to note that  $\alpha$  and  $\alpha_c$  given by (6.46) are implicit since  $\tilde{Q}$  and  $\tilde{P}$  are functions of  $\alpha$  and  $\alpha_c$ . However, the optimal robust reduced-order controller gains and the scaling parameters  $\alpha$  and  $\alpha_c$  can be determined simultaneously within a numerical optimization algorithm using  $\frac{\partial \mathcal{J}}{\partial \alpha} = 0$  and  $\frac{\partial \mathcal{J}}{\partial \alpha_c} = 0$ . For details of this fact, see Section 6.10.

## 6.7. Additive Controller Uncertainty and Guaranteed Cost Bound

In this section we assign a different structure to the uncertainty set  $\mathcal{U}_c$  and consequently the bounding functions  $\Omega_i(\cdot)$ ,  $i = 1, 2, 3$ . Specifically, the uncertainty set  $\mathcal{U}_c$  is assumed to be of the form

$$\mathcal{U}_c \triangleq \{(\Delta A_c, \Delta B_c, \Delta C_c) : \Delta A_c = \delta \mathcal{I}_{A_c}, \Delta B_c = \delta \mathcal{I}_{B_c}, \Delta C_c = \delta \mathcal{I}_{C_c}, |\delta| \leq \gamma_c^{-1}\}, \quad (6.47)$$

where  $\mathcal{I}_{A_c}$ ,  $\mathcal{I}_{B_c}$ , and  $\mathcal{I}_{C_c}$  are ones matrices of dimension  $\mathbb{R}^{n_c \times n_c}$ ,  $\mathbb{R}^{n_c \times l}$ , and  $\mathbb{R}^{m \times n_c}$ , respectively,  $\delta$  is an uncertain real parameter, and  $\gamma_c$  is a given positive number. Note that, unlike the multiplicative uncertainty characterization addressed in Section 6.4,

the uncertainty characterization given by (6.47) can capture controller gain variations with zero entries in the nominal gain matrices  $(A_c, B_c, C_c)$ . With this additive (absolute) uncertainty characterization, the closed-loop system (6.6) has structured uncertainty of the form

$$\Delta \tilde{A} = \tilde{B}_0 \tilde{F} \tilde{C}_0, \quad (6.48)$$

where

$$\tilde{B}_0 \triangleq \begin{bmatrix} B_0 & 0 & 0 & B \\ 0 & I_{n_c} & \mathcal{I}_{B_c} & 0 \end{bmatrix}, \quad \tilde{F} \triangleq \begin{bmatrix} F & 0 & 0 & 0 \\ 0 & \delta I_{n_c} & 0 & 0 \\ 0 & 0 & \delta I_l & 0 \\ 0 & 0 & 0 & \delta I_m \end{bmatrix}, \quad \tilde{C}_0 \triangleq \begin{bmatrix} C_0 & 0 \\ 0 & \mathcal{I}_{A_c} \\ C & 0 \\ 0 & \mathcal{I}_{C_c} \end{bmatrix}. \quad (6.49)$$

For the structure of  $\mathcal{U} \times \mathcal{U}_c$  as specified by (6.18) and (6.47), the bounding functions  $\Omega_1(\tilde{Q})$ ,  $\Omega_2(B_c)$ , and  $\Omega_3(C_c)$  can now be given a concrete form. For the statement of the next result, define  $\tilde{R}_{c_2} \triangleq \tilde{E}_{c_2}^T \tilde{E}_{c_2}$  and  $\tilde{V}_{c_2} \triangleq \tilde{D}_{c_2}^T \tilde{D}_{c_2}$ , where

$$\tilde{E}_{c_2} \triangleq \begin{bmatrix} 0 & E_2 \mathcal{I}_{C_c} \end{bmatrix}, \quad \tilde{D}_{c_2} \triangleq \begin{bmatrix} 0 \\ \mathcal{I}_{B_c} D_2 \end{bmatrix}.$$

Furthermore, to enforce the block-structure of the uncertainty matrix  $\tilde{F}$ , define the set of compatible scaling matrices  $\mathcal{D}$  by

$$\mathcal{D} \triangleq \{ \tilde{D}_0 > 0 : \tilde{F} \tilde{D}_0 = \tilde{D}_0 \tilde{F}, \tilde{F}^T \tilde{F} \leq \tilde{N} \},$$

where

$$\tilde{N} \triangleq \begin{bmatrix} \gamma^2 I_r & 0 \\ 0 & \gamma_c^2 I_{(n_c+l+m)} \end{bmatrix}.$$

The condition  $\tilde{F} \tilde{D}_0 = \tilde{D}_0 \tilde{F}$  in  $\mathcal{D}$  is analogous to the commuting assumption between the  $D$ -scales and  $\Delta$  blocks in  $\mu$ -analysis and synthesis which accounts for the structure in the uncertainty  $\tilde{F}$ . It is easy to see that there *always exists* such a matrix  $\tilde{D}_0$  even if  $\tilde{F}$  is *neither diagonal nor symmetric*. For example, if  $F = f I_r$ , where  $f$  is a scalar uncertainty, then  $\tilde{D}_0$  can be an arbitrary positive definite matrix. Alternatively, if  $F \in \mathbb{R}^{r \times r}$  is nondiagonal, then one can always choose  $\tilde{D}_0 = \text{block-diag}[d I_r, D_0]$ ,

where  $d$  is a scalar and  $D_0 \in \mathbb{R}^{(n_c+l+m) \times (n_c+l+m)}$  is an arbitrary matrix. Of course,  $\tilde{F}$  and  $\tilde{D}_0$  may have more intricate structure, for example, they may be block-diagonal with commuting blocks situated on the diagonal.

**Proposition 6.2.** Let  $\alpha_1 > 0$ ,  $\alpha_2 > 0$ , and let  $\tilde{D}_0 \in \mathcal{D}$ . Furthermore, let  $\mathcal{U}$  and  $\mathcal{U}_c$  be defined by (6.18) and (6.47), respectively, and define  $\Omega_1(\cdot)$ ,  $\Omega_2(\cdot)$ , and  $\Omega_3(\cdot)$  by

$$\Omega_1(\tilde{Q}) = \tilde{Q}\tilde{C}_0^T\tilde{D}_0\tilde{N}\tilde{D}_0\tilde{C}_0\tilde{Q} + \tilde{B}_0\tilde{D}_0^{-2}\tilde{B}_0^T, \quad (6.50)$$

$$\Omega_2(B_c) = \alpha_1^{-1}\gamma_c^{-2}\tilde{V}_{c_1} + (\alpha_1 + \gamma_c^{-2})\tilde{V}_{c_2}, \quad (6.51)$$

$$\Omega_3(C_c) = \alpha_2^{-1}\gamma_c^{-2}\tilde{R}_{c_1} + (\alpha_2 + \gamma_c^{-2})\tilde{R}_{c_2}. \quad (6.52)$$

Then (6.9)–(6.11) are satisfied.

**Proof.** Note that with  $\tilde{D}_0 \in \mathcal{D}$

$$\begin{aligned} 0 &\leq \left[ \tilde{B}_0\tilde{D}_0^{-1} - \tilde{Q}\tilde{C}_0^T\tilde{D}_0\tilde{F}^T \right] \left[ \tilde{B}_0\tilde{D}_0^{-1} - \tilde{Q}\tilde{C}_0^T\tilde{D}_0\tilde{F}^T \right]^T \\ &\leq \tilde{B}_0\tilde{D}_0^{-2}\tilde{B}_0^T + \tilde{Q}\tilde{C}_0^T\tilde{D}_0\tilde{N}\tilde{D}_0\tilde{C}_0\tilde{Q} - (\Delta\tilde{A}\tilde{Q} + \tilde{Q}\Delta\tilde{A}^T), \end{aligned}$$

which proves (6.9) with  $\mathcal{U}$  and  $\mathcal{U}_c$  given by (6.18) and (6.47), respectively. Next, note that

$$\Delta\tilde{V} = \delta\tilde{D}_{c_1}\tilde{D}_{c_2}^T + \delta\tilde{D}_{c_2}\tilde{D}_{c_1}^T + \delta^2\tilde{D}_{c_2}\tilde{D}_{c_2}^T.$$

Now, since  $\delta^2\tilde{D}_{c_2}\tilde{D}_{c_2}^T \leq \gamma_c^{-2}\tilde{D}_{c_2}\tilde{D}_{c_2}^T$  and

$$\begin{aligned} 0 &\leq \left[ \alpha_1^{\frac{1}{2}}\tilde{D}_{c_2} - \alpha_1^{-\frac{1}{2}}\Delta\tilde{D}_{c_1} \right] \left[ \alpha_1^{\frac{1}{2}}\tilde{D}_{c_2} - \alpha_1^{-\frac{1}{2}}\Delta\tilde{D}_{c_1} \right]^T \\ &\leq \alpha_1\tilde{D}_{c_2}\tilde{D}_{c_2}^T + \alpha_1^{-1}\gamma_c^{-2}\tilde{D}_{c_1}\tilde{D}_{c_1}^T - \delta(\tilde{D}_{c_1}\tilde{D}_{c_2}^T + \tilde{D}_{c_2}\tilde{D}_{c_1}^T), \end{aligned}$$

it follows that

$$\Delta\tilde{V} \leq (\alpha_1 + \gamma_c^{-2})\tilde{V}_{c_2} + \alpha_1^{-1}\gamma_c^{-2}\tilde{V}_{c_1},$$

which proves (6.10) with  $\mathcal{U}_c$  given by (6.47). Finally, a similar construction proves (6.11).  $\square$

Next, using Theorem 6.1 and Proposition 6.2 we have the following immediate result.

**Theorem 6.4.** Let  $\alpha_1, \alpha_2 > 0$ ,  $\tilde{D}_0 \in \mathcal{D}$ , and suppose there exists a matrix  $\tilde{Q} \in \mathbb{N}^{\tilde{n}}$  satisfying

$$0 = \tilde{A}\tilde{Q} + \tilde{Q}\tilde{A}^T + \tilde{Q}\tilde{C}_0^T\tilde{D}_0\tilde{N}\tilde{D}_0\tilde{C}_0\tilde{Q} + \tilde{B}_0\tilde{D}_0^{-2}\tilde{B}_0^T + \tilde{V} + \alpha_1^{-1}\gamma_c^{-2}\tilde{V}_{c_1} + (\alpha_1 + \gamma_c^{-2})\tilde{V}_{c_2}. \quad (6.53)$$

Then  $(\tilde{A} + \Delta\tilde{A}, \tilde{D} + \Delta\tilde{D})$  is stabilizable for all  $(\Delta A, \Delta A_c, \Delta B_c, \Delta C_c) \in \mathcal{U} \times \mathcal{U}_c$  if and only if  $\tilde{A} + \Delta\tilde{A}$  is asymptotically stable for all  $(\Delta A, \Delta A_c, \Delta B_c, \Delta C_c) \in \mathcal{U} \times \mathcal{U}_c$ . In this case,

$$\tilde{Q}_\Delta \leq \tilde{Q}, \quad (\Delta A, \Delta A_c, \Delta B_c, \Delta C_c) \in \mathcal{U} \times \mathcal{U}_c, \quad (6.54)$$

where  $\tilde{Q}_\Delta$  satisfies (6.8), and

$$J(A_c, B_c, C_c) \leq \text{tr } \tilde{Q} \left[ \tilde{R} + \alpha_2^{-1}\gamma_c^{-2}\tilde{R}_{c_1} + (\alpha_2 + \gamma_c^{-2})\tilde{R}_{c_2} \right]. \quad (6.55)$$

## 6.8. Decentralized Static Output Feedback Formulation

As in Section 6.5, note that for every dynamic controller (6.3), (6.4) with gain variations  $(\Delta A_c, \Delta B_c, \Delta C_c) \in \mathcal{U}_c$  given by (6.47), the closed-loop system (6.1)–(6.4) can be written as

$$\begin{bmatrix} \dot{x}(t) \\ \dot{x}_c(t) \end{bmatrix} = \begin{bmatrix} A + B_0FC_0 & BC_c + \delta B\mathcal{I}_{C_c} \\ B_cC + \delta\mathcal{I}_{B_c}C & A_c + \delta\mathcal{I}_{A_c} \end{bmatrix} \begin{bmatrix} x(t) \\ x_c(t) \end{bmatrix} + \begin{bmatrix} D_1 \\ B_cD_2 + \delta\mathcal{I}_{B_c}D_2 \end{bmatrix} w(t). \quad (6.56)$$

Furthermore, by treating  $A_c$ ,  $B_c$ , and  $C_c$  as decentralized static output feedback gains with additive uncertainty as shown in Figure 6.2, we can pull the uncertainty into the plant model obtaining

$$\dot{\tilde{x}}(t) = (\mathcal{A} + \Delta\mathcal{A})\tilde{x}(t) + \sum_{i=1}^3 \mathcal{B}_{u_i}u_i(t) + (\mathcal{B}_w + \Delta\mathcal{B}_w)w(t), \quad t \in [0, \infty), \quad (6.57)$$

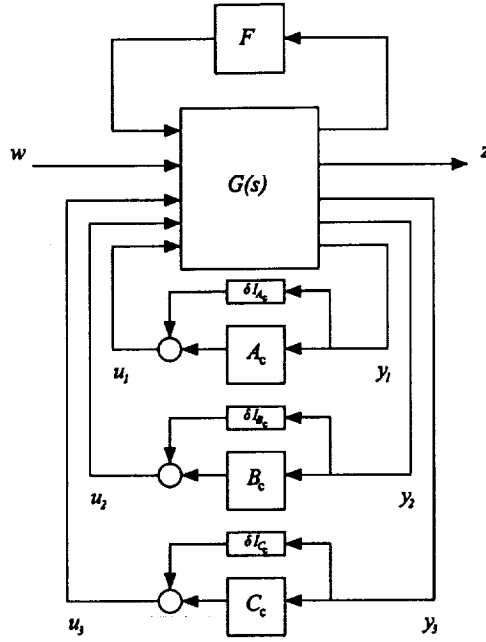


**Figure 6.2:** Decentralized static output feedback: Additive controller uncertainty

$$y_i(t) = C_{y_i} \tilde{x}(t) + D_{y_w} w(t), \quad i = 1, 2, 3, \quad (6.58)$$

$$z(t) = (C_z + \Delta C_z) \tilde{x}(t) + \sum_{i=1}^3 D_{z u_i} u_i(t), \quad (6.59)$$

where  $u_i(t)$ ,  $i = 1, 2, 3$ , are given by (6.32) and

$$\Delta \mathcal{A} \triangleq \begin{bmatrix} B_0 F C_0 & \delta B \mathcal{I}_{C_c} \\ \delta \mathcal{I}_{B_c} C & \delta \mathcal{I}_{A_c} \end{bmatrix}, \quad \Delta \mathcal{B}_w \triangleq \begin{bmatrix} 0 \\ \delta \mathcal{I}_{B_c} D_2 \end{bmatrix}, \quad \Delta C_z \triangleq [0 \quad \delta E_2 \mathcal{I}_{C_c}].$$

The uncertain closed-loop system is now given by

$$\dot{\tilde{x}}(t) = (\tilde{A} + \Delta \tilde{A}) \tilde{x}(t) + (\tilde{D} + \Delta \tilde{D}) w(t), \quad t \in [0, \infty), \quad (6.60)$$

$$z(t) = (\tilde{E} + \Delta \tilde{E}) \tilde{x}(t), \quad (6.61)$$

where  $\Delta \tilde{A} \triangleq \Delta \mathcal{A}$ ,  $\Delta \tilde{D} \triangleq \Delta \mathcal{B}_w$ , and  $\Delta \tilde{E} \triangleq \Delta C_z$ .

Now, as in the multiplicative controller uncertainty case, we introduce an Auxiliary Optimization Problem by considering

$$\mathcal{J}(\mathcal{K}) = \text{tr} \tilde{Q} \left[ \tilde{R} + \alpha_2^{-1} \gamma_c^{-2} \tilde{R}_{c_1} + (\alpha_2 + \gamma_c^{-2}) \tilde{R}_{c_2} \right], \quad (6.62)$$

with  $\tilde{Q} \in \mathbb{N}^{\tilde{n}}$  satisfying (6.53), and proceed by determining controller gains that minimize  $\mathcal{J}(\mathcal{K})$ .

## 6.9. Sufficient Conditions for Fixed-Order Resilient Compensation with Additive Uncertainty

In this section we state sufficient conditions for characterizing dynamic output feedback controllers guaranteeing robust stability and robust  $\mathcal{H}_2$  performance with respect to system plant uncertainty and additive controller gain variations.

**Theorem 6.5.** Let  $\alpha_1, \alpha_2 > 0$ , and let  $\tilde{D}_0 \in \mathcal{D}$ . Suppose there exist matrices  $\tilde{Q}, \tilde{P} \in \mathbb{N}^{\tilde{n}}$  satisfying

$$0 = \tilde{A}\tilde{Q} + \tilde{Q}\tilde{A}^T + \tilde{Q}\tilde{C}_0^T\tilde{D}_0\tilde{N}\tilde{D}_0\tilde{C}_0\tilde{Q} + \tilde{B}_0\tilde{D}_0^{-2}\tilde{B}_0^T + \tilde{V} + \alpha_1^{-1}\gamma_c^{-2}\tilde{V}_{c_1} + (\alpha_1 + \gamma_c^{-2})\tilde{V}_{c_2}, \quad (6.63)$$

$$0 = \left( \tilde{A} + \tilde{Q}\tilde{C}_0^T\tilde{D}_0\tilde{N}\tilde{D}_0\tilde{C}_0 \right)^T \tilde{P} + \tilde{P} \left( \tilde{A} + \tilde{Q}\tilde{C}_0^T\tilde{D}_0\tilde{N}\tilde{D}_0\tilde{C}_0 \right) + \tilde{R} + \alpha_2^{-1}\gamma_c^{-2}\tilde{R}_{c_1} + (\alpha_2 + \gamma_c^{-2})\tilde{R}_{c_2}, \quad (6.64)$$

and let  $(A_c, B_c, C_c)$  satisfy

$$0 = B_{u_1}^T \tilde{P} \tilde{Q} C_{y_1}^T, \quad (6.65)$$

$$0 = B_{u_2}^T \tilde{P} \tilde{D} D_{yw_2}^T + B_{u_2}^T \tilde{P} \tilde{Q} C_{y_2}^T + \alpha_1^{-1} \gamma_c^{-2} B_{u_2}^T \tilde{P} B_u \mathcal{K} D_{yw} D_{yw_2}^T, \quad (6.66)$$

$$0 = B_{u_3}^T \tilde{P} \tilde{Q} C_{y_3}^T + D_{zu_3}^T \tilde{E} \tilde{Q} C_{y_3}^T + \alpha_2^{-1} \gamma_c^{-2} D_{zu_3}^T D_{zu} \mathcal{K} C_y \tilde{Q} C_{y_3}^T. \quad (6.67)$$

Then  $(\tilde{A} + \Delta\tilde{A}, \tilde{D} + \Delta\tilde{D})$  is stabilizable for all  $(\Delta A, \Delta A_c, \Delta B_c, \Delta C_c) \in \mathcal{U} \times \mathcal{U}_c$  if and only if  $\tilde{A} + \Delta\tilde{A}$  is asymptotically stable for all  $(\Delta A, \Delta A_c, \Delta B_c, \Delta C_c) \in \mathcal{U} \times \mathcal{U}_c$ . In this case, the worst-case  $\mathcal{H}_2$  performance of the closed-loop system (6.7) satisfies the bound

$$J(A_c, B_c, C_c) \leq \text{tr} \tilde{Q} \left[ \tilde{R} + \alpha_2^{-1} \gamma_c^{-2} \tilde{R}_{c_1} + (\alpha_2 + \gamma_c^{-2}) \tilde{R}_{c_2} \right]. \quad (6.68)$$

**Proof.** The proof is similar to the proof of Theorem 6.1.  $\square$

As in Section 6.6, one can view  $\alpha_i$ ,  $i = 1, 2$ , and  $\tilde{D}_0$  as free parameters and optimize the performance criterion  $\mathcal{J}(\mathcal{K})$  given by (6.62) with respect to  $\alpha_i$ ,  $i = 1, 2$ , and  $\tilde{D}_0$ . In particular, setting  $\frac{\partial \mathcal{J}}{\partial \alpha_i} = 0$ ,  $i = 1, 2$ , and  $\frac{\partial \mathcal{J}}{\partial \tilde{D}_0} = 0$  yields, respectively,

$$\alpha_1 = \frac{1}{\gamma_c} \left[ \frac{\text{tr } \tilde{P} \tilde{V}_{c_1}}{\text{tr } \tilde{P} \tilde{V}_{c_2}} \right]^{\frac{1}{2}}, \quad \alpha_2 = \frac{1}{\gamma_c} \left[ \frac{\text{tr } \tilde{Q} \tilde{R}_{c_1}}{\text{tr } \tilde{Q} \tilde{R}_{c_2}} \right]^{\frac{1}{2}}, \quad (6.69)$$

$$0 = \tilde{N} \tilde{D}_0 \tilde{C}_0 \tilde{Q} \tilde{P} \tilde{Q} \tilde{C}_0^T - \tilde{D}_0^{-1} \tilde{B}_0^T \tilde{P} \tilde{B}_0 \tilde{D}_0^{-2}. \quad (6.70)$$

## 6.10. Quasi-Newton Optimization Algorithm

As mentioned in Section 2.3, the optimization algorithm was initialized with an LQG controller for full-order controller designs, while for reduced-order control, the algorithm was initialized with a balanced truncated LQG controller. A large value was chosen for  $\gamma$  and then a feasible value of  $\gamma_c$  was calculated. The quasi-Newton optimization algorithm was used to find the controller gains  $A_c$ ,  $B_c$ , and  $C_c$ . After each iteration,  $\gamma_c$  was decreased and the current values of the controller gains ( $A_c$ ,  $B_c$ ,  $C_c$ ) were then used as the starting point for the next iteration. When  $\gamma_c$  could not be decreased any further,  $\gamma$  was decreased and a feasible  $\gamma_c$  was calculated for the new value of  $\gamma$  and the process was repeated.

## 6.11. Second-Order Unstable System

To demonstrate the design of robust resilient controllers, consider the second-order unstable system originally presented in [29] to illustrate the lack of guaranteed gain margins for LQG controllers. Specifically, the state space system is given by

$$\begin{aligned} \dot{x}(t) &= \begin{bmatrix} 1 & 1 \\ 0 & 1 \end{bmatrix} x(t) + \begin{bmatrix} 0 \\ 1 \end{bmatrix} u(t), \quad t \in [0, \infty) \\ y(t) &= [1 \ 0] x(t). \end{aligned}$$

The matrices  $D_1$ ,  $D_2$ ,  $E_1$ , and  $E_2$  are chosen to be

$$D_1 = \begin{bmatrix} \sqrt{60} & 0 \\ \sqrt{60} & 0 \end{bmatrix}, \quad D_2 = [0 \quad 1], \quad E_1 = \begin{bmatrix} \sqrt{60} & \sqrt{60} \\ 0 & 0 \end{bmatrix}, \quad E_2 = \begin{bmatrix} 0 \\ 1 \end{bmatrix}.$$

Here we consider uncertainty in the (2, 1) component of the dynamics matrix. Using the uncertainty structure given by (6.18), the actual dynamics are given by  $A + B_0 f C_0$ , where  $B_0 = [1 \quad 0]^T$  and  $C_0 = [0 \quad 1]$ .

The quasi-Newton optimization algorithm discussed in Section 6.10 was used to compute full-order controllers ( $n_c = 2$ ) that minimize the cost bound  $\mathcal{J}$  for several values of  $\gamma$  and  $\gamma_c$  for both the multiplicative and additive uncertainty characterizations. The actual  $\mathcal{H}_2$  cost was computed for a range of values of the controller error parameter  $\delta$  and the plant uncertainty  $f$ . The cost dependence for the multiplicative (relative) uncertainty characterization (6.19) is shown in Figure 6.4. As  $\gamma_c$  decreases, the  $\mathcal{H}_2$  cost of the nominal closed-loop system increases while the  $\mathcal{H}_2$  cost of the perturbed closed-loop system remains near the nominal value for a larger range of perturbations. The LQG controller stabilizes the closed-loop system for only small perturbations in the controller error parameter, while the resilient controllers stabilize the closed-loop system and provide performance close to the optimal level for much larger perturbations in the controller error parameter. Hence, robust performance over a large range of the uncertain parameter is achieved for some increase in the  $\mathcal{H}_2$  cost above the optimal.

The effects of both plant uncertainty and controller uncertainty can be seen in the parameter plot shown in Figure 6.5. In this case, the stability of the closed-loop system was checked over a grid of the uncertain parameters for both the LQG and a robust resilient controller. The dashed line shows the region of asymptotic stability of the LQG controller, the solid line corresponds to the robust resilient controller, and 'x' marks the point corresponding to the nominal conditions. It is evident from the

figure that the robust resilient controller renders the closed-loop system more robust to perturbations in both the plant and controller.

Next, Figure 6.6 shows the Nyquist plots of the loop gain of the system for the LQG controller and three different robust resilient controller designs. These plots clearly demonstrate the resiliency of the non-fragile controllers over the LQG controller in terms of their increased gain and phase margins. Figures 6.7–6.9 give the same plots for the case of additive (absolute) controller uncertainty. Once again, the achieved robustness of the robust resilient controllers over the LQG controller is obvious. Figure 6.7 also shows the cost dependence of an  $\mathcal{H}_\infty$  robust controller which shows that although the  $\mathcal{H}_\infty$  controller is robust against plant variations, it is highly fragile with respect to controller gain variations. The Nyquist plots of the loop gain of the  $\mathcal{H}_\infty$  robust controller and the robust resilient controller corresponding to identical plant uncertainty levels are shown in Figure 6.10, which clearly shows the relative stability superiority of the robust resilient controller over the robust  $\mathcal{H}_\infty$  controller.

## 6.12. Two-Mass Benchmark Problem

Consider the two-mass system shown in Figure 6.3 with  $m_1 = m_2 = 1$  and an

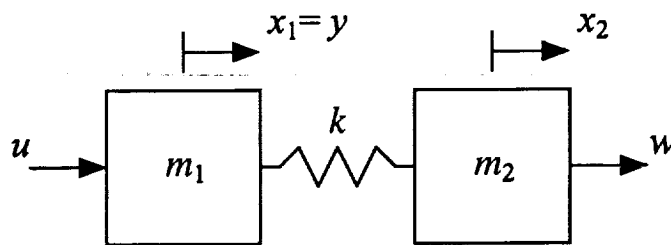


Figure 6.3: Two mass oscillator

uncertain spring stiffness  $k$  [114]. A control force acts on mass 1 and the position of mass 2 is measured, resulting in a noncolocated control problem. The nominal system

dynamics with  $k_{\text{nom}} = 1$  and states defined in the figure are given by

$$\begin{aligned} \dot{x}(t) &= \begin{bmatrix} 0 & 0 & 1 & 0 \\ 0 & 0 & 0 & 1 \\ -1 & 1 & 0 & 0 \\ 1 & -1 & 0 & 0 \end{bmatrix} x(t) + \begin{bmatrix} 0 \\ 0 \\ 1 \\ 0 \end{bmatrix} u(t) + \begin{bmatrix} 0 & 0 \\ 0 & 0 \\ 0 & 0 \\ 1 & 0 \end{bmatrix} w(t), \\ y(t) &= [0 \ 1 \ 0 \ 0] x(t) + [0 \ 1] w(t). \end{aligned}$$

Using the uncertainty structure given by (6.18), the actual dynamics are given by  $A + B_0 f C_0$ , where  $B_0 = [0 \ 0 \ -1 \ 1]^T$  and  $C_0 = [1 \ -1 \ 0 \ 0]$ . The matrices  $E_1$  and  $E_2$  are chosen to be

$$E_1 = \begin{bmatrix} 0 & 1 & 0 & 0 \\ 0 & 0 & 0 & 0 \end{bmatrix}, \quad E_2 = \begin{bmatrix} 0 \\ \sqrt{0.001} \end{bmatrix}.$$

As in Section 6.11, the quasi-Newton optimization algorithm was used to compute full-order controllers ( $n_c = 4$ ) that minimize the cost bound  $\mathcal{J}$ . The cost dependence for the multiplicative uncertainty characterization is shown in Figure 6.11. The Nyquist plots of the LQG controller and three robust resilient controllers are shown in Figure 6.12. For the additive uncertainty characterization, the cost dependence is compared to the LQG controller and an  $\mathcal{H}_\infty$  robust controller in Figure 6.13. The asymptotic stability regions of the LQG controller and the robust resilient controller are shown in Figure 6.14. Finally, the Nyquist plots of the LQG controller and three robust resilient controllers are shown in Figure 6.15, while the Nyquist plots of the  $\mathcal{H}_\infty$  robust controller and the robust resilient controller corresponding to identical plant uncertainty levels are shown in Figure 6.16. In all cases, the robust resilient controllers are superior in their ability to tolerate plant *and* controller uncertainty as compared to the LQG and robust  $\mathcal{H}_\infty$  controllers. Furthermore, the robust resilient controllers possess far superior gain and phase margins.

## 6.13. Conclusion

In this chapter, we extended the robust fixed-structure guaranteed cost controller synthesis framework to synthesize robust resilient controllers for controller gain variations and system parametric uncertainty. Specifically, the guaranteed cost approach of [10] and [13] was used to develop sufficient conditions for robust stability and  $\mathcal{H}_2$  performance via fixed-order dynamic compensation. A quasi-Newton optimization algorithm was used to obtain robust controllers for two illustrative examples.

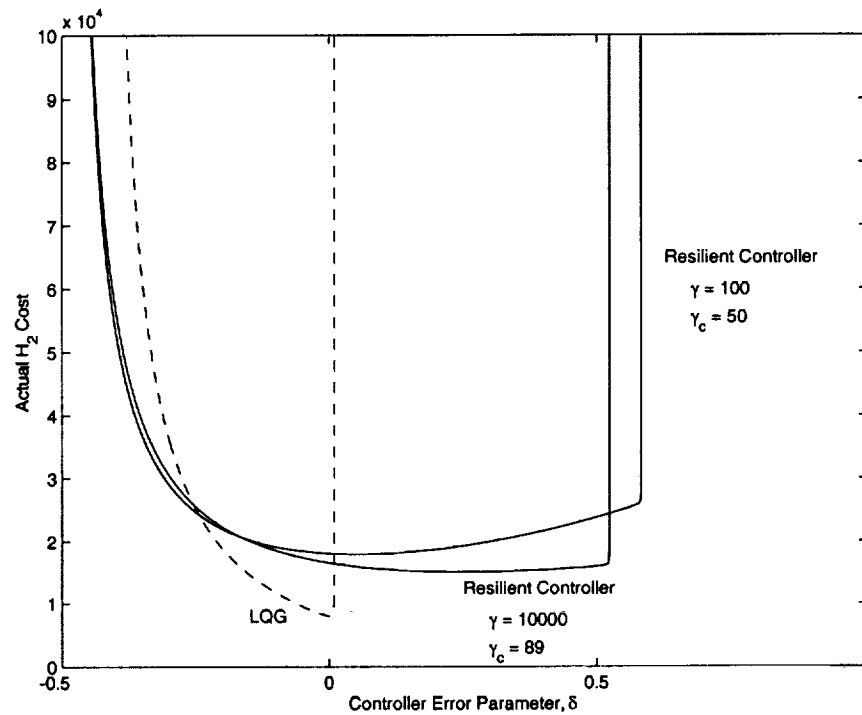


Figure 6.4: Dependence of the  $\mathcal{H}_2$  cost on the controller error parameter

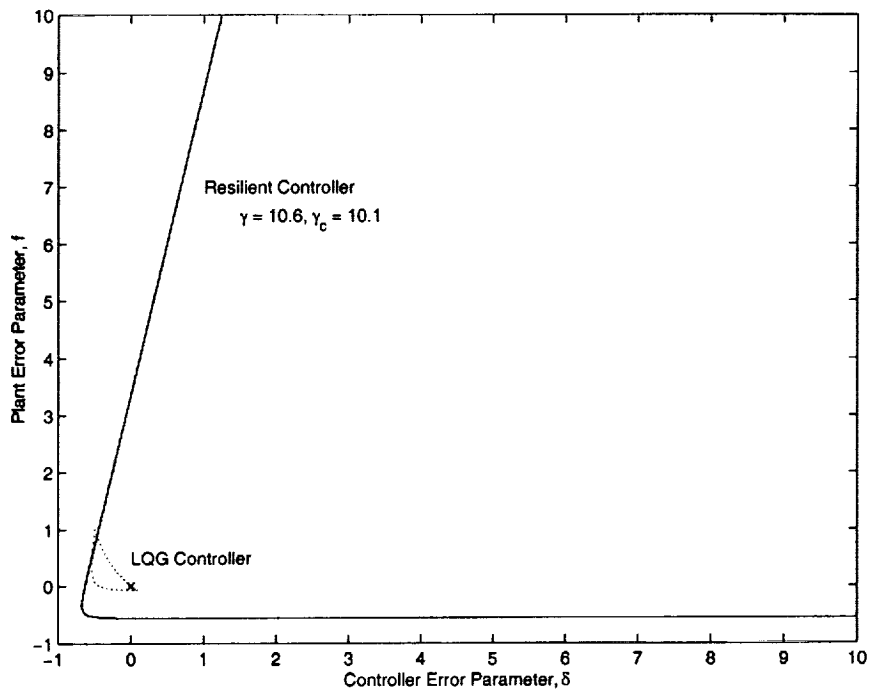


Figure 6.5: Asymptotic stability regions

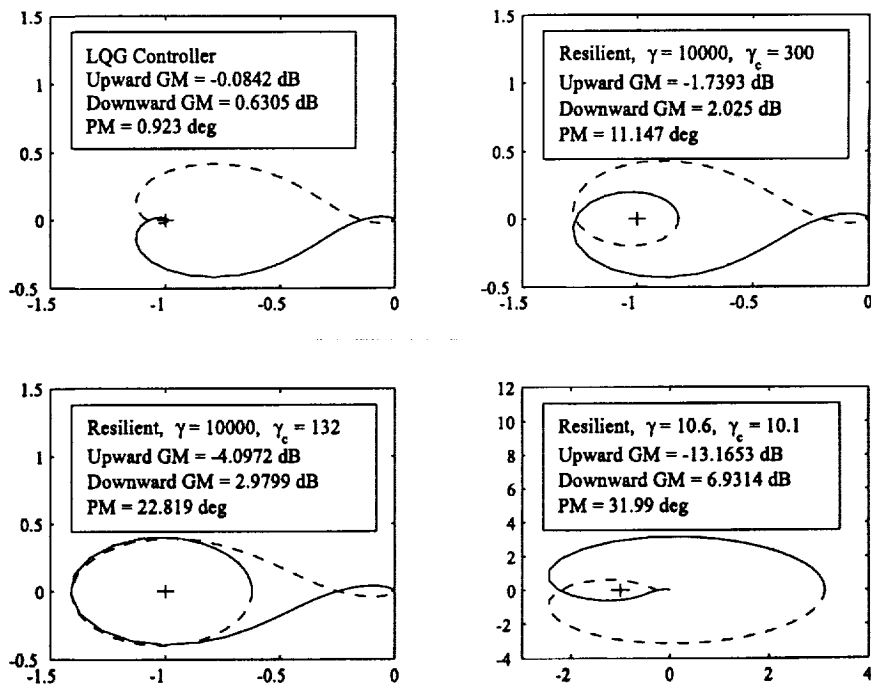


Figure 6.6: Loop gain Nyquist plots

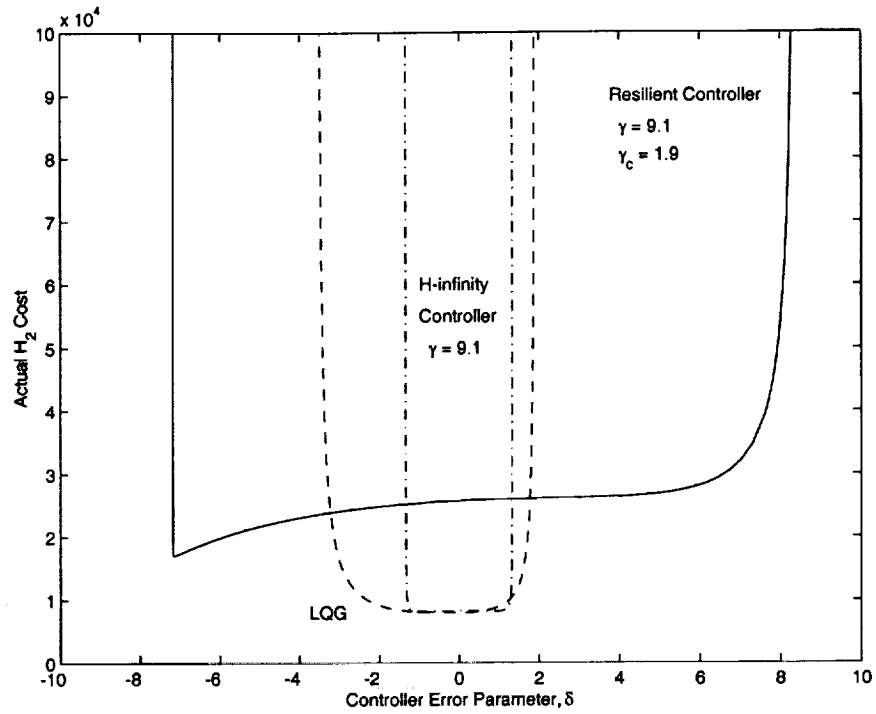


Figure 6.7: Dependence of the  $\mathcal{H}_2$  cost on the controller error parameter

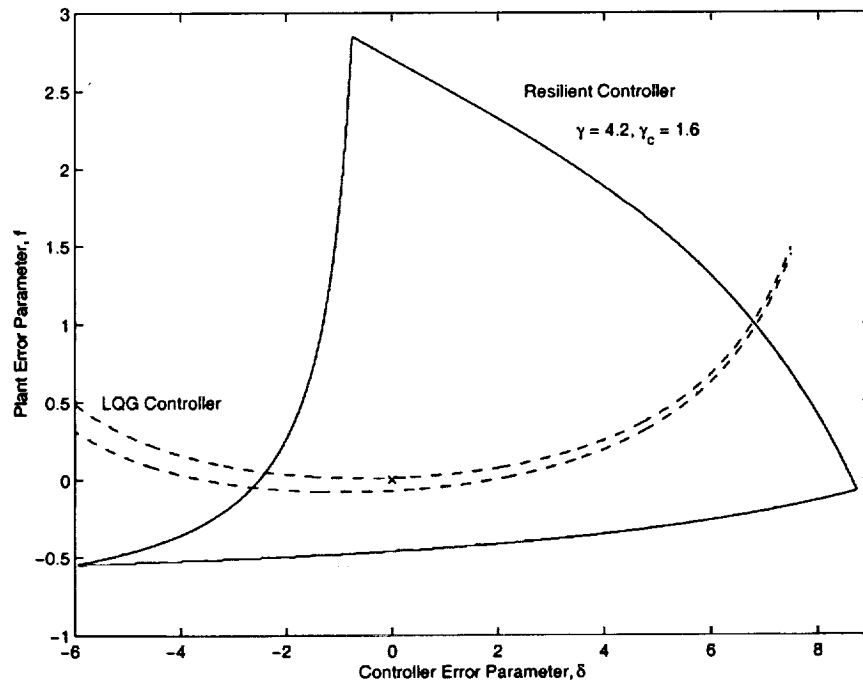


Figure 6.8: Asymptotic stability regions

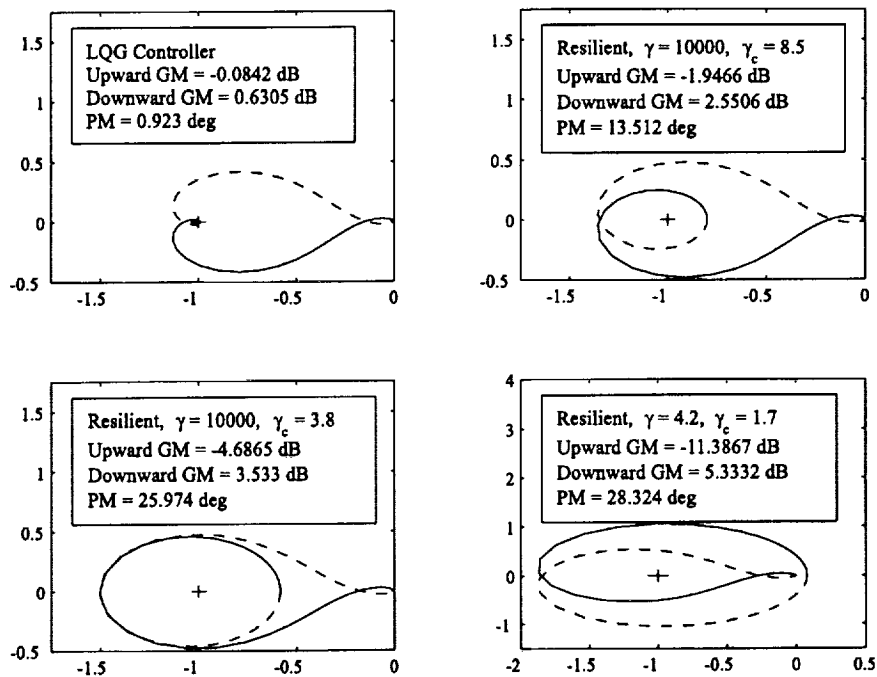


Figure 6.9: Loop gain Nyquist plots

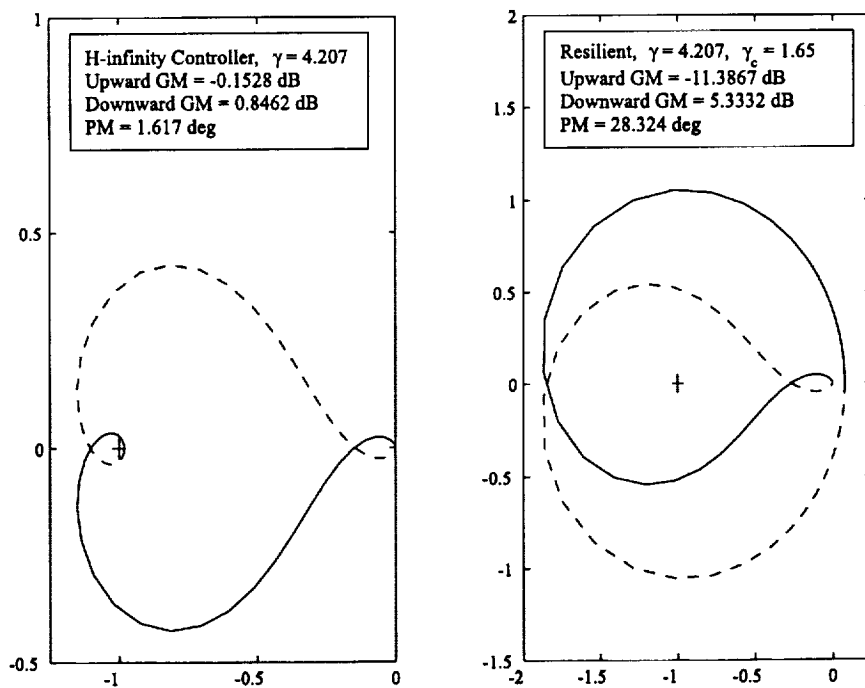


Figure 6.10: Loop gain Nyquist plots

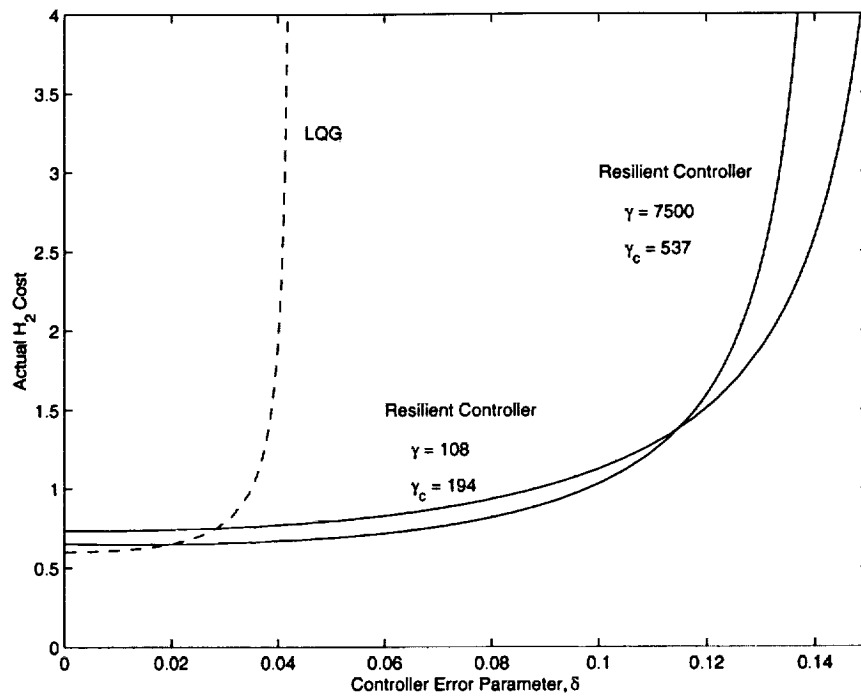


Figure 6.11: Dependence of the  $\mathcal{H}_2$  cost on the controller error parameter

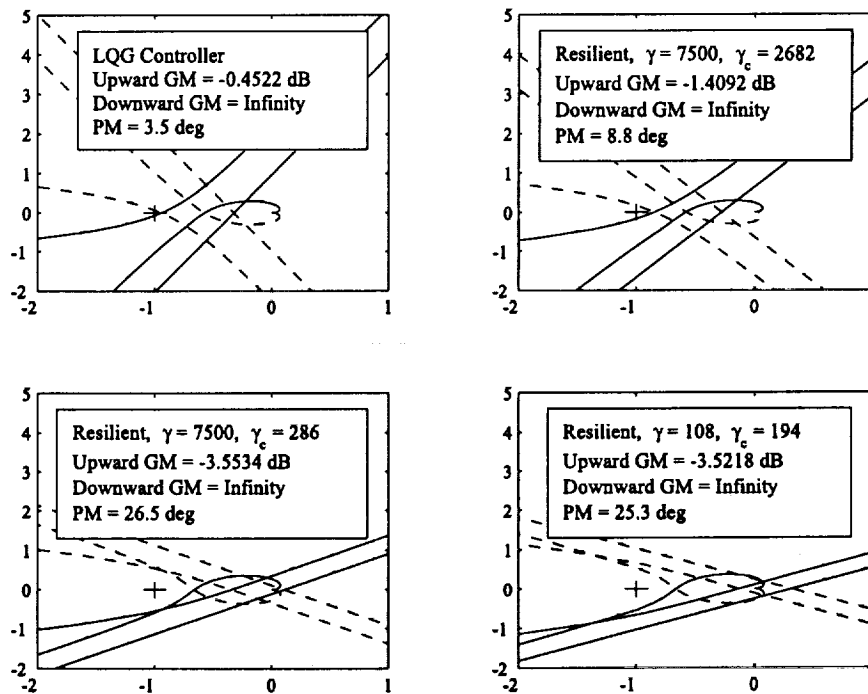


Figure 6.12: Loop gain Nyquist plots

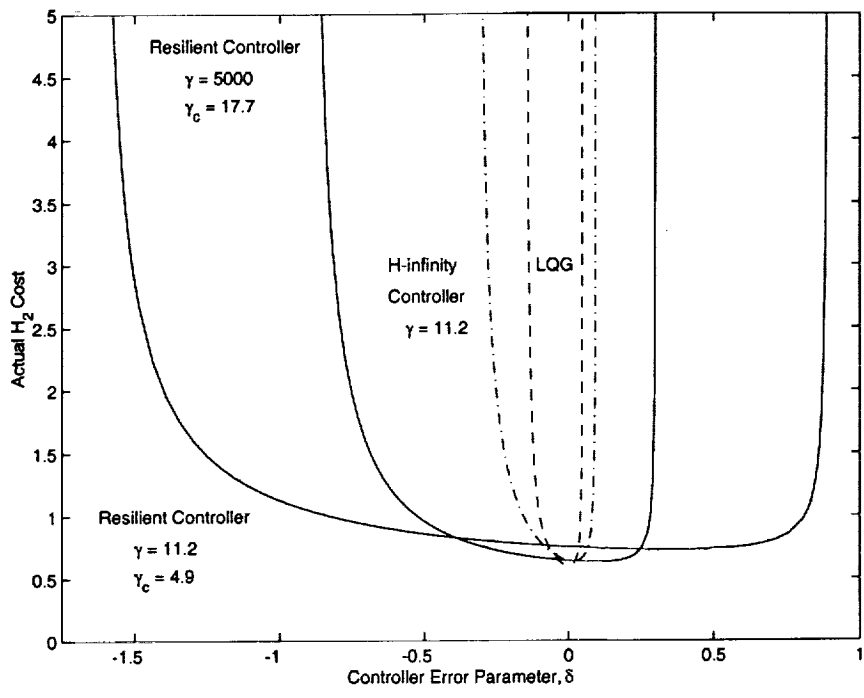


Figure 6.13: Dependence of the  $\mathcal{H}_2$  cost on the controller error parameter

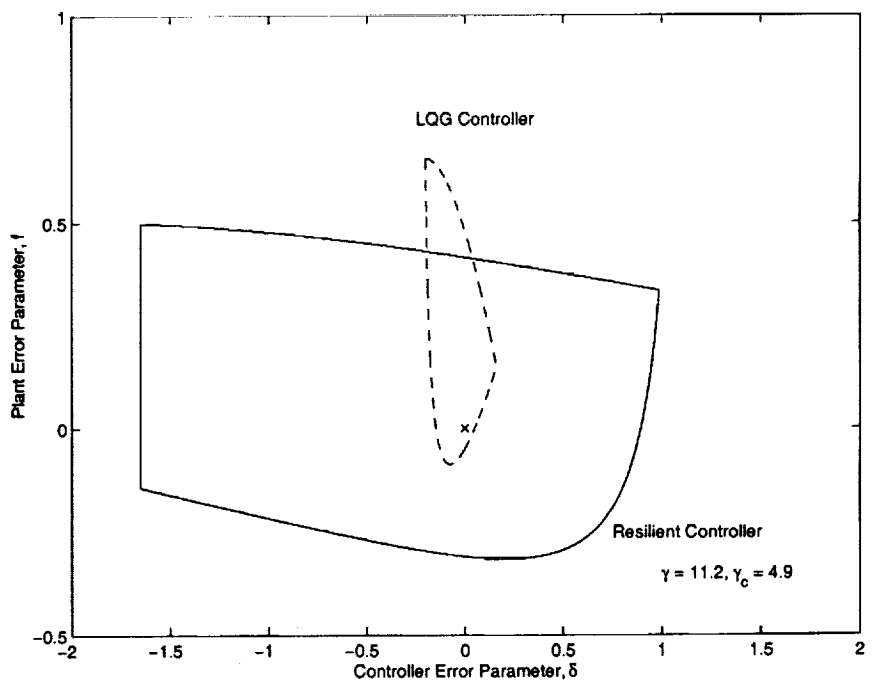


Figure 6.14: Asymptotic stability regions

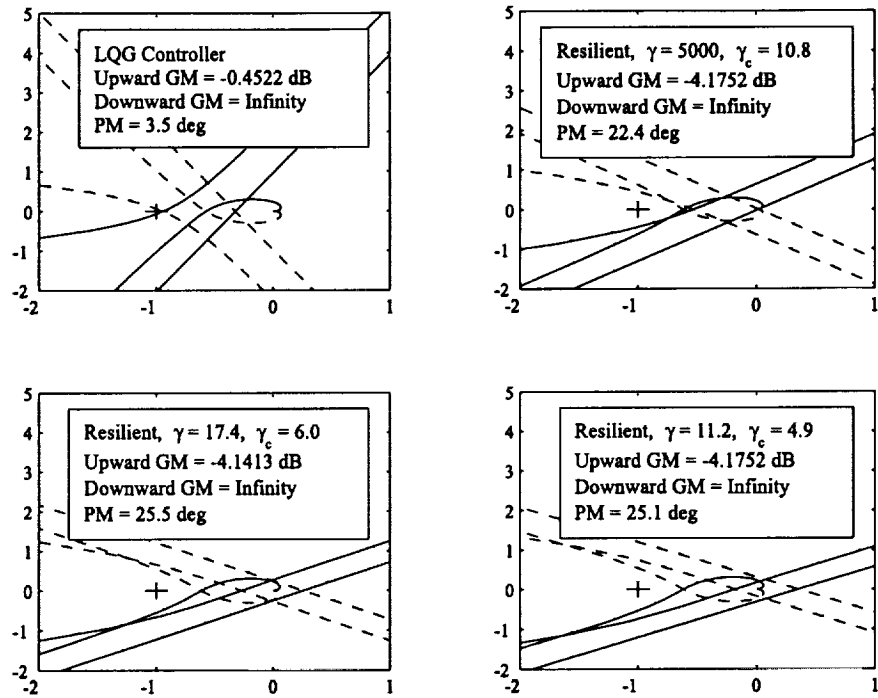


Figure 6.15: Loop gain Nyquist plots

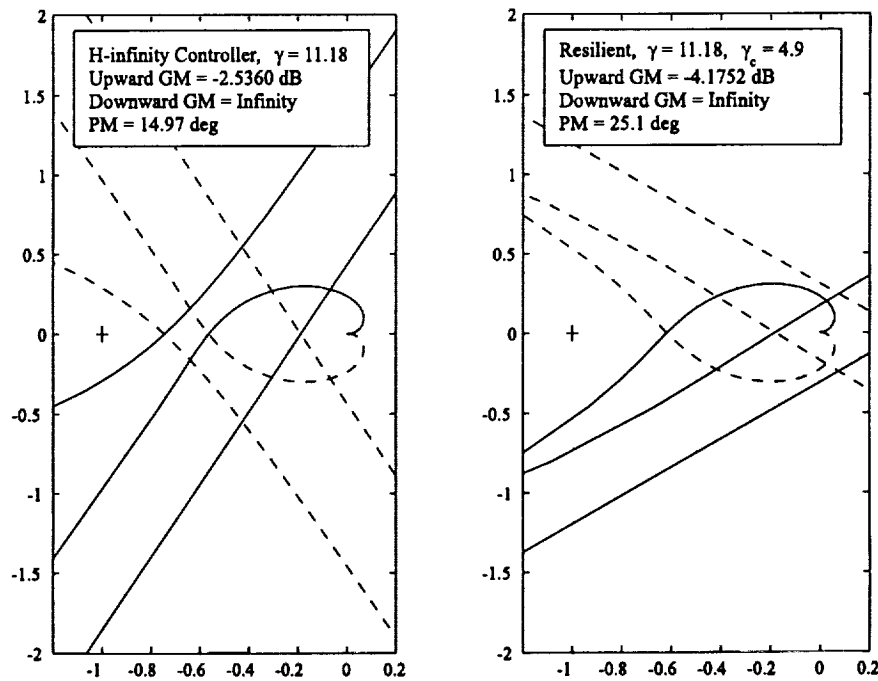


Figure 6.16: Loop gain Nyquist plots



# CHAPTER 7

## Fixed-Structure Controller Design for Axial Flow Compression Systems

### 7.1. Introduction

The desire to develop an integrated control system-design methodology for advanced propulsion systems has led to significant activity in modeling and control of flow compression systems in recent years (see, for example, [7, 79, 83, 90, 98] and the references therein). Two of the main design constraints limiting jet engine compression system performance are the compressor aerodynamic instabilities of rotating stall and surge. Rotating stall is an inherently three-dimensional<sup>1</sup> fluid dynamic instability which is characterized by regions of flow that rotate at a fraction of the compressor rotor speed while surge is a one-dimensional axisymmetric global compression system oscillation which involves axial flow oscillations, and in some cases even axial flow reversal, which can damage engine components and cause flameout to occur.

A fundamental development in compression system modeling for low speed axial compressors is the Moore-Greitzer model given in [90]. Specifically, utilizing a one-

---

<sup>1</sup>When analyzing high hub-to-tip ratio compressors, rotating stall can be approximated as a two-dimensional local compression system oscillation.

mode expansion of the disturbance velocity potential in the compression system and assuming a cubic characteristic for the compressor pressure-flow performance map, the authors in [90] develop a low-order three-state nonlinear model involving the mean flow in the compressor, the pressure rise, and the amplitude of the rotating stall. Starting from infinitesimal perturbations in the flow field, the model captures the development of rotating stall and surge. In particular, the model predicts the experimentally verified pitchfork hard subcritical bifurcation at the onset of rotating stall [89].

Using the Moore-Greitzer model, a bifurcation-based controller for rotating stall and surge was developed by Liaw and Abed [84]. In particular, the Liaw and Abed static nonlinear controller is given by

$$\gamma_{\text{throt}}(A) = \gamma_0 + kA^2, \quad (7.1)$$

where  $\gamma_{\text{throt}}(A)$  is the control throttle,  $A$  is the amplitude of the rotating stall, and  $\gamma_0$  and  $k$  are constants. The locally stabilizing bifurcation-based controller given by (7.1) essentially changes the bifurcation structure of the controlled system at the onset of rotating stall from a hard subcritical bifurcation to a soft supercritical bifurcation to soften the transition into rotating stall. However, as noted by Evekter *et al.* [36], even though the Liaw and Abed controller reduces the abrupt transition into rotating stall, it is ineffective for surge. Modifying the static nonlinear controller given by (7.1) to

$$\gamma_{\text{throt}}(A, \dot{\Phi}) = \gamma_0 + k_1 A^2 - k_2 \dot{\Phi}, \quad (7.2)$$

where  $\dot{\Phi}$  is the time rate of change of the mean flow in the compressor<sup>2</sup> and  $k_1$  and

<sup>2</sup>Even though a patented differentiation scheme for sensing the time rate of change of the mean flow in the compressor is given in [36], the calculation of  $\dot{\Phi}$  can be simply obtained by the most elementary equations of fluid dynamics. For example, under the assumption of one-dimensional flow, the unsteady axial momentum equation as applied to the bulk of the fluid in the inlet duct yields  $\dot{\Phi} = -\frac{1}{\rho L U} \Delta P$ , where  $\rho$  is the fluid density,  $L$  is the duct length,  $U$  is the rotor wheel speed, and  $\Delta P$  is the change in static pressure.

$k_2$  are constants, Badmus *et al.* [8] considerably extended the domain of attraction of the Liaw and Abed controller. A fundamental shortcoming of the aforementioned controllers is the demanding two-dimensional sensing requirements for implementing these controllers. Specifically, measuring rotating stall amplitude is quite challenging, requiring pressure sensor arrays distributed circumferentially around the compressor annulus, along with discrete Fourier transform software for spatial and temporal filtering for computing the first circumferential spatial harmonic of rotating stall. As an alternative to the locally stabilizing nonlinear controllers developed in [8, 36, 84], the authors in [56, 78, 79] develop globally stabilizing controllers for controlling rotating stall and surge in axial flow compression systems. In particular, Lyapunov-based recursive backstepping globally stabilizing static *full-state* feedback nonlinear controllers requiring rotating stall amplitude measurements are constructed in [56], while a globally stabilizing static *output* feedback nonlinear controller is given in [79]. Specifically, the Krstić *et al.* [79] static output feedback controller is given by

$$\gamma_{\text{throt}}(\Phi, \Psi) = \frac{\Gamma + c_1\Psi - c_2\Phi}{\sqrt{\Psi}}, \quad (7.3)$$

where  $\Psi$  is the pressure rise in the compressor,  $\Phi$  is the circumferentially averaged flow in the compressor,<sup>3</sup> and  $\Gamma$ ,  $c_1$ , and  $c_2$  are constants. Even though (7.3) provides a simplified sensing architecture over (7.1) and (7.2), the controller is static, possessing gain at all frequencies. Furthermore, none of the above controllers have any disturbance rejection guarantees.

In this chapter we develop *linear*, time-invariant, *pressure rise* feedback reduced-order dynamic compensators for the nonlinear Moore-Greitzer axial flow compressor model. Specifically, we construct a modified Riccati equation whose solution guarantees that the nonlinear closed-loop axial flow compression system is locally asymptot-

---

<sup>3</sup>Mean flow is relatively simple to measure and is usually measured using pitot probes located in the bell mouth of an engine.

ically stable and the closed-loop output system energy is less than the net weighted input energy at any time  $T$  in the face of  $\mathcal{L}_2$  exogenous disturbances. Using the modified Riccati equation, constructive sufficient conditions for fixed-order (i.e., full- and reduced-order) pressure rise feedback dynamic compensators guaranteeing local asymptotic stability and disturbance rejection are developed. These sufficient conditions are in the form of a coupled system of algebraic Riccati equations providing explicit design equations for characterizing pressure rise feedback dynamic compensators that account for compression system nonlinearities and exogenous disturbances with a guaranteed domain of attraction. Unlike the nonlinear static and relative degree zero controllers possessing gain at all frequencies discussed above, the proposed linear dynamic compensators explicitly account for compressor performance versus sensor accuracy, compressor performance versus processor throughput, and compressor performance versus disturbance rejection. Furthermore, the proposed controller is predicated on *only* pressure rise measurements, providing a considerable simplification in the sensing architecture.

## 7.2. Output Feedback Disturbance Rejection Control for Axial Flow Compression Systems

In this section we introduce the output feedback disturbance rejection control problem for axial flow compression systems. The goal of the problem is to determine a *linear*, time-invariant, fixed-order dynamic *output* feedback compensator that stabilizes a given parameterization of the nonlinear Moore-Greitzer axial flow compressor model using only pressure rise measurements while guaranteeing closed-loop disturbance rejection and optimality of a quadratic performance criterion involving weighted state and control variables.

To capture post-stall transients in axial flow compression systems, we use the

one-mode Galerkin approximation model for the partial differential equation characterizing the disturbance velocity potential at the compressor inlet proposed by Moore and Greitzer [90]. Specifically, we consider the basic compression system shown in Figure 7.1, consisting of an inlet duct, a compressor, an outlet duct, a plenum, and a control throttle. We assume that the plenum dimensions are large compared to the compressor-duct dimensions so that the fluid velocity and acceleration in the plenum are negligible. In this case, the pressure in the plenum is spatially uniform. Furthermore, we assume that the flow is controlled by a throttle at the plenum exit. Finally, we assume a low speed compression system with oscillation frequencies much lower than the acoustic resonance frequencies so that the flow can be considered incompressible. However, we do assume that the gas in the plenum is compressible, and therefore acts as a gas spring.

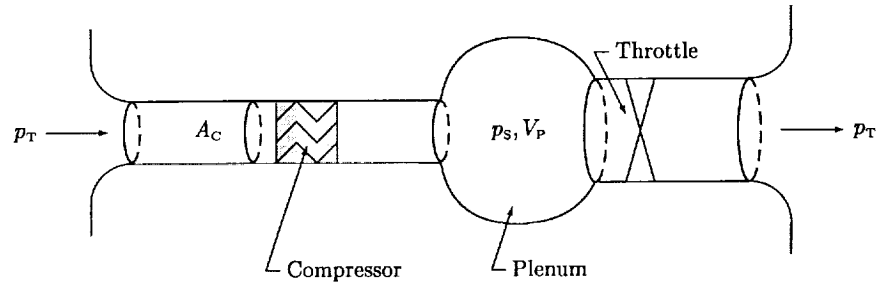


Figure 7.1: Compressor system geometry

Now, invoking a momentum balance across the compression system, conservation of mass in the plenum, and using a Galerkin projection based on a one-mode circumferential spatial harmonic approximation for the non-axisymmetric flow disturbances yields [90]

$$\dot{A}(t) = \frac{\sigma}{3\pi} \int_0^{2\pi} \Psi_C(\Phi(t) + A(t) \sin(\theta)) \sin(\theta) d\theta, \quad t \in [0, \infty), \quad (7.4)$$

$$\dot{\Phi}(t) = -\Psi(t) + \frac{1}{2\pi} \int_0^{2\pi} \Psi_C(\Phi(t) + A(t) \sin(\theta)) d\theta, \quad (7.5)$$

$$\dot{\Psi}(t) = \frac{1}{\beta^2}[\Phi(t) - \Phi_T(t)], \quad (7.6)$$

where  $\Phi$  is the circumferentially averaged axial mass flow in the compressor,  $\Psi$  is the total-to-static pressure rise,  $A$  is the normalized stall cell amplitude of angular variation capturing a measure of nonuniformity in the flow,  $\Phi_T$  is the mass flow through the throttle,  $\sigma$  and  $\beta$  are positive constant parameters, and  $\Psi_C(\cdot)$  is a given compressor pressure-flow map. The compliance coefficient  $\beta$  is a function of the compressor rotor speed and plenum size. For large values of  $\beta$ , a surge limit cycle can occur, while rotating stall can occur for any value of  $\beta$ . Now, assuming that the compressor pressure-flow map  $\Psi_C(\cdot)$  is analytic, the integral terms in (7.4) and (7.5) can be expressed in terms of an infinite Taylor expansion about the circumferentially averaged flow to give

$$\dot{A}(t) = \frac{\sigma}{3\pi} \sum_{k=1}^{\infty} \frac{1}{k!(k-1)!} \left. \frac{d^{2k-1}\Psi_C(\xi)}{d\xi^{2k-1}} \right|_{\xi=\Phi(t)} \left( \frac{A(t)}{2} \right)^{2k-1}, \quad t \in [0, \infty), \quad (7.7)$$

$$\dot{\Phi}(t) = -\Psi(t) + \sum_{k=0}^{\infty} \frac{1}{(k!)^2} \left. \frac{d^{2k}\Psi_C(\xi)}{d\xi^{2k}} \right|_{\xi=\Phi(t)} \left( \frac{A(t)}{2} \right)^{2k}, \quad (7.8)$$

$$\dot{\Psi}(t) = \frac{1}{\beta^2}[\Phi(t) - \Phi_T(t)]. \quad (7.9)$$

The specific compressor pressure-flow map,  $\Psi_C(\cdot)$ , which was considered in [90] is

$$\Psi_C(\Phi) = \Psi_{C_0} + 1 + \frac{3}{2}\Phi - \frac{1}{2}\Phi^3, \quad (7.10)$$

where  $\Psi_{C_0}$  is a constant parameter. In this case, (7.7)–(7.9) become

$$\dot{A}(t) = \frac{\sigma}{2}A(t)[1 - \Phi^2(t) - \frac{1}{4}A^2(t)] + \beta_1 w_1(t), \quad t \in [0, \infty), \quad (7.11)$$

$$\dot{\Phi}(t) = -\Psi(t) + \Psi_C(\Phi(t)) - \frac{3}{4}\Phi(t)A^2(t) + \beta_2 w_2(t), \quad (7.12)$$

$$\dot{\Psi}(t) = \frac{1}{\beta^2}[\Phi(t) - \Phi_T(t)] + \beta_3 w_3(t), \quad (7.13)$$

to which we have added the  $\mathcal{L}_2$  external disturbance signals  $w_1(t)$ ,  $w_2(t)$ , and  $w_3(t)$ ,  $t \in [0, \infty)$ , with scaling factors  $\beta_1, \beta_2, \beta_3 \in \mathbb{R}$ . The proposed additive disturbance

model can be used to capture combustion noise and turbine speed fluctuations. For example,  $w_3(t)$ ,  $t \in [0, \infty)$ , might reflect back-pressure disturbances to the compressor from the combustor.

Next, note that for fixed values of flow through the throttle,  $\Phi_T(t) \equiv \Phi_{T_{\text{eq}}}$ , (7.11)–(7.13) have an equilibrium point given by

$$(A_{\text{eq}}, \Phi_{\text{eq}}, \Psi_{\text{eq}}) = (0, \Phi_{T_{\text{eq}}}, \Psi_C(\Phi_{\text{eq}})). \quad (7.14)$$

Defining the shifted state variables  $x_1 \triangleq A$ ,  $x_2 \triangleq \Phi - \Phi_{\text{eq}}$ , and  $x_3 \triangleq \Psi - \Psi_{\text{eq}}$ , so that for a given equilibrium point on the axisymmetric branch of the compressor characteristic pressure-flow map the system equilibrium is translated to the origin, it follows that the translated nonlinear system is given by

$$\begin{aligned} \dot{x}_1(t) = & \frac{\sigma}{2}(1 - \lambda^2)x_1(t) - \frac{\sigma}{2}\left[\frac{1}{4}x_1^3(t) + x_1(t)x_2^2(t) + 2\lambda x_1(t)x_2(t)\right] \\ & + \beta_1 w_1(t), \quad t \in [0, \infty), \end{aligned} \quad (7.15)$$

$$\begin{aligned} \dot{x}_2(t) = & -x_3(t) + \frac{3}{2}(1 - \lambda^2)x_2(t) - \frac{1}{2}x_2^3(t) - \frac{3}{2}\lambda x_2^2(t) - \frac{3}{4}\lambda x_1^2(t) - \frac{3}{4}x_1^2(t)x_2(t) \\ & + \beta_2 w_2(t), \end{aligned} \quad (7.16)$$

$$\dot{x}_3(t) = \frac{1}{\beta^2}[x_2(t) - u(t)] + \beta_3 w_3(t), \quad (7.17)$$

where  $\lambda \triangleq \Phi_{T_{\text{eq}}}$  and  $u \triangleq \Phi_T - \lambda$ . Decomposing (7.15)–(7.17) into a linear and a nonlinear part, we obtain the state space model

$$\begin{aligned} \begin{bmatrix} \dot{x}_1(t) \\ \dot{x}_2(t) \\ \dot{x}_3(t) \end{bmatrix} = & \begin{bmatrix} \frac{\sigma}{2}(1 - \lambda^2) & 0 & 0 \\ 0 & \frac{3}{2}(1 - \lambda^2) & -1 \\ 0 & \frac{1}{\beta^2} & 0 \end{bmatrix} \begin{bmatrix} x_1(t) \\ x_2(t) \\ x_3(t) \end{bmatrix} + \begin{bmatrix} -\frac{\sigma}{8} & 0 \\ 0 & -\frac{1}{4} \\ 0 & 0 \end{bmatrix} \phi(y_0(t)) \\ & + \begin{bmatrix} 0 \\ 0 \\ -\frac{1}{\beta^2} \end{bmatrix} u(t) + \begin{bmatrix} \beta_1 & 0 & 0 \\ 0 & \beta_2 & 0 \\ 0 & 0 & \beta_3 \end{bmatrix} \begin{bmatrix} w_1(t) \\ w_2(t) \\ w_3(t) \end{bmatrix}, \end{aligned} \quad (7.18)$$

where

$$y_0(t) = \begin{bmatrix} 1 & 0 & 0 \\ 0 & 1 & 0 \end{bmatrix} \begin{bmatrix} x_1(t) \\ x_2(t) \\ x_3(t) \end{bmatrix}, \quad \phi(y_0(t)) = \begin{bmatrix} x_1^3(t) + 4x_1(t)x_2^2(t) + 8\lambda x_1(t)x_2(t) \\ 3\lambda x_1^2(t) + 3x_1^2(t)x_2(t) + 6\lambda x_2^2(t) + 2x_2^3(t) \end{bmatrix}.$$

Now, it can be shown that the linear part of (7.18) is linearly stabilizable for  $\lambda > 1$ , while for  $\lambda = 1$ , corresponding to the maximum pressure rise equilibrium point, the linear part of (7.18) is linearly unstabilizable. With the system written in this form, we can now state the dynamic output feedback control problem for axial flow compression systems. Here, for generality of exposition, we present the formulation for an  $n$ -dimensional dynamical compression system.

**Dynamic Output Feedback Control for Axial Flow Compression Systems.** Given the  $n^{\text{th}}$ -order stabilizable and detectable<sup>4</sup> nonlinear dynamical system

$$\dot{x}(t) = Ax(t) + B_0\phi(y_0(t)) + Bu(t) + D_1w(t), \quad t \in [0, \infty), \quad (7.19)$$

$$y_0(t) = C_0x(t), \quad (7.20)$$

with output measurements

$$y(t) = Cx(t) + D_2w(t), \quad (7.21)$$

where  $u(t) \in \mathbb{R}^m$ ,  $y(t) \in \mathbb{R}^l$ ,  $y_0(t) \in \mathbb{R}^{l_0}$ ,  $t \in [0, \infty)$ ,  $\phi : \mathbb{R}^{l_0} \rightarrow \mathbb{R}^{m_0}$ , and where  $w(t) \in \mathbb{R}^d$ ,  $t \in [0, \infty)$ , is an exogenous  $\mathcal{L}_2$  signal, each of whose components has norm less than one, determine an  $n_c^{\text{th}}$ -order linear, time-invariant dynamic compensator

$$\dot{x}_c(t) = A_c x_c(t) + B_c y(t), \quad t \in [0, \infty), \quad (7.22)$$

$$u(t) = C_c x_c(t), \quad (7.23)$$

that satisfies the following design criteria:

1. the undisturbed ( $w(t) \equiv 0$ ) closed-loop nonlinear system (7.19)–(7.23) is asymptotically stable;

---

<sup>4</sup>Here, stabilizability and detectability are defined with respect to the linear part of the dynamical system (7.19)–(7.21).

2. the disturbed closed-loop system (7.19)–(7.23) from  $\mathcal{L}_2$  disturbances  $w(\cdot)$  to performance variables

$$z(t) = E_1 x(t) + E_2 u(t), \quad (7.24)$$

satisfies the disturbance rejection constraint

$$\int_0^T z^T(s)z(s) ds < \gamma_d^2 \int_0^T w^T(s)w(s) ds + V(\tilde{x}(0)), \quad T \geq 0, \quad w(\cdot) \in \mathcal{L}_2, \quad (7.25)$$

where  $z(t) \in \mathbb{R}^p$ ,  $t \in [0, \infty)$ ,  $\gamma_d > 0$  is a given constant,  $\tilde{x}(t) \triangleq [x^T(t) \quad x_c^T(t)]^T$ , and  $V(\cdot)$  is a Lyapunov function for the closed-loop system (7.19)–(7.23); and

3. the quadratic performance functional

$$J(A_c, B_c, C_c) \triangleq \int_0^\infty z^T(t)z(t) dt, \quad (7.26)$$

with  $w(t) \equiv 0$  is minimized.

For the three-state parameterized Moore-Greitzer model given by (7.18), the system matrices in (7.19) and (7.20) are given by

$$A = \begin{bmatrix} \frac{\sigma}{2}(1 - \lambda^2) & 0 & 0 \\ 0 & \frac{3}{2}(1 - \lambda^2) & -1 \\ 0 & \frac{1}{\beta^2} & 0 \end{bmatrix}, \quad B_0 = \begin{bmatrix} -\frac{\sigma}{8} & 0 \\ 0 & -\frac{1}{4} \\ 0 & 0 \end{bmatrix}, \quad C_0 = \begin{bmatrix} 1 & 0 & 0 \\ 0 & 1 & 0 \end{bmatrix}, \quad (7.27)$$

$$B = \begin{bmatrix} 0 \\ 0 \\ -\frac{1}{\beta^2} \end{bmatrix}, \quad D_1 = \begin{bmatrix} \beta_1 & 0 & 0 \\ 0 & \beta_2 & 0 \\ 0 & 0 & \beta_3 \end{bmatrix}. \quad (7.28)$$

Furthermore, for pressure rise sensor measurements,

$$C = [0 \quad 0 \quad 1]. \quad (7.29)$$

### 7.3. Sufficient Conditions for Closed-Loop Stability and Disturbance Rejection

In this section we provide a Riccati equation that guarantees asymptotic stability of the undisturbed ( $w(t) \equiv 0$ ) closed-loop system (7.19)–(7.23) as well as disturbance

rejection of the disturbed closed-loop system in the face of  $\mathcal{L}_2$  exogenous disturbances. First, however, note that the closed-loop system (7.19)–(7.23) has a state-space representation given by

$$\dot{\tilde{x}}(t) = \tilde{A}\tilde{x}(t) + \tilde{B}_0\phi(y_0(t)) + \tilde{D}w(t), \quad t \in [0, \infty), \quad (7.30)$$

$$y_0(t) = \tilde{C}_0\tilde{x}(t), \quad (7.31)$$

$$z(t) = \tilde{E}\tilde{x}(t), \quad (7.32)$$

where

$$\tilde{B}_0 \triangleq \begin{bmatrix} B_0 \\ 0_{n_c \times m_0} \end{bmatrix}, \quad \tilde{C}_0 \triangleq [ C_0 \quad 0_{l_0 \times n_c} ].$$

Furthermore, we assume that the nonlinear part of (7.19), or, equivalently, (7.30), is such that  $\phi(\cdot) \in \Phi_{\mathcal{D}}$ , where

$$\Phi_{\mathcal{D}} \triangleq \{ \phi : \mathcal{D} \rightarrow \mathbb{R}^{m_0} : \phi(0) = 0, \|\phi(y_0)\|_2^2 \leq \gamma_n^{-2} \|y_0\|_2^2, y_0 \in \mathcal{D} \}, \quad (7.33)$$

where  $\mathcal{D} \subseteq \mathbb{R}^{l_0}$  is a closed set and  $\gamma_n > 0$  is given. For the statement of the main result of this section, define the notation  $\tilde{n} \triangleq n + n_c$ ,  $\tilde{R} \triangleq \tilde{E}^T \tilde{E}$ , and  $\tilde{V} \triangleq \tilde{D} \tilde{D}^T$  and set  $\mathcal{D} = \mathbb{R}^{l_0}$ .

**Theorem 7.1.** Let  $(A_c, B_c, C_c)$  be given and suppose there exists a matrix  $\tilde{P} \in \mathbb{P}^{\tilde{n}}$  and scalars  $\epsilon, \gamma_d, \gamma_n > 0$  satisfying

$$0 = \tilde{A}^T \tilde{P} + \tilde{P} \tilde{A} + \gamma_d^{-2} \tilde{P} \tilde{V} \tilde{P} + \gamma_n^{-2} \tilde{P} \tilde{B}_0 \tilde{B}_0^T \tilde{P} + \tilde{C}_0^T \tilde{C}_0 + \epsilon \tilde{P} + \tilde{R}. \quad (7.34)$$

Then the function

$$V(\tilde{x}) = \tilde{x}^T \tilde{P} \tilde{x}, \quad (7.35)$$

is a Lyapunov function that guarantees that the undisturbed ( $w(t) \equiv 0$ ) closed-loop system (7.30)–(7.32) is globally asymptotically stable for all  $\phi(\cdot) \in \Phi_{\mathbb{R}^{l_0}}$ . Furthermore, the solution  $\tilde{x}(t)$ ,  $t \in [0, \infty)$ , of the nonlinear system (7.30)–(7.32) satisfies the

disturbance rejection constraint

$$\int_0^T z^T(s)z(s) ds < \gamma_d^2 \int_0^T w^T(s)w(s) ds + V(\tilde{x}_0), \quad T \geq 0, \quad w(\cdot) \in \mathcal{L}_2. \quad (7.36)$$

Finally, in the case where  $w(t) \equiv 0$ , the performance functional (7.26) satisfies the bound

$$J(\tilde{x}_0, A_c, B_c, C_c) = \int_0^\infty z(t)^T z(t) dt < V(\tilde{x}_0). \quad (7.37)$$

**Proof.** First note that since  $\tilde{P} \in \mathbb{P}^{\tilde{n}}$ , it follows that the Lyapunov function candidate  $V(\tilde{x})$ ,  $\tilde{x} \in \mathbb{R}^{\tilde{n}} \setminus \{0\}$ , given by (7.35), is positive definite. The corresponding Lyapunov derivative along the trajectories  $\tilde{x}(t)$ ,  $t \in [0, \infty)$ , of the undisturbed ( $w(t) \equiv 0$ ) closed-loop system (7.30)–(7.32) is given by

$$\begin{aligned} \dot{V}(\tilde{x}(t)) &\triangleq V'(\tilde{x}(t))[\tilde{A}\tilde{x}(t) + \tilde{B}_0\phi(y_0(t))] \\ &= \tilde{x}^T(t)(\tilde{A}^T\tilde{P} + \tilde{P}\tilde{A})\tilde{x}(t) + 2\phi^T(y_0(t))\tilde{B}_0^T\tilde{P}\tilde{x}(t), \quad t \in [0, \infty), \end{aligned} \quad (7.38)$$

or, equivalently, using (7.34)

$$\begin{aligned} \dot{V}(\tilde{x}(t)) &= -\tilde{x}^T(t) \left[ \epsilon\tilde{P} + \gamma_d^{-2}\tilde{P}\tilde{V}\tilde{P} + \tilde{R} \right] \tilde{x}(t) - \gamma_n^{-2}\tilde{x}^T(t)\tilde{P}\tilde{B}_0\tilde{B}_0^T\tilde{P}\tilde{x}(t) \\ &\quad - \tilde{x}^T(t)\tilde{C}_0^T\tilde{C}_0\tilde{x}(t) + \phi^T(y_0(t))\tilde{B}_0^T\tilde{P}\tilde{x}(t) + \tilde{x}^T(t)\tilde{P}\tilde{B}_0\phi(y_0(t)), \quad t \in [0, \infty). \end{aligned} \quad (7.39)$$

Now, adding and subtracting  $\gamma_n^2\phi^T(y_0(t))\phi(y_0(t))$ ,  $t \in [0, \infty)$ , to and from (7.39) and grouping terms yields

$$\begin{aligned} \dot{V}(\tilde{x}(t)) &= -\tilde{x}^T(t)[\epsilon\tilde{P} + \gamma_d^{-2}\tilde{P}\tilde{V}\tilde{P} + \tilde{R}]\tilde{x}(t) + \gamma_n^2\phi^T(y_0(t))\phi(y_0(t)) - y_0^T(t)y_0(t) \\ &\quad - \left[ \gamma_n^{-1}\tilde{B}_0^T\tilde{P}\tilde{x}(t) - \gamma_n\phi(y_0(t)) \right]^T \left[ \gamma_n^{-1}\tilde{B}_0^T\tilde{P}\tilde{x}(t) - \gamma_n\phi(y_0(t)) \right], \quad t \in [0, \infty). \end{aligned} \quad (7.40)$$

Since  $\epsilon\tilde{P}$  is positive definite,  $\gamma_d^{-2}\tilde{P}\tilde{V}\tilde{P} + \tilde{R}$  is nonnegative definite, and  $\gamma_n^2\phi^T\phi - y_0^T y_0 \leq 0$ , it follows that  $\dot{V}(\tilde{x}(t)) < 0$ ,  $t \in [0, \infty)$ , and hence the undisturbed ( $w(t) \equiv 0$ ) nonlinear closed-loop system (7.30)–(7.32) is globally asymptotically stable.

Next, to show that the disturbance rejection constraint (7.36) holds, note that for all  $w \in \mathbb{R}^d$ ,

$$\begin{aligned}
0 &\leq (\gamma_d^{-1} \tilde{D}^T \tilde{P} \tilde{x} - \gamma_d w)^T (\gamma_d^{-1} \tilde{D}^T \tilde{P} \tilde{x} - \gamma_d w) \\
&= \gamma_d^{-2} \tilde{x}^T \tilde{P} \tilde{V} \tilde{P} \tilde{x} + \gamma_d^2 w^T w - 2 \tilde{x}^T \tilde{P} \tilde{D} w \\
&= \gamma_d^{-2} \tilde{x}^T \tilde{P} \tilde{V} \tilde{P} \tilde{x} + \tilde{x}^T \tilde{R} \tilde{x} + \gamma_d^2 w^T w - z^T z - 2 \tilde{x}^T \tilde{P} \tilde{D} w.
\end{aligned} \tag{7.41}$$

Now, let  $w(\cdot) \in \mathcal{L}_2$  and let  $\tilde{x}(t)$ ,  $t \in [0, \infty)$ , denote the solution of the nonlinear closed-loop system (7.30)–(7.32). Then

$$\dot{V}(\tilde{x}(t)) = \tilde{x}^T(t) (\tilde{A}^T \tilde{P} + \tilde{P} \tilde{A}) \tilde{x}(t) - 2 \phi^T(y_0(t)) \tilde{B}_0^T \tilde{P} \tilde{x}(t) + 2 \tilde{x}^T(t) \tilde{P} \tilde{D} w(t), \quad t \in [0, \infty), \tag{7.42}$$

which, using (7.34) and (7.41), implies

$$\begin{aligned}
\dot{V}(\tilde{x}(t)) &< 2 \tilde{x}^T(t) \tilde{P} \tilde{D} w(t) - \gamma_d^{-2} \tilde{x}^T(t) \tilde{P} \tilde{V} \tilde{P} \tilde{x}(t) - \tilde{x}^T(t) \tilde{R} \tilde{x}(t) \\
&\leq \gamma_d^2 w^T(t) w(t) - z^T(t) z(t), \quad t \in [0, \infty).
\end{aligned} \tag{7.43}$$

Now, integrating (7.43) over  $[0, T]$  yields

$$V(\tilde{x}(T)) < \int_0^T [\gamma_d^2 w^T(s) w(s) - z^T(s) z(s)] ds + V(\tilde{x}(0)), \quad T \geq 0, \quad w(\cdot) \in \mathcal{L}_2, \tag{7.44}$$

which, by noting that  $V(\tilde{x}(T)) \geq 0$ ,  $T \geq 0$ , yields (7.36).

Finally, to show that the performance functional (7.26) satisfies the bound (7.37), note that (7.40) implies

$$\dot{V}(\tilde{x}(t)) < \tilde{x}^T(t) \tilde{R} \tilde{x}(t). \tag{7.45}$$

Now, integrating (7.45) over  $[0, \infty)$  yields

$$\int_0^\infty z^T(t) z(t) dt < - \int_0^\infty \dot{V}(\tilde{x}(t)) dt. \tag{7.46}$$

Next, since  $\tilde{x}(t) \rightarrow 0$  as  $t \rightarrow \infty$ , where  $\tilde{x}(t)$ ,  $t \in [0, \infty)$ , satisfies (7.30) with  $w(t) \equiv 0$ , we obtain

$$\begin{aligned} J(\tilde{x}_0, A_c, B_c, C_c) &< V(\tilde{x}(0)) - \lim_{t \rightarrow \infty} V(\tilde{x}(t)) \\ &= V(\tilde{x}(0)) \\ &= \tilde{x}_0^T \tilde{P} \tilde{x}_0. \end{aligned} \quad \square$$

Theorem 7.1 guarantees global asymptotic stability if  $\phi(\cdot) \in \Phi_{\mathcal{D}}$  with  $\mathcal{D} = \mathbb{R}^{l_0}$ . However, for the three-state axial compressor model given by (7.18),  $\phi(\cdot) \in \Phi_{\mathcal{D}}$  is not satisfied for  $\mathcal{D} = \mathbb{R}^{l_0}$ . Hence, to obtain a *local* stability result for the parameterized compressor model given by (7.18), we restrict  $\mathcal{D}$  to the set  $\mathcal{D}_c$ , where  $\mathcal{D}_c$  is the smallest compact set given by

$$\mathcal{D}_c \triangleq \{y_0 \in \mathbb{R}^{l_0} : \|\phi(y_0)\|_2^2 \leq \gamma_n^{-2} \|y_0\|_2^2\}, \quad (7.47)$$

where  $\phi(y_0)$ ,  $y_0 \in \mathbb{R}^{l_0}$ , is the nonlinear part of (7.18).

**Proposition 7.1.** For the axial flow compression system given by (7.18),  $\mathcal{D}_c$  is not empty.

**Proof.** Defining

$$f(y_0) \triangleq \gamma_n^{-2} y_0^T y_0 - \phi^T(y_0) \phi(y_0), \quad (7.48)$$

it follows that

$$f(y_0) = \gamma_n^{-2} (x_1^2 + x_2^2) - x_1^2 [x_1^2 + 4x_2(2\lambda + x_2)]^2 - [3x_1^2(\lambda + x_2) + 2x_2^2(3\lambda + x_2)]^2. \quad (7.49)$$

Now, since  $f'(0) = 0$ , where  $f'(0)$  denotes the Frechét derivative of  $f(\cdot)$  at the origin, and

$$f''(0) = \begin{bmatrix} 2\gamma_n^{-2} & 0 \\ 0 & 2\gamma_n^{-2} \end{bmatrix} > 0, \quad (7.50)$$

where  $f''(0)$  denotes the Hessian at the origin, it follows that the origin is a local minimum of  $f(\cdot)$ . Thus, since  $f(\cdot)$  is continuous, there exists a neighborhood of the origin where  $f(y_0) > 0$ ,  $y_0 \in \mathbb{R}^{l_0} \setminus \{0\}$ , and hence  $\mathcal{D}_c$  is not empty.  $\square$

The size and shape of the set  $\mathcal{D}_c$  for various values of the parameter  $\gamma_n$  with  $\lambda = 1.1$  are shown in Figure 7.2.

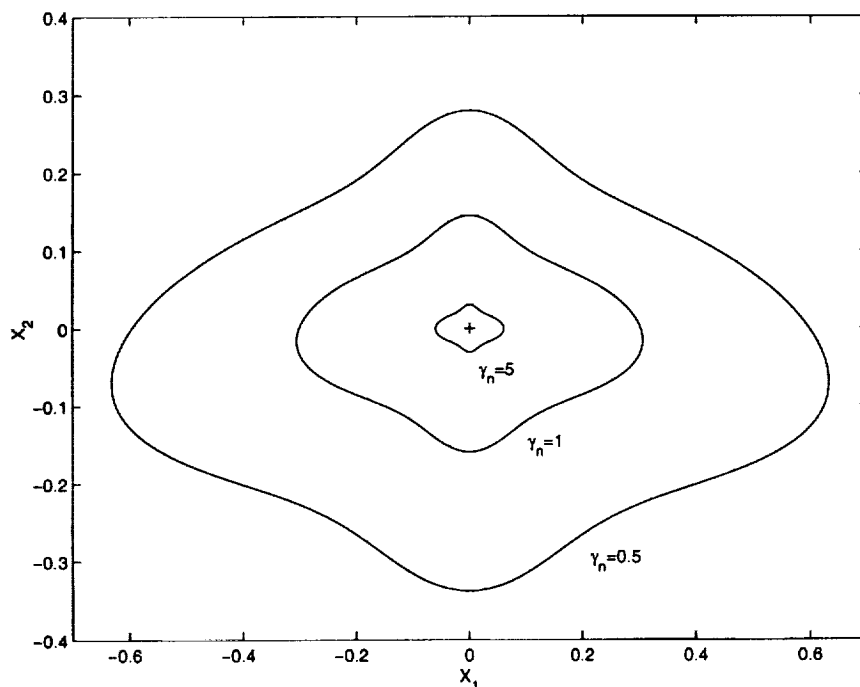


**Figure 7.2:** Regions,  $\mathcal{D}_c$ , satisfying the sector bound (7.47)

Next, note that  $J(\tilde{x}_0, A_c, B_c, C_c) < \tilde{x}_0^T \tilde{P} \tilde{x}_0 = \text{tr } \tilde{P} \tilde{x}_0 \tilde{x}_0^T$ , which has the same form as the standard  $\mathcal{H}_2$  cost appearing in standard LQG theory. Hence, we replace  $\tilde{x}_0 \tilde{x}_0^T$  by

$$\hat{V} \triangleq \begin{bmatrix} \hat{V}_1 & 0 \\ 0 & B_c \hat{V}_2 B_c^T \end{bmatrix}, \quad (7.51)$$

where  $\hat{V}_1 \in \mathbb{R}^{n \times n}$  and  $\hat{V}_2 \in \mathbb{R}^{l \times l}$  are arbitrary design weights such that  $\hat{V}_1 \geq 0$  and  $\hat{V}_2 > 0$ , and proceed by determining controller gains that minimize  $\text{tr } \tilde{P} \hat{V}$ . Before proceeding, however, we shall require for technical reasons that  $V_2 \triangleq D_2 D_2^T = \alpha^2 \hat{V}_2$ ,

where the positive scalar  $\alpha$  is a design variable such that  $\alpha \equiv 0$  if and only if  $D_2 \equiv 0$ . Next, in the spirit of [11],  $\mathcal{J}(\tilde{P}, A_c, B_c, C_c) \triangleq \text{tr } \tilde{P}\hat{V}$  can be interpreted as an auxiliary cost which leads to the following optimization problem.

**Optimization Problem.** Determine controller gains  $(A_c, B_c, C_c)$  that minimizes  $\mathcal{J}(\tilde{P}, A_c, B_c, C_c) \triangleq \text{tr } \tilde{P}\hat{V}$  with  $\tilde{P} \in \mathbb{P}^{\tilde{n}}$  subject to (7.34) and such that  $(A_c, B_c, C_c)$  is minimal.

It follows from Theorem 7.1 that by deriving necessary conditions for the Optimization Problem, we obtain sufficient conditions for characterizing dynamic output feedback controllers guaranteeing closed-loop system stability and disturbance rejection to  $\mathcal{L}_2$  exogenous disturbances.

## 7.4. Reduced-Order Dynamic Control for Axial Flow Compressors

In this section we present our main theorem characterizing fixed-order disturbance rejection controllers for axial flow compression systems. For design flexibility, the compensator order,  $n_c$ , may be less than the plant order,  $n$ . For convenience in stating this result, define the notation  $S \triangleq (I_n + \alpha^2 \gamma_d^{-2} Q \hat{P})^{-1}$  for arbitrary matrices  $Q, \hat{P} \in \mathbb{N}^n$ , and  $A_\epsilon \triangleq A + \frac{1}{2}\epsilon I_n$ . Note that since  $Q, \hat{P} \in \mathbb{N}^n$  are nonnegative definite and the eigenvalues of  $Q\hat{P}$  coincide with the eigenvalues of the nonnegative definite matrix  $Q^{1/2}\hat{P}Q^{1/2}$ , it follows that  $Q\hat{P}$  has nonnegative eigenvalues. Thus the eigenvalues of  $I_n + \alpha^2 \gamma_d^{-2} Q\hat{P}$  are all greater than one, so that  $S$  exists. Furthermore, define

$$\mathcal{D}_\beta \triangleq \{\tilde{x} \in \mathbb{R}^{\tilde{n}}: \tilde{C}_0 \tilde{x} \in \mathcal{D}_c \text{ and } \tilde{x}^T \tilde{P} \tilde{x} \leq \beta\}, \quad (7.52)$$

where  $\tilde{P} \in \mathbb{N}^{\tilde{n}}$  satisfies (7.34) for a given compensator  $(A_c, B_c, C_c)$  and  $\beta > 0$ .

**Theorem 7.2.** Let  $n_c \leq n$  and let  $\epsilon, \gamma_n, \gamma_d, \alpha > 0$ . Furthermore, using the

results of Lemma 5.2, suppose there exist matrices  $P, Q, \hat{P}, \hat{Q} \in \mathbb{N}^m$  satisfying

$$0 = A_\epsilon^T P + P A_\epsilon + P[\gamma_n^{-2} B_0 B_0^T + \gamma_d^{-2} V_1] P + R_1 + C_0^T C_0 - P \Sigma P + \tau_\perp^T P \Sigma P \tau_\perp, \quad (7.53)$$

$$0 = (A_\epsilon + [\gamma_n^{-2} B_0 B_0^T + \gamma_d^{-2} V_1][P + \hat{P}]) Q + Q (A_\epsilon + [\gamma_n^{-2} B_0 B_0^T + \gamma_d^{-2} V_1][P + \hat{P}])^T \\ + \hat{V}_1 - S Q \bar{\Sigma} Q S^T + \tau_\perp S Q \bar{\Sigma} Q S^T \tau_\perp^T, \quad (7.54)$$

$$0 = (A_\epsilon - S Q \bar{\Sigma} + [\gamma_n^{-2} B_0 B_0^T + \gamma_d^{-2} V_1] P)^T \hat{P} + \hat{P} (A_\epsilon - S Q \bar{\Sigma} + [\gamma_n^{-2} B_0 B_0^T + \gamma_d^{-2} V_1] P) \\ + \hat{P} (\gamma_n^{-2} B_0 B_0^T + \gamma_d^{-2} [V_1 + \alpha^2 S Q \bar{\Sigma} Q S^T]) \hat{P} + P \Sigma P - \tau_\perp^T P \Sigma P \tau_\perp, \quad (7.55)$$

$$0 = (A_\epsilon + [\gamma_n^{-2} B_0 B_0^T + \gamma_d^{-2} V_1 - \Sigma] P) \hat{Q} + \hat{Q} (A_\epsilon + [\gamma_n^{-2} B_0 B_0^T + \gamma_d^{-2} V_1 - \Sigma] P)^T \\ + S Q \bar{\Sigma} Q S^T - \tau_\perp S Q \bar{\Sigma} Q S^T \tau_\perp^T, \quad (7.56)$$

$$\text{rank } \hat{Q} = \text{rank } \hat{P} = \text{rank } \hat{Q} \hat{P} = n_c, \quad (7.57)$$

and let  $(A_c, B_c, C_c)$  be given by

$$A_c = \Gamma [A - S Q \bar{\Sigma} + (\gamma_n^{-2} B_0 B_0^T + \gamma_d^{-2} V_1 - \Sigma) P] G^T, \quad (7.58)$$

$$B_c = \Gamma S Q C^T \hat{V}_2^{-1}, \quad (7.59)$$

$$C_c = -R_2^{-1} B^T P G^T. \quad (7.60)$$

Then

$$\tilde{P} = \begin{bmatrix} P + \hat{P} & -\hat{P} G^T \\ -G \hat{P} & G \hat{P} G^T \end{bmatrix}, \quad (7.61)$$

satisfies (7.34) and  $(A_c, B_c, C_c)$  is an extremal of  $\mathcal{J}(\tilde{P}, A_c, B_c, C_c)$ . Furthermore, the undisturbed ( $w(t) \equiv 0$ ) closed-loop system (7.30)–(7.32) is globally asymptotically stable for all  $\phi(\cdot) \in \Phi_{\mathbb{R}^{n_0}}$ . In addition, if  $\phi(\cdot) \in \Phi_{\mathcal{D}_c}$ , then the undisturbed ( $w(t) \equiv 0$ ) closed-loop system (7.30)–(7.32) is locally asymptotically stable, and  $\mathcal{D}_A$  defined by

$$\mathcal{D}_A \triangleq \{\tilde{x} \in \mathbb{R}^{\tilde{n}}: \tilde{C}_0 \tilde{x} \in \mathcal{D}_c \text{ and } \tilde{x}^T \tilde{P} \tilde{x} \leq v_\beta\}, \quad (7.62)$$

where  $v_\beta = \max\{\beta > 0 : \mathcal{D}_\beta \subset \mathbb{R}^{\tilde{n}}\}$  is a subset of the domain of attraction of the closed-loop system. Moreover, the solution  $\tilde{x}(t)$ ,  $t \in [0, \infty)$ , of the disturbed closed-loop system (7.30)–(7.32) satisfies the disturbance rejection constraint (7.36). Finally,

the cost  $\mathcal{J}(\tilde{P}, A_c, B_c, C_c)$  is given by

$$\mathcal{J}(\tilde{P}, A_c, B_c, C_c) = \text{tr}[(P + \hat{P})\hat{V}_1 + \hat{P}SQ\bar{\Sigma}QS^T]. \quad (7.63)$$

**Proof.** The proof is constructive in nature. Specifically, we first obtain necessary conditions for the Optimization Problem and then show by construction that these conditions serve as sufficient conditions for closed-loop stability and disturbance rejection. For  $\phi(\cdot) \in \Phi_{\mathcal{D}_c}$  and  $w(t) \equiv 0$ , the estimate of the domain of attraction  $\mathcal{D}_A$  is immediate using maximal closed sublevel sets. For details of a similar proof, see [11, 58].  $\square$

Since our design methodology yields *reduced-order* controllers, we are reducing control system complexity by assuring the implementation of a simpler controller for achieving disturbance rejection than the full-order controller. By “simple”, we are referring to a reduction in control system complexity measured by computer memory. In the full-order case,  $n_c = n$ , set  $G = \Gamma = \tau = I_n$ , so that  $\tau_{\perp} = 0$ . Now the last term in each of (7.53)–(7.56) can be deleted and  $G$  and  $\Gamma$  in (7.58)–(7.60) can be taken to be the identity. Furthermore,  $\hat{Q}$  plays no role, so (7.56) is superfluous. If, alternatively, the reduced-order constraint is retained and the disturbance rejection constraint is sufficiently relaxed, i.e.,  $\gamma_d \rightarrow \infty$ , then considerable simplification arises in (7.53)–(7.56).

To solve the design equations (7.53)–(7.56), we employed the homotopic continuation method presented in [58]. Homotopy algorithms operate by first replacing the original problem with a simpler problem having a known solution. The desired solution is then reached by integrating along the homotopy path that connects the starting problem to the original problem. The algorithm was initialized with  $\gamma_n = \gamma_d = \infty$ , and the LQG gains designed for the linear part of (7.18). For given values of the parameters  $\gamma_n$  and  $\gamma_d$ , the algorithm was used to find  $(A_c, B_c, C_c)$ . After each iter-

ation,  $\gamma_n$  and  $\gamma_d$  were decreased and the current values of  $(A_c, B_c, C_c)$  were used to find feasible values for  $\gamma_n$  and  $\gamma_d$  which were then used as the starting point for the next iteration. Complete details of the algorithm are provided in [58].

## 7.5. Active Dynamic Control of an Axial Flow Compressor

In this section we use the design equations (7.53)–(7.56) to design a full-order ( $n_c=3$ ) disturbance rejection, pressure rise feedback, dynamic controller for the non-linear Moore-Greitzer axial flow compressor model given in Section 7.2. Specifically, we chose the data parameter values of  $\sigma = 3.6$ ,  $\beta = 0.356$ , and  $\Psi_{C_0} = 0.72$ , and set  $\lambda = 1.1$  in the parameterization given by (7.18). Note that with  $\lambda = 1.1$ , the linear part of (7.18) is linearly stabilizable, with (7.18) providing an equilibrium point close to the desired ( $\lambda = 1.0$ ) maximum pressure rise compressor operating point. Furthermore, we set  $\gamma_n = 12.59$  and  $\gamma_d = 2.3$ , and chose design weights

$$V_1 = \hat{V}_1 = BB^T, \quad V_2 = \hat{V}_2 = 1, \quad E_1 = [ 10 \ 1 \ 1 ], \quad E_2 = \begin{bmatrix} 0 \\ 1 \end{bmatrix}.$$

Using the initial conditions  $A_0 = 1.0$ ,  $\Phi_0 = 1.866$ , and  $\Psi_0 = 3.22$  to capture system transients in the compressor, simulations of the Moore-Greitzer model were run in both the open-loop ( $\gamma_{\text{throt}}(t) = \gamma_0 = 0.6689$ ) configuration and with the designed controller given by (7.58)–(7.60) in the feedback loop. Figure 7.3 shows the phase portrait of pressure rise versus flow in the compressor for the case where no external disturbances are included in the simulation. It is seen from this plot that the controlled system converges to an equilibrium point close to the maximum pressure rise equilibrium point, whereas the constant throttle opening drives the system to a stalled equilibrium point. Figure 7.4 shows the phase portrait of pressure rise versus flow for a set of initial conditions chosen with various radii at angular intervals of

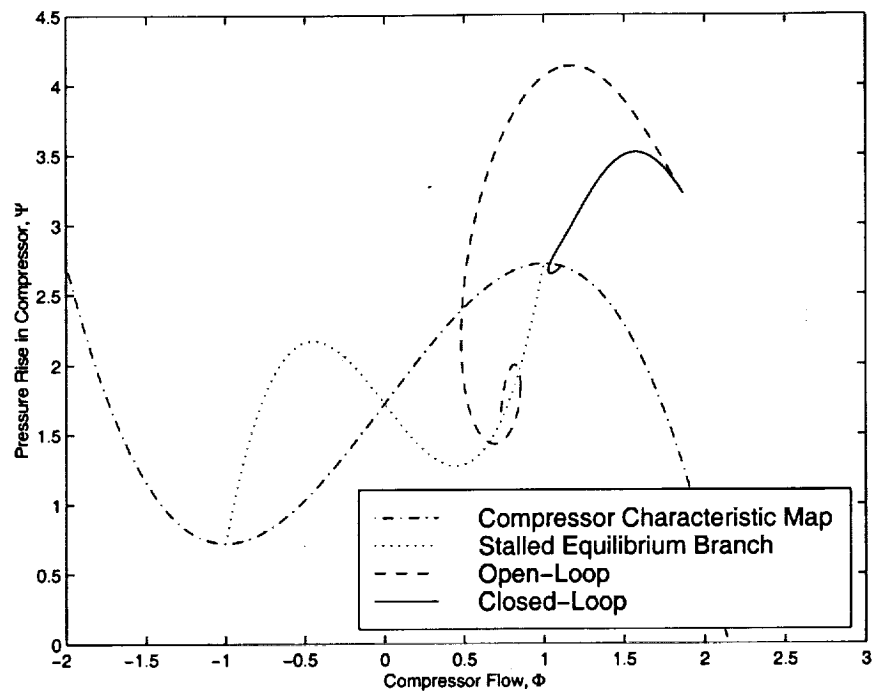


Figure 7.3: Phase portrait of pressure versus flow

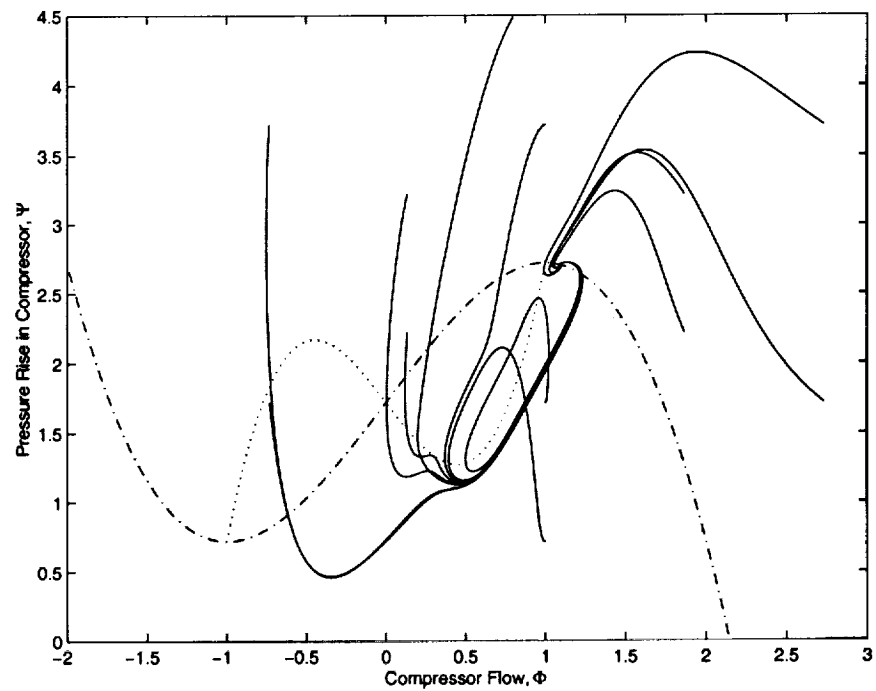


Figure 7.4: Phase portrait of pressure versus flow

$\pi/6$  about the maximum pressure rise operating point. Figure 7.5 shows the phase

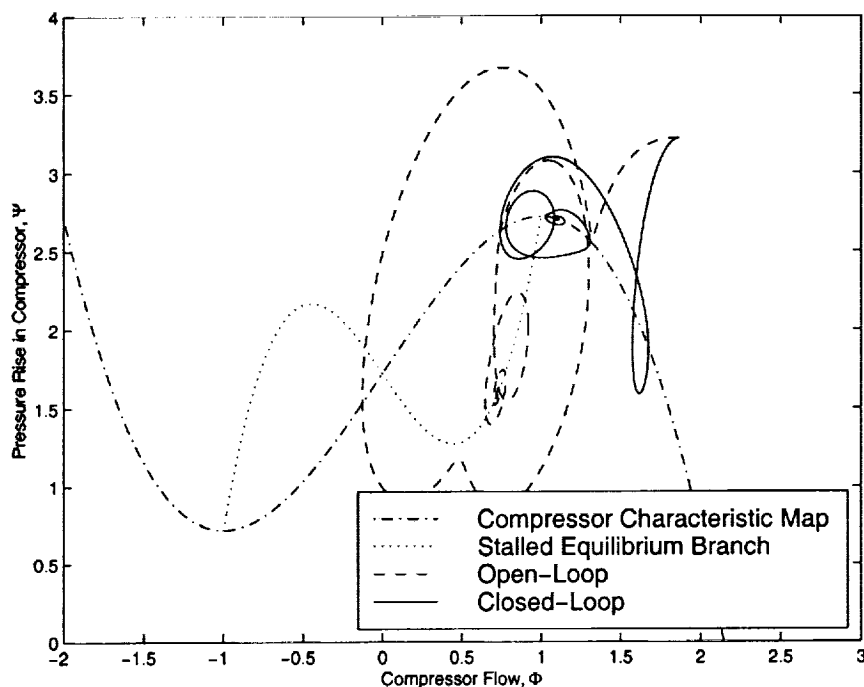


Figure 7.5: Phase portrait of pressure versus flow with exogenous disturbances

portrait of pressure rise versus flow in the compressor when the exogenous  $\mathcal{L}_2$  signal given by

$$w(t) = \begin{bmatrix} 0.9e^{-t/5} \sin(t + 2) \\ 1.2e^{-t/10} \sin(t/2 + 1) \end{bmatrix},$$

is included in the simulations. Once again, the closed-loop system converges to a point near the maximum pressure rise equilibrium point while the constant throttle opening drives the system to a stalled equilibrium point.

Figures 7.6–7.9 show the time histories of the stall cell amplitude  $A(t)$ , the compressor flow  $\Phi(t)$ , the pressure rise in the compressor  $\Psi(t)$ , and the control throttle opening  $\gamma_{\text{throt}}(t)$ , with the exogenous  $\mathcal{L}_2$  disturbance included in the simulations for the constant throttle opening, the closed-loop system with the disturbance rejection controller (7.58)–(7.60), the Liaw and Abed [83] controller given by (7.1) with  $k = 1$ , and the Badmus *et al.* [8] controller given by (7.2) with  $k_1 = 1$  and  $k_2 = 1$ . As seen in

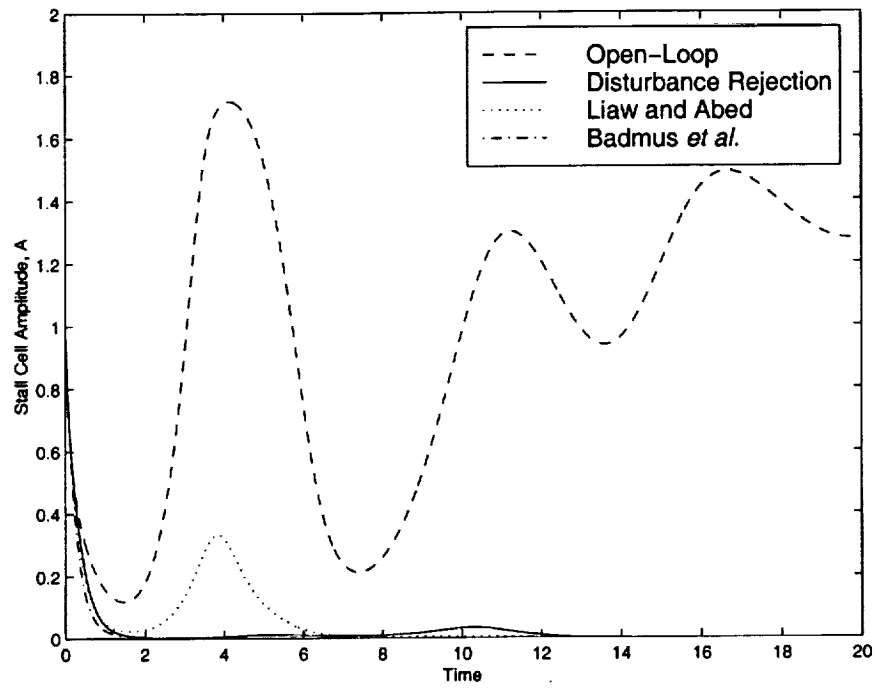


Figure 7.6: Stall cell amplitude versus time

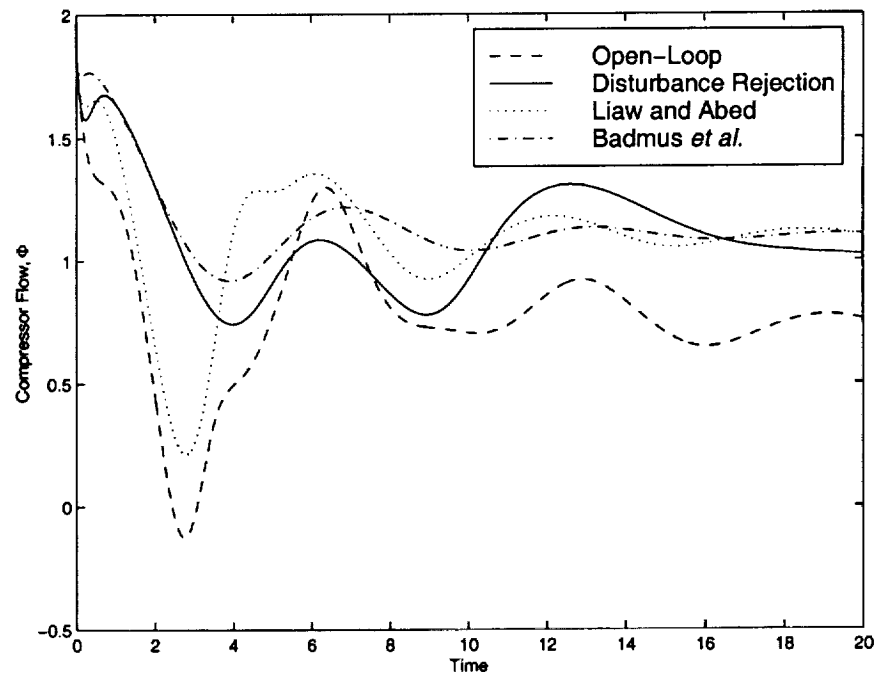


Figure 7.7: Compressor flow versus time

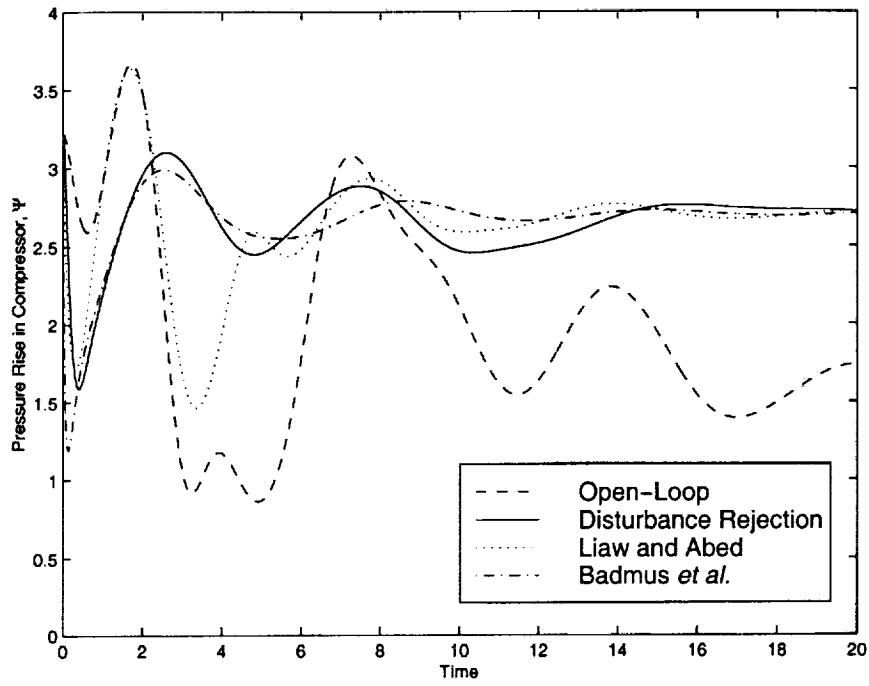


Figure 7.8: Pressure rise in compressor versus time

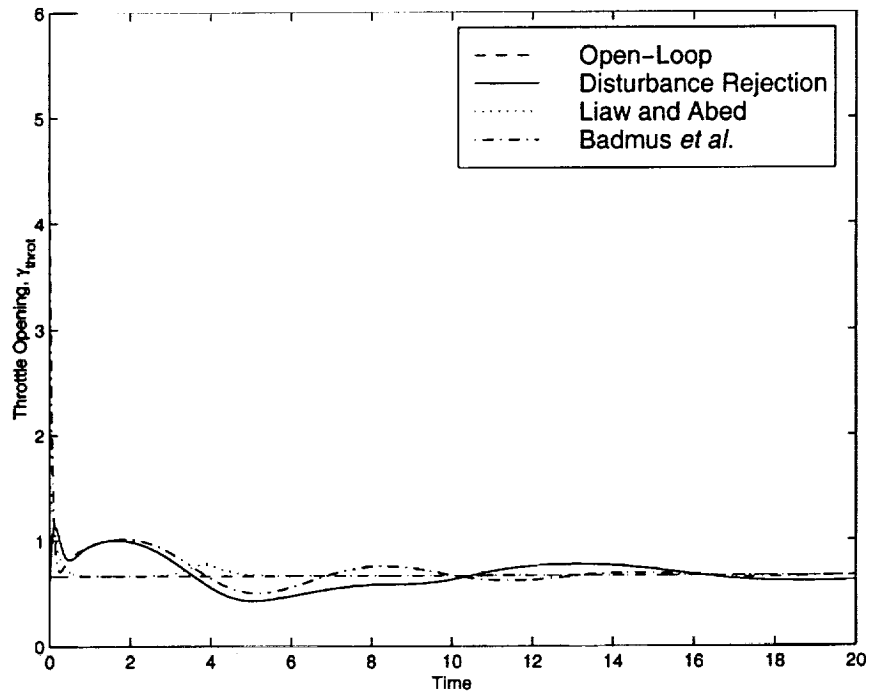


Figure 7.9: Throttle opening versus time

Figure 7.6, the disturbance rejection controller rejects the exogenous disturbance and drives the stall cell amplitude to zero, while the constant throttle opening is unable to reject the exogenous disturbance, driving the system to a stalled equilibrium. The Liaw and Abed [83] controller does stabilize the maximum pressure rise point but has poor disturbance rejection properties. Alternatively, even though, for the given disturbance, the Badmus *et al.* [8] controller has comparable disturbance rejection properties to the proposed controller, it requires a considerably more complex sensing architecture in practice. Figure 7.9 shows a comparison of the throttle opening for the three controllers considered as well as the constant throttle opening. It should be noted that the maximum throttle opening amplitude of the disturbance rejection controller is 1.1286, whereas the maximum throttle opening amplitude for the Liaw and Abed [83] controller is 1.669, and the Badmus *et al.* [8] controller is 5.018. The

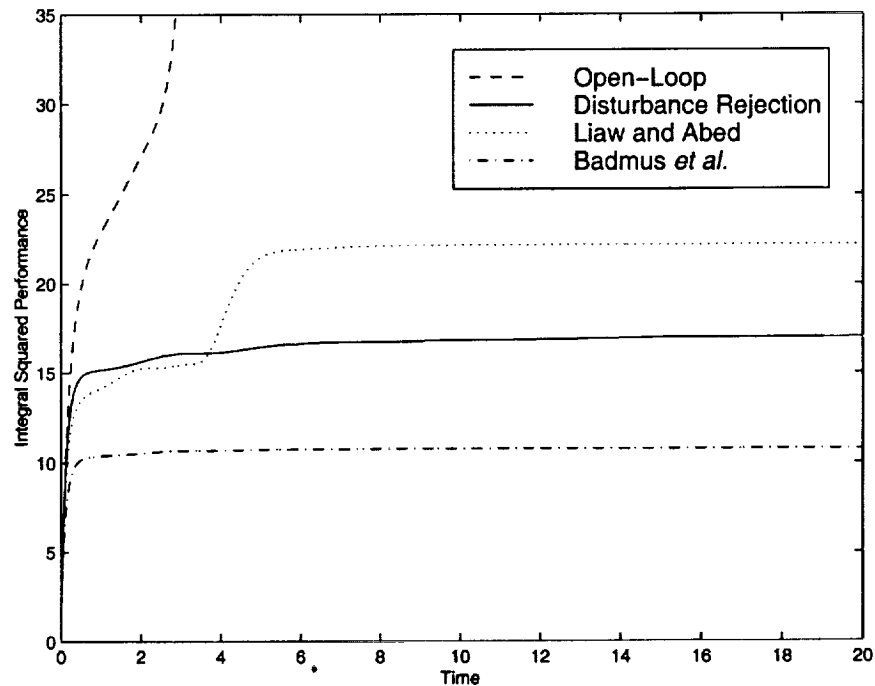


Figure 7.10: Integral squared performance versus time

Badmus *et al.* [8] controller has a significantly larger throttle opening amplitude than

the other two controllers and therefore can violate actuator limitation constraints in practice. Finally, Figure 7.10 shows the integral squared performance response  $\int_0^T z^T(t)z(t) dt$  versus time for the three designs.

## 7.6. Conclusion

A linear, fixed-order (i.e., full- and reduced-order) pressure rise feedback dynamic compensation framework for axial flow compression systems was developed. Unlike the nonlinear bifurcation-based and backstepping controllers proposed in the literature, the proposed dynamic compensator framework explicitly accounts for compressor performance versus sensor noise, compressor performance versus controller order, and compressor performance versus disturbance rejection. Furthermore, the proposed pressure rise feedback controllers provide a considerable simplification in the sensing architecture required for controlling rotating stall and surge. Finally, we note that bifurcation-based controllers discussed in the Introduction are dependent only upon measured quantities as opposed to the proposed controller which requires a model for the performance characteristic map. However, it is important to recognize that since the proposed controller guarantees *robust* stability for all  $\phi(\cdot) \in \Phi_{\mathcal{D}_c}$ , an accurate representation of the performance characteristic map is *not* required.

# CHAPTER 8

## Fixed-Structure Controller Synthesis for Real and Complex Multiple Block-Structured Uncertainty

### 8.1. Introduction

The ability of the structured singular value to account for complex, real, and mixed uncertainty provides a powerful framework for robust stability and performance problems in both analysis and synthesis (see [30, 37, 97, 105, 123] and the numerous references therein). Since exact computation of the structured singular value is, in general, an intractable problem, the development of practically implementable bounds remains a high priority in robust control research. Recent work in this area includes upper and lower bounds for mixed uncertainty [37, 81, 123] as well as LMI-based computational techniques [18, 41].

An alternative approach to developing bounds for the structured singular value is to specialize absolute stability criteria for sector-bounded nonlinearities to the case of linear uncertainty [53]. This approach, which has been explored in [23, 46, 48, 49, 51, 52, 57, 61], demonstrates the direct applicability of the classical theory of absolute stability

to the modern structured singular value framework. In particular, the rich theory of multiplier-based absolute stability criteria due to Luré and Postnikov [1, 82, 94, 103], Popov [102], Yakubovitch [119, 120], Zames and Falb [125], and numerous others can be seen to have a close and fundamental relationship with recently developed structured singular value bounds.

The objective of this chapter is to use the absolute stability results of [53], which unify and extend existing structured singular value bounds for mixed uncertainty, to obtain fixed-structure controllers and fixed-order stability multipliers which provide robust stability and performance. Using the results of [53], the robust controller synthesis technique proposed here permits the treatment of fully populated real uncertain blocks which may, in addition, possess internal structure. Such problems arise in a variety of applications, such as the study of modal dynamics, in which transformation to 'standard' diagonal form may introduce additional conservatism, computational complexity, as well as destroying the parameter space of the original uncertainty characterization [53]. The ability to address real uncertain blocks is based on the use of an appropriate class of multipliers whose structure is compatible with the real block uncertainty. Hence, tailoring the multipliers to the structure of the uncertainty not only leads to the ability to address more general uncertainty characterizations but can also lead to less conservative controllers than obtained from the standard mixed- $\mu$  synthesis techniques. This more general class of multipliers has no counterpart in standard mixed- $\mu$  theory [37, 105, 123].

## **8.2. Absolute Stability Criterion with Generalized Positive Real Stability Multipliers**

In this section we review the absolute stability criterion for multivariable systems with generalized positive real stability multipliers given in [53]. This criterion involves

a square nominal (open-loop or feedback) transfer function  $G(s)$  in a negative feedback interconnection with a complex, square, uncertain matrix  $\Delta$  as shown in Figure 8.1. Here, we consider the set of block-diagonal matrices with possibly repeated blocks

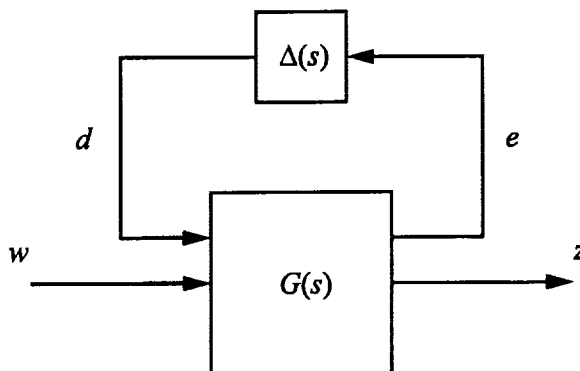


**Figure 8.1:** Standard feedback uncertainty representation

defined by

$$\begin{aligned} \Delta_{\text{bs}} \triangleq \{ \Delta \in \mathbb{C}^{p \times p} : \Delta = \text{block-diag} [ & I_{\psi_1} \otimes \Delta_1^r, \dots, I_{\psi_r} \otimes \Delta_r^r, \\ & I_{\psi_{r+1}} \otimes \Delta_{r+1}^c, \dots, I_{\psi_{r+c}} \otimes \Delta_{r+c}^c ] ; \Delta_i^r \in \mathbb{R}^{p_i \times p_i}, i = 1, \dots, r ; \\ & \Delta_i^c \in \mathbb{C}^{p_i \times p_i}, i = r + 1, \dots, r + c \}, \end{aligned}$$

where the dimension  $p_i$  of each block and the number of repetitions  $\psi_i$  of each block are given such that  $\sum_{i=1}^v \psi_i p_i = p$ , where  $v = r + c$  is the number of *distinct* uncertain blocks. Furthermore, define the subset  $\Delta \subseteq \Delta_{\text{bs}}$  consisting of sector-bounded matrices

$$\Delta \triangleq \{ \Delta \in \Delta_{\text{bs}} : 2(\Delta - M_1)^*(M_2 - M_1)^{-1}(\Delta - M_1) \leq (\Delta - M_1) + (\Delta - M_1)^* \},$$

where  $M_1, M_2 \in \Delta_{\text{bs}}$  are Hermitian matrices such that  $M \triangleq M_2 - M_1$  is positive definite. Note that  $M_1$  and  $M_2$  are elements of  $\Delta$ . Alternate characterizations of  $\Delta$  are given in [53].

To draw connections with the structured singular value for real and complex block-structured uncertainty, we specialize the set  $\Delta$  to the case of norm-bounded, internally

block-structured uncertainty. Specifically, by letting  $M_1 = -\gamma^{-1}I$  and  $M_2 = \gamma^{-1}I$ , where  $\gamma > 0$ , it follows that  $M = 2\gamma^{-1}I$  so that  $M^{-1} = \frac{1}{2}\gamma I$ . In this case,  $\Delta$  becomes

$$\Delta_\gamma = \{\Delta \in \Delta_{\text{bs}} : \gamma(\Delta + \gamma^{-1}I)^*(\Delta + \gamma^{-1}I) \leq (\Delta + \gamma^{-1}I) + (\Delta + \gamma^{-1}I)^*\}.$$

Now,  $\Delta \in \Delta_\gamma$  if and only if  $\sigma_{\max}(\Delta) \leq \gamma^{-1}$ . Therefore,  $\Delta_\gamma$  is given by

$$\Delta_\gamma = \{\Delta \in \Delta_{\text{bs}} : \sigma_{\max}(\Delta) \leq \gamma^{-1}\}.$$

Next we give the multivariable absolute stability criterion for sector-bounded uncertain matrices. To state this criterion, we define the sets  $\mathcal{D}$  and  $\mathcal{N}$  of Hermitian rational scaling matrix functions by

$$\mathcal{D} \triangleq \{D : \mathbb{C} \rightarrow \mathbb{C}^{p \times p} : D(j\omega) \geq 0, D(j\omega)\Delta = \Delta D(j\omega), \omega \in \mathbb{R}, \Delta \in \Delta_{\text{bs}}\},$$

$$\mathcal{N} \triangleq \{N : \mathbb{C} \rightarrow \mathbb{C}^{p \times p} : N(j\omega) = N^*(j\omega), N(j\omega)\Delta = \Delta^* N(j\omega), \omega \in \mathbb{R}, \Delta \in \Delta_{\text{bs}}\}.$$

Furthermore, define the set  $\mathcal{Z}$  of rational multiplier functions by

$$\mathcal{Z} \triangleq \{Z : \mathbb{C} \rightarrow \mathbb{C}^{q \times q} : Z(j\omega) = D(j\omega) - j\omega N(j\omega), D(\cdot) \in \mathcal{D}, N(\cdot) \in \mathcal{N}\}.$$

Note that if  $Z(\cdot) \in \mathcal{Z}$ ,  $D(\cdot) \in \mathcal{D}$ , and  $N(\cdot) \in \mathcal{N}$ , then  $Z(j\omega) = D(j\omega) - j\omega N(j\omega)$  if and only if  $D(j\omega) = \text{He } Z(j\omega)$  and  $N(j\omega) = \frac{-1}{j\omega} \text{Sh } Z(j\omega)$ ,  $\omega \neq 0$ . Hence, since  $D(j\omega) \geq 0$ ,  $\omega \in \mathbb{R} \cup \infty$ ,  $Z(\cdot) \in \mathcal{Z}$  consists of generalized positive real functions [3].

**Remark 8.1.** Although the condition  $D(j\omega)\Delta = \Delta D(j\omega)$  in  $\mathcal{D}$  arises in complex and mixed- $\mu$  analysis [37], the condition  $N(j\omega)\Delta = \Delta^* N(j\omega)$  in  $\mathcal{N}$  has no counterpart in [37]. As shown in [53], this condition generalizes mixed- $\mu$  analysis to address nondiagonal real matrices which are not considered in standard mixed- $\mu$  theory. The condition  $N(j\omega)\Delta = \Delta^* N(j\omega)$  is an extension of the condition used in [46] for Popov controller synthesis with constant real matrix uncertainty.

We now state our main robust stability result.

**Theorem 8.1** [53]. Suppose  $(I + G(s)M_1)^{-1}G(s)$  is asymptotically stable. If there exists  $Z(\cdot) \in \mathcal{Z}$  such that

$$\operatorname{Re} [Z(s)(M^{-1} + (I + G(s)M_1)^{-1}G(s))] > 0, \quad (8.1)$$

for all  $s = j\omega$ ,  $\omega \in \mathbb{R} \cup \infty$ , then the negative feedback interconnection of  $G(s)$  and  $\Delta$  is asymptotically stable for all  $\Delta \in \overline{\Delta}$ .

### 8.3. Stability Multiplier Structure

To ensure the commutability of the rational scaling matrix functions  $D(s)$  and  $N(s)$  with the uncertainty set  $\Delta$ , we must structure  $Z(s) = C_m(sI - A_m)^{-1}B_m + D_m$  so that  $Z(s) \in \mathcal{Z}$ . To assure this, we construct the multiplier  $Z(s)$  from the constituent multipliers  $D(s)$  and  $N(s)$ . Furthermore, instead of obtaining a realization for  $N(s)$ , we obtain a realization for  $sN(s)$  directly since  $Z(s) = D(s) - sN(s)$ . We therefore choose multiplier realizations

$$D(s) \sim \left[ \begin{array}{c|c} A_d & B_d \\ \hline C_d & D_d \end{array} \right], \quad N(s) \sim \left[ \begin{array}{c|c} A_n & B_n \\ \hline C_n & 0 \end{array} \right],$$

where  $A_d \in \mathcal{S}_{A_d}$ ,  $A_n \in \mathcal{S}_{A_n}$ ,  $B_d \in \mathcal{S}_{B_d}$ ,  $B_n \in \mathcal{S}_{B_n}$ ,  $C_d \in \mathcal{S}_{C_d}$ ,  $C_n \in \mathcal{S}_{C_n}$ , and  $D_d \in \mathcal{S}_{D_d}$ . The sets  $\mathcal{S}_{A_d}$ ,  $\mathcal{S}_{A_n}$ ,  $\mathcal{S}_{B_d}$ ,  $\mathcal{S}_{B_n}$ ,  $\mathcal{S}_{C_d}$ ,  $\mathcal{S}_{C_n}$ , and  $\mathcal{S}_{D_d}$  are chosen to enforce the diagonal structure of  $D(s)$  and  $N(s)$  given by

$$D(s) = C_d(sI - A_d)^{-1}B_d + D_d = \text{block-diag}[D_1(s) \otimes I_{p_1}, \dots, D_v(s) \otimes I_{p_v}],$$

$$N(s) = C_n(sI - A_n)^{-1}B_n = \text{block-diag}[N_1(s) \otimes I_{p_1}, \dots, N_v(s) \otimes I_{p_v}],$$

where

$$0 \leq D_i(s) \in \mathbb{C}^{\psi_i \times \psi_i}, \quad i = 1, \dots, v,$$

$$N_i(s) = N_i^*(s) \in \mathbb{C}^{\psi_i \times \psi_i}, N_i(s)\Delta_i = N_i(s)\Delta_i^*, \quad i = 1, \dots, v.$$

The structure chosen for the rational functions representing  $D(s)$  and  $N(s)$  in this chapter is similar to the one for the curve-fitting operation in standard  $\mu$ -synthesis [9].

In particular, we define  $\mathcal{S}_{A_d}$ ,  $\mathcal{S}_{A_n}$ ,  $\mathcal{S}_{B_d}$ ,  $\mathcal{S}_{B_n}$ ,  $\mathcal{S}_{C_d}$ ,  $\mathcal{S}_{C_n}$ , and  $\mathcal{S}_{D_d}$  as follows:

$$\begin{aligned} \mathcal{S}_{A_d} \triangleq \{ & A_d = \text{block-diag}[I_{\psi_1 p_1} \otimes A_{d_1}, \dots, I_{\psi_v p_v} \otimes A_{d_v}] : A_{d_i} \in \mathbb{R}^{n_{d_i} \times n_{d_i}}, \\ & A_{d_i} \text{ is in controllable canonical companion form with the 1}^{\text{st}} \\ & \text{row} = \begin{bmatrix} 0 & a_{d_i,2} & 0 & a_{d_i,4} & \cdots & 0 & a_{d_i,n_{d_i}} \end{bmatrix}, \text{sgn } a_{d_i,j} = (-1)^{(j/2)+1}, \\ & i = 1, \dots, v, j = 1, \dots, n_{d_i} \}, \end{aligned} \quad (8.2)$$

$$\begin{aligned} \mathcal{S}_{A_n} \triangleq \{ & A_n = \text{block-diag}[I_{\psi_1 p_1} \otimes A_{n_1}, \dots, I_{\psi_v p_v} \otimes A_{n_v}] : A_{n_i} \in \mathbb{R}^{n_{n_i} \times n_{n_i}}, \\ & A_{n_i} \text{ is in controllable canonical companion form with the 1}^{\text{st}} \\ & \text{row} = \begin{bmatrix} 0 & a_{n_i,2} & 0 & a_{n_i,4} & \cdots & 0 & a_{n_i,n_{n_i}} \end{bmatrix}, i = 1, \dots, v \}, \end{aligned} \quad (8.3)$$

$$\begin{aligned} \mathcal{S}_{B_d} \triangleq \{ & B_d = \text{block-diag}[I_{\psi_1 p_1} \otimes B_{d_1}, \dots, I_{\psi_v p_v} \otimes B_{d_v}] : B_{d_i} \in \mathbb{R}^{n_{d_i} \times 1}, \\ & B_{d_i}^T = \begin{bmatrix} 1 & 0 & \cdots & 0 \end{bmatrix}, i = 1, \dots, v \}, \end{aligned} \quad (8.4)$$

$$\begin{aligned} \mathcal{S}_{B_n} \triangleq \{ & B_n = \text{block-diag}[I_{\psi_1 p_1} \otimes B_{n_1}, \dots, I_{\psi_v p_v} \otimes B_{n_v}] : B_{n_i} \in \mathbb{R}^{n_{n_i} \times 1}, \\ & B_{n_i}^T = \begin{bmatrix} 1 & 0 & \cdots & 0 \end{bmatrix}, i = 1, \dots, v \}, \end{aligned} \quad (8.5)$$

$$\begin{aligned} \mathcal{S}_{C_d} \triangleq \{ & C_d = \text{block-diag}[I_{\psi_1 p_1} \otimes C_{d_1}, \dots, I_{\psi_v p_v} \otimes C_{d_v}] : C_{d_i} \in \mathbb{R}^{1 \times n_{d_i}}, \\ & C_{d_i} = \begin{bmatrix} 0 & c_{d_i,2} & 0 & c_{d_i,4} & \cdots & 0 & c_{d_i,n_{d_i}} \end{bmatrix}, \text{sgn } c_{d_i,j} = (-1)^{j/2}, \\ & i = 1, \dots, v, j = 1, \dots, n_{d_i} \}, \end{aligned} \quad (8.6)$$

$$\begin{aligned} \mathcal{S}_{C_n} \triangleq \{ & C_n = [\text{block-diag}[I_{\psi_1 p_1} \otimes C_{n_1}, \dots, I_{\psi_v p_v} \otimes C_{n_v}]] : C_{n_i} \in \mathbb{R}^{1 \times n_{n_i}}, \\ & C_{n_i} = \begin{bmatrix} c_{n_i,1} & 0 & c_{n_i,3} & \cdots & 0 & c_{n_i,n_{n_i}-1} & 0 \end{bmatrix}, i = 1, \dots, v \}, \end{aligned} \quad (8.7)$$

$$\begin{aligned} \mathcal{S}_{D_d} \triangleq \{ & D_d = \text{block-diag}[d_{d_1} I_{\psi_1 p_1}, \dots, d_{d_v} I_{\psi_v p_v}] : d_{d_i} \in \mathbb{R}, d_{d_i} > 0, \\ & i = 1, \dots, v \}, \end{aligned} \quad (8.8)$$

where  $n_{d_i}$  and  $n_{n_i}$  are the *a priori* fixed even orders of the rational functions representing the  $i^{\text{th}}$  diagonal element of the multipliers  $D(s)$  and  $N(s)$ , respectively. Thus we see that  $n_d$  and  $n_n$ , defined as

$$n_d \triangleq \sum_{i=1}^v n_{d_i} \psi_i, \quad n_n \triangleq \sum_{i=1}^v n_{n_i} \psi_i, \quad (8.9)$$

are the total number of states describing  $D(s)$  and  $N(s)$ , respectively.

To construct  $Z(s) = D(s) - sN(s)$ , we obtain the augmented realizations

$$A_m = \text{block-diag}[A_d, A_n], \quad (8.10)$$

$$B_m = \begin{bmatrix} B_d \\ B_n \end{bmatrix}, \quad (8.11)$$

$$C_m = [C_d \quad -C_n], \quad (8.12)$$

$$D_m = D_d, \quad (8.13)$$

where  $A_d \in \mathcal{S}_{A_d}$ ,  $A_n \in \mathcal{S}_{A_n}$ ,  $B_d \in \mathcal{S}_{B_d}$ ,  $B_n \in \mathcal{S}_{B_n}$ ,  $C_d \in \mathcal{S}_{C_d}$ ,  $C_n \in \mathcal{S}_{C_n}$ , and  $D_d \in \mathcal{S}_{D_d}$ . Note that  $A_m \in \mathbb{R}^{n_m \times n_m}$ , where  $n_m = n_d + n_n$ . Furthermore note that there is no contribution to  $D_m$  from the  $sN(s)$  term. This is due to the fact that the rational function  $N(s)$  is strictly proper and has only even powers of  $s$ . Thus  $N(s)$  necessarily has a relative degree of two and hence  $sN(s)$  is strictly proper.

Next, we note that with

$$Z(s) \sim \left[ \begin{array}{c|c} A_m & B_m \\ \hline C_m & D_m \end{array} \right],$$

as defined in (8.10)–(8.13), we obtain the necessary commutability properties, as well as ensuring that  $D(s) > 0$  and  $N(s) = N^*(s)$ . However, to satisfy the condition  $N(s)\Delta = \Delta^*N(s)$ , we require that the  $i^{\text{th}}$  block of  $N(s)$  be zero whenever the  $i^{\text{th}}$  uncertainty block  $\Delta_i$  is complex. Thus, in the case where  $\Delta_i \in \mathbb{C}^{p_i \times p_i}$ , we require that the realization of  $N_i(s)$  be given by

$$A_{n_i} = [ \quad ]_{0 \times 0}, \quad B_{n_i} = [ \quad ]_{0 \times 1}, \quad C_{n_i} = [ \quad ]_{1 \times 0},$$

where  $[ ]_{0 \times j}$  is the  $0 \times j$  empty matrix [96]. Thus, in this case, the  $i^{\text{th}}$  block of  $N(s)$  is given by

$$N_i(s) = C_{n_i}(sI - A_{n_i})^{-1}B_{n_i} = 0.$$

Finally, we note that the stability multipliers cannot have arbitrary realizations and still be elements of their appropriate sets  $\mathcal{S}_{A_d}$ ,  $\mathcal{S}_{A_n}$ ,  $\mathcal{S}_{B_d}$ ,  $\mathcal{S}_{B_n}$ ,  $\mathcal{S}_{C_d}$ ,  $\mathcal{S}_{C_n}$ , and  $\mathcal{S}_{D_d}$ . Thus we recast the stability multiplier matrices so that the free parameters appear along the diagonal of a separate matrix,  $\mathcal{K}_m$ . The stability multipliers can then be constructed as

$$\begin{aligned} A_m &= A_{mC} + A_{mL}\mathcal{K}_mA_{mR}, & B_m &= B_{mC}, \\ C_m &= C_{mL}\mathcal{K}_mC_{mR}, & D_m &= D_{mL}\mathcal{K}_mD_{mR}, \end{aligned}$$

where the matrices  $A_{mC}$ ,  $A_{mL}$ ,  $A_{mR}$ ,  $B_{mC}$ ,  $C_{mL}$ ,  $C_{mR}$ ,  $D_{mL}$ , and  $D_{mR}$  are structured appropriately. To illustrate the structure of these matrices, consider the scalar multiplier

$$Z(s) = d_{d_1} + \frac{c_{d_{1,2}}}{s^2 - a_{d_{1,2}}} - \frac{c_{n_{1,1}}s}{s^2 - a_{n_{1,2}}}.$$

The gain and structure matrices for the stability multiplier with  $n_n = n_d = 2$  are then given by

$$\mathcal{K}_m = \begin{bmatrix} a_{d_{1,2}} & 0 & 0 & 0 & 0 \\ 0 & c_{d_{1,2}} & 0 & 0 & 0 \\ 0 & 0 & d_{d_1} & 0 & 0 \\ 0 & 0 & 0 & a_{n_{1,2}} & 0 \\ 0 & 0 & 0 & 0 & c_{n_{1,1}} \end{bmatrix},$$

$$A_{mC} = \begin{bmatrix} 0 & 0 & 0 & 0 \\ 1 & 0 & 0 & 0 \\ 0 & 0 & 0 & 0 \\ 0 & 0 & 1 & 0 \end{bmatrix}, \quad A_{mL} = \begin{bmatrix} 1 & 0 & 0 & 0 & 0 \\ 0 & 0 & 0 & 0 & 0 \\ 0 & 0 & 0 & 1 & 0 \\ 0 & 0 & 0 & 0 & 0 \end{bmatrix}, \quad A_{mR} = \begin{bmatrix} 0 & 1 & 0 & 0 \\ 0 & 0 & 0 & 0 \\ 0 & 0 & 0 & 0 \\ 0 & 0 & 0 & 1 \\ 0 & 0 & 0 & 0 \end{bmatrix},$$

$$B_{mC} = \begin{bmatrix} 1 \\ 0 \\ 1 \\ 0 \end{bmatrix}, \quad C_{mR} = \begin{bmatrix} 0 & 0 & 0 & 0 \\ 0 & 1 & 0 & 0 \\ 0 & 0 & 0 & 0 \\ 0 & 0 & 0 & 0 \\ 0 & 0 & 1 & 0 \end{bmatrix}, \quad D_{mR} = \begin{bmatrix} 0 \\ 0 \\ 1 \\ 0 \\ 0 \end{bmatrix},$$

$$C_{mL} = [0 \ 1 \ 0 \ 0 \ -1], \quad D_{mL} = [0 \ 0 \ 1 \ 0 \ 0].$$

With these definitions, we see that

$$A_m = \begin{bmatrix} 0 & a_{d_{1,2}} & 0 & 0 \\ 1 & 0 & 0 & 0 \\ 0 & 0 & 0 & a_{n_{1,2}} \\ 0 & 0 & 1 & 0 \end{bmatrix}, \quad B_m = \begin{bmatrix} 1 \\ 0 \\ 1 \\ 0 \end{bmatrix},$$

$$C_m = [0 \ c_{d_{1,2}} \ -c_{n_{1,1}} \ 0], \quad D_m = [d_{d_1}],$$

and thus

$$Z(s) = C_m(sI - A_m)^{-1}B_m + D_m = d_{d_1} + \frac{c_{d_{1,2}}}{s^2 - a_{d_{1,2}}} - \frac{c_{n_{1,1}}s}{s^2 - a_{n_{1,2}}}.$$

## 8.4. Decentralized Static Output Feedback Formulation

In this section we review the decentralized static output feedback problem formulation for fixed-structure controller synthesis [14, 34]. Consider the  $(m + q + 1)$ -vector-input,  $(m + q + 1)$ -vector-output decentralized system shown in Figure 8.2, where  $e_i$  and  $d_i$ ,  $i = 1, \dots, q$ , are used to account for model uncertainty,  $w$  is the exogenous disturbance input,  $z$  is the performance variable, and the signals  $y_i$  and  $u_i$ ,  $i = 1, \dots, m$ , are measurement and control signals, respectively. The decentralized static output feedback multi vector-input, multi vector-output system shown in Figure 8.2 is characterized by the dynamics

$$\dot{\tilde{x}}(t) = \mathcal{A}\tilde{x}(t) + \sum_{j=1}^m \mathcal{B}_{u_j} u_j(t) + \sum_{k=1}^q \mathcal{B}_{d_k} d_k(t) + \mathcal{B}_w w(t), \quad t \in [0, \infty), \quad (8.14)$$

$$y_i(t) = \mathcal{C}_{y_i} \tilde{x}(t) + \sum_{j=1}^m \mathcal{D}_{y u_{ij}} u_j(t) + \sum_{k=1}^q \mathcal{D}_{y d_{ik}} d_k(t) + \mathcal{D}_{y w_i} w(t), \quad i = 1, 2, \dots, m, \quad (8.15)$$

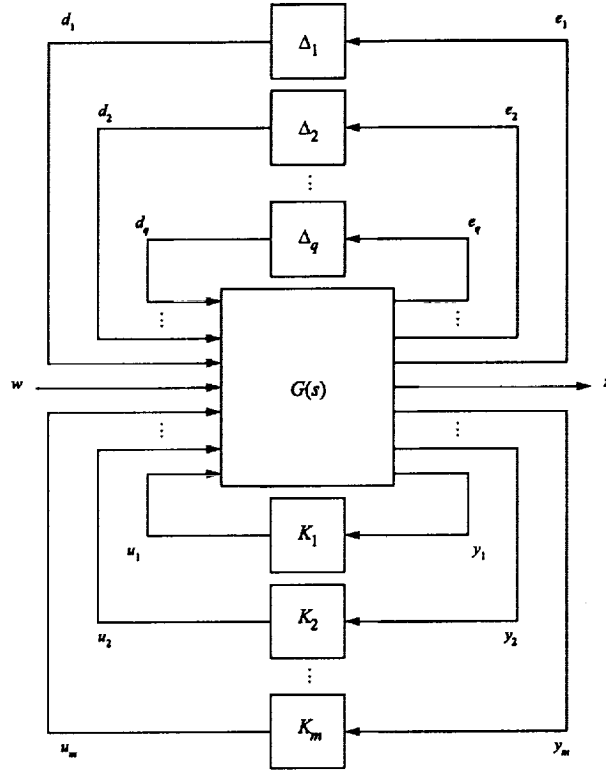


Figure 8.2: Decentralized static output feedback framework

$$e_i(t) = C_{e_i} \tilde{x}(t) + \sum_{j=1}^m \mathcal{D}_{eu_{ij}} u_j(t) + \sum_{k=1}^q \mathcal{D}_{ed_{ik}} d_k(t) + \mathcal{D}_{ew_i} w(t), \quad i = 1, 2, \dots, q, \quad (8.16)$$

$$z(t) = C_z \tilde{x}(t) + \sum_{j=1}^m \mathcal{D}_{zu_j} u_j(t) + \sum_{k=1}^q \mathcal{D}_{zd_k} d_k(t) + \mathcal{D}_{zw} w(t). \quad (8.17)$$

In the above formulation, model uncertainty is represented by the decentralized static output feedback map

$$d_i(t) = \Delta_i e_i(t), \quad i = 1, \dots, q, \quad (8.18)$$

where the uncertain matrices  $\Delta_i$  are not necessarily distinct. To represent decentralized static output feedback control with possibly repeated gains, we consider

$$u_i(t) = \mathcal{K}_i y_i(t), \quad i = 1, \dots, m, \quad (8.19)$$

where the matrices  $\mathcal{K}_i$  are not necessarily distinct. Reordering the variables in (8.18)

and (8.19) if necessary and defining

$$\hat{u}(t) = \begin{bmatrix} u_1(t) \\ \vdots \\ u_m(t) \end{bmatrix}, \hat{y}(t) = \begin{bmatrix} y_1(t) \\ \vdots \\ y_m(t) \end{bmatrix}, \hat{d}(t) = \begin{bmatrix} d_1(t) \\ \vdots \\ d_q(t) \end{bmatrix}, \hat{e}(t) = \begin{bmatrix} e_1(t) \\ \vdots \\ e_q(t) \end{bmatrix}, \quad (8.20)$$

$$\mathcal{B}_u \triangleq [\mathcal{B}_{u_1} \ \cdots \ \mathcal{B}_{u_m}], \mathcal{B}_d \triangleq [\mathcal{B}_{d_1} \ \cdots \ \mathcal{B}_{d_q}], \mathcal{D}_{zu} \triangleq [\mathcal{D}_{zu_1} \ \cdots \ \mathcal{D}_{zu_m}], \quad (8.21)$$

$$\mathcal{C}_y \triangleq \begin{bmatrix} \mathcal{C}_{y_1} \\ \vdots \\ \mathcal{C}_{y_m} \end{bmatrix}, \mathcal{D}_{yu} \triangleq \begin{bmatrix} \mathcal{D}_{yu_{11}} & \cdots & \mathcal{D}_{yu_{1m}} \\ \vdots & \ddots & \vdots \\ \mathcal{D}_{yu_{m1}} & \cdots & \mathcal{D}_{yu_{mm}} \end{bmatrix}, \mathcal{D}_{yd} \triangleq \begin{bmatrix} \mathcal{D}_{yd_{11}} & \cdots & \mathcal{D}_{yd_{1q}} \\ \vdots & \ddots & \vdots \\ \mathcal{D}_{yd_{m1}} & \cdots & \mathcal{D}_{yd_{mq}} \end{bmatrix}, \quad (8.22)$$

$$\mathcal{C}_e \triangleq \begin{bmatrix} \mathcal{C}_{e_1} \\ \vdots \\ \mathcal{C}_{e_q} \end{bmatrix}, \mathcal{D}_{eu} \triangleq \begin{bmatrix} \mathcal{D}_{eu_{11}} & \cdots & \mathcal{D}_{eu_{1m}} \\ \vdots & \ddots & \vdots \\ \mathcal{D}_{eu_{q1}} & \cdots & \mathcal{D}_{eu_{qm}} \end{bmatrix}, \mathcal{D}_{ed} \triangleq \begin{bmatrix} \mathcal{D}_{ed_{11}} & \cdots & \mathcal{D}_{ed_{1q}} \\ \vdots & \ddots & \vdots \\ \mathcal{D}_{ed_{q1}} & \cdots & \mathcal{D}_{ed_{qq}} \end{bmatrix}, \quad (8.23)$$

$$\mathcal{D}_{zd} \triangleq [\mathcal{D}_{zd_1} \ \cdots \ \mathcal{D}_{zd_q}], \mathcal{D}_{yw} \triangleq \begin{bmatrix} \mathcal{D}_{yw_1} \\ \vdots \\ \mathcal{D}_{yw_m} \end{bmatrix}, \mathcal{D}_{ew} \triangleq \begin{bmatrix} \mathcal{D}_{ew_1} \\ \vdots \\ \mathcal{D}_{ew_q} \end{bmatrix}, \quad (8.24)$$

(8.18) and (8.19) can be rewritten

$$\hat{d}(t) = \Delta \hat{e}(t), \quad (8.25)$$

$$\hat{u}(t) = \mathcal{K} \hat{y}(t), \quad (8.26)$$

where  $\Delta$  and  $\mathcal{K}$  have the form

$$\Delta \triangleq \text{block-diag} [I_{\psi_1} \otimes \Delta_1, \dots, I_{\psi_v} \otimes \Delta_v], \quad (8.27)$$

$$\mathcal{K} \triangleq \text{block-diag} [I_{\phi_1} \otimes \mathcal{K}_1, \dots, I_{\phi_g} \otimes \mathcal{K}_g], \quad (8.28)$$

where  $v$  is the number of *distinct* uncertainties  $\Delta_i \in \mathbb{C}^{p_i \times p_i}$  or  $\mathbb{R}^{p_i \times p_i}$ ,  $\psi_i$  is the number of repetitions of uncertainty  $\Delta_i$ ,  $g$  is the number of *distinct* gains  $\mathcal{K}_i \in \mathbb{R}^{r_i \times c_i}$  and  $\phi_i$  is the number of repetitions of gain  $\mathcal{K}_i$ . Note that  $\mathcal{K}_1, \dots, \mathcal{K}_g$  are not necessarily square matrices, and  $\sum_{i=1}^v \psi_i = q$  and  $\sum_{i=1}^g \phi_i = m$ .

With the definitions in (8.20)–(8.24), the transfer function  $G(s)$  from  $[\hat{u}^T, \hat{d}^T, w^T]^T$  to  $[\hat{y}^T, \hat{e}^T, z^T]^T$  of the decentralized system has the realization

$$G(s) \sim \left[ \begin{array}{c|ccc} \mathcal{A} & \mathcal{B}_u & \mathcal{B}_d & \mathcal{B}_w \\ \hline \mathcal{C}_y & \mathcal{D}_{yu} & \mathcal{D}_{yd} & \mathcal{D}_{yw} \\ \hline \mathcal{C}_e & \mathcal{D}_{eu} & \mathcal{D}_{ed} & \mathcal{D}_{ew} \\ \hline \mathcal{C}_z & \mathcal{D}_{zu} & \mathcal{D}_{zd} & \mathcal{D}_{zw} \end{array} \right], \quad (8.29)$$

which represents the linear, time-invariant dynamic system

$$\dot{\tilde{x}}(t) = \mathcal{A}\tilde{x}(t) + \mathcal{B}_u\hat{u}(t) + \mathcal{B}_d\hat{d}(t) + \mathcal{B}_w w(t), \quad t \in [0, \infty), \quad (8.30)$$

$$\hat{y}(t) = \mathcal{C}_y\tilde{x}(t) + \mathcal{D}_{yu}\hat{u}(t) + \mathcal{D}_{yd}\hat{d}(t) + \mathcal{D}_{yw}w(t), \quad (8.31)$$

$$\hat{e}(t) = \mathcal{C}_e\tilde{x}(t) + \mathcal{D}_{eu}\hat{u}(t) + \mathcal{D}_{ed}\hat{d}(t) + \mathcal{D}_{ew}w(t), \quad (8.32)$$

$$z(t) = \mathcal{C}_z\tilde{x}(t) + \mathcal{D}_{zu}\hat{u}(t) + \mathcal{D}_{zd}\hat{d}(t) + \mathcal{D}_{zw}w(t), \quad (8.33)$$

which is equivalent to (8.14)–(8.17). Furthermore, by rewriting the decentralized control signals (8.19) in the compact form given by (8.26), the closed-loop system realization from  $[\hat{d}^T, w^T]^T$  to  $[\hat{e}^T, z^T]^T$  is given by

$$\tilde{G}(s) \sim \left[ \begin{array}{c|cc} \tilde{A} & \tilde{B}_0 & \tilde{D} \\ \hline \tilde{C}_0 & \tilde{D}_0 & \tilde{D}_1 \\ \hline \tilde{E} & \tilde{E}_1 & \tilde{E}_0 \end{array} \right], \quad (8.34)$$

where

$$\begin{aligned} \tilde{A} &\triangleq \mathcal{A} + \mathcal{B}_u \mathcal{K} L_{\mathcal{K}}^{-1} \mathcal{C}_y, & \tilde{B}_0 &\triangleq \mathcal{B}_d + \mathcal{B}_u \mathcal{K} L_{\mathcal{K}}^{-1} \mathcal{D}_{yd}, & \tilde{D} &\triangleq \mathcal{B}_w + \mathcal{B}_u \mathcal{K} L_{\mathcal{K}}^{-1} \mathcal{D}_{yw}, \\ \tilde{C}_0 &\triangleq \mathcal{C}_e + \mathcal{D}_{eu} \mathcal{K} L_{\mathcal{K}}^{-1} \mathcal{C}_y, & \tilde{D}_0 &\triangleq \mathcal{D}_{ed} + \mathcal{D}_{eu} \mathcal{K} L_{\mathcal{K}}^{-1} \mathcal{D}_{yd}, & \tilde{D}_1 &\triangleq \mathcal{D}_{ew} + \mathcal{D}_{eu} \mathcal{K} L_{\mathcal{K}}^{-1} \mathcal{D}_{yw}, \\ \tilde{E} &\triangleq \mathcal{C}_z + \mathcal{D}_{zu} \mathcal{K} L_{\mathcal{K}}^{-1} \mathcal{C}_y, & \tilde{E}_1 &\triangleq \mathcal{D}_{zd} + \mathcal{D}_{zu} \mathcal{K} L_{\mathcal{K}}^{-1} \mathcal{D}_{yd}, & \tilde{E}_0 &\triangleq \mathcal{D}_{zw} + \mathcal{D}_{zu} \mathcal{K} L_{\mathcal{K}}^{-1} \mathcal{D}_{yw}, \end{aligned}$$

and where  $L_{\mathcal{K}} \triangleq I - \mathcal{D}_{yu} \mathcal{K}$ . Note that we assume  $\det(L_{\mathcal{K}}) \neq 0$  for all  $\mathcal{K}$  given by (8.28) to ensure the well-posedness of the feedback interconnection.

Finally, given the closed-loop system realization given by (8.34) with  $\tilde{D}_0 \equiv 0$ ,  $\tilde{D}_1 \equiv 0$ ,  $\tilde{E}_1 \equiv 0$ , and  $\tilde{E}_0 \equiv 0$ , and the multiplier realization given by

$$Z(s) \sim \left[ \begin{array}{c|c} A_m & B_m \\ \hline C_m & D_m \end{array} \right],$$

the realization of  $\hat{G}(s) \triangleq Z(s)(M^{-1} + (I + \tilde{G}_{ed}(s)M_1)^{-1}\tilde{G}_{ed}(s))$ , where  $\tilde{G}_{ed}(s)$  is the closed-loop transfer function from uncertainty inputs  $\hat{d}(t)$  to uncertainty signals  $\hat{e}(t)$ , is given by

$$\hat{G}(s) \sim \left[ \begin{array}{c|c} \hat{A} & \hat{B}_0 \\ \hline \hat{C}_0 & \hat{D}_0 \end{array} \right],$$

where

$$\hat{A} \triangleq \left[ \begin{array}{cc} \tilde{A} - \tilde{B}_0 M_1 \tilde{C}_0 & 0 \\ B_m \tilde{C}_0 & A_m \end{array} \right], \quad \hat{B}_0 \triangleq \left[ \begin{array}{c} \tilde{B}_0 \\ B_m M^{-1} \end{array} \right],$$

$$\hat{C}_0 \triangleq [ D_m \tilde{C}_0 \quad C_m ], \quad \hat{D}_0 \triangleq [ D_m M^{-1} ].$$

## 8.5. Specialization to Centralized Strictly Proper Dynamic Compensation

In order to give a more concrete illustration of the decentralized static output feedback framework, in this section we provide an example with a single uncertain block using a centralized, strictly proper dynamic controller. Specifically, consider the uncertain dynamical system

$$\dot{x}(t) = Ax(t) + Bu(t) + B_0 d(t) + D_1 w(t), \quad t \in [0, \infty), \quad (8.35)$$

$$y(t) = Cx(t) + Du(t) + F_1 d(t) + D_2 w(t), \quad (8.36)$$

$$e(t) = C_0 x(t) + F_2 u(t), \quad (8.37)$$

$$z(t) = E_1 x(t) + E_2 u(t), \quad (8.38)$$

with uncertain plant perturbations  $\Delta A = B_0 \Delta C_0$ ,  $\Delta B = B_0 \Delta F_2$ ,  $\Delta C = F_1 \Delta C_0$ ,  $\Delta D = F_1 \Delta F_2$ , of the nominal system matrices  $(A, B, C, D)$ .

The dynamics of the centralized, strictly proper controller are given by

$$\dot{x}_c(t) = A_c x_c(t) + B_c y(t), \quad t \in [0, \infty), \quad (8.39)$$

$$u(t) = C_c x_c(t), \quad (8.40)$$

so that the closed-loop system can be written as

$$\dot{\tilde{x}}(t) = \tilde{A}\tilde{x}(t) + \tilde{B}_0d(t) + \tilde{D}w(t), \quad t \in [0, \infty), \quad (8.41)$$

$$e(t) = \tilde{C}_0\tilde{x}(t), \quad (8.42)$$

$$z(t) = \tilde{E}\tilde{x}(t), \quad (8.43)$$

where

$$\tilde{x}(t) \triangleq \begin{bmatrix} x(t) \\ x_c(t) \end{bmatrix}, \quad \tilde{A} \triangleq \begin{bmatrix} A & BC_c \\ B_cC & A_c + B_cDC_c \end{bmatrix}, \quad \tilde{B}_0 \triangleq \begin{bmatrix} B_0 \\ B_cF_1 \end{bmatrix}, \quad \tilde{D} \triangleq \begin{bmatrix} D_1 \\ B_cD_2 \end{bmatrix},$$

$$\tilde{C}_0 \triangleq [C_0 \quad F_2C_c], \quad \tilde{E} \triangleq [E_1 \quad E_2C_c].$$

Writing this system in the decentralized static output feedback framework, we obtain

$$\dot{\tilde{x}}(t) = \mathcal{A}\tilde{x}(t) + \sum_{j=1}^3 \mathcal{B}_{u_j}u_j(t) + \mathcal{B}_d d(t) + \mathcal{B}_w w(t), \quad t \in [0, \infty), \quad (8.44)$$

$$y_i(t) = \mathcal{C}_{y_i}\tilde{x}(t) + \sum_{j=1}^3 \mathcal{D}_{y_{u_{ij}}}u_j(t) + \mathcal{D}_{y_d}d(t) + \mathcal{D}_{y_w}w(t), \quad i = 1, 2, 3, \quad (8.45)$$

$$e(t) = \mathcal{C}_e\tilde{x}(t) + \sum_{j=1}^3 \mathcal{D}_{e_{u_j}}u_j(t), \quad (8.46)$$

$$z(t) = \mathcal{C}_z\tilde{x}(t) + \sum_{j=1}^3 \mathcal{D}_{z_{u_j}}u_j(t), \quad (8.47)$$

and

$$u_1(t) = A_c y_1(t), \quad u_2(t) = B_c y_2(t), \quad u_3(t) = C_c y_3(t),$$

where

$$\mathcal{A} \triangleq \begin{bmatrix} A & 0 \\ 0 & 0 \end{bmatrix}, \quad \mathcal{B}_{u_1} \triangleq \begin{bmatrix} 0 \\ I_{n_c} \end{bmatrix}, \quad \mathcal{B}_{u_2} \triangleq \begin{bmatrix} 0 \\ I_{n_c} \end{bmatrix}, \quad \mathcal{B}_{u_3} \triangleq \begin{bmatrix} B \\ 0 \end{bmatrix}, \quad \mathcal{B}_d \triangleq \begin{bmatrix} B_0 \\ 0 \end{bmatrix}, \quad \mathcal{B}_w \triangleq \begin{bmatrix} D_1 \\ 0 \end{bmatrix},$$

$$\mathcal{C}_{y_1} \triangleq [0 \quad I_{n_c}], \quad \mathcal{D}_{y_{u_{11}}} \triangleq 0, \quad \mathcal{D}_{y_{u_{12}}} \triangleq 0, \quad \mathcal{D}_{y_{u_{13}}} \triangleq 0, \quad \mathcal{D}_{y_{d_1}} \triangleq 0, \quad \mathcal{D}_{y_{w_1}} \triangleq 0,$$

$$\mathcal{C}_{y_2} \triangleq [C \quad 0], \quad \mathcal{D}_{y_{u_{21}}} \triangleq 0, \quad \mathcal{D}_{y_{u_{22}}} \triangleq 0, \quad \mathcal{D}_{y_{u_{23}}} \triangleq D, \quad \mathcal{D}_{y_{d_2}} \triangleq F_1, \quad \mathcal{D}_{y_{w_2}} \triangleq D_2,$$

$$\mathcal{C}_{y_3} \triangleq [0 \quad I_{n_c}], \quad \mathcal{D}_{y_{u_{31}}} \triangleq 0, \quad \mathcal{D}_{y_{u_{32}}} \triangleq 0, \quad \mathcal{D}_{y_{u_{33}}} \triangleq 0, \quad \mathcal{D}_{y_{d_3}} \triangleq 0, \quad \mathcal{D}_{y_{w_3}} \triangleq 0,$$

$$\mathcal{C}_e \triangleq [C_0 \quad 0], \quad \mathcal{D}_{e_{u_1}} \triangleq 0, \quad \mathcal{D}_{e_{u_2}} \triangleq 0, \quad \mathcal{D}_{e_{u_3}} \triangleq F_2,$$

$$\mathcal{C}_z \triangleq [E_1 \quad 0], \quad \mathcal{D}_{z_{u_1}} \triangleq 0, \quad \mathcal{D}_{z_{u_2}} \triangleq 0, \quad \mathcal{D}_{z_{u_3}} \triangleq E_2.$$

Next, defining

$$\hat{u}(t) \triangleq \begin{bmatrix} u_1(t) \\ u_2(t) \\ u_3(t) \end{bmatrix}, \quad \hat{y}(t) \triangleq \begin{bmatrix} y_1(t) \\ y_2(t) \\ y_3(t) \end{bmatrix},$$

$$\begin{aligned} \mathcal{B}_u &\triangleq [\mathcal{B}_{u1} \ \mathcal{B}_{u2} \ \mathcal{B}_{u3}], \quad \mathcal{D}_{eu} \triangleq [\mathcal{D}_{eu1} \ \mathcal{D}_{eu2} \ \mathcal{D}_{eu3}], \quad \mathcal{D}_{zu} \triangleq [\mathcal{D}_{zu1} \ \mathcal{D}_{zu2} \ \mathcal{D}_{zu3}], \\ \mathcal{C}_y &\triangleq \begin{bmatrix} \mathcal{C}_{y1} \\ \mathcal{C}_{y2} \\ \mathcal{C}_{y3} \end{bmatrix}, \quad \mathcal{D}_{yu} \triangleq \begin{bmatrix} \mathcal{D}_{yu11} & \mathcal{D}_{yu12} & \mathcal{D}_{yu13} \\ \mathcal{D}_{yu21} & \mathcal{D}_{yu22} & \mathcal{D}_{yu23} \\ \mathcal{D}_{yu31} & \mathcal{D}_{yu32} & \mathcal{D}_{yu33} \end{bmatrix}, \quad \mathcal{D}_{yd} \triangleq \begin{bmatrix} \mathcal{D}_{yd1} \\ \mathcal{D}_{yd2} \\ \mathcal{D}_{yd3} \end{bmatrix}, \quad \mathcal{D}_{yw} \triangleq \begin{bmatrix} \mathcal{D}_{yw1} \\ \mathcal{D}_{yw2} \\ \mathcal{D}_{yw3} \end{bmatrix}, \end{aligned}$$

and rewriting the decentralized control signals in the compact form

$$\hat{u}(t) = \mathcal{K}\hat{y}(t),$$

where

$$\mathcal{K} \triangleq \begin{bmatrix} A_c & 0 & 0 \\ 0 & B_c & 0 \\ 0 & 0 & C_c \end{bmatrix},$$

the system matrices  $\tilde{A}$ ,  $\tilde{B}_0$ ,  $\tilde{D}$ ,  $\tilde{C}_0$ , and  $\tilde{E}$  in the closed-loop dynamics

$$\dot{\tilde{x}}(t) = \tilde{A}\tilde{x}(t) + \tilde{B}_0d(t) + \tilde{D}w(t), \quad t \in [0, \infty), \quad (8.48)$$

$$e(t) = \tilde{C}_0\tilde{x}(t), \quad (8.49)$$

$$z(t) = \tilde{E}\tilde{x}(t), \quad (8.50)$$

can now be written as

$$\begin{aligned} \tilde{A} &= \mathcal{A} + \mathcal{B}_u\mathcal{K}L_{\mathcal{K}}^{-1}\mathcal{C}_y = \begin{bmatrix} A & BC_c \\ B_cC & A_c + B_cDC_c \end{bmatrix}, \\ \tilde{B}_0 &= \mathcal{B}_w + \mathcal{B}_u\mathcal{K}L_{\mathcal{K}}^{-1}\mathcal{D}_{yw} = \begin{bmatrix} B_0 \\ B_cF_1 \end{bmatrix}, \\ \tilde{D} &= \mathcal{B}_w + \mathcal{B}_u\mathcal{K}L_{\mathcal{K}}^{-1}\mathcal{D}_{yw} = \begin{bmatrix} D_1 \\ B_cD_2 \end{bmatrix}, \\ \tilde{C}_0 &= \mathcal{C}_z + \mathcal{D}_{zu}\mathcal{K}L_{\mathcal{K}}^{-1}\mathcal{C}_y = [C_0 \ F_2C_c], \\ \tilde{E} &= \mathcal{C}_z + \mathcal{D}_{zu}\mathcal{K}L_{\mathcal{K}}^{-1}\mathcal{C}_y = [E_1 \ E_2C_c]. \end{aligned}$$

Furthermore, closing the uncertainty loop from  $d(t)$  to  $e(t)$  yields the closed-loop realization

$$\tilde{G}_{\Delta}(s) \sim \left[ \frac{\tilde{A} + \tilde{B}_0\Delta\tilde{C}_0}{\tilde{E}} \middle| \frac{\tilde{D}}{0} \right].$$

## 8.6. Robust Stability and Performance

In this section we present sufficient conditions for robust stability of the feedback system given in Figure 8.1 and a robust  $\mathcal{H}_2$  performance bound for  $\|\tilde{G}_{zw}(s)\|_2^2$ . Specifically, the following theorem provides a sufficient condition for ensuring that  $Z(s)[M^{-1} + [I + \tilde{G}_{ed}(s)M_1]^{-1}\tilde{G}_{ed}(s)]$  is strongly positive real [48], as well as providing a robust performance bound for  $\|\tilde{G}_{zw}(s)\|_2^2$ . For the statement of the next theorem define the notation

$$\hat{E} \triangleq \begin{bmatrix} \tilde{E} & 0 \end{bmatrix}, \quad \hat{D} \triangleq \begin{bmatrix} \tilde{D} \\ 0 \end{bmatrix},$$

and recall the definition for a strongly positive real transfer function [48].

**Theorem 8.2.** Suppose there exists  $\hat{P} \in \mathbb{N}^{\hat{n}+n_m}$  satisfying

$$0 = \hat{A}^T \hat{P} + \hat{P} \hat{A} + (\hat{B}_0^T \hat{P} - \hat{C}_0)(\hat{D}_0 + \hat{D}_0^T)^{-1}(\hat{B}_0^T \hat{P} - \hat{C}_0)^T + \hat{E}^T \hat{E}. \quad (8.51)$$

Then  $Z(s)[M^{-1} + [I + \tilde{G}_{ed}(s)M_1]^{-1}\tilde{G}_{ed}(s)]$  is strongly positive real. Consequently, the feedback interconnection of  $G(s)$  and  $\Delta$  is asymptotically stable for all  $\Delta \in \Delta$ . Furthermore,

$$\|\tilde{G}_{zw}(s)\|_2^2 \leq \text{tr } \hat{P} \hat{D} \hat{D}^T. \quad (8.52)$$

To apply Theorem 8.2 to controller synthesis, we use the modified Riccati equation (8.51) to guarantee that the closed-loop system is robustly stable. This leads to the following optimization problem.

**Optimization Problem.** Determine gain matrices  $\mathcal{K} \in \mathbb{R}^{\sum_{i=1}^g r_i \times \sum_{i=1}^g c_i}$  and  $\mathcal{K}_m \in \mathbb{R}^{(n_m+v) \times (n_m+v)}$  that minimize

$$\mathcal{J}(\mathcal{K}, \mathcal{K}_m) \triangleq \text{tr } \hat{P} \hat{D} \hat{D}^T, \quad (8.53)$$

where  $\hat{P} \in \mathbb{N}^{\hat{n}}$  satisfies (8.51), and where  $\hat{n} \triangleq \tilde{n} + n_m$ .

## 8.7. Sufficient Conditions for Fixed-Order Robust Compensation with Dynamic Multipliers

In this section we state sufficient conditions for characterizing dynamic output feedback controllers and dynamic stability multipliers guaranteeing robust stability and robust  $\mathcal{H}_2$  performance. For the statement of the next theorem, partition the matrices  $\hat{P}$  and  $\hat{Q}$  as

$$\hat{P} = \begin{bmatrix} P_{11} & P_{12} \\ P_{12}^T & P_{22} \end{bmatrix}, \quad \hat{Q} = \begin{bmatrix} Q_{11} & Q_{12} \\ Q_{12}^T & Q_{22} \end{bmatrix},$$

where  $P_{11}, Q_{11} \in \mathbb{N}^{\hat{n}}$  and  $P_{22}, Q_{22} \in \mathbb{N}^{m}$ , and define

$$Q_{L_{ij}} \triangleq \begin{bmatrix} 0_{r_1 \phi_1 \times r_i} \\ 0_{r_2 \phi_2 \times r_i} \\ \vdots \\ 0_{r_{i-1} \phi_{i-1} \times r_i} \\ 0_{r_i(j-1) \times r_i} \\ I_{r_i} \\ 0_{r_i(\phi_i-j) \times r_i} \\ 0_{r_{i+1} \phi_{i+1} \times r_i} \\ \vdots \\ 0_{r_v \phi_v \times r_i} \end{bmatrix}, \quad Q_{R_{ij}} \triangleq \begin{bmatrix} 0_{c_1 \phi_1 \times c_i} \\ 0_{c_2 \phi_2 \times c_i} \\ \vdots \\ 0_{c_{i-1} \phi_{i-1} \times c_i} \\ 0_{c_i(j-1) \times c_i} \\ I_{c_i} \\ 0_{c_i(\phi_i-j) \times c_i} \\ 0_{c_{i+1} \phi_{i+1} \times c_i} \\ \vdots \\ 0_{c_v \phi_v \times c_i} \end{bmatrix}^T, \quad (8.54)$$

where  $r_i$  and  $c_i$  are the dimensions of the  $i^{\text{th}}$  controller gain,  $\mathcal{K}_i \in \mathbb{R}^{r_i \times c_i}$ ,  $i = 1, \dots, v$ , and  $j = 1, \dots, \phi_i$ .

**Theorem 8.3.** Suppose there exists  $\hat{n} \times \hat{n}$  nonnegative definite matrices  $\hat{P}$  and  $\hat{Q}$  satisfying

$$0 = \hat{A}^T \hat{P} + \hat{P} \hat{A} + (\hat{B}_0^T \hat{P} - \hat{C}_0)(\hat{D}_0 + \hat{D}_0^T)^{-1}(\hat{B}_0^T \hat{P} - \hat{C}_0)^T + \hat{E}^T \hat{E}, \quad (8.55)$$

$$0 = \left( \hat{A} - \hat{B}_0(\hat{D}_0 + \hat{D}_0^T)^{-1}(\hat{B}_0^T \hat{P} - \hat{C}_0) \right) \hat{Q} + \hat{Q} \left( \hat{A} - \hat{B}_0(\hat{D}_0 + \hat{D}_0^T)^{-1}(\hat{B}_0^T \hat{P} - \hat{C}_0) \right)^T + \hat{D} \hat{D}^T, \quad (8.56)$$

and let  $\mathcal{K}_i$  satisfy

$$0 = 2 \sum_{j=1}^{\phi_i} Q_{L_{ij}}^T (I + \mathcal{D}_{yu}^T L_{\mathcal{K}}^{-T} \mathcal{K}^T) \left[ \mathcal{B}_u^T (P_1 Q_1 + P_{12} Q_{12}^T) (C_y^T - \tilde{C}_0^T M_1 \mathcal{D}_{yd}^T) + \mathcal{B}_u^T P_1 \tilde{B}_w \mathcal{D}_{yw}^T \right]$$

$$\begin{aligned}
& +\mathcal{D}_{zu}^T \tilde{C}_z Q_1 C_y^T + \mathcal{D}_{eu}^T [B_m^T (P_{12}^T Q_1 + P_2 Q_{12}^T) - M_1 \tilde{B}_d^T (P_1 Q_1 + P_{12} Q_{12}^T)] C_y^T \\
& + B_u^T [(P_1 Q_1 + P_{12} Q_{12}^T) (P_1 \tilde{B}_d + P_{12} B_m M^{-1} - \tilde{C}_e^T D_m) \\
& \quad + (P_1 Q_{12} + P_{12} Q_2) (P_{12}^T \tilde{B}_d + P_2 B_m M^{-1} - C_m^T)] (D_m M^{-1} + M^{-1} D_m)^{-1} \mathcal{D}_{yd}^T \\
& - \mathcal{D}_{eu}^T D_m (D_m M^{-1} + M^{-1} D_m)^{-1} [(P_1 \tilde{B}_d + P_{12} B_m M^{-1} - \tilde{C}_e^T D_m)^T Q_1 \\
& \quad + (P_{12}^T \tilde{B}_d + P_2 B_m M^{-1} - C_m^T)^T Q_{12}^T] C_y^T \Big] L_{\mathcal{K}}^{-T} Q_{R_{ij}}^T. \tag{8.57}
\end{aligned}$$

Furthermore, let  $\mathcal{K}_m$  satisfy

$$\begin{aligned}
0 = & \text{diag}\{2A_{mL}^T (P_{12}^T Q_{12} + P_2 Q_2) A_{mR}^T \\
& - 2C_{mL}^T (D_m M^{-1} + M^{-1} D_m)^{-1} (T_1^T Q_{12} + T_2^T Q_2) C_{mR}^T \\
& - 2D_{mL}^T (D_m M^{-1} + M^{-1} D_m)^{-1} (T_1^T Q_1 + T_2^T Q_{12}^T) \tilde{C}_e^T D_{mR}^T \\
& - D_{mL}^T (D_m M^{-1} + M^{-1} D_m)^{-1} (M^{-1} T_1^T Q_1 T_1 + T_1^T Q_1 T_1 M^{-1} \\
& \quad + M^{-1} T_2^T Q_2 T_2 + T_2^T Q_2 T_2 M^{-1} + 2M^{-1} T_1^T Q_{12} T_2 + 2T_2^T Q_{12}^T T_1 M^{-1}) \\
& \cdot (D_m M^{-1} + M^{-1} D_m)^{-1} D_{mR}^T\}, \tag{8.58}
\end{aligned}$$

where

$$T_1 \triangleq P_1 \tilde{B}_d + P_{12} B_m M^{-1} - \tilde{C}_e^T D_m, \quad T_2 \triangleq P_{12}^T \tilde{B}_d + P_2 B_m M^{-1} - C_m^T.$$

Then  $Z(s)[M^{-1} + [I + \tilde{G}_{ed}(s)M_1]^{-1}\tilde{G}_{ed}(s)]$  is strongly positive real. Thus the closed-loop system from  $w(t)$  to  $z(t)$  is asymptotically stable for all  $\Delta \in \Delta$ . Furthermore, the worst-case  $\mathcal{H}_2$  performance of the closed-loop system satisfies the bound

$$\|\tilde{G}_{zw}(s)\|_2^2 \leq \text{tr } \hat{P} \hat{D} \hat{D}^T. \tag{8.59}$$

**Proof.** First we obtain necessary conditions for the Optimization Problem and then show, by construction, that these conditions serve as sufficient conditions for closed-loop stability and robust  $\mathcal{H}_2$  performance. Thus, to optimize (8.53) subject to

(8.51), form the Lagrangian

$$\mathcal{L}(\mathcal{K}, \mathcal{K}_m, \hat{Q}, \lambda) \triangleq \text{tr} \left[ \lambda \hat{P} \hat{D} \hat{D}^T + \hat{Q} \left( \hat{A}^T \hat{P} + \hat{P} \hat{A} \right. \right. \\ \left. \left. + (\hat{B}_0^T \hat{P} - \hat{C}_0)(\hat{D}_0 + \hat{D}_0^T)^{-1}(\hat{B}_0^T \hat{P} - \hat{C}_0)^T + \hat{E}^T \hat{E} \right) \right],$$

where the Lagrange multipliers  $\lambda \geq 0$  and  $\hat{Q} \in \mathbb{R}^{\hat{n} \times \hat{n}}$  are not both zero. By viewing  $\mathcal{K}$ ,  $\mathcal{K}_m$ , and  $\hat{P}$  as independent variables, we obtain

$$\frac{\partial \mathcal{L}}{\partial \hat{P}} = \left( \hat{A} - \hat{B}_0(\hat{D}_0 + \hat{D}_0^T)^{-1}(\hat{B}_0^T \hat{P} - \hat{C}_0) \right) \hat{Q} \\ + \hat{Q} \left( \hat{A} - \hat{B}_0(\hat{D}_0 + \hat{D}_0^T)^{-1}(\hat{B}_0^T \hat{P} - \hat{C}_0) \right)^T + \lambda \hat{D} \hat{D}^T. \quad (8.60)$$

If  $\left( \hat{A} - \hat{B}_0(\hat{D}_0 + \hat{D}_0^T)^{-1}(\hat{B}_0^T \hat{P} - \hat{C}_0) \right)$  is Hurwitz, then  $\lambda = 0$  implies  $\hat{Q} = 0$ . Hence, it can be assumed without loss of generality that  $\lambda = 1$ . Furthermore, note that  $\hat{Q}$  is nonnegative definite. Thus the stationary conditions with  $\lambda = 1$  are given by

$$\frac{\partial \mathcal{L}}{\partial \hat{P}} = \left( \hat{A} - \hat{B}_0(\hat{D}_0 + \hat{D}_0^T)^{-1}(\hat{B}_0^T \hat{P} - \hat{C}_0) \right) \hat{Q} \\ + \hat{Q} \left( \hat{A} - \hat{B}_0(\hat{D}_0 + \hat{D}_0^T)^{-1}(\hat{B}_0^T \hat{P} - \hat{C}_0) \right)^T + \hat{D} \hat{D}^T = 0, \\ \frac{\partial \mathcal{L}}{\partial \mathcal{K}_i} = 2 \sum_{j=1}^{\phi_i} Q_{Lij}^T \left( I + \mathcal{D}_{yu}^T L_{\mathcal{K}}^{-T} \mathcal{K}^T \right) \left[ \mathcal{B}_u^T (P_1 Q_1 + P_{12} Q_{12}^T) (\mathcal{C}_y^T - \tilde{C}_0^T M_1 \mathcal{D}_{yd}^T) \right. \\ \left. + \mathcal{B}_u^T P_1 \tilde{B}_w \mathcal{D}_{yw}^T + \mathcal{D}_{zu}^T \tilde{C}_z Q_1 \mathcal{C}_y^T + \mathcal{D}_{eu}^T [B_m^T (P_{12}^T Q_1 + P_2 Q_{12}^T) \right. \\ \left. - M_1 \tilde{B}_d^T (P_1 Q_1 + P_{12} Q_{12}^T)] \mathcal{C}_y^T + \mathcal{B}_u^T [(P_1 Q_1 + P_{12} Q_{12}^T) (P_1 \tilde{B}_d + P_{12} B_m M^{-1} - \tilde{C}_e^T D_m) \right. \\ \left. + (P_1 Q_{12} + P_{12} Q_2) (P_{12}^T \tilde{B}_d + P_2 B_m M^{-1} - C_m^T)] (D_m M^{-1} + M^{-1} D_m)^{-1} \mathcal{D}_{yd}^T \right. \\ \left. - \mathcal{D}_{eu}^T D_m (D_m M^{-1} + M^{-1} D_m)^{-1} [(P_1 \tilde{B}_d + P_{12} B_m M^{-1} - \tilde{C}_e^T D_m)^T Q_1 \right. \\ \left. + (P_{12}^T \tilde{B}_d + P_2 B_m M^{-1} - C_m^T)^T Q_{12}^T] \mathcal{C}_y^T \right] L_{\mathcal{K}}^{-T} Q_{Rij}^T = 0, \\ \frac{\partial \mathcal{L}}{\partial \mathcal{K}_m} = \text{diag} \{ 2 A_{mL}^T (P_{12}^T Q_{12} + P_2 Q_2) A_{mR}^T \\ - 2 C_{mL}^T (D_m M^{-1} + M^{-1} D_m)^{-1} (T_1^T Q_{12} + T_2^T Q_2) C_{mR}^T \\ - 2 D_{mL}^T (D_m M^{-1} + M^{-1} D_m)^{-1} (T_1^T Q_1 + T_2^T Q_{12}^T) \tilde{C}_e^T D_{mR}^T \}$$

$$\begin{aligned}
& -D_{\text{mL}}^{\text{T}}(D_{\text{m}}M^{-1} + M^{-1}D_{\text{m}})^{-1} (M^{-1}T_1^{\text{T}}Q_1T_1 + T_1^{\text{T}}Q_1T_1M^{-1} \\
& + M^{-1}T_2^{\text{T}}Q_2T_2 + T_2^{\text{T}}Q_2T_2M^{-1} + 2M^{-1}T_1^{\text{T}}Q_{12}T_2 + 2T_2^{\text{T}}Q_{12}^{\text{T}}T_1M^{-1}) \\
& \cdot (D_{\text{m}}M^{-1} + M^{-1}D_{\text{m}})^{-1}D_{\text{mR}}^{\text{T}}\} = 0,
\end{aligned}$$

which are equivalent to (8.56)–(8.58). Equation (8.55) is a restatement of (8.51). It now follows from Theorem 8.2 that if  $Z(s)[M^{-1} + [I + \tilde{G}_{ed}(s)M_1]^{-1}\tilde{G}_{ed}(s)]$  is positive real then  $\hat{A} + \hat{B}_0\Delta\hat{C}_0$  is asymptotically stable for all  $\Delta \in \Delta$ . Finally, the  $\mathcal{H}_2$  performance bound (8.59) is a restatement of (8.53).  $\square$

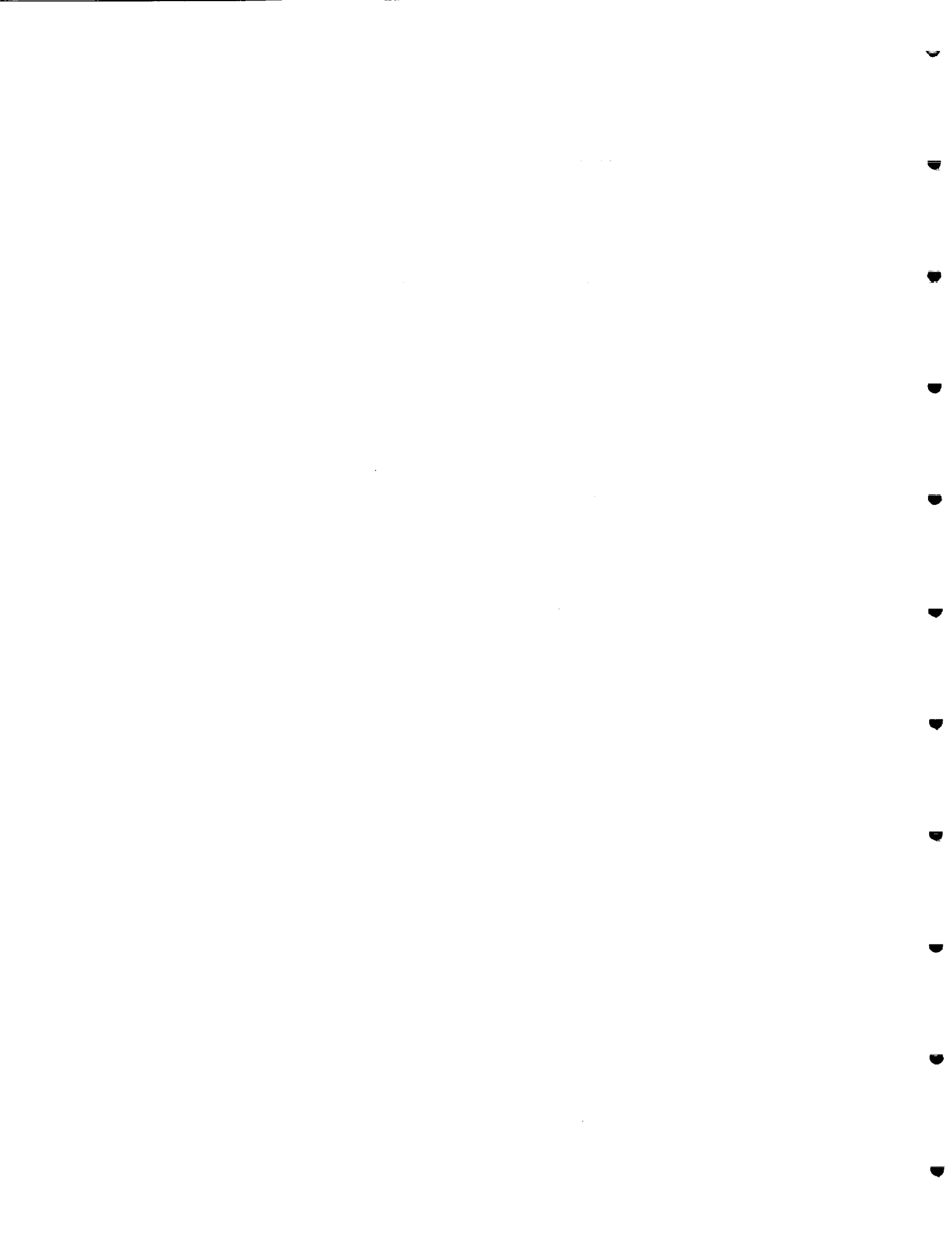
Equations (8.55)–(8.58) provide constructive sufficient conditions that yield dynamic controllers for robust fixed-order (i.e., full- and reduced-order) output feedback compensation. By using these equations within a numerical optimization algorithm, the optimal robust fixed-order controllers and stability multipliers can be determined *simultaneously*, thus avoiding  $D$ ,  $N - K$  iterations.

## 8.8. Quasi-Newton Optimization Algorithm

A general-purpose BFGS quasi-Newton algorithm [26] can be used to calculate the controller gains and the stability matrices, as described in Section 2.3. One requirement of gradient-based optimization algorithms is an initial stabilizing design. For full-order controller design, the algorithm can be initialized with an LQG controller, while for reduced-order control, the algorithm can be initialized with a balanced truncation of an LQG controller. Small values should be chosen for  $M_1$  and  $M_2$  so that the design equations (8.55) and (8.56) can be solved. The quasi-Newton optimization algorithm can then be used to find the controller gains  $A_c$ ,  $B_c$ , and  $C_c$  and the multiplier gains  $A_m$ ,  $B_m$ ,  $C_m$  and  $D_m$ . After each iteration,  $M_1$  and  $M_2$  are increased and the current values of the controller gains ( $A_c, B_c, C_c$ ) and multiplier gains ( $A_m, B_m, C_m, D_m$ ) are then used as the starting point for the next iteration.

## 8.9. Conclusion

This chapter used the absolute stability results of [53] to obtain fixed-structure controllers and fixed-order stability multipliers which provide robust stability and performance. By satisfying certain commutability properties with the uncertainty set, the stability multipliers designed by the robust controller synthesis technique proposed here permit the treatment of fully populated real and complex uncertain blocks which may, in addition, possess internal structure. Hence, tailoring the multipliers to the structure of the uncertainty not only leads to the ability to address more general uncertainty characterizations but can also lead to less conservative controllers than obtained from the standard mixed- $\mu$  synthesis techniques. Furthermore, since the numerical optimization routine optimizes over the free parameters in the controller and the stability multipliers *simultaneously*, this methodology avoids the  $D, N - K$  iterations of standard mixed- $\mu$  synthesis techniques.



# CHAPTER 9

## Concluding Remarks and Recommendations for Future Research

### 9.1. Conclusions

In this report, we introduced a decentralized static output feedback framework for fixed-structure dynamic controller synthesis. As a special case of this framework, we showed how a centralized dynamic output feedback control problem can be transformed to a decentralized static output feedback form. By using this format, a numerical optimization scheme can be used to optimize the controller gains with respect to a given cost function and constraint equation. Furthermore, we demonstrated its effectiveness on the ACTEX flight experiment.

Next, we used the decentralized static output feedback framework to synthesize stable  $\mathcal{H}_2$ -optimal controllers by including the  $\mathcal{H}_2$  cost of the controller in the Lagrangian and using a multiobjective optimization technique. It was numerically shown that for some systems, namely minimum phase, open-loop unstable or non-minimum phase, open-loop stable plants, a stable controller can rival the performance of an unstable  $\mathcal{H}_2$ -optimal LQG controller and yet not be constrained by the loop margins of unstable controllers. For other systems, however, there could be a significant

degradation in performance by requiring the controller to remain stable, although this technique provided controllers yielding the minimal  $\mathcal{H}_2$  closed-loop cost for all stable linear controllers.

By exploiting the ability of the decentralized static output feedback framework to *a priori* fix the structure of the controller, we were able to synthesize  $\mathcal{H}_2$ -optimal relative degree two controllers. This was accomplished by cascading two strictly proper dynamic controllers in the feedback loop and optimizing over the free controller parameters. It was shown that constraining the controller to have a relative degree of at least two only marginally increased the  $\mathcal{H}_2$  cost of the closed-loop system, though it was noted that changing the order of the separate cascaded controllers in the feedback loop does significantly affect the  $\mathcal{H}_2$  cost of the closed-loop system and the natural frequencies and break frequencies of the controller dynamics.

Next we focused on robust control by extending the implicit small gain guaranteed cost bound [54] to controller synthesis. Specifically, the implicit small gain guaranteed cost bound was used to address the problem of robust stability and  $\mathcal{H}_2$  performance via fixed-order dynamic compensation, and a quasi-Newton optimization algorithm was used to solve the coupled nonlinear design equations.

We then extended the robust fixed-structure guaranteed cost controller synthesis framework to synthesize robust resilient controllers, or controllers which are robust in the face of system parametric uncertainty *and* variations in the controller gains themselves. Specifically, the guaranteed cost approach of [10] and [13] was used to develop sufficient conditions for robust stability and  $\mathcal{H}_2$  performance via fixed-order dynamic compensation.

The robust fixed-structure control framework was then used to develop linear, fixed-order (i.e., full- and reduced-order) pressure rise feedback dynamic compensators for axial flow compression systems. Unlike the nonlinear bifurcation-based and

backstepping controllers proposed in the literature, the proposed dynamic compensator framework explicitly accounts for compressor performance versus sensor noise, compressor performance versus controller order, and compressor performance versus disturbance rejection. Furthermore, the proposed pressure rise feedback controllers provide a considerable simplification in the sensing architecture required for controlling rotating stall and surge.

Finally, we used the absolute stability results of [53] to obtain fixed-structure controllers and fixed-order stability multipliers which provide robust stability and performance. By tailoring the multipliers to the structure of the uncertainty, we could permit the treatment of fully populated real and complex uncertain blocks which may, in addition, possess internal structure. This not only leads to the ability to address more general uncertainty characterizations but can also lead to less conservative controllers than obtained from the standard mixed- $\mu$  synthesis techniques. Furthermore, by using a numerical optimization routine, we could optimize over the free parameters in the controller and the stability multipliers *simultaneously*, thus avoiding the  $D, N - K$  iterations of standard mixed- $\mu$  synthesis techniques.

## 9.2. Recommendations for Future Research

The decentralized static output feedback formulation and the quasi-Newton optimization algorithm discussed in Chapter 2 are programmed into a MATLAB toolbox [35]. However, in its present form, it is not the most user-friendly program, and making it easier to use would most likely spread its use. Also, as it now stands, the quasi-Newton optimization algorithm has only one search method. Adding routines such as “double dog-leg” searches or locally constrained optimal “hook” steps [26] to the Armijo-type routine already programmed would enhance the robustness of the

optimization routine. Furthermore, adding numerical gradient computations instead of relying solely on analytical gradient computations will extend the range of the problems the routine will be able to solve.

In Chapter 4, we designed controllers with a minimum guaranteed (vector) relative degree of two. However, the theory itself is very general, and we can use the same formulation to design controllers of (vector) relative degree  $r$ . Furthermore, the methodology used to obtain relative degree two controllers was solely based on the structure of the controllers, and was not constrained to a particular notion of optimality. In Chapter 4, we designed  $\mathcal{H}_2$ -optimal controllers, but we could just as easily design  $\mathcal{H}_\infty$ -optimal (vector) relative degree two or even relative degree two robust controllers.

In Chapter 5, robustness was guaranteed by bounding the effects of the uncertain terms in the Lyapunov equation. However, this was just one particular bound, and it may not be the best bound for certain applications. Further work may be able to find new bounds which can reduce conservatism and therefore give better performance for particular problems.

As noted in Chapter 6, almost *all* robust control theory available in the literature address either the issue of (structured or unstructured) plant uncertainty or the issue of uncertain exogenous disturbance rejection. However, the stability of closed-loop systems could be very sensitive to numerical errors in the controller gains themselves. Hence, an important issue in robust control should be the robustness of compensators with respect to implementation errors arising from floating point accuracy in the processor. While we presented bounds to deal with controller gain variations for linear control problems, extending the results of Chapter 6 to address the robustness of nonlinear compensators is of utmost importance and remains essentially an untapped area of future research.

The general fixed-structure positive real stability multipliers developed for real parameter uncertainty in Chapter 8 are structured to handle real block uncertainty, but the diagonal structure of  $Z(s)$  is not the most general form for the case of repeated uncertainties. For example, if the uncertainty matrix is

$$\Delta = \begin{bmatrix} \delta_1 & 0 & 0 & 0 \\ 0 & \delta_1 & 0 & 0 \\ 0 & 0 & \delta_2 & 0 \\ 0 & 0 & 0 & \delta_2 \end{bmatrix},$$

then the commutative property  $\Delta D(s) = D(s)\Delta$  will hold for a multiplier of the form

$$D(s) = \begin{bmatrix} d_{11}(s) & d_{12}(s) & 0 & 0 \\ d_{12}(s) & d_{13}(s) & 0 & 0 \\ 0 & 0 & d_{21}(s) & d_{22}(s) \\ 0 & 0 & d_{22}(s) & d_{23}(s) \end{bmatrix}.$$

Similarly, a generalization of the structure of  $N(s)$  can be made which will result in a nondiagonal multiplier which will still satisfy the condition  $N(s)\Delta = \Delta^*N(s)$ . Further work on this problem can generalize the multiplier structure to handle such a case. Furthermore, this structure for the multiplier  $Z(s)$  only allows us to consider *realizable* multipliers. However, this precludes us from considering the famous Popov multiplier,  $Z(s) = I + Ns$ . When using the Popov multiplier, one must assume that  $(I + Ns)G_s(s)$  is realizable, where  $G_s(s) = M^{-1} + (I + \tilde{G}_{ed}(s)M_1)\tilde{G}_{ed}(s)$ . Thus, instead of assuming that  $Z(s)$  is realizable, we can take

$$Z(s) = D_r(s) - sN_r(s) + sD_1 + s^2D_2 + \dots + s^rD_r - sN_1 - s^2N_2 - \dots - s^rN_r,$$

where  $D_r(s)$  and  $N_r(s)$  are the realizable portions of the multipliers,  $D_i$  and  $N_i$  are constant matrix scales, and  $r$  is chosen such that  $s^rG_s(s)$  is realizable.

Finally, although the theory for designing linear output feedback controllers is quite mature, nonlinear *output* feedback controller synthesis remains relatively undeveloped. In numerous real world applications, system nonlinearities such as saturation, relay, deadzone, quantization, geometric and material nonlinearities require

nonlinear output feedback controllers. Furthermore, for linear plants with parametric uncertainty and nonquadratic performance criteria, nonlinear controllers exist that generate superior performance over the best linear controller. A fruitful area of research is to develop a fixed-structure controller synthesis framework for nonlinear control. The motivation for fixed-structure nonlinear control theory is to address controller synthesis within a class of candidate nonlinear feedback controller structures. Specifically, control Lyapunov functions can be used to provide a controller synthesis framework by assuring global or local asymptotic stability for an *a priori* fixed class of nonlinear feedback controllers. A specific controller within this class can now be chosen to optimize a given performance functional. Thus, this provides a constructive framework where Lyapunov theory is used to guarantee global or local asymptotic stability over a class of nonlinear feedback controllers while optimization is performed over the free controller gains so as to minimize a specific performance functional.

# Appendix

## Controller Configuration 2

For this configuration, the controller given by (2.37) can be expressed as

$$A_c = \begin{bmatrix} 0 & 1 & 0 & 0 \\ -\omega_1^2 & -0.3\omega_1 & 0 & 0 \\ 0 & 0 & 0 & 1 \\ 0 & \omega_1 & -\omega_2^2 & -0.3\omega_2 \end{bmatrix}, \quad B_c = \begin{bmatrix} 0 \\ 1 \\ 0 \\ 0 \end{bmatrix},$$
$$C_c = [0 \ 0 \ k_3\omega_2^2 \ 0].$$

Note that there are three free parameters, namely,  $\omega_1$ ,  $\omega_2$ , and  $k_3$ . Thus

$$K = \begin{bmatrix} \omega_1 & 0 & 0 \\ 0 & \omega_2 & 0 \\ 0 & 0 & k_3 \end{bmatrix},$$

and

$$K_0 = \begin{bmatrix} 0 & 1 & 0 & 0 & 0 & 0 & 0 & 0 & 0 \\ 0 & 0 & 0 & 0 & 0 & 0 & 0 & 0 & 0 \\ 0 & 0 & 0 & 1 & 0 & 0 & 0 & 0 & 0 \\ 0 & 0 & 0 & 0 & 0 & 0 & 0 & 0 & 0 \\ 0 & 0 & 0 & 0 & 0 & 0 & 0 & 0 & 0 \\ 0 & 0 & 0 & 0 & 1 & 0 & 0 & 0 & 0 \\ 0 & 0 & 0 & 0 & 0 & 0 & 0 & 0 & 0 \\ 0 & 0 & 0 & 0 & 0 & 0 & 0 & 0 & 0 \\ 0 & 0 & 0 & 0 & 0 & 0 & 0 & 0 & 0 \end{bmatrix},$$

$$L_1 = \begin{bmatrix} 0 & 0 & 0 \\ -0.3 & 0 & 0 \\ 0 & 0 & 0 \\ 1 & -0.3 & 0 \\ 0 & 0 & 0 \\ 0 & 0 & 0 \\ 0 & 0 & 0 \\ 0 & 0 & 0 \end{bmatrix}, \quad L_2 = \begin{bmatrix} 0 & 0 & 0 \\ -1 & 0 & 0 \\ 0 & 0 & 0 \\ 0 & -1 & 0 \\ 0 & 0 & 0 \\ 0 & 0 & 0 \\ 0 & 0 & 0 \\ 0 & 0 & 0 \end{bmatrix}, \quad L_3 = \begin{bmatrix} 0 & 0 & 0 \\ 0 & 0 & 0 \\ 0 & 0 & 0 \\ 0 & 0 & 0 \\ 0 & 0 & 0 \\ 0 & 0 & 0 \\ 0 & 0 & 0 \\ 0 & 1 & 0 \end{bmatrix},$$

$$R_1 = \begin{bmatrix} 0 & 0 & 0 \\ 1 & 0 & 0 \\ 0 & 0 & 0 \\ 0 & 1 & 0 \\ 0 & 0 & 0 \\ 0 & 0 & 0 \\ 0 & 0 & 0 \\ 0 & 0 & 0 \end{bmatrix}^T, \quad R_2 = \begin{bmatrix} 1 & 0 & 0 \\ 0 & 0 & 0 \\ 0 & 1 & 0 \\ 0 & 0 & 0 \\ 0 & 0 & 0 \\ 0 & 0 & 0 \\ 0 & 0 & 0 \\ 0 & 0 & 0 \end{bmatrix}^T, \quad R_3 = \begin{bmatrix} 0 & 0 & 0 \\ 0 & 0 & 0 \\ 0 & 0 & 0 \\ 0 & 0 & 0 \\ 0 & 0 & 0 \\ 0 & 0 & 0 \\ 0 & 0 & 1 \\ 0 & 0 & 0 \end{bmatrix}^T, \quad M_3 = \begin{bmatrix} 0 & 0 & 0 \\ 0 & 0 & 1 \\ 0 & 0 & 0 \end{bmatrix}.$$

### Controller Configuration 3

For this configuration, the controller given by (2.38) can be expressed as

$$A_c = \begin{bmatrix} 0 & 1 & 0 & 0 \\ -\omega_1^2 & -0.3\omega_1 & 0 & 0 \\ 0 & 0 & 0 & 1 \\ \omega_1^2 & 0 & -\omega_2^2 & -0.3\omega_2 \end{bmatrix}, \quad B_c = \begin{bmatrix} 0 \\ 1 \\ 0 \\ 0 \end{bmatrix},$$

$$C_c = [0 \ 0 \ k_3\omega_2^2 \ 0].$$

Note that there are three free parameters, namely,  $\omega_1$ ,  $\omega_2$ , and  $k_3$ . Thus

$$K = \begin{bmatrix} \omega_1 & 0 & 0 \\ 0 & \omega_2 & 0 \\ 0 & 0 & k_3 \end{bmatrix},$$

and

$$K_0 = \begin{bmatrix} 0 & 1 & 0 & 0 & 0 & 0 & 0 & 0 & 0 \\ 0 & 0 & 0 & 0 & 0 & 0 & 0 & 0 & 0 \\ 0 & 0 & 0 & 1 & 0 & 0 & 0 & 0 & 0 \\ 0 & 0 & 0 & 0 & 0 & 0 & 0 & 0 & 0 \\ 0 & 0 & 0 & 0 & 0 & 0 & 0 & 0 & 0 \\ 0 & 0 & 0 & 0 & 1 & 0 & 0 & 0 & 0 \\ 0 & 0 & 0 & 0 & 0 & 0 & 0 & 0 & 0 \\ 0 & 0 & 0 & 0 & 0 & 0 & 0 & 0 & 0 \\ 0 & 0 & 0 & 0 & 0 & 0 & 0 & 0 & 0 \end{bmatrix},$$

$$L_1 = \begin{bmatrix} 0 & 0 & 0 \\ -0.3 & 0 & 0 \\ 0 & 0 & 0 \\ 1 & -0.3 & 0 \\ 0 & 0 & 0 \\ 0 & 0 & 0 \\ 0 & 0 & 0 \\ 0 & 0 & 0 \\ 0 & 0 & 0 \end{bmatrix}, \quad L_2 = \begin{bmatrix} 0 & 0 & 0 \\ -1 & 0 & 0 \\ 0 & 0 & 0 \\ 1 & -1 & 0 \\ 0 & 0 & 0 \\ 0 & 0 & 0 \\ 0 & 0 & 0 \\ 0 & 0 & 0 \\ 0 & 0 & 0 \end{bmatrix}, \quad L_3 = \begin{bmatrix} 0 & 0 & 0 \\ 0 & 0 & 0 \\ 0 & 0 & 0 \\ 0 & 0 & 0 \\ 0 & 0 & 0 \\ 0 & 0 & 0 \\ 0 & 0 & 0 \\ 0 & 0 & 0 \\ 0 & 1 & 0 \end{bmatrix},$$

$$R_1 = \begin{bmatrix} 0 & 0 & 0 \\ 1 & 0 & 0 \\ 0 & 0 & 0 \\ 0 & 1 & 0 \\ 0 & 0 & 0 \\ 0 & 0 & 0 \\ 0 & 0 & 0 \\ 0 & 0 & 0 \\ 0 & 0 & 0 \end{bmatrix}^T, \quad R_2 = \begin{bmatrix} 1 & 0 & 0 \\ 0 & 0 & 0 \\ 0 & 1 & 0 \\ 0 & 0 & 0 \\ 0 & 0 & 0 \\ 0 & 0 & 0 \\ 0 & 0 & 0 \\ 0 & 0 & 0 \\ 0 & 0 & 0 \end{bmatrix}^T, \quad R_3 = \begin{bmatrix} 0 & 0 & 0 \\ 0 & 0 & 0 \\ 0 & 0 & 0 \\ 0 & 0 & 0 \\ 0 & 0 & 0 \\ 0 & 0 & 0 \\ 0 & 0 & 0 \\ 0 & 0 & 1 \\ 0 & 0 & 0 \end{bmatrix}^T, \quad M_3 = \begin{bmatrix} 0 & 0 & 0 \\ 0 & 0 & 1 \\ 0 & 0 & 0 \end{bmatrix}.$$

## Controller Configuration 4

For this configuration, the controller given by (2.39) can be expressed as

$$A_c = \begin{bmatrix} 0 & 1 & 0 & 0 & 0 & 0 \\ -\omega_1^2 & -0.3\omega_1 & 0 & 0 & 0 & 0 \\ 0 & 0 & 0 & 1 & 0 & 0 \\ 0 & \omega_1 & -\omega_2^2 & -0.3\omega_2 & 0 & 0 \\ 0 & 0 & 0 & 0 & 0 & 1 \\ 0 & 0 & \omega_2^2 & 0 & -\omega_3^2 & -0.3\omega_3 \end{bmatrix}, \quad B_c = \begin{bmatrix} 0 \\ 1 \\ 0 \\ 0 \\ 0 \\ 0 \end{bmatrix},$$

$$C_c = [0 \ 0 \ 0 \ 0 \ 0 \ k_3\omega_3^2 \ 0].$$

Note that there are four free parameters, namely,  $\omega_1$ ,  $\omega_2$ ,  $\omega_3$ , and  $k_3$ . Thus

$$K = \begin{bmatrix} \omega_1 & 0 & 0 & 0 \\ 0 & \omega_2 & 0 & 0 \\ 0 & 0 & \omega_3 & 0 \\ 0 & 0 & 0 & k_3 \end{bmatrix},$$

and

$$K_0 = \begin{bmatrix} 0 & 1 & 0 & 0 & 0 & 0 & 0 & 0 & 0 & 0 & 0 & 0 & 0 \\ 0 & 0 & 0 & 0 & 0 & 0 & 0 & 0 & 0 & 0 & 0 & 0 & 0 \\ 0 & 0 & 0 & 1 & 0 & 0 & 0 & 0 & 0 & 0 & 0 & 0 & 0 \\ 0 & 0 & 0 & 0 & 0 & 0 & 0 & 0 & 0 & 0 & 0 & 0 & 0 \\ 0 & 0 & 0 & 0 & 0 & 1 & 0 & 0 & 0 & 0 & 0 & 0 & 0 \\ 0 & 0 & 0 & 0 & 0 & 0 & 0 & 0 & 0 & 0 & 0 & 0 & 0 \\ 0 & 0 & 0 & 0 & 0 & 0 & 0 & 0 & 0 & 0 & 0 & 0 & 0 \\ 0 & 0 & 0 & 0 & 0 & 0 & 0 & 0 & 0 & 0 & 0 & 0 & 0 \\ 0 & 0 & 0 & 0 & 0 & 0 & 0 & 0 & 0 & 0 & 0 & 0 & 0 \\ 0 & 0 & 0 & 0 & 0 & 0 & 0 & 0 & 0 & 0 & 0 & 0 & 0 \\ 0 & 0 & 0 & 0 & 0 & 0 & 0 & 0 & 0 & 0 & 0 & 0 & 0 \\ 0 & 0 & 0 & 0 & 0 & 0 & 0 & 0 & 0 & 0 & 0 & 0 & 0 \\ 0 & 0 & 0 & 0 & 0 & 0 & 0 & 0 & 0 & 0 & 0 & 0 & 0 \end{bmatrix},$$

$$L_1 = \begin{bmatrix} 0 & 0 & 0 & 0 \\ -0.3 & 0 & 0 & 0 \\ 0 & 0 & 0 & 0 \\ 1 & -0.3 & 0 & 0 \\ 0 & 0 & 0 & 0 \\ 0 & 0 & -0.3 & 0 \\ 0 & 0 & 0 & 0 \\ 0 & 0 & 0 & 0 \\ 0 & 0 & 0 & 0 \\ 0 & 0 & 0 & 0 \\ 0 & 0 & 0 & 0 \\ 0 & 0 & 0 & 0 \\ 0 & 0 & 0 & 0 \\ 0 & 0 & 0 & 0 \end{bmatrix}, \quad L_2 = \begin{bmatrix} 0 & 0 & 0 & 0 \\ -1 & 0 & 0 & 0 \\ 0 & 0 & 0 & 0 \\ 0 & -1 & 0 & 0 \\ 0 & 0 & 0 & 0 \\ 0 & 1 & -1 & 0 \\ 0 & 0 & 0 & 0 \\ 0 & 0 & 0 & 0 \\ 0 & 0 & 0 & 0 \\ 0 & 0 & 0 & 0 \\ 0 & 0 & 0 & 0 \\ 0 & 0 & 0 & 0 \\ 0 & 0 & 0 & 0 \\ 0 & 0 & 0 & 0 \end{bmatrix}, \quad L_3 = \begin{bmatrix} 0 & 0 & 0 & 0 \\ 0 & 0 & 0 & 0 \\ 0 & 0 & 0 & 0 \\ 0 & 0 & 0 & 0 \\ 0 & 0 & 0 & 0 \\ 0 & 0 & 0 & 0 \\ 0 & 0 & 0 & 0 \\ 0 & 0 & 0 & 0 \\ 0 & 0 & 0 & 0 \\ 0 & 0 & 0 & 0 \\ 0 & 0 & 0 & 0 \\ 0 & 0 & 0 & 0 \\ 0 & 0 & 0 & 0 \\ 0 & 0 & 1 & 0 \end{bmatrix},$$

$$R_1 = \begin{bmatrix} 0 & 0 & 0 & 0 \\ 1 & 0 & 0 & 0 \\ 0 & 0 & 0 & 0 \\ 0 & 1 & 0 & 0 \\ 0 & 0 & 0 & 0 \\ 0 & 0 & 1 & 0 \\ 0 & 0 & 0 & 0 \\ 0 & 0 & 0 & 0 \\ 0 & 0 & 0 & 0 \\ 0 & 0 & 0 & 0 \\ 0 & 0 & 0 & 0 \\ 0 & 0 & 0 & 0 \\ 0 & 0 & 0 & 0 \end{bmatrix}^T, \quad R_2 = \begin{bmatrix} 1 & 0 & 0 & 0 \\ 0 & 0 & 0 & 0 \\ 0 & 1 & 0 & 0 \\ 0 & 0 & 0 & 0 \\ 0 & 0 & 1 & 0 \\ 0 & 0 & 0 & 0 \\ 0 & 0 & 0 & 0 \\ 0 & 0 & 0 & 0 \\ 0 & 0 & 0 & 0 \\ 0 & 0 & 0 & 0 \\ 0 & 0 & 0 & 0 \\ 0 & 0 & 0 & 0 \\ 0 & 0 & 0 & 0 \end{bmatrix}^T, \quad R_3 = \begin{bmatrix} 0 & 0 & 0 & 0 \\ 0 & 0 & 0 & 0 \\ 0 & 0 & 0 & 0 \\ 0 & 0 & 0 & 0 \\ 0 & 0 & 0 & 0 \\ 0 & 0 & 0 & 0 \\ 0 & 0 & 0 & 0 \\ 0 & 0 & 0 & 0 \\ 0 & 0 & 0 & 0 \\ 0 & 0 & 0 & 0 \\ 0 & 0 & 0 & 0 \\ 0 & 0 & 0 & 1 \\ 0 & 0 & 0 & 0 \end{bmatrix}^T, \quad M_3 = \begin{bmatrix} 0 & 0 & 0 & 0 \\ 0 & 0 & 0 & 0 \\ 0 & 0 & 0 & 1 \\ 0 & 0 & 0 & 0 \end{bmatrix}.$$



## References

- [1] M. A. Aizerman and F. R. Gantmacher, *Absolute Stability of Regulator Systems*. San Francisco, CA: Holden-Day, 1964.
- [2] A. Albert, "Conditions for positive and nonnegative definiteness in terms of pseudo inverse," *SIAM Journal on Control and Optimization*, vol. 17, pp. 434–440, 1969.
- [3] B. D. O. Anderson and J. B. Moore, "Algebraic structure of generalized positive real matrices," *SIAM Journal of Control*, vol. 6, pp. 615–625, 1968.
- [4] B. D. O. Anderson and J. B. Moore, *Optimal Control: Linear Quadratic Methods*. Englewood Cliffs, NJ: Prentice-Hall, 1990.
- [5] B. D. O. Anderson and S. Vongpanitlerd, *Network Analysis and Synthesis: A Modern Systems Approach*. Englewood Cliffs, NJ: Prentice-Hall, 1973.
- [6] M. Athans, "The role and use of the stochastic linear quadratic gaussian problem in control system design," *IEEE Trans. Autom. Contr.*, vol. 34, pp. 293–305, 1971.
- [7] O. O. Badmus, S. Chowdhury, and C. N. Nett, "Nonlinear control of surge in axial compression systems," *Automatica*, vol. 32, no. 1, pp. 59–70, 1996.
- [8] O. O. Badmus, C. N. Nett, and F. J. Schork, "An integrated, full-range surge control/rotating stall avoidance compressor control system," in *Proc. Amer. Contr. Conf.*, (Boston, MA), pp. 3173–3180, June 1991.
- [9] G. J. Balas, J. C. Doyle, K. Glover, A. Packard, and R. Smith,  *$\mu$ -Analysis and Synthesis Toolbox: Matlab Functions for the Analysis and Design of Robust Control Systems*. Natick, MA: The MathWorks, 1991.
- [10] D. S. Bernstein and W. M. Haddad, "The optimal projection equations with Petersen-Hollot bounds: Robust stability and performance via fixed-order dynamic compensation for systems with structured real-valued parameter uncertainty," *IEEE Trans. Autom. Contr.*, vol. 33, pp. 578–582, 1988.

- [11] D. S. Bernstein and W. M. Haddad, "LQG control with an  $\mathcal{H}_\infty$  performance bound: A Riccati equation approach," *IEEE Trans. Autom. Contr.*, vol. 34, pp. 293–305, 1989.
- [12] D. S. Bernstein and W. M. Haddad, "Robust stability and performance analysis for state space systems via quadratic Lyapunov functions," *SIAM Journal of Matrix Analysis and Applications*, vol. 11, pp. 239–271, 1990.
- [13] D. S. Bernstein and W. M. Haddad, "Robust stability and performance via fixed-order dynamic compensation with guaranteed cost bounds," *Math. Contr. Sig. Sys.*, vol. 3, pp. 139–163, 1990.
- [14] D. S. Bernstein, W. M. Haddad, and C. N. Nett, "Minimal complexity control law synthesis, Part 2: Problem solution via  $\mathcal{H}_2/\mathcal{H}_\infty$  optimal static output feedback," in *Proc. Amer. Contr. Conf.*, (Pittsburgh, PA), pp. 2506–2511, June 1989, Also appears in *Recent Advances in Robust Control*, pp. 288–293, P. Dorato and R. K. Yedavalli, Eds., IEEE Press, 1990.
- [15] D. S. Bernstein, W. M. Haddad, and A. G. Sparks, "A Popov criterion for uncertain linear multivariable systems," *Automatica*, vol. 31, pp. 1061–1064, 1995.
- [16] D. S. Bernstein and D. C. Hyland, "Optimal projection approach to robust, fixed-structure control design," in *Mechanics and Control of Space Structures* (J. Junkins, ed.), pp. 237–293, AIAA, Washington, D.C., 1993.
- [17] H. S. Black, "Stabilized feedback amplifiers," U.S. Patent No. 2,102,671, 1927.
- [18] S. Boyd, L. El Ghaoui, E. Feron, and V. Balakrishnan, *Linear Matrix Inequalities in Systems and Control Theory*, vol. 15 of *Studies in Applied Mathematics*. SIAM, 1994.
- [19] R. W. Brockett, "The status of stability theory for deterministic systems," *IEEE Trans. Autom. Contr.*, vol. 12, pp. 596–606, 1967.
- [20] R. W. Brockett and J. L. Willems, "Frequency domain stability criteria, Parts I and II," *IEEE Trans. Autom. Contr.*, vol. 10, pp. 255–261, 1965.
- [21] S. L. Campbell and C. D. Meyer, *Generalized Inverses of Linear Transformations*. Marshfield, MA: Pitman, 1979. Reprinted by Dover, New York, 1991.
- [22] R. H. Cannon, Jr. and D. E. Rosenthal, "Experiments in control of flexible structures with noncolocated sensors and actuators," *AIAA J. Guid. Contr. Dyn.*, vol. 7, pp. 546–553, 1984.
- [23] R. Y. Chiang and M. G. Safonov, "Real  $k_m$ -synthesis via generalized Popov multipliers," in *Proc. Amer. Contr. Conf.*, (Chicago, IL), pp. 2417–2418, June 1992.

- [24] E. G. Collins, Jr., W. M. Haddad, and S. S. Ying, "Construction of low-authority, nearly non-minimal LQG compensators for reduced-order control design," in *Proc. Amer. Contr. Conf.*, (Baltimore, MD), pp. 3411–3415, June 1994.
- [25] M. A. Dahleh and I. J. Diaz-Bobillo, *Control of Uncertain Systems: A Linear Programming Approach*. Englewood Cliffs, NJ: Prentice-Hall, 1995.
- [26] J. E. Dennis, Jr. and R. B. Schnabel, *Numerical Methods for Unconstrained Optimization and Nonlinear Equations*. Englewood Cliffs, NJ: Prentice-Hall, 1983.
- [27] P. Dorato and R. K. Yedavalli, Eds., *Recent Advances in Robust Control*. New York, NY: IEEE Press, 1990.
- [28] P. Dorato, Ed., *Robust Control*. New York, NY: IEEE Press, 1987.
- [29] J. C. Doyle, "Guaranteed margins for LQG regulators," *IEEE Trans. Autom. Contr.*, vol. 23, pp. 756–757, 1978.
- [30] J. C. Doyle, "Analysis of feedback systems with structured uncertainties," *IEE Proceedings, Part D*, pp. 242–250, 1982.
- [31] J. C. Doyle, K. Glover, P. P. Khargonekar, and B. A. Francis, "State-space solutions to standard  $\mathcal{H}_2$  and  $\mathcal{H}_\infty$  control problems," *IEEE Trans. Autom. Contr.*, vol. 34, pp. 831–847, 1989.
- [32] J. C. Doyle and G. Stein, "Robustness with observers," *IEEE Trans. Aut. Control*, vol. 24, pp. 607–611, 1979.
- [33] J. C. Doyle and G. Stein, "Multivariable feedback design: Concepts for a classical/modern synthesis," *IEEE Trans. Autom. Contr.*, vol. 26, no. 1, pp. 4–16, 1981.
- [34] R. S. Erwin, A. G. Sparks, and D. S. Bernstein, "Decentralized real structured singular value synthesis," in *Proc. 13th IFAC World Congress*, vol. C: Control Design I, (San Francisco, CA), pp. 79–84, July 1996.
- [35] R. S. Erwin, A. G. Sparks, D. S. Bernstein, J. R. Corrado, V. Chellaboina, and W. M. Haddad, *The Robust Fixed-Structure Control Toolbox*. preprint.
- [36] K. M. Eveker, D. L. Gysling, C. N. Nett, and O. P. Sharma, "Integrated control of rotating stall and surge in aeroengines," in *SPIE Conf. on Sensing, Actuation, and Control in Aeropropulsion*, (Orlando, FL), April 1995.
- [37] M. K. H. Fan, A. L. Tits, and J. C. Doyle, "Robustness in the presence of mixed parametric uncertainty and unmodeled dynamics," *IEEE Trans. Autom. Contr.*, vol. 36, pp. 25–38, 1991.

- [38] T. Feng and D. S. Bernstein, "Shifted quadratic guaranteed cost bounds for robust stability and performance," in *Proc. 13th IFAC World Congress*, vol. G: Education, Robust Control I, (San Francisco, CA), pp. 285–290, July 1996.
- [39] B. A. Francis, *A Course in  $\mathcal{H}_\infty$  Control Theory*. New York: Springer-Verlag, 1987.
- [40] J. H. Friedman and D. S. Bernstein, "Maximum entropy controller synthesis for collocated and noncollocated systems," *AIAA Journal of Guidance, Control, and Dynamics*, vol. 17, pp. 859–862, 1993.
- [41] P. Gahinet, A. Nemirovskii, A. J. Laub, and M. Chilali, *LMI Lab: A Package for Manipulating and Solving LMIs, v. 2.0*. The Math Works, Inc., 1994.
- [42] C. Ganesh and J. B. Pearson, " $\mathcal{H}_2$ -optimization with stable controllers," *Automatica*, vol. 25, pp. 629–634, 1989.
- [43] S. C. O. Grocott, D. G. MacMartin, and D. W. Miller, "Experimental implementation of a multi-model design technique for robust control of the MACE test article," in *Proc. Third Int. Conf. Adaptive Structures*, (San Diego, CA), pp. 375–387, November 1992.
- [44] W. M. Haddad, *Robust Optimal Projection Control-System Synthesis*. PhD thesis, Florida Institute of Technology, Melbourne, FL, 1987.
- [45] W. M. Haddad and D. S. Bernstein, "Generalized Riccati equations for the full- and reduced-order mixed-norm  $\mathcal{H}_2/\mathcal{H}_\infty$  standard problem," *Syst. Contr. Lett.*, vol. 14, pp. 185–197, 1990.
- [46] W. M. Haddad and D. S. Bernstein, "Parameter-dependent Lyapunov functions, constant real parameter uncertainty, and the Popov criterion in robust analysis and synthesis, Parts I and II," in *Proc. IEEE Conf. Dec. Contr.*, (Brighton, UK), pp. 2274–2279, 2632–2633, December 1991.
- [47] W. M. Haddad and D. S. Bernstein, "Robust stabilization with positive real uncertainty: Beyond the small gain theorem," *Systems and Control Letters*, vol. 17, pp. 191–208, 1991.
- [48] W. M. Haddad and D. S. Bernstein, "Explicit construction of quadratic Lyapunov functions for the small gain, positivity, circle, and Popov theorems and their application to robust stability, Part I: Continuous-time theory," *Int. J. Robust Nonlinear Contr.*, vol. 3, pp. 313–319, 1993.
- [49] W. M. Haddad and D. S. Bernstein, "Explicit construction of quadratic Lyapunov functions for the small gain, positivity, circle, and Popov theorems and their application to robust stability, Part II: Discrete-time theory," *Int. J. Robust Nonlin. Contr.*, vol. 4, pp. 249–265, 1994.

- [50] W. M. Haddad and D. S. Bernstein, "Parameter-dependent Lyapunov functions and the discrete-time Popov criterion for robust analysis," *Automatica*, vol. 30, pp. 1015–1021, 1994.
- [51] W. M. Haddad and D. S. Bernstein, "The octomorphic criterion for real parameter uncertainty: Real  $\mu$ -bounds without circles and  $d$ ,  $n$ -scales," *Sys. Contr. Lett.*, vol. 25, pp. 175–183, 1995.
- [52] W. M. Haddad and D. S. Bernstein, "Parameter-dependent Lyapunov functions and the Popov criterion in robust analysis and synthesis," *IEEE Trans. Autom. Contr.*, vol. 40, pp. 536–543, 1995.
- [53] W. M. Haddad, D. S. Bernstein, and V. Chellaboina, "Generalized mixed- $\mu$  bounds for real and complex multiple-block uncertainty with internal matrix structure," *Int. J. Contr.*, vol. 64, pp. 789–806, 1996.
- [54] W. M. Haddad, V. Chellaboina, and D. S. Bernstein, "An implicit small gain condition and an upper bound for the real structured singular value," *Sys. Contr. Lett.*, vol. 29, pp. 197–205, 1997.
- [55] W. M. Haddad, E. G. Collins, Jr., and D. S. Bernstein, "Robust stability analysis using the small gain, circle, positivity, and Popov theorems: A comparative study," *IEEE Trans. Contr. Syst. Tech.*, vol. 1, pp. 290–293, 1993.
- [56] W. M. Haddad, J. L. Fausz, V. Chellaboina, and A. Leonessa, "Nonlinear robust disturbance rejection controllers for rotating stall and surge in axial flow compressors," in *Proc. IEEE Conf. Contr. Appl.*, (Hartford, CT), pp. 767–772, September 1997.
- [57] W. M. Haddad, J. P. How, S. R. Hall, and D. S. Bernstein, "Extensions of mixed- $\mu$  bounds to monotonic and odd monotonic nonlinearities using absolute stability theory," *International Journal of Control*, vol. 60, pp. 905–951, 1994.
- [58] W. M. Haddad and V. Kapila, "Fixed-order controller synthesis for systems with input-output time-varying nonlinearities," *Int. J. Robust and Nonlinear Control*, vol. 7, pp. 675–710, 1997.
- [59] Y. Halevi, "Stable LQG controllers," *IEEE Trans. Aut. Control*, vol. 39, no. 10, pp. 2104–2106, 1994.
- [60] Y. Halevi, D. S. Bernstein, and W. M. Haddad, "On stable full-order and reduced-order LQG controllers," *Opt. Contr. Appl. Meth.*, vol. 12, pp. 163–172, 1991.
- [61] J. P. How and S. R. Hall, "Connections between the Popov stability criterion and bounds for real parameter uncertainty," in *Proc. Amer. Contr. Conf.*, (San Francisco, CA), pp. 1084–1089, June 1993.

- [62] D. C. Hyland and D. S. Bernstein, "The optimal projection equations for fixed-order dynamic compensation," *IEEE Trans. Autom. Contr.*, vol. 29, pp. 1034–1037, 1984.
- [63] D. C. Hyland and D. S. Bernstein, "The optimal projection equations for model reduction and the relationship among the methods of Wilson, Skelton, and Moore," *IEEE Trans. Autom. Contr.*, vol. 30, pp. 1201–1211, 1985.
- [64] M. Jacobus, M. Jamshidi, C. Abdallah, P. Dorato, and D. Bernstein, "Suboptimal strong stabilization using fixed-order dynamic compensation," in *Proc. Amer. Contr. Conf.*, (San Diego, CA), pp. 2659–2660, May 1990.
- [65] E. I. Jury and B. W. Lee, "On the absolute stability of nonlinear sampled-data systems," *IEEE Trans. Autom. Contr.*, vol. 9, pp. 551–554, 1964.
- [66] E. I. Jury and B. W. Lee, "On the stability of a class of nonlinear sampled-data systems," *IEEE Trans. Autom. Contr.*, vol. 9, pp. 51–61, 1964.
- [67] R. E. Kalman, "Contributions to the theory of optimal control," *Boltein de la Sociedad Matematica Mexicana*, vol. 5, pp. 102–119, 1960.
- [68] R. E. Kalman, "A new approach to linear filtering and prediction problems," *J. Basic Engineering, Trans. ASME*, vol. 82, pp. 35–45, 1960.
- [69] R. E. Kalman, "Lyapunov functions for the problem of Lur'e in automatic control," *Proc. Natl. Acad. Sci.*, vol. 49, pp. 201–205, 1963.
- [70] R. E. Kalman, "When is a linear control system optimal?," *J. Basic Engineering, Trans. ASME*, vol. 86, pp. 51–60, 1964.
- [71] R. E. Kalman and J. E. Bertram, "Control system analysis and design via the "Second Method" of Lyapunov, Part I: Continuous-time systems," *J. Basic Engineering, Trans. ASME*, vol. 82, pp. 371–393, 1960.
- [72] R. E. Kalman and J. E. Bertram, "Control system analysis and design via the "Second Method" of Lyapunov, Part II: Discrete-time systems," *J. Basic Engineering, Trans. ASME*, vol. 82, pp. 394–400, 1960.
- [73] R. E. Kalman and R. S. Bucy, "New results in linear filtering and prediction theory," *J. Basic Engineering, Trans. ASME*, vol. 83, pp. 95–108, 1961.
- [74] V. Kapila, W. M. Haddad, R. S. Erwin, and D. S. Bernstein, "Robust controller synthesis via shifted parameter-dependent quadratic cost bounds," *IEEE Trans. Autom. Contr.*, vol. 43, pp. 1003–1007, 1998.
- [75] L. H. Keel and S. P. Bhattacharyya, "Robust, fragile, or optimal?," *IEEE Trans. Autom. Contr.*, vol. 42, pp. 1098–1105, 1997.

- [76] P. P. Khargonekar, I. R. Petersen, and K. Zhou, "Robust stabilization of uncertain linear systems: Quadratic stabilizability and  $\mathcal{H}_\infty$  control theory," *IEEE Trans. Autom. Contr.*, vol. 35, pp. 356–361, 1990.
- [77] P. P. Khargonekar and K. Poola, "Robust stabilization of disturbed systems," *Automatica*, vol. 22, pp. 77–84, 1986.
- [78] M. Krstić and P. V. Kokotović, "Lean backstepping design for a jet engine compressor model," in *Proc. IEEE Conf. Contr. Appl.*, (Albany, NY), pp. 1047–1052, September 1995.
- [79] M. Krstić, J. M. Protz, J. D. Paduano, and P. V. Kokotović, "Backstepping designs for jet engine stall and surge control," in *Proc. IEEE Conf. Dec. Contr.*, (New Orleans, LA), pp. 3049–3055, December 1995.
- [80] H. Kwakernaak and R. Sivan, *Linear Optimal Control Systems*. New York: Wiley-Interscience, 1972.
- [81] L. Lee and A. L. Tits, "Linear fractional transformations for the approximation of various uncertainty sets," in *Control of Uncertain Dynamic Systems*, edited by S. Bhattacharyya and L. Keel, pp. 53–62, CRC Press, 1991.
- [82] S. Lefschetz, *Stability of Nonlinear Control Systems*. New York: Academic Press, 1965.
- [83] D. C. Liaw and E. H. Abed, "Stability analysis and control of rotating stall," *IFAC Nonlinear Control Systems*, pp. 295–300, 1992.
- [84] D. C. Liaw and E. H. Abed, "Active control of compressor stall inception: A bifurcation-theoretic approach," *Automatica*, vol. 32, pp. 109–115, 1996.
- [85] A. G. J. MacFarlane and N. Karcanias, "Poles and zeros of linear multivariable systems: A survey of the algebraic, geometric, and complex-variable theory," *Int. J. Contr.*, vol. 24, pp. 33–74, 1976.
- [86] D. G. MacMartin, S. R. Hall, and D. S. Bernstein, "Fixed-order multi-model estimation and control," in *Proc. Amer. Contr. Conf.*, (Boston, MA), pp. 2113–2118, June 1991.
- [87] D. G. MacMartin and J. P. How, "Implementation and prevention of unstable compensators," in *Proc. Amer. Contr. Conf.*, (Baltimore, MD), pp. 2190–2195, June 1994.
- [88] A. N. Madiwale, W. M. Haddad, and D. S. Bernstein, "Robust  $\mathcal{H}_\infty$  control design for systems with structured parameter uncertainty," *Systems and Control Letters*, vol. 12, pp. 393–407, 1989.

- [89] F. E. McCaughan, "Bifurcation analysis of axial flow compressor stability," *SIAM Journal Applied Mathematics*, vol. 20, pp. 1232–1253, 1990.
- [90] F. K. Moore and E. M. Greitzer, "A theory of post-stall transients in axial compression systems, Parts I and II," *Journal of Engineering for Gas Turbines and Power*, vol. 108, pp. 68–76, 1986.
- [91] K. S. Narendra and Y. S. Cho, "Stability analysis of nonlinear and time-varying discrete systems," *SIAM Journal of Control*, vol. 6, pp. 625–646, 1968.
- [92] K. S. Narendra and C. P. Neuman, "Stability of a class of differential equations with a single monotone nonlinearity," *SIAM Journal of Control*, vol. 4, pp. 295–308, 1966.
- [93] K. S. Narendra and C. P. Neuman, "Stability of continuous-time dynamical systems with  $m$ -feedback nonlinearities," *AIAA Journal*, vol. 5, pp. 2021–2027, 1967.
- [94] K. S. Narendra and J. H. Taylor, *Frequency Domain Criteria for Absolute Stability*. New York: Academic Press, 1973.
- [95] C. N. Nett, D. S. Bernstein, and W. M. Haddad, "Minimal complexity control law synthesis, Part 1: Problem formulation and reduction to optimal static output feedback," in *Proc. Amer. Contr. Conf.*, (Pittsburgh, PA), pp. 2056–2064, June 1989.
- [96] C. N. Nett and W. M. Haddad, "A system-theoretic appropriate realization of the empty matrix concept," *IEEE Trans. Autom. Contr.*, vol. 38, pp. 771–775, 1993.
- [97] A. Packard and J. Doyle, "The complex structured singular value," *Automatica*, vol. 29, pp. 71–109, 1993.
- [98] J. D. Paduano, L. Valavani, A. H. Epstein, E. M. Greitzer, and G. R. Guenette, "Modeling for control of rotating stall," *Automatica*, vol. 30, no. 9, pp. 1357–1373, 1994.
- [99] I. R. Petersen, "Disturbance attenuation and  $\mathcal{H}_\infty$  optimization: A design method based on the algebraic Riccati equation," *IEEE Trans. Autom. Contr.*, vol. 32, pp. 427–429, 1987.
- [100] I. R. Petersen and C. V. Hollot, "A Riccati equation approach to the stabilization of uncertain systems," *Automatica*, vol. 22, pp. 397–411, 1986.
- [101] L. S. Pontryagin, V. G. Boltyanskii, R. V. Gamkrelidze, and E. F. Mischenko, *The Mathematical Theory of Optimal Process*. K. N. Tirogoff (transl.) and L. W. Newstadt (ed.), New York: Interscience, 1962.

- [102] V. M. Popov, "Absolute stability of nonlinear systems of automatic control," *Automation and Remote Control*, vol. 22, pp. 857–875, 1962.
- [103] V. M. Popov, *Hyperstability of Automatic Control Systems*. New York: Springer-Verlag, 1973.
- [104] M. G. Safonov, *Stability and Robustness of Multivariable Feedback Systems*. Cambridge, MA: MIT Press, 1980.
- [105] M. G. Safonov and R. Y. Chiang, "Real/complex  $K_m$ -synthesis without curve fitting," *Control and Dynamic Systems*, vol. 56, pp. 303–324, 1993.
- [106] A. G. Sparks and D. S. Bernstein, "Real structured singular value synthesis using the scaled Popov criterion," *AIAA J. Guid. Contr. Dyn.*, vol. 18, pp. 1244–1252, 1995.
- [107] Special Issue on the Linear Quadratic Gaussian Problem *IEEE Trans. Autom. Contr.*, vol. 16, 1971.
- [108] G. Stein and M. Athans, "The LQG/LQR procedure for multivariable feedback control design," *IEEE Trans. Autom. Contr.*, vol. 32, pp. 105–114, 1987.
- [109] Y. Z. Tsytkin, "A criterion for absolute stability of automatic pulse systems with monotonic characteristics of the nonlinear element," *Sov. Phys.-Doklady*, vol. 9, pp. 263–266, 1964.
- [110] M. Vidyasagar, *Control System Synthesis*. Cambridge, MA: The MIT Press, 1985.
- [111] M. Vidyasagar, *Nonlinear Systems Analysis*. Englewood Cliffs, NJ: Prentice-Hall, 1993.
- [112] Y. W. Wang and D. S. Bernstein, " $\mathcal{H}_2$  -suboptimal stable stabilization," *Automatica*, vol. 30, pp. 1797–1800, 1994.
- [113] Y. W. Wang, W. M. Haddad, and D. S. Bernstein, "Stable stabilization with  $\mathcal{H}_2$  and  $\mathcal{H}_\infty$  performance constraints," *Journal of Mathematical Systems, Estimation, and Control*, vol. 6, no. 2, pp. 181–194, 1996.
- [114] B. Wei and D. S. Bernstein, "Benchmark problems for robust control design," *AIAA J. Guid. Contr. Dyn.*, vol. 15, pp. 1057–1059, 1992.
- [115] W. M. Wonham, *Linear Multivariable Control: A Geometric Approach*. New York: Springer-Verlag, 2nd ed., 1979.
- [116] V. A. Yakubovitch, "Absolute stability of nonlinear control systems in critical cases, Part I," *Avtomatika i Telemekhanika*, vol. 24, pp. 293–303, 1963.

- [117] V. A. Yakubovitch, "Absolute stability of nonlinear control systems in critical cases, Part II," *Avtomatika i Telemekhanika*, vol. 24, pp. 717–731, 1963.
- [118] V. A. Yakubovitch, "Absolute stability of nonlinear control systems in critical cases, Part III," *Avtomatika i Telemekhanika*, vol. 25, pp. 601–612, 1963.
- [119] V. A. Yakubovitch, "Frequency conditions for the absolute stability and dissipativity of control systems with a single differentiable nonlinearity," *Soviet Mathematics*, vol. 6, pp. 98–101, 1965.
- [120] V. A. Yakubovitch, "The method of matrix inequalities in the theory of the stability of nonlinear control systems II: Absolute stability in a class of nonlinearities with a condition on the derivative," *Automatic and Remote Control*, vol. 26, pp. 577–592, 1965.
- [121] D. C. Youla, J. J. Bongiorno, and C. N. Lu, "Single loop feedback-stabilization of linear multivariable dynamical plants," *Automatica*, vol. 10, pp. 159–173, 1974.
- [122] P. M. Young, "Controller design with mixed uncertainties," in *Proc. Amer. Contr. Conf.*, (Baltimore, MD), pp. 2333–2337, June 1994.
- [123] P. M. Young, M. Newlin, and J. Doyle, " $\mu$ -analysis with real parameter uncertainty," in *Proc. IEEE Conf. Dec. Contr.*, (Brighton, UK), pp. 1251–1256, December 1991.
- [124] A. Yousuff and R. E. Skelton, "An optimal controller reduction by covariance equivalent realizations," *IEEE Trans. Autom. Contr.*, vol. 31, pp. 56–60, 1986.
- [125] G. Zames and P. L. Falb, "Stability conditions for systems with monotone and slope-restricted nonlinearities," *SIAM Journal on Control and Optimization*, vol. 4, pp. 89–108, 1968.
- [126] K. Zhou, J. C. Doyle, and K. Glover, *Robust and Optimal Control*. Englewood Cliffs, NJ: Prentice-Hall, 1996.